Analysis of Epidermis and Mesophyll-specific Transcript Accumulation after Syringolin A Application in Powdery Mildew-inoculated Wheat Leaves

Dissertation

zur

Erlangung der naturwissenschaftlichen Doktorwürde

(Dr. sc. nat.)

vorgelegt der

Mathematisch-naturwissenschaftlichen Fakultät

der

Universität Zürich

von

Olaf Abderhalden

von

Ebnat-Kappel SG

Begutachtet von

Prof. Dr. Robert Dudler

Prof. Dr. Beat Keller

Zürich 2006

Die vorliegende Arbeit wurde von der Mathematisch-naturwissenschaftlichen Fakultät der Universität Zürich auf Antrag von Prof. Dr. Beat Keller und
Prof. Dr. Ueli Grossniklaus als Dissertation angenommen.

1. Summary

The powdery mildew fungus *Blumeria graminis* (DC) Speer is one of the most important foliar diseases of cereals. It is an obligate biotrophic organism exclusively colonizing the surface of the host plant, which makes it highly suitable to study plant-pathogen interactions at the cytological and molecular level. An important component of the plant defense is the induction of localized cellular suicide called the 'hypersensitive response' (HR), which restricts the propagation of pathogens inside the host organism. It is hypothesized that the induction of HR can be suppressed by pathogenic isolates of powdery mildew. Recently, it was discovered that a cyclic tetrapeptide (syringolin) secreted by phytopathogenic strains of *Pseudomonas syringae* pv. *syringae* re-induced HR in powdery mildew-infected wheat epidermal cells. By this means, the fungus is efficiently eradicated from the host surface and it was hypothesized that syringolin action might specifically target the control of cellular survival in wheat. The goal of the present study was to identify genes activated in powdery mildew-infected wheat upon treatment with syringolin. Subsequent investigations were aimed to differentiate between genes generally induced by syringolin treatment and genes involved in the induction of HR.

cDNA subtraction of sample material collected 2 h, 6 h, 12 h, and 24 h after syringolin treatment of powdery mildew-infected wheat yielded 498 cDNA fragments which were tested for syringolin responsiveness by reverse dot blot hybridization experiments. Subsequent DNA sequence analysis resulted in the identification of 158 candidate genes of plant origin which were analyzed further. For these purposes, a microarray containing 1666 cDNA probes was designed. One hundred glass slides which carried PCR products corresponding to the 158 candidate genes as well as to additional genes derived from other screenings were fabricated. With the aim to distinguish between generally induced and HR-specific genes, the microarray slides were hybridized with different cDNA targets. These corresponded to epidermal and mesophyll tissue of powdery mildew-infected and uninfected wheat leaves collected at 12 h and 24 h after treatment with syringolin. A total number of 124 genes was confirmed to be transcriptionally regulated by syringolin treatment, 103 were derived from cDNA subtraction. A considerable proportion of more than 20 % of putative proteins encoded by syringolin responsive genes exhibited similarity to proteins of unknown function. The rest was found to cover a broad range of biological activity. Surprisingly, all of the genes were also found to be regulated by the activity of syringolin alone and none of them showed exclusive transcript accumulation in the presence of powdery mildew. Moreover, none of the genes was found to be transcribed exclusively in the epidermis, where the syringolin-induced HR is located at.

Essentially, no overlap of gene transcription was found upon comparisons between the plant response to syringolin and to the contact fungicide cyprodinil. This indicated that different molecular mechanisms underlie eradication of powdery mildew by syringolin.

In parallel to microarray investigations, thirty genes were selected and tested for their functional participation in the induction of HR occurring upon infection of wheat expressing the *Pm3b* resistance gene with a powdery mildew isolate carrying the cognate avirulence factor. Therefore, a biolistic transient transformation system was used to study suppression of transcript accumulation by induction of RNA interference, which should lead to increased susceptibility of transformed cells to the fungal pathogen. However, none of the genes favored elevated fungal colonization of the plant upon transient induction of RNA interference. This strongly indicated that the reprogramming of infected wheat epidermal cells to undergo hypersensitive cell death is controlled by a different, thus far unconsidered mechanism.

Microscopical investigations as well as further microarray analyses at 2 h and 48 h after syringolin treatment indicated that the HR induced by syringolin occurs later than previously expected. On the basis of comprehensive analyses of biological functions of syringolin-induced genes this lead to a novel hypothesis according to which syringolin may act as a virulence factor, capable of suppressing host defense and induction of HR in wheat. Implications of this model with respect to known characteristics of syringolin action are discussed.

In addition, further microarray analyses of the interaction of resistant wheat with different powdery mildew isolates resulted in the identification of 2 putative HR marker genes encoding proteins of unknown molecular function. Both of them were derived from cDNA subtraction in syringolin-treated wheat.

2. Zusammenfassung

Der echte Mehltaupilz (*Blumeria graminis* (DC) Speer) ist eine der wichtigsten Blattkrankheiten in Getreide. Es handelt sich um einen obligat biotrophen Organismus, welcher sich ausschliesslich auf der Blattoberfläche seiner Wirtspflanze auszubreiten vermag. Dies macht ihn zu einem ausgezeichneten Studienobjekt für Pflanzen-Pathogen-Interaktionen auf zytologischer und molekularer Ebene. Eine wichtige Komponente der pflanzlichen Abwehr, welche die Ausbreitung von Erregern im Wirtsorganismus einzudämmen vermag, ist die Induktion eines zellulären Suizidprogramms, die 'Hypersensitive Reaktion' (HR) genannt wird. Es wird angenommen, dass die Induktion von HR von virulenten Mehltauisolaten unterdrückt werden kann. Kürzlich wurde entdeckt, dass ein zyklisches Tetrapeptid (Syringolin), welches von pflanzenpathogenen Stämmen von *Pseudomonas syringae* pv. *syringae* sezerniert wird, die HR in mehltaubefallenen Epidermiszellen von Weizen reaktiviert. Dabei wird der Mehltau auf effiziente Weise auf der ganzen Blattoberfläche vernichtet und es entstand die Annahme, dass die Syringolinwirkung spezifisch auf die Kontrolle des zellulären Überlebens beim Weizen abzielt. Ziel der vorliegenden Studie war die Identifizierung von transkriptionell induzierten Genen, die bei der Syringolinbehandlung von mehltaubefallenem Weizen aktiviert werden. Die folgenden Untersuchungen zielten darauf ab, Gene, welche eine generelle Induktion durch Syringolinbehandlung aufweisen, von solchen zu unterscheiden, welche spezifisch für das Zustandekommen von HR verantwortlich sind.

cDNA-Subtraktion von Probenmaterial, welches 2 h, 6 h, 12 h, und 24 h nach Syringolinbehandlung von mehltauinfiziertem Weizen gesammelt wurde, ergab 498 cDNA Fragmente, die anschliessend mittels reverser Dotblot-Hybridisierung auf ihre Syringolinempfindlichkeit hin getestet wurden. Darauf folgende DNA Sequenzanalyse resultierte in der Identifizierung von 158 pflanzlichen Kandidatengenen, welche weiteren Analysen unterzogen wurden. Zu diesem Zweck wurde ein Mikroarray bestehend aus 1666 cDNA Proben entworfen. Einhundert Objektträger mit PCR-Produkten der 158 Kandidatengene sowie weiterer Gene, welche von anderen Screenings herrührten, wurden hergestellt. Mit dem Ziel, generell und HR-spezifisch induzierte Gene voneinander unterscheiden zu können, wurden die Mikroarrayobjektträger mit verschiedensten cDNA-Targets hybridisiert. Diese entsprachen Epidermis- und Mesophyllgewebe von mehltauinfizierten Weizenpflanzen, welche 12 h und 24 h nach Behandlung mit Syringolin gesammelt wurden. Die transkriptionelle Regulation durch Einwirkung von Syringolin von insgesamt 124 Genen wurde hierbei bestätigt, 103 davon stammten aus der cDNA-

Subtraktion. Ein beträchtlicher Anteil von über 20 % der mutmasslichen Proteine, welche von syringolinempfindlichen Genen kodiert werden, zeigte Ähnlichkeit zu Proteinen unbekannter Funktion. Der Rest deckte einen weiten Bereich biologischer Aktivität ab. Überraschenderweise waren sämtliche Gene auch durch die alleinige Einwirkung von Syringolin reguliert und keines zeigte ausschliessliche Akkumulation von Transkripten bei Anwesenheit des Pilzes. Des Weiteren zeigte keines der Gene ausschliesslich epidermisspezifische Transkription, obschon die syringolininduzierte HR ausschliesslich in der Epidermis stattfindet.

Bei Vergleichen zwischen der pflanzlichen Antwort auf Syringolin und auf das Kontaktfungizid Cyprodinil wurde im Wesentlichen keine Überlappung der Gentranskription festgestellt. Dies deutete darauf hin, dass der Vernichtung von Mehltau durch Syringolin unterschiedliche molekulare Mechanismen zu Grunde liegen.

Parallel zu Mikroarrayanalysen wurden dreissig Gene selektioniert und auf ihre mögliche Funktion bei der Induktion von HR getestet, welche im Zuge der Infektion von Weizen mit Mehltau durch einen pilzlichen Avirulenzfaktor in Anwesenheit des pflanzlichen *Pm3b* Resistenzgenprodukts ausgelöst wird. Dabei wurde die Akkumulation von Transkripten durch Induktion von RNA-Interferenz mit Hilfe eines biolistischen transienten Transformationssystems unterdrückt, was zu erhöhter Anfälligkeit transformierter Zellen gegenüber Pilzbefall führen sollte. Es zeigte sich jedoch, dass keines der Gene bei transienter Induktion von RNA-Interferenz die Kolonisierung der Pflanze durch den Pilz begünstigte. Dies deutete darauf hin, dass die Reprogrammierung infizierter epidermaler Weizenzellen hypersensitiven Zelltod zu initiieren durch einen anderen, bislang unberücksichtigten Mechanismus zu Stande kommt.

Sowohl mikroskopische als auch weitere Mikroarrayuntersuchungen 2 h und 48 h nach Syringolinbehandlung deuteten darauf hin, dass die syringolininduzierte HR später als ursprünglich erwartet eintritt. Auf der Basis umfassender Analysen biologischer Funktionen von syringolininduzierten Genen führte dies schliesslich zu einer neuen Hypothese, wonach Syringolin als Virulenzfaktor wirken könnte, welcher die Wirtsabwehr und Induktion von HR zu unterdrücken vermag. Die Diskussion möglicher Folgerungen aus diesem Modell im Hinblick auf bekannte Charakteristika der Syringolinaktivität ist Teil der vorliegenden Arbeit.

Im Weiteren führten zusätzliche Mikroarrayuntersuchungen der Interaktion von resistentem Weizen mit verschiedenen Mehltauisolaten zur Identifizierung von 2 mutmasslichen HR-Markergenen, welche Proteine unbekannter molekularer Funktion kodieren. Beide Gene stammen aus der cDNA-Subtraktion in syringolinbehandeltem Weizen.

3. Introduction

Like all organisms, plants are exposed to a constant onrush of bacterial or fungal microbes as well as myriads of viral particles. Their master role in energy and carbon fixation and thus their basal position in the global food chain might even make them particularly attractive for fungal and bacterial intruders. In contrast to animals, plants are immobile and thus, they are lacking specialized cells, analogs of animal B- or T-lymphocytes, destined to combat and eradicate potential pathogens. Consequently distinct strategies to overcome microbial attacks constituting the plant defense system have evolved.

The effectiveness of the innate defense system has always been hived into a hot spot of interest due to the great agronomical importance of many plants. Yield losses caused by epidemic spread of plant diseases repeatedly caused famines in the western world history and still do so world wide. Modern monocropping systems comprising of large contiguous areas cultivated with the same plant species even enhance the risk of epidemics requiring the application of tons of chemical fungicides and insecticides. In 2003, the global market of chemical crop protection products reached € 23.6 billion. Yet, application of large quantities of chemical agents is not only cost intensive but also entails problematical environmental burdens to the whole ecosystem.

Alternatively, centuries of plant breeding created cultivated plants exhibiting desirable characteristics such as high yield and high resistance towards prevalent plant diseases. However, breeding firstly involves undirected crossing of appropriate parental plants and requires laborious selection and back-crossing of filial generations. A central and widely discussed aspect in the generation of elevated plant resistance in traditional and modern plant breeding is circumscribed by the term 'durability of resistance'. The importance of durable resistance resides in a remarkable flexibility and ability of pathogens to overcome plant defense mechanisms. Recent advances in biotechnology have offered the possibility to selectively transfer specific genes or modulate their activity, thereby circumventing the recombination of two complete genomes. However, transformation efficiency in wheat is relatively low because *Agrobacterium tumefaciens*-aided stable gene transfection is still not possible. In addition, transformation is still restricted to only a number of wheat cultivars and thus, the application is still primarily confined to scientific purposes. As opposed to traditional breeding, targeted molecular modification requires profound knowledge about the biochemical and molecular reactions on the plant and pathogen side. Thus, great efforts are put into investigations of these complex interactions.

3.1. Powdery mildew

Blumeria graminis (DC.) Speer, the causal agent of cereal powdery mildew belongs to the family of Erysiphaceae in the phylum of Ascomycota. Classification into eight formae speciales (ff.spp.) including f.sp. *hordei* on *Hordeum vulgare* and f.sp. *tritici* on *Triticum aestivum* is based on strict host specialization. The genetic variation of grass powdery mildews with regard to geographical distribution and pathogen/host co-evolution was investigated recently (Wyand and Brown, 2003). Powdery mildews are growing on the leaf surface of their host plants. In the hot summer season, hyphal growth on infected plants and the formation of conidiophores during the asexual propagation overlays leaves with a white fungal powder (Figure 3.10, p23). Conidia are distributed by wind and frequently cause epidemic spread of the pathogen in monocropping cultures of host plants. If infection occurs early in the crop cycle, powdery mildew can cause major yield losses of up to 30 % in susceptible wheat. While the season precedes, sexual reproduction sets in, resulting in the formation of cleistothecia visible as black spots on the leaf surface. Hibernation of the asci is taking place inside the fruit body and maturation of the ascospores generally happens in spring (Figure 3.1).

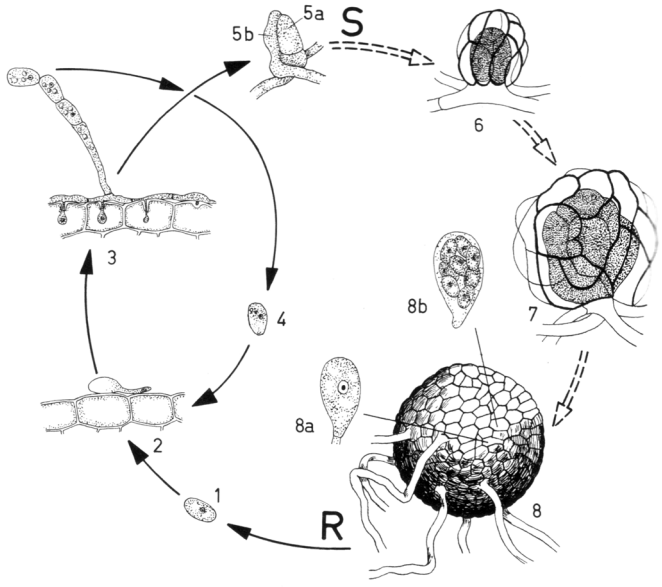

Figure 3.1: Blumeria life cycle. 1 ascospore, 2 germ tube, 3 elongating secondary hyphae and formation of conidiophores, 4 conidiospore, 5a ascogon, 5b antheridium, 6 & 7 developing cleistothecium, 8 fertile cleistothecium, 8a kariogamy in the ascus, 8b mature ascus with 8 ascospores R reduction division, S sexual reproduction. (Schwantes and Weberling, 1981)

Unlike for example downy mildew or leaf rust, powdery mildew exclusively infects epidermal host cells and only spreads at the surface of infected plants. It is an obligate biotrophic pathogen which only can live and reproduce on living host plants. Infection of host plant epidermal cells begins after landing of a conidial spore on the plant. *B. graminis* produces two different germ tubes and initiation of germination is independent from inducing factors on the host plant (Bélanger et al., 2002). The primary germ tube ensures attaching of the fungal germling and might be involved in fungal water supply and surface

recognition (Carver et al., 1995; Carver et al., 1999). Germination of the secondary germ tube at around 3 hours after spore landing is particularly stimulated on host cell surfaces and recognition of substratum characteristics by the elongating germ tube initiates the differentiation of an appressorium. The appressorial lobe at the tip of the secondary germ tube corresponds to the fungal infection structure. Penetration of the host epidermal cell is achieved by combined enzymatic degradation and high turgor pressure, driving a penetration peg through the cell cuticle and cell wall from beneath the appressorial lobe (Pryce-Jones et al., 1999). The penetration stage is shown in Figure 3.2A.

After penetration, the hyphal tip grows into the epidermal cell and forms a fungal absorption structure called the haustorium (Figure 3.2B). The haustorium is enclosed by the extrahaustorial matrix and the invaginated host plasma membrane and the whole structure is termed the haustorial complex (Bélanger et al., 2002). The haustorium is responsible for nutrient transfer from the host plant to the fungus and photoassimilates are thought to enter the haustorium in the form of glucose (Sutton et al., 1999). One haustorium is capable to acquire enough nutrients to supply a whole fungal colony during the entire asexual life cycle (Shirasu et al., 1999). In addition, haustorial structures of obligate biotrophic fungi might play important roles in mediating host defense suppression (reviewed by Panstruga, 2003).

Defeat of the plant defense and successful colonization by the fungus is followed by the formation of elongating hyphae (Figure 3.2.C) and finally results in a dense mycelium covering the leaf surface. The time course of a compatible interaction between wheat and powdery mildew is illustrated in Figure 3.3A-D.

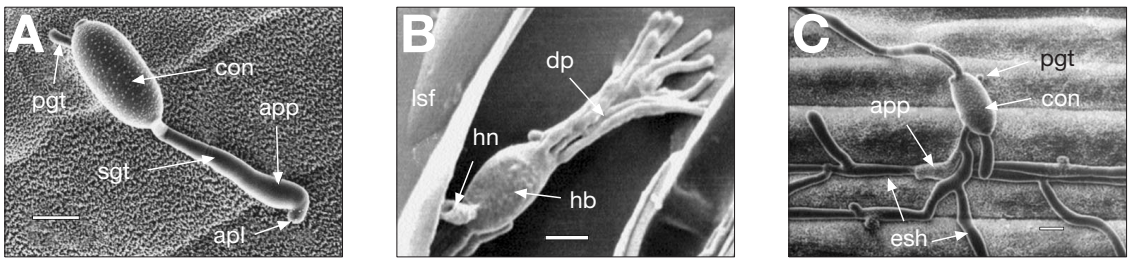

Figure 3.2: Colonization of epidermal cells by *Blumeria graminis*. A: Appressorial penetration attempt, B: Fully developed haustorium inside an epidermal cell, C: Compatible interaction and successful colonization. con = conidium; pgt = primary germ tube; sgt = secondary germ tube; app = appressorium; apl = appressorial lobe; lsf = leaf surface; hn = haustorial neck; hb = haustorial body; dp = digitate processes; esh = elongating secondary hyphae. Scale bar = 10 µm. (Carver et al., 2001).

3.2. Plant Defense

In general, the ability of pathogens to multiply in certain plant species requires the presence or absence of multiple factors in the plant and pathogen and can therefore be

viewed to be based on compatibility of two interacting partners. In the case of powdery mildew, the pathogenicity spectrum is restricted to plants of a certain genus (e.g. *Triticum*). Corresponding plants are thus referred to as host plants. For plant species of another genus such as for example *Hordeum*, the pathogen is not virulent and the interaction is termed 'incompatible interaction'. Corresponding plants are per definition 'nonhost plants' and in this specific interaction, the putative pathogen is called 'nonhost pathogen'.

3.2.1. Defense mechanisms

To defend themselves against pathogen attack, plants have evolved a whole repertoire of inducible defense mechanisms. These include assembly of cell wall appositions (structural barriers called papillae) or synthesis of toxic secondary metabolites called phytoalexins (reviewed by Dixon, 2001) and reactive oxygen intermediates (ROI). Of the latter, the hydroxyl radical ($HO^{\bullet}$) is the most toxic due to the ability to spontaneously react with proteins and other organic molecules. A very efficient tool to prevent systemic proliferation of infection is the induction of the hypersensitive response (HR) which denotes induction of a rapid localized cell death at sites of infection.

Papilla

Deposition of papilla material occurs at the inner surface of the epidermal cell wall at the penetration site. This cell wall fortification called papilla is formed in incompatible as well as compatible interactions. Induction of papilla formation by the plant is preceded by translocation of the nucleus close to sites of attempted penetration and local cytoplasm aggregation beneath the fungal appressorial lobe (Zeyen et al., 2002). The papilla consists of polyphenolics, callose, lignin silicates and proteins such as peroxidases cross-linked by the activity of ROIs (Thordal-Christensen et al., 1997; von Röpenack et al., 1998; Zeyen et al., 2002; Hückelhoven and Kogel, 2003). Initiation occurs at around 10 hours after infection (hai; Figure 3.3.E) and the deposition process consists of several stages. Papilla formation is dependent on a large re-organization of actin microfilaments into radial arrangements beneath fungal contact sites mediating transport of components by vesicles (Kobayashi et al., 1997; Hückelhoven et al., 1999; Collins et al., 2003; Opalski et al., 2005). Strikingly, effective papillae strongly accumulate H_2O_2 and intense yellow autofluorescence based on phenolic compounds is observed in the epidermal cell wall halo surrounding the papilla and the papilla itself whereas H_2O_2 accumulation and autofluorescence is weak in the compatible case (Koga et al., 1980; Carver et al., 1994; Hückelhoven and Kogel, 2003).

PR-genes

The induction of plant defense is accompanied by transcriptional upregulation of various classes of specific defense-related genes called pathogen-related (PR) genes (compiled in Muthukrishnan et al., 2001). Corresponding gene products may either exhibit direct antimicrobial activity such as for example the PR-3 class chitinases (Sela-Buurlage et al., 1993) or they alternatively can be involved in the production of phytoalexins (e.g. chalcone synthase Nugroho et al., 2002) or redox-reactions like for example oxalate oxidases (Lane et al., 1991; Lane et al., 1993; Schweizer et al., 1999a) or PR-9 class peroxidases (Altpeter et al., 2005). In the interaction of wheat with powdery mildew, several gene transcripts accumulating upon powdery mildew infection were cloned (WIR genes, Schweizer et al., 1989) and two of them significantly enhanced resistance upon transient overexpression in wheat epidermal cells (Schweizer et al., 1999b). Interestingly, induction of PR gene transcription is commonly observed in both compatible and incompatible interactions, respectively, but upregulation is generally stronger and prolonged in the incompatible case (Kmecl et al., 1995).

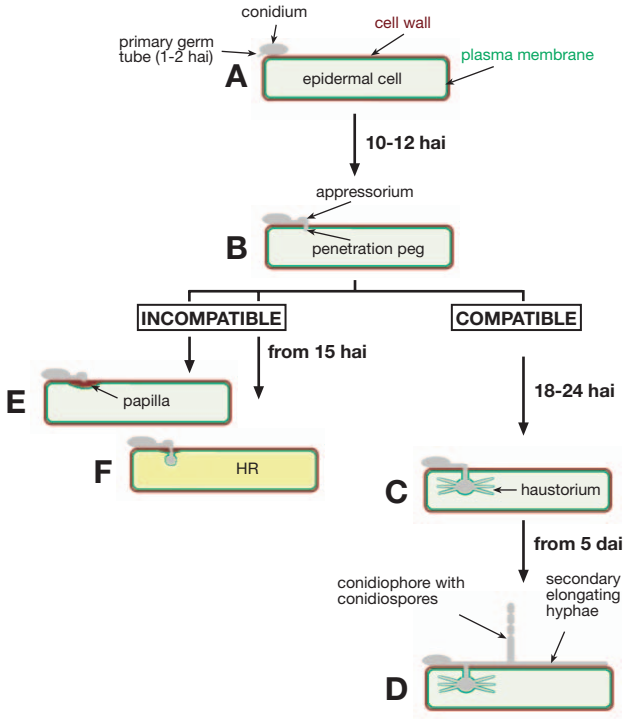

Figure 3.3: Schematic time course of the interaction of powdery mildew and wheat. A) After landing of a conidiospore on the leaf surface, the spore produces a primary germ tube. B) An appressorium is built at the end of a secondary germ tube and the fungus tries to penetrate the plant cell wall. C) After penetration, a haustorial feeding structure is built inside colonized cells. D) The fungal mycelium expands on the leaf surface and formation of new conidiophores is initiated at around 5 to 7 days after infection (dai). Penetration can either be stopped by the formation of papillae (between 10 and 15 hai) (E) or later by the induction of cell death (HR) (F). (Schulze-Lefert and Vogel, 2000, modified).

The plant hypersensitive response

Resistant plants respond to pathogen attack by induction of localized single cell death called the hypersensitive response (HR) which requires the activity of the host transcriptional machinery (Heath, 1998). The hypersensitive cell death of wheat or barley epidermal cells upon fungal attack is accompanied by whole cell autofluorescence under blue light (Figure 3.4). The cellular autofluorescence which is caused by polymerization of phenolic compounds was for a long time known to occur in the consecution of cell death as indicated by the inability of corresponding cells to exhibit plasmolysis (Koga et al., 1988; Carver et al., 1994).

The hypersensitive response is associated with a biphasic oxidative burst. Accumulation of reactive oxygen intermediates (ROI) such as hydrogen peroxide (H_2O_2) or superoxide ($O_2^{\bullet -}$) plays a complex role in plant defense, signaling and induction of cell death which is not entirely understood (reviewed by Lamb and Dixon, 1997; Jabs, 1999; Grant and Loake, 2000). For example, H_2O_2 exhibits direct defensive activity by cross-linking of phenolic compounds and proteins during the formation of plant structural barriers called papillae (Thordal-Christensen et al., 1997). In animals, H_2O_2 triggers apoptosis associated with a decrease in the concentration of $O_2^{\bullet -}$. The induction of HR in plants was actually found to depend on balanced amounts of nitric oxide (NO) and H_2O_2, respectively and is counteracted by high concentrations of $O_2^{\bullet -}$ (Delledonne et al., 2001). There are multiple enzymatic sources for ROI production including peroxidases, NADPH oxidases, amine oxidases and germin-like oxalate oxidases (Mittler et al., 2004). Studies of O_3-induced HR in *Arabidopsis* epidermal cells revealed that generation of H_2O_2 mainly raised from mitochondria in the first peak of the oxidative burst whereas the second peak is dependent on the presence of plasma membrane-bound NADPH oxidase (Joo et al., 2005). The timing of ROI accumulation in the interaction of barley and powdery mildew was found to include three phases (Hückelhoven and Kogel, 2003). The first accumulation of H_2O_2 already occurs during formation of the primary germ tube around 3 hai. The second phase encompasses attempted penetration (compare to Figure 3.3) around 14 hai and accumulation is localized to the emerging papilla and the surrounding cytoplasm.

In incompatible interactions, H_2O_2 accumulation during phase II is stronger and normally is followed by induction of HR and cell death accompanied by the third and strongest accumulation spreading over the whole cell. In contrast, $O_2^{\bullet -}$ only accumulates after successful penetration in the vicinity of haustorial initials around 20 hours after infection (hai) and is thought to counteract induction of cell death (Hückelhoven and Kogel, 2003).

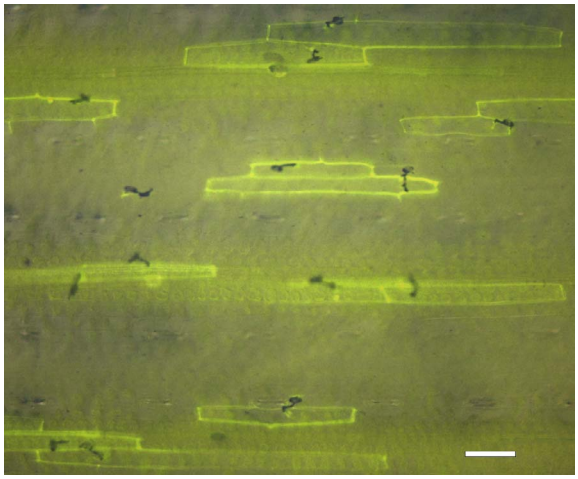

Figure 3.4: HR induction during interaction of wheat cv. Michigan Amber and *Blumeria graminis* f.sp. *tritici* (isolate *BgtAvr1*). Fungal attempts to penetrate wheat epidermal cells cause HR as evidenced by whole cell autofluorescence of corresponding cells. Blue light incident fluorescence microscopy image (excitation filter 450-490 nm; bypass filter 515-565 nm) overlaid on bright field microscopy image. Scale bar = 100 µm.

The decision of a cell between living or dying is viewed to depend on survival signals and death of the cell is the default path. In plants, programmed cell death (PCD) is involved in many aspects of life including formation of tracheary elements or aerenchyma, leaf senescence, megaspore formation and pathogenesis-related PCD.

The plant hormone salicylic acid (SA) may play a dual role in some of the signaling pathways and promotes cell death only at high concentrations whereas low concentrations prevent PCD (Lam, 2004). SA promotes the production of reactive oxygen intermediates (ROI) and similarly SA abundance is regulated by ROI feedback control (León et al., 1995). SA signaling is dependent on functional *pad4* and *eds1* genes encoding triacylglycerol lipases which break down triacylglycerols into fatty acids (Falk et al., 1999; Jirage et al., 1999). This may provide a link to phospholipid signaling. In *Arabidopsis*, phospholipase D activity attenuates activation of cell death probably via alteration of phosphatidic acid levels (Meijer and Munnik, 2003; Zhang et al., 2003). A current model of SA signaling during induction of HR including additional components is shown in Figure 3.5.

During compatible interactions plant cells are sometimes specifically killed by the activity of the pathogens. An important role in this type of cell death appears to be played by the pro-apoptotic sphingolipid ceramide and its phosphorylated derivatives (reviewed by Khurana et al., 2005). Ceramide signaling is also involved in apoptosis in animal systems

(Kolesnick and Fuks, 2003). *Arabidopsis* plants mutated in the *Pseudomonas*-induced *acd5* ceramide kinase accumulate more ceramide and conditionally exhibit apoptosis-like PCD indicating that ceramide-induced PCD may be important in the compatible interaction of *Arabidopsis* and *P. syringae* (Liang et al., 2003).

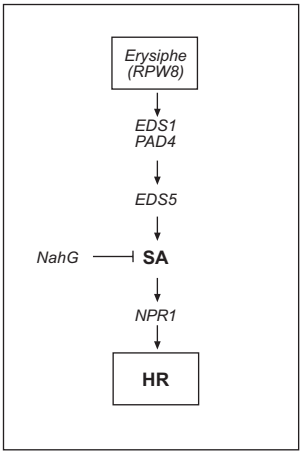

Figure 3.5: Simplified model of SA-induced HR investigated during *RPW8*-related defense in *Arabidopsis*. *RPW8*: Resistance to powdery mildew, unique type of plant disease resistance gene; *EDS1 & EDS5:* Enhanced disease susceptibility, *PAD4*: Phytoalexin deficient, *NahG*: Salicylate hydroxylase metabolizing SA to inactive catechol, plants expressing *NahG* do not accumulate SA. *NPR1*: Non-expressor of PR genes (= *Nim1*). Arrows: Activation, Bars: Inhibition. (Xiao et al., 2005, modified)

HR induced during interaction with *Pseudomonas syringae* morphologically involves formation of apoptotic bodies, mitochondrial swelling and cristae disorganization reminiscent of animal apoptosis (reviewed by Greenberg and Yao, 2004). There is increasing evidence that regulation of pathogenesis-related PCD occurs in an apoptosis-like manner. For example cell death triggered by various stimuli in *Arabidopsis* involves early mitochondrial permeability transition (Yao et al., 2004).

The term apoptosis was introduced by Kerr et al. (1972) to distinguish the PCD involving nuclear condensation and partition of cytoplasm and nucleus into apoptotic bodies from the necrotic type of PCD which is characterized by organelle swelling and membrane rupture. In addition, Clarke (1990) distinguished another form of PCD called autophagic PCD which is characterized by the formation of autophagic vacuoles. Because diverse triggers such as for example heat shock or oxidative stress can induce apoptotic as well as necrotic PCD and many signaling mechanisms are shared, the different types of PCD are presently viewed to represent just extreme cases of a wide range of possible morphological deaths (Kane et al., 1993; Leist and Nicotera, 1997). Whereas low cellular ATP levels appear to favor necrotic cell death, apoptosis requires high ATP levels (Nicotera and Leist, 1997; Tsujimoto, 1997).

Induction of apoptosis has been well studied and involves the activity of specific cysteinyl aspartate-specific proteases called caspases (reviewed by Hengartner, 2000). Two major apoptotic pathways converge at procaspase-3 activation (illustrated in

Figure 3.6). Activation in the death receptor pathways occurs via ligand binding of membrane bound receptors such as CD95 and includes caspase-8 self activation and autocatalytic caspase cascade activity (Martinova, 2003). In the mitochondrial pathway, mitochondria can be targeted by a multitude of stimuli to release pro-apoptotic proteins from the mitochondrial intermembrane space such as cytochrome c, apoptosis inducing factor (AIF), Smac/DIABLO and various procaspases (Ferri and Kroemer, 2001; Bras et al., 2005). Release of cytochrome *c* stimulates the assembly of a protein complex called the apoptosome which activates procaspase-3. Release of pro-apoptotic factors involves mitochondrial membrane permeabilization (MMP) conferred by the formation of a permeability transition pore complex (PTPC) between the adenine nucleotide translocase (ANT) at the inner membrane and the voltage-dependent anion channel (VDAC) at the outer mitochondrial membrane. MMP is under the control of pro- and anti-apoptotic factors of the Bcl-2 protein family (Adams and Cory, 2001). Members of the Bcl-2 family may either modulate cell death induction by forming channels in the outer mitochondrial membrane or by stabilizing or perturbing pre-existing channels like the PTPC. Modulation of VDAC opening has been shown in the case of the pro-apoptotic Bax and tBid or the anti-apoptotic Bcl-x_L (Shimizu et al., 1999; Rostovtseva et al., 2004).

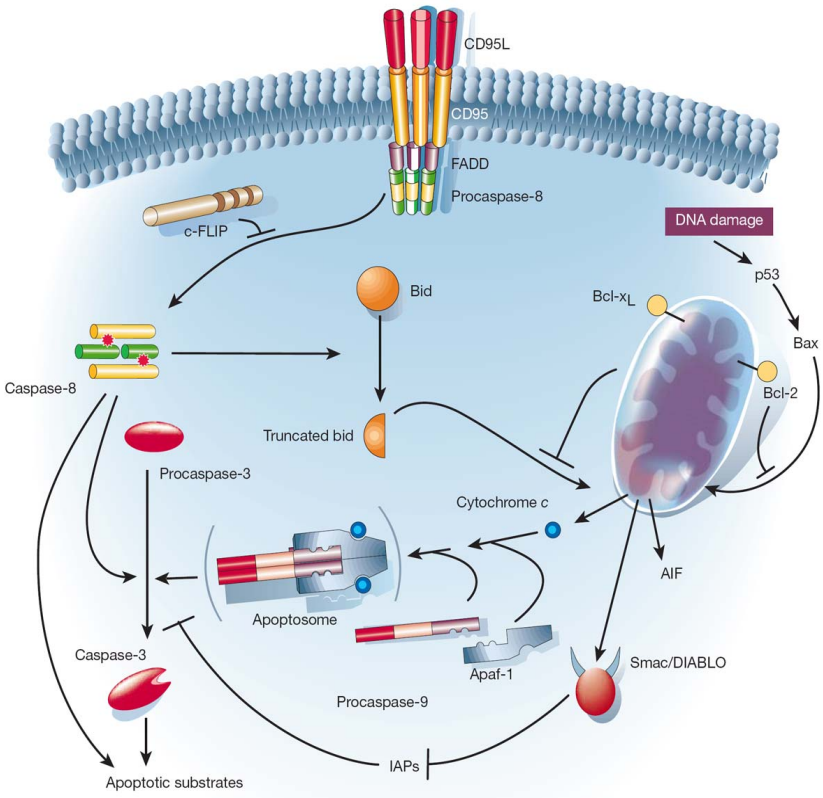

Figure 3.6: Induction of mammalian apoptotic cell death. The death receptor pathway is triggered by members of the death-receptor superfamily (left pathway. The mitochondrial pathway involves mitochondrial membrane permeabilization and control by pro- and anti-apoptotic Bcl-2 family proteins. IAP: inhibitor of apoptosis, AIF: apoptosis inducing factor. Arrows: Activation, Bars: Inhibition. (by Hengartner, 2000).

Activation of caspases results in cleavage of specific targets such as caspase-activated DNase (CAD), nuclear lamins, cytoskeletal proteins or polyADP-ribose polymerase (PARP). Usually, caspase-mediated cleavage results in inactivation of the target proteins but in the case of CAD, caspase-mediated cleavage of the inactive form (ICAD) is required for the enzyme to be activated and to generate the characteristic apoptotic DNA laddering (Liu et al., 1997; Enari et al., 1998).

The existence of similar plant PCD mechanisms is the subject of much debate since no genes orthologous to caspases or Bcl-2 family regulators were found in plants by sequence similarity searches. Still, there is strong evidence for a crucial role played by proteins exhibiting caspase-like protease activity (CLP) and the function of candidates is currently being investigated (reviewed by Woltering et al., 2002; Woltering, 2004; Rotari et al., 2005; Sanmartin et al., 2005). Intriguingly, extracts form plants undergoing cell death exhibit proteolytic activity against various caspase substrates and natural substrates such as PARP are cleaved at caspase cleavage sites by plant proteases. Moreover, application of specific caspase inhibitors suppresses cell death also in plants (Woltering, 2004).

CLP candidates essentially include three groups of plant cysteine proteases which exhibit (Asp)-specific cleavage activity. Plant legumains and metacaspases share structural homology to caspases whereas the subtilisin-like serine proteases are not related to caspases. Legumains (also referred to as vacuolar processing enzymes, VPE) are involved in maturation of proteins in seeds and they are located in vacuoles and protease precursor vesicles (Shimada et al., 2003). A mutation in the *Arabidopsis vpe*γ gene compromises activation of caspase activity and increases susceptibility to infection with incompatible *Pseudomonas syringae* pv. *tomato* (Rojo et al., 2004). Two structurally different classes of metacaspases are found in plants. Whereas type I metacaspases are predicted to be located in mitochondria and chloroplasts, type II metacaspases are thought to be cytosolic (compiled in Sanmartin et al., 2005). Transcription of the two *Arabidopsis* type I metacaspases *AtMCP1b* and *AtMCP1c* is upregulated in response to pathogen infection or treatment with bacterial peptides Flg22 and NPP1 (Sanmartin et al., 2005). Subtilisin-like proteases called saspases are involved in the proteolytic generation of bioactive peptides and are translocated to the apoplast upon initiation of PCD (Coffeen and Wolpert, 2004). Altogether, induced expression of various plant CLPs during PCD indicates that the regulation of caspase activity in plants might be at the transcriptional level whereas regulation of apoptosis in animals is post-transcriptional via proteolytic digestion of inactive precursors (zymogens).

Whether plant mitochondria play similar regulatory roles during apoptosis like in animals is still unclear (Lam et al., 2001; Watanabe and Lam, 2004). An apoptosis-like early

loss of mitochondrial membrane potential ($\Delta\Psi_m$) together with cytochrome *c* release into the cytosol is observed during PCD in *Arabidopsis* protoplasts but the cytochrome *c*-release is not obligatory for the control of PCD (Yao et al., 2004). Intriguingly, despite the absence of mitochondrial permeability regulatory Bcl-2 homologues in plants and yeast, transgenic plants expressing animal or viral anti-apoptotic regulators such as Bcl-2, Bcl-x_L or the baculovirus Op-IAP exhibit resistance to necrotrophic fungal pathogens (Dickman et al., 2001). In addition, heterologous expression of Bax in tobacco triggers HR-like cell death correlating with accumulation of *PR1* transcripts (Lacomme and Cruz, 1999).

The only animal apoptosis regulator that is conserved in plants is the BAX inhibitor-1 (BI-1) which corresponds to a Bcl-2 unrelated protein of 5-7 transmembrane α-helices located in the endoplasmic reticulum (Kawai-Yamada et al., 2001). Overexpression of plant BI-1 suppresses BAX-induced cell death in plants and animals (reviewed by Lam, 2004). During the interaction of barley and powdery mildew, BI-1 is rapidly induced in resistant and delayed in susceptible plants. Transient overexpression of BI-1 enhances susceptibility of barley to powdery mildew and it is thought that BI-1 is a suppressor of PCD (Hückelhoven et al., 2003). Suppression of BI-1 expression in tobacco increased susceptibility to autophagy (organelle recycling by phagocytosis) in response to sucrose starvation (Bolduc and Brisson, 2002). Animal autophagic cell death morphologically differs form apoptosis and possible overlaps of autophagic and apoptotic modes in plant PCD are currently discussed (Lam, 2004).

The genome of *A. thaliana* contains three homologues of the BAX inhibitor-1 (BI-1, BI-2 and BI-3) differing in their N-terminal region. A gene family of 13 genes with similarity to the corresponding region of BI-2 is referred to as *A. thaliana* BI-2-related (ABR) genes and is exclusively found in plants (Lam et al., 2001). The biological function of ABR gene products is unknown and it is speculated that they might be the plant counterparts of Bcl-2-related proteins (Lam, 2004).

Other putative plant specific regulators of PCD include LSD1 (lesions stimulating disease) and MLO (modulator of defense and cell death) which both occur in monocots and dicots and negatively regulate PCD (reviewed Lam, 2004). LSD1 is thought to act downstream of EDS1 and PAD4 and *Arabidopsis lsd1* mutant plants are defective in cell death restriction and exhibit runaway cell death. In barley, mutations of MLO which is thought to act in a Ca^{2+}-dependent manner result in spontaneous cell death of mesophyll cells. In addition, mutant plants show strong papilla-based resistance towards infection with the powdery mildew fungus.

3.2.2. Nonhost and race-specific resistance

Nonhost resistance is based on the fact that, as a basic principle, plants are not compatible with putative pathogens. Since nonhost resistance is very effective and durable, implication of related mechanisms into modern plant breeding is commonly considered to hold great potentials. Nonhost resistance against powdery mildew exhibits a great field of specificity for there are various levels like true or conditional nonhosts (reviewed by Bushnell in Bélanger et al., 2002). Whereas true nonhosts are incompatible with any member of the Erysiphaceae, conditional nonhosts exhibit susceptibility only towards specific powdery mildew species. A special case of conditional nonhosts is the compatibility with only certain formae speciales (f.sp.) of powdery mildew like the one of wheat and the wheat powdery mildew. The present knowledge about nonhost mechanisms increases a lot and it is found that different cases of resistance share common signaling components. In a recent review by H. Thordal-Christensen (2003), the plant-pathogen interaction was illustrated to sequentially rely on different obstacles like (1) signals required for pathogen differentiation, (2) plant pre-formed barriers, (3) plant ancient inducible barriers, (4) nutrient acquisition from the host and (5) avoidance of recognition by multiple sensors capable to induce effective plant defense mechanisms. Failure to overcome one of those obstacles inevitably causes nonhost resistance of the plant.

In the case of powdery mildew, the variability of nonhost levels are reflected by the inability to cope with different barriers. Reduced germination depends on the relation of true nonhosts and is ascribed to inhibitory factors on the leaf surface. In contrast, invasive conidiospores efficiently sporulate and produce appressorial infection structures in the interaction between *Blumeria graminis* f.sp. *hordei* and wheat. Thus, development of powdery mildew incompatible at the *f. sp.* level is mainly hindered at the subsequent stage of hyphal feeding structures whereas conditional and true nonhosts are already highly impaired at the former stage (Johnson et al., 1982; reviewed in Bélanger et al., 2002).

Barriers involved in nonhost resistance can be induced by perception of conserved pathogen-derived molecules, so called PAMPs (pathogen-associated molecular patterns). In mammals, PAMP perception occurs by Leu-rich repeat (LRR) Toll-like receptors that associate with LRR transmembrane kinases mediating ligand-specific signal perception and intracellular signal transduction (Roeder et al., 2004; Rifkin et al., 2005; Takeda and Akira, 2005). Reminiscent of the animal innate immunity systems, perception of the bacterial flagellin protein in *Arabidopsis* involves an (LRR) receptor kinase (FLS2) and leads to the production of reactive oxygen species (ROS) and activation of mitogen-activated protein kinases (MAPK) controlling specific WRKY-domain transcription factors (Gomez-Gomez et

al., 1999; Asai et al., 2002). Similarly, MAPK activity is also required for induction of PR gene transcription by the harpin protein, another PAMP of plant pathogenic bacteria like *Erwinia* and *Pseudomonas* (Lee et al., 2001). Yet, no corresponding plant receptor has been cloned thus far but harpin is forming conducting pores in lipid bilayers and direct interactions with plant proteins via protein binding sites are currently being investigated (Eden Bioscience, 2004; Li et al., 2005a).

The induction of a well studied inducible barrier in barley is related to the *mlo* resistance locus which confers durable papilla-related pre-penetration resistance (Jorgensen, 1992; reviewed by Stein and Somerville, 2002). Interestingly, the resistance is conferred by a recessive mutation in the *Mlo* wild type gene which encodes a 60 kDa protein of a seven-transmembrane protein family, which is exclusively found in higher plants and bryophytes. Its architecture and location in the plasma membrane is reminiscent of animal G-protein-coupled receptors. Little is still known about the biological function of the wild type protein but *Bgh*-induced late mesophyll cell death and spontaneous accelerated leaf senescence in *mlo* plants suggest a role as negative regulator of cell death during pathogen attack and senescence (Piffanelli et al., 2002). mlo resistance is dependent on the presence of the wild type proteins Ror1 and Ror2 (required for mlo-specified resistance ,Freialdenhoven et al., 1996). The latter is a functional homologue of the *Arabidopsis PEN1* gene (penetration1) which encodes a syntaxin and is plays a role in mediating fusion of vesicles at the plasma membrane during attempted invasion by powdery mildew in epidermal cells (Collins et al., 2003; Assaad et al., 2004).

The 5th obstacle in plant-pathogen interaction similarly includes the situation of a single pathogen effector (avirulence factor; Avr) interacting with a single plant sensor (R-protein), resulting in plant defense. Whereas PAMPs generally represent conserved molecules, avirulence factors are present in only certain races of the pathogen. This special case of rejection of the pathogen by the nominal host plant follows a gene for gene concept, for it requires the presence of both, the single avirulence factor and the single R-protein (resistance protein). It is called 'race-specific resistance' (syn. 'vertical resistance'). Host varieties carrying the R-protein exhibit a resistant phenotype towards pathogens carrying the avirulence factor whereas susceptibility occurs when the R-protein is lacking. On the other hand, pathogens lacking the avirulence factor are virulent on both types of hosts. Early studies suggested that *R*-genes encode selective receptors for cognate avr factors. Yet, direct interaction between R-proteins and corresponding Avr-factors have rarely been demonstrated.

The largest class of resistance genes encodes structurally related intracellular NB-LRR proteins containing two to three domains (reviewed by Dangl and Jones, 2001). The intra- or extracellular leucine-rich repeat (LRR) domain mediates protein-protein interactions. A nucleotide-binding domain (NB) is present in R-proteins with intracellular LRR-domain. Some R-proteins additionally contain an N-terminal coiled-coil (CC) domain or a Toll-interleukin-like TIR domain which may be absent in monocots (Madsen et al., 2003). In *Arabidopsis*, signaling of CC-NB-LRR proteins requires the NDR1 protein (non-race-specific disease resistance 1) and is often dependent on *PBS2,* an *Arabidopsis* homologue of the barley *Rar1* gene. Signaling of TIR-NB-LRR proteins is dependent on the EDS1 protein (enhanced disease susceptibility) and often requires PAD4 (phytoalexin-deficient 4) (Bonas and Lahaye, 2002).

In barley, numerous CC-NB-LRR proteins are encoded at the *Mla* (mildew-resistance locus A) locus and confer race-specific resistance to the barley powdery mildew (Jorgensen, 1994; Wei et al., 2002). At present it is speculated that R-proteins generally are present as hetero-multimeric complexes (Shirasu and Schulze-Lefert, 2003). Following the 'guard hypothesis', avirulence factors are thought to be recognized via cofactors resulting in the activation of downstream components mediated by the R-protein Figure 3.7. In *Arabidopsis*, the RIN4 (RPM1-interacting) protein which might regulate basal defense is targeted by AvrB and other avirulence factors and similarly resides in a complex with RPM1 and RPS2, CC-NB-LRR proteins conferring resistance against *Pseudomonas syringae* carrying cognate avirulence factors (Mackey et al., 2002). RIN4 is directly targeted by the *Pseudomonas* AvrRpt2 protease resulting in dissociation of the recognition complex necessary for activation of defense responses by RPS2 (Day et al., 2005).

The small number of about 120 NBS-LRR proteins in *Arabidopsis* contrasts the almost infinite diversity achieved by somatic recombination in the vertebrate immunoglobulin receptor system. This circumstance is assumed to be compensated by their characteristic to keep critical key proteins which are indispensable for colonization by pathogens under strict surveillance (Schulze-Lefert and Bieri, 2005). Downstream signaling for numerous barley Mla but also other resistance proteins like RPS2 or RPM1 depends on the RAR1 (required for Mla12 resistance) and SGT1 (suppressor of G-two allele of skp1) proteins, which physically interact with each other (Schulze-Lefert and Vogel, 2000; Azevedo et al., 2002; Shirasu and Schulze-Lefert, 2003).

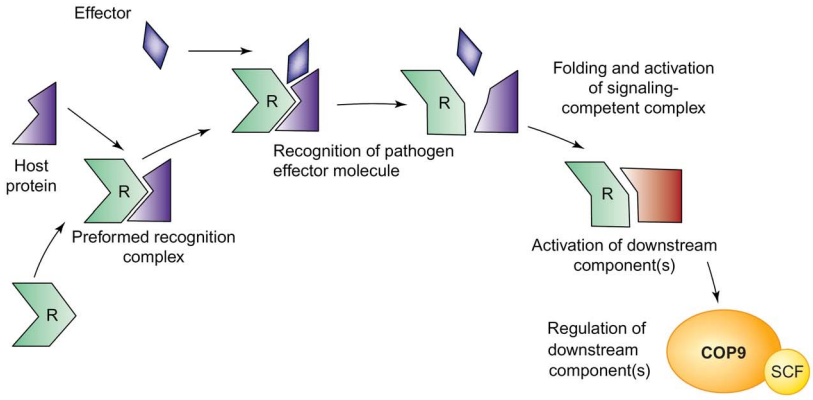

Figure 3.7: Guard hypothesis. R proteins reside in recognition complexes and signaling is achieved only in the presence of additional host proteins like RIN4. (Shirasu and Schulze-Lefert, 2003, modified).

The involvement of SGT1 directly links disease resistance with ubiquitination for SGT1 associates via SKP1 (S-phase kinase-associated protein) with the E3 ubiquitin ligase SCF (SKP1/CULLIN/F-box) which is responsible for the targeting of cell cycle proteins for degradation by ubiquitination in yeast (reviewed by Nishimura and Somerville, 2002). In addition, in *Arabidopsis* SGT1b interacts with the 19S proteasome-like COP9 signalosome which modulates repressor-degradation on Auxin-inducible genes via SCF^{TIR1} (Schwechheimer et al., 2001). Figure 3.8 visualizes a possible model illustrating the complexity by which signals from different resistance genes might be transduced.

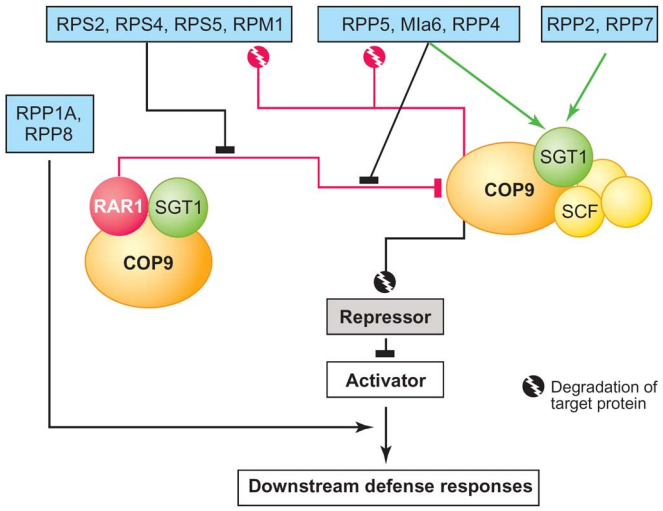

Figure 3.8: Possible signal transduction via RAR1, SGT1 and the COP9 signalosome. Arrows: Positive regulation. Bars: Negative regulation. The activity of defense response repressor(s) (gray box) is controlled by degradation or modification via interaction with COP9 complexes of variable composition. In some instances, degradation of R-proteins in the absence of RAR1 indicates negative feedback regulation of resistance signaling limiting defense response activation. (Nishimura and Somerville, 2002).

The identity of negative regulators of defense targeted by RAR1 and SGT1 is presently unknown but candidates include LSD1, EDR1, BI-1, barley MLO or ROM1 (restoration of Mla12-specified resistance). It was hypothesized that RAR1 and SGT1 alternatively might be required for putative activating elements like MAPK (mitogen-activated protein kinase) cascades, CDPK (calcium-dependent protein kinase) or NADPH oxidase regulators (Nishimura and Somerville, 2002; Shirasu and Schulze-Lefert, 2003).

Recent investigations in barley uncovered interesting overlaps between the classical nonhost and race-specific resistance and revealed that RAR1 and ROM1 are active in both types of resistance. The interaction with the nonhost pathogen *Bgt* was found to strictly being stopped before penetration of host cells but mutations of *Rar1* strongly reduced the percentage of HR-committing cells as compared to wild type plants whereas mutations of *Rom1* lead to hyper-induction of HR (Freialdenhoven et al., 2005).

In wheat, race-specific resistance to *Bgt* is conferred by the *Pm* resistance genes (Zeller et al., 1993; Chen and Chelkowski, 1999; Huang et al., 2004). It was found that a heterologous barley probe of *Mla1* in wheat mapped close to the wheat *Pm3* locus on chromosome 1AS but the two resistance loci were found to be clearly separated by a genetic distance of 0.7 cM (Zhou et al., 2001). *Pm3b* was recently cloned and encodes a CC-NB-LRR protein of a length of 1415 amino acids (Yahiaoui et al., 2004).

Besides, defense not only occurs upon recognition of a pathogen by the plant but also during susceptible interactions. This type of defense reaction is generally referred to as 'background resistance'. It's strength can vary with type and age of different plant cells. The long epidermal cells of barley leaves are five-times less susceptible than short cells (Koga et al., 1990) and in wheat, slim cells located between trichomes were found to exhibit enhanced resistance towards fungal penetration (Schweizer et al., 1999b). Similarly, young cells in newly emerging barley leaves are highly susceptible towards infection with barley powdery mildew whereas older cells only show 10% infection rates (Bélanger et al., 2002, chapt. 1). In general, such differences in susceptible interactions are ascribed to variations of background resistance.

3.2.3. Induced resistance

A different mode of resistance involves pre-induction of defense mechanisms by various stimuli such as attempted infection by incompatible pathogens or chemical treatment. Pre-induced defense mechanisms cause immunization and increase the plant resistance against subsequent infection with virulent pathogens. The mechanism is termed induced resistance (IR). In monocots, induced resistance is restricted to the site of induction and near surrounding area (local acquired resistance; LAR). LAR in cereals was described in barley, wheat and rice (Ouchi et al., 1976; Schweizer et al., 1989).

In dicots, local induction of resistance can trigger a systemic resistance induction in the whole plant and the phenomenon is called systemic acquired resistance (SAR). An efficient protection of the plant conferred by LAR and SAR can last for several days or weeks. SAR has been known for a long time and first studies were published by Ross (Ross,

1961a, b). He showed that systemic induction of resistance against tobacco mosaic virus (TMV), tobacco necrosis virus (TNV) and bacterial plant pathogens is obtained after previous local infection with TMV. Like in some cases of HR, induction of SAR is dependent on the plant hormone salicylic acid (SA) and transgenic plants expressing the salicylate hydroxylase NahG are incapable to induce SAR. However, grafting experiments with wild type and NahG-expressing plants revealed that although required for SAR induction, SA is not responsible for the systemic propagation of resistance. At present the mobile signal required for SAR still lacks identification.

SAR can also be triggered chemically by application of (1,2,3) thiadiazole-7-carbothioic acid S-methyl ester (BTH) and 2,6-dichloroisonicotinic acid (INA). In both cases, SA is not required for the transcriptional upregulation of an SAR-specific set of genes and SAR is also triggered in transgenic *NahG* plants (Ward et al., 1991; Gaffney et al., 1993; Lawton et al., 1996). Signal transduction of biologically and chemically induced SAR is dependent on NPR1 (Cao et al., 1994; Delaney et al., 1995) which also acts downstream of SA signaling upon induction of HR (Figure 3.5).

Chemical treatment of monocots with BTH causes SAR. However, apart from *PR1*, a different set of genes is induced as compared to dicots and the corresponding wheat genes are called WCI (wheat chemically induced Goerlach et al., 1996; Schaffrath et al., 1997; Schweizer et al., 1999c).

3.3. Syringolin

Rice blast is the most important fungal disease in rice which is caused by *Pyricularia oryzae* (telomorph: *Magnaporthe grisea*). Biological control of this disease includes acquired resistance induced by inoculation with the nonhost pathogen *Pseudomonas syringae* pv. *syringae* (Smith and Métraux, 1991). Syringolin is an unusual cyclic tetrapeptide secreted by *P. syringae* and it confers partial resistance against rice blast caused by *P. oryzae* (Wäspi et al., 1998a). Induction of acquired resistance by *Pseudomonas* is not restricted to strains producing syringolin and thus syringolin is one of several determinants by which rice plants are able to recognize the nonhost pathogen. It contains the nonproteinogenic amino acids 5-methyl-4-amino-2-hexenoic acid and 3,4-dehydrolysine bound to two valins which are interconnected via a urea moiety (Figure 3.9).

Six structurally closely related bioactive members designated syringolin A to F are secreted by *Pseudomonas* and the most abundant is syringolin A (sylA, Wäspi et al., 1999). All syringolin variants are synthesized nonribosomally probably by the same nonribosomal peptide synthetase encoded on a single operon (Amrein et al., 2004).

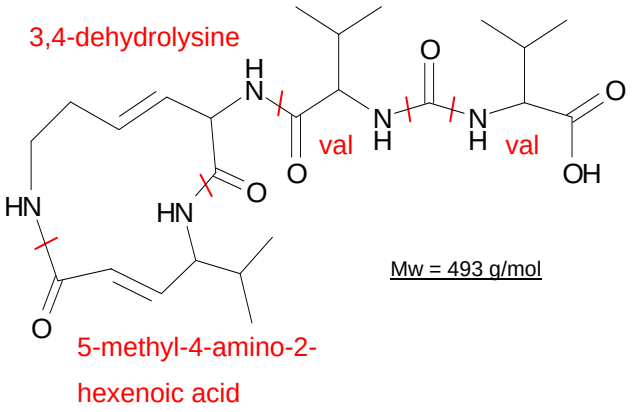

Figure 3.9: Chemical structure of syringolin A (sylA): A 12-membered ring structure consisting of 5-methyl-4-amino-2-hexenoic acid and 3,4-dehydrolysine is connected to two valins. Valins are interconnected via a urea moiety. Red lines delimit amino acids. (Amrein et al., 2004).

Structurally, syringolin is most closely related to the anti-tumor antibiotics glidobactins and cepafungins which contain a related 12-membered ring structure linked to an acetylated L-threonine residue (Oka et al., 1988a; Shoji et al., 1990). Unlike the two antibiotics, syringolin lacks the acyl group which is important for antifungal activity of glidobactins (Oka et al., 1988b).

The biological function of syringolin is subject of ongoing investigations. Its production is controlled by the bacterial *lemA/gacA* two-component regulatory system (Wäspi et al., 1998a). The latter is necessary for pathogenicity of *Pseudomonas* on host plants and also controls the synthesis of the phytotoxin syringomycin probably via the salA regulon (Hrabak and Willis, 1992, 1993; Lu et al., 2005). It is therefore speculated that syringolin might account for virulence in compatible interactions of *Pseudomonas syringa*e pv. *syringae* with appropriate host plants.

SylA treatment of rice leaves induces a very transient accumulation of several common defense-related transcripts and is intimately connected to the accumulation of *Pir7b* (*Pseudomonas* induced rice gene). Monitored by the accumulation of *Pir7b,* perception of syringolin occurs at lowest concentrations of 6.25 nM in cultured rice cells (Wäspi et al., 1998a). *Pir7b* encodes an esterase of the α/β hydrolase fold proteins and accumulation of corresponding transcripts only occurs in response to inoculation with *Pseudomonas* producing syringolin (Reimmann et al., 1995; Wäspi et al., 1998a). Since secretion of syringolin is not a prerequisite for acquired resistance, the induction of *Pir7b* transcription appears not to be directly linked to the activation of the plant defense but

rather might be part of a detoxification reaction. Induction of *Pir7b* transcription in rice requires activity of the protein synthesis machinery and is dependent on dephosphorylation by type 1 and 2A protein phosphatases but not on the activity of serine/threonine or tyrosine protein kinases or Ca^{2+} ion fluxes.

In wheat (*Triticum aestivum* L.), syringolin treatment induces resistance which protects the plant from subsequent infection with virulent isolates of *Blumeria graminis* f.sp. *tritici* (Wäspi et al., 2001). Disease symptoms are drastically reduced to about 15 % when plants are pre-treated with a 40 µM solution of sylA. As monitored by two-dimensional SDS PAGE analysis of in vitro translation reactions, the induction of resistance is associated with the accumulation of numerous transcripts of unknown function. One of the products is cross-hybridizing with an antibody raised against the rice Pir7b esterase, indicating that like rice, wheat responds to sylA treatment with the induction of the specific marker gene. In sharp contrast to the response of rice, none of multiple defense-related PR genes such as the *WIR* or the *WCI* genes exhibit activation of gene transcription in response to sylA treatment (Wäspi et al., 2001).

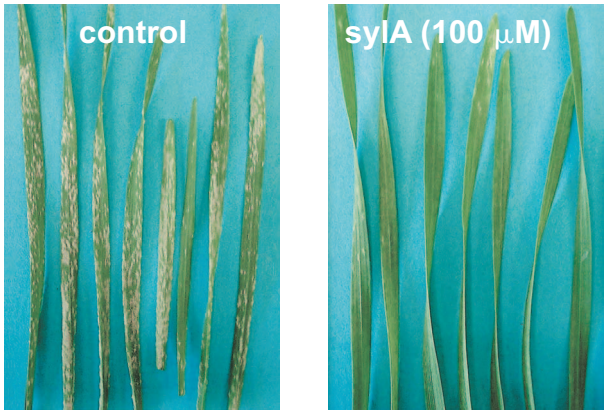

Figure 3.10: Syringolin A treatment of wheat suppresses colonization by *Blumeria graminis* f.sp. *tritici*, the powdery mildew fungus. The images illustrate curative activity of sylA. Leaves were heavily infected with *Bgt* conidiospores and treated with a 100 µM solution of sylA (right) or control solution (left) at 2 days after infection. Pictures were taken 7 days after infection.

Intriguingly, the most efficient protection of wheat from colonization by powdery mildew is obtained when sylA is applied curatively at 2 days after the infection (Figure 3.10). This mode of activity is reminiscent of fungicides such as cyprodinil (Knauf-Beiter et al., 1995). Due to the obligate biotrophy of *Blumeria graminis*, fungicidal activity of sylA can not entirely be excluded by in vitro experiments. Yet, microscopically the situation resembles a race-specific incompatible interaction, where the pathogen is sometimes stopped at later stages of the infection. Likewise, differences in the colonization by the pathogen between control- and sylA-treated plants only become apparent later than 24 hours after the infection (hai) when sylA is sprayed before infection. SylA does not exhibit fungitoxic activity against

numerous fungi tested such as *Pyricularia oryzae*, *Rhodotorula pilimanae*, *Fusarium graminearum* or *Trichoderma viride* (Wäspi et al., 2001). In contrast to treatment with the fungicide cyprodinil, sylA treatment causes autofluorescence indicative for HR in more than 95 % of all infected cells (Figure 3.11). Cell death induction by sylA treatment is correlated with the inability of corresponding cells to undergo plasmolysis. It is exclusively found in infected cells and no autofluorescence occurs in uninfected tissue (Wäspi et al., 2001).

Normally, abundance of transcripts corresponding to PR-genes rapidly increases in response to the infection with virulent and avirulent powdery mildew but the accumulation is much more transient and transcript levels decrease faster in the compatible interaction as compared to incompatible interactions (Kmecl et al., 1995). Interestingly, the sylA-induced HR on infected cells in this nominally compatible interaction is accompanied by a re-induced transcription of PR genes at 2 days after treatment (Wäspi et al., 2001). This re-induction is not observed after treatment with fungicides such as cyprodinil and it only affects a subset of PR gene transcripts including *WIR1* and *WIR2* (Rebmann et al., 1991; Bull et al., 1992).

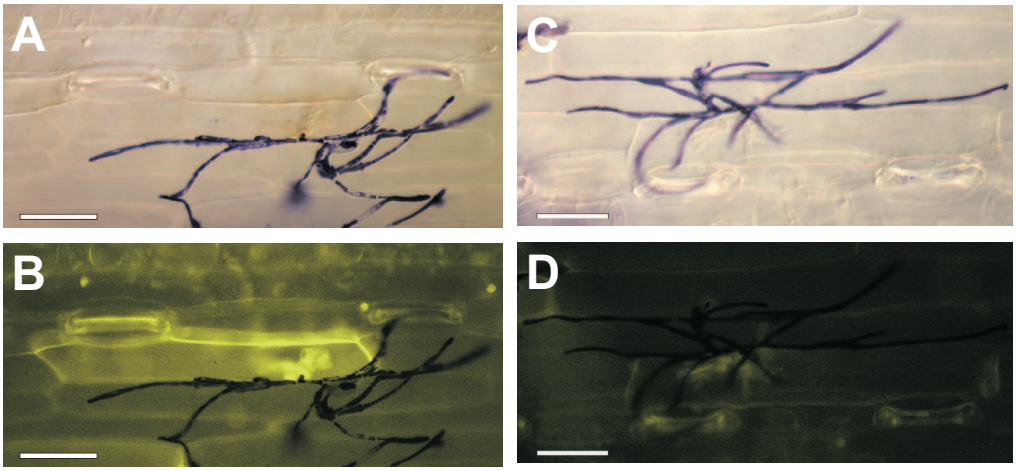

Figure 3.11: Induction of HR by application of 100 µM sylA in powdery mildew-infected wheat. Leaves were infected with wheat powdery mildew and sprayed with 100 µM sylA (A & B) or 888 µM cyprodinil (C & D). Top images: Bright field microscopy, bottom images: Blue light incident fluorescence microscopy (excitation filter 450-490 nm; bypass filter 515-565 nm). Scale bar = 50 µM.

The ability of syringolin to re-induce PR gene transcription is hypothesized to be part of a re-induction of the plant defense which normally is suppressed by the activity of the virulent powdery mildew fungus. The theory of suppression of plant defense by the activity of pathogens such as powdery mildew is based on observations of induced susceptibility for avirulent powdery mildew species after the infection with virulent species. Induced susceptibility of barley coleoptiles for the nonhost pathogen *Erysiphe pisi* following infection

with *Blumeria graminis* f.sp. *hordei* was found by Kuno *et. al.* (1985; 1986). Lingkjaer and Carver (1999) showed that infection of epidermal barley cells by barley powdery mildew lead to increased accessibility to subsequent infections by the same pathogen. The fact that syringolin application alone does not induce accumulation of important PR genes in wheat but similarly triggers HR and transcription of PR gene upon attack with powdery mildew indicates that syringolin might relieve colonized plant cells from suppression of defense reactions (Wäspi et al., 2001).

3.4. Aim of the study

Durability of plant resistance is an important aspect of modern plant breeding and is conferred by nonhost resistance which appears to share common defense signaling components with race-specific resistance (reviewed by Thordal-Christensen, 2003). Plant defense to pathogens consists of a whole repertoire of mechanisms which act synergistically and which are differentially initiated to give rise to the dynamic palette of defense reactions induced against all different kinds of pathogens. The hypersensitive response is involved in many defense reactions and might similarly be involved into plant defense against biotrophic pathogens as well as into virulence of necrotrophic pathogens. Investigation of the HR induced in the course of plant defense is difficult for it constitutes an integral part of the whole defense response.

With respect to this, syringolin was considered to be a helpful tool not only to detect gene induction during induced wheat nonhost resistance but also to similarly identify genes involved in true defense-related HR which might be specifically initiated by sylA treatment of powdery mildew-infected wheat. However, screening for differentially expressed gene products in the allo-hexaploid wheat system (chromosomes 2n = 42, genome size 16 Gb) is highly demanding with respect to sensitivity and resolution for the method due to elevated crosshybridization in a highly complex transcriptome. Subtractive hybridization has been further developed by Diatchenko and coworkers (Diatchenko et al., 1996; Diatchenko et al., 1999) and represents a powerful method to identify differentially expressed genes (Gurskaya et al., 1996). The modified technique termed suppression subtractive hybridization (SSH) perfectly meets the requirements for it is highly sensitive and it exhibits a high resolution.

Our main interest was to identify genes exhibiting transcriptional upregulation before the re-induction of PR gene transcription. Thus, sylA treatment or treatment with control solution was carried out on wheat leaves pre-infected with powdery mildew. Samples were collected at 2, 6, 12, and 24 hours after treatment and subjected to SSH analysis.

Subsequent investigation and characterization of cloned cDNAs by cDNA microarray hybridization experiments was aimed to distinguish genes involved into the general plant response to sylA treatment from genes involved into initiation or succession of the hypersensitive cell death. Two strategies were followed: On the one hand, genes involved in HR were expected to be regulated differently in sylA-treated leaves that had previously been infected as compared to uninfected leaves. Second, microarray analysis was carried out on stripped epidermis and the remainder of the leaf in order to identify genes which are transcriptionally regulated in epidermal tissue, the site of direct fungal interaction.

To address biological functions of relevant genes by studying overexpression or loss of gene function, a transient expression system had been established previously (Schweizer et al., 1999b; Schweizer et al., 2000). Transient gene silencing by induction of RNA interference (RNAi) was intended to test genes of interest for their functional involvement into the initiation and succession of the plant hypersensitive response.

4. Results

4.1. Identification of sylA-induced genes and isolation of corresponding cDNAs

4.1.1. Experimental setup

Seven-day-old seedlings of winter wheat (*Triticum aestivum cv.* Fidel) were infected at high spore density on the primary leaf with a highly virulent Swiss field isolate of wheat powdery mildew *(Blumeria graminis* f.sp. *tritici)*. Forty-eight hours after infection, the plants were sprayed with a 100 µM solution of syringolin A (referred to as sylA or syringolin for simplicity) or a control solution. Plant material was harvested 2 h, 6 h, 12 h, and 24 h after syringolin treatment. Total RNA was extracted and two pools representing two time points each were created by combining the respective total RNA at a ratio of 1:1 (w/w): Early time point α (2 h and 6 h) and late time point β (12 h and 24 h). The procedure is illustrated in Figure 4.1.

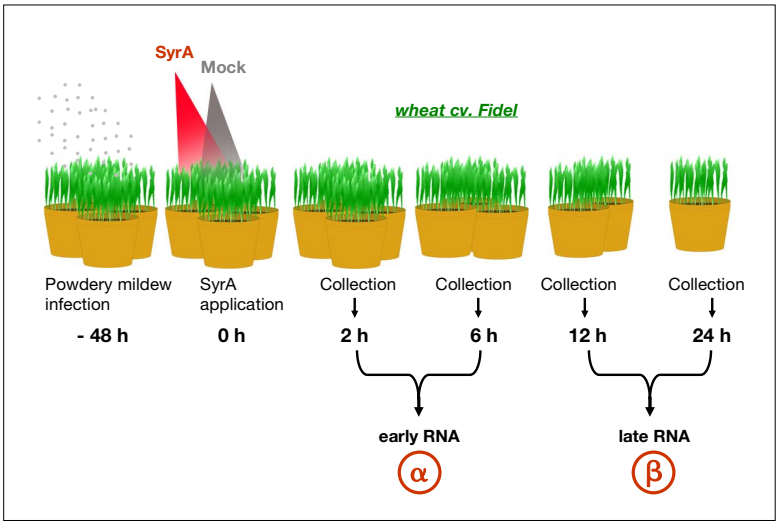

Figure 4.1: Illustration of experimental setup for suppression subtractive hybridization. Powdery mildew infection occurred at minus 48 h. Total RNA was extracted from leaves collected at four different time points. Starting material for SSH was obtained by combining total RNA derived from the two earlier and the two later time points at a ratio of 1:1 (w/w).

4.1.2. Subtraction

Suppression subtractive hybridization (Diatchenko et al., 1999) was carried out at the early (α) and the late (β) time point. In order to get information also on syringolin-induced downregulation of specific genes, the realization of reverse subtraction was taken into consideration. Whereas control treatment-derived cDNA is subtracted off the syringolin treatment-derived cDNA in the forward subtraction, the reciprocal arrangement is applied in the reverse subtraction. The former should result in an enrichment of syringolin-induced

upregulated transcripts, while the latter should result in the enrichment of syringolin-mediated downregulated transcripts. However, significant increases of fungal biomass in the control samples as compared to interrupted fungal development in the syringolin-treated test sample had to be taken into account. Thus, owing to substantial differences of fungal tissue in the two samples, a great number of cDNA fragments corresponding to the whole fungal transcriptome were supposed to strongly prevent substantial enrichment of syringolin downregulated wheat transcripts. Anyhow, availability of reverse subtracted cDNA was reported to be highly beneficial for downstream analysis of subtraction products (Diatchenko et al., 1999). Therefore, both forward and reverse subtraction were carried out for each of the two time points. The whole subtraction process is schematically illustrated (Figure 4.2).

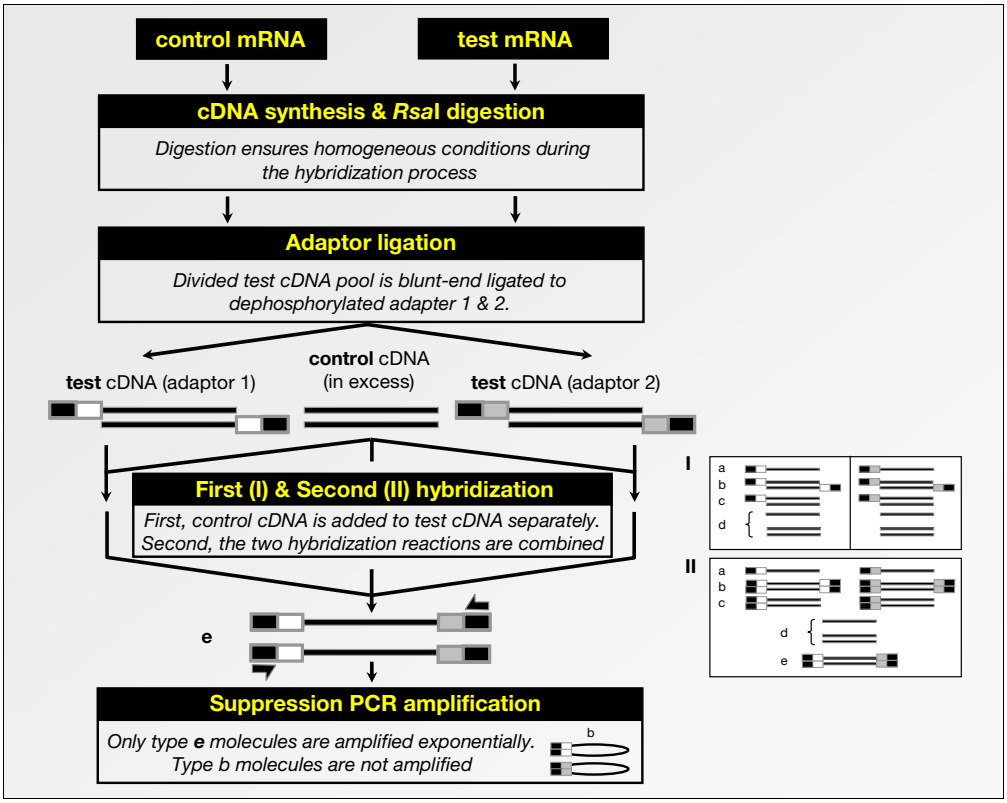

Figure 4.2: Schematic overview illustrating the suppression subtractive hybridization technique. Preceded by heat denaturation, hybridizations are carried out at permanent high temperature of 68°C. Hybridizations I and II are carried out sequentially. Control cDNA is added in excess to the separated test cDNA pools. Resulting types of DNA hybrids are shown for the first hybridization (Box I, left and right panel) and for the second hybridization (after fill in reaction of the ends; box II). The following cDNA hybrids are created during the first and second hybridization: d: No adapter sequences (no PCR amplification). a and c: Only one adapter (only linear PCR amplification). b: Two identical adapters (no PCR amplification due to PCR suppression). e: Two different adapter sequences (exponential amplification). (Diatchenko et al., 1999, modified).

Starting with poly(A)$^+$ RNA, double-stranded cDNA was synthesized by reverse transcription and subsequent second strand cDNA synthesis. The cDNA was then cut into smaller pieces by *Rsa*I digestion. Next, the cDNA pool containing DNA fragments of interest (referred to as test cDNA) was divided into two portions and ligated to two different types of DNA adapters. Following heat denaturation, template DNA for subsequent PCR amplification was enriched for upregulated genes owing to complex hybridization kinetics during two hybridization reactions. Finally, enriched DNA fragments were subjected to PCR amplification resulting in exponential amplification of genes of interest (type e hybrids, Figure 4.2). For further investigation, the amplified cDNA pool was subcloned into a standard cloning vector and transformed into *E. coli*.

In principle, the procedure rests on two core features. First, DNA fragments carrying different adapters are selectively amplified in the final PCR reactions. This event is based on a PCR suppression effect acting on DNA fragments carrying identical adapters on both ends. Owing to the high affinity of complementary ends, amplification of the latter is strongly suppressed due to formation of stable fold back loops of corresponding single stranded molecules (Figure 4.2). Second, adaptor-linked cDNA fragments corresponding to constitutively expressed genes are neutralized for subsequent amplification by preferential pairing with excess control cDNA lacking DNA adapters in the first hybridization. Thus, formation of asymmetrically flanked template DNA in the second hybridization is highly favored for DNA sequences present in elevated copy number in the test cDNA pool. In addition, second order kinetics of hybridization favors neutralization of cDNA fragments corresponding to high copy transcripts as compared to low copy transcripts. Thus, preferential formation of asymmetrically flanked template DNA is accompanied by an equalization effect balancing relative abundance of high and low copy differentially expressed genes (Diatchenko et al., 1999).

4.1.3. Subtraction efficiency

Reflected by the degree of removal of constitutively expressed 'housekeeping' genes, subtraction efficiency can be monitored by semi-quantitative PCR using gene specific primers on the subtracted cDNA pool. One of the standard housekeeping genes is glyceraldehyde-3-phosphate dehydrogenase (G3PDH) and its transcript levels are commonly used as reference insensitive to a variety of treatments and conditions (von Stein et al., 1997; Zierold et al., 2005).

Surprisingly, indicative for low subtraction efficiency, corresponding cDNAs were still found to be present in high numbers after subtraction. This was reflected by the appearance of a specific band after 18 cycles of PCR using wheat G3PDH specific primers on the

forward subtracted DNA pool of the β-subtraction (Figure 4.3A). Conversely, efficient removal of corresponding cDNAs was observed in the reverse subtracted pool (a faint signal was detected only after 33 cycles of PCR. (Semi-quantitative PCR using G3PDH specific primers was carried out only in the β-subtraction but not in the α-subtraction.)

Alternatively, efficiency of the subtraction procedure was also tested by the use of wheat α-tubulin specific primers. Reflected by the complete absence of PCR product in the forward subtraction, SSH resulted in a clear drop in the abundance of the corresponding PCR fragments as compared to the unsubtracted sample (Figure 4.3B). The same situation was found when tested with the α-subtraction and equal reduction of α-tubulin was observed in the reverse-subtracted samples (data not shown).

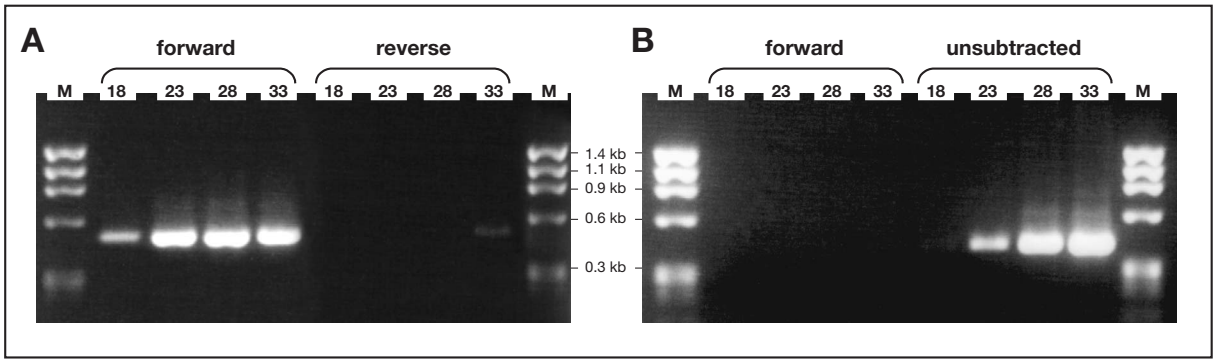

Figure 4.3: Monitoring subtraction efficiency by semi-quantitative PCR in the β-subtraction. PCR using gene specific primers was carried out on equally concentrated diluted secondary PCR of the forward and reverse subtraction or on diluted secondary PCR of unsubtracted DNA fragments derived from an unhybridized mixture of test cDNA carrying both adapters respectively (panel B). 5 µl aliquots were removed from the PCR after 18, 23, 28 and 33 cycles and analyzed on a 2 % agarose gel. M: 250 ng ϕX174 DNA/*Hae*III (fragment sizes are given aside). Panel A: Semi-quantitative PCR using wheat glyceraldehyde-3-phosphate dehydrogenase specific primers. Panel B: Semi-quantitative PCR using wheat α-tubulin specific primers.

Successful removal of putative housekeeping genes by SSH in both the α- and β-subtraction was demonstrated by semi-quantitative PCR using wheat α-tubulin specific primers. The failure of reduction of fragments corresponding to G3PDH in the β-subtraction was interpreted to indicate elevated transcript levels in syringolin-treated samples.

To monitor SSH-mediated cDNA enrichment of upregulated gene transcripts by semi-quantitative PCR, knowledge of specific DNA sequence information of respective transcripts is required for primer design. As shown earlier by immunological methods, the only known protein accumulating in response to syringolin treatment was a wheat homologue of the rice Pir7b esterase (Wäspi et al., 2001). However, no sequence information on the *Pir7b* wheat homolog was obtained by searching DNA databases with the rice sequence using blastn and tblastx algorithms. Chances of successfully designing

wheat specific primers based on the rice Pir7b DNA sequence were considered to be low since no crosshybridization of radioactively labeled rice probes of *Pir7b* was observed on northern-blots of RNA derived from syringolin treated wheat seedlings (U. Wäspi, personal communication).

In addition, none of the PR genes reported to be re-induced upon sylA treatment of powdery mildew-infected wheat was shown to be upregulated within the first 24 h after syringolin treatment (Wäspi et al., 2001). Indeed, when tested with *WIR2*-specific DNA primers in the β-subtraction, corresponding fragments were effectively subtracted off in the forward and reverse subtraction (data not shown).

In summary, the removal of α-tubulin from the forward and the reverse β-subtraction lead to the conclusion that transcription levels of α-tubulin remained unaffected by syringolin application. Furthermore, suppression subtractive hybridization was demonstrated to effectively remove cDNA fragments corresponding to undifferentially expressed genes from the subtracted pool.

4.1.4. Subtraction products

PCR fragments from the α- and β-screen were subcloned into standard cloning vector pCRII-TOPO (Invitrogen BV, Groningen, The Netherlands) carrying the *LacZα* gene and transformed into *E. coli* strain TOP10F' (Invitrogen BV, Groningen, The Netherlands) suitable for IPTG/X-Gal-dependent blue-white color selection of transformants. Following induction of *LacZα* transcription, 3 different types of colonies could be distinguished: White, dark blue and light blue colonies, the latter frequently showing a blue stained centre surrounded by white bacterial zone. Light blue coloration was considered to result from in-frame insertions of DNA fragments smaller than 500 bp. Therefore they were also used for liquid culture amplification together with white colonies. In contrast, dark blue colonies were not selected.

Six 96-well plates of liquid cultures were inoculated with 564 colonies of transformed *E. coli* (12 cultures were reserved for negative hybridization controls). 50 % of all cultures were derived from the α-screen and 50 % from the β-screen. In total, 22 % corresponded to light blue colonies whereas the rest was found to remain white upon blue-white color selection. Inserted DNA fragments were successfully amplified from 1 µl of liquid culture using SSH-derived universal primers and one prolonged denaturation step at the beginning of the cycling.

Representative results are shown in Figure 4.4. Sizes of subcloned PCR products were estimated by agarose gel electrophoresis and ranged from 50 bp to 3.0 kb (550 bp on average). Average sizes of fragments corresponding to light blue and white colonies were found to be equal. The proportion of cultures giving rise to a single PCR band was found to be 85 %. 12 % were not resulting in any PCR product whereas 3 % showed more than one band on the agarose gel. In total, 498 PCR fragments of variable size (including the multiple banded ones) were successfully amplified from all 564 colonies tested and they were subjected to further analysis.

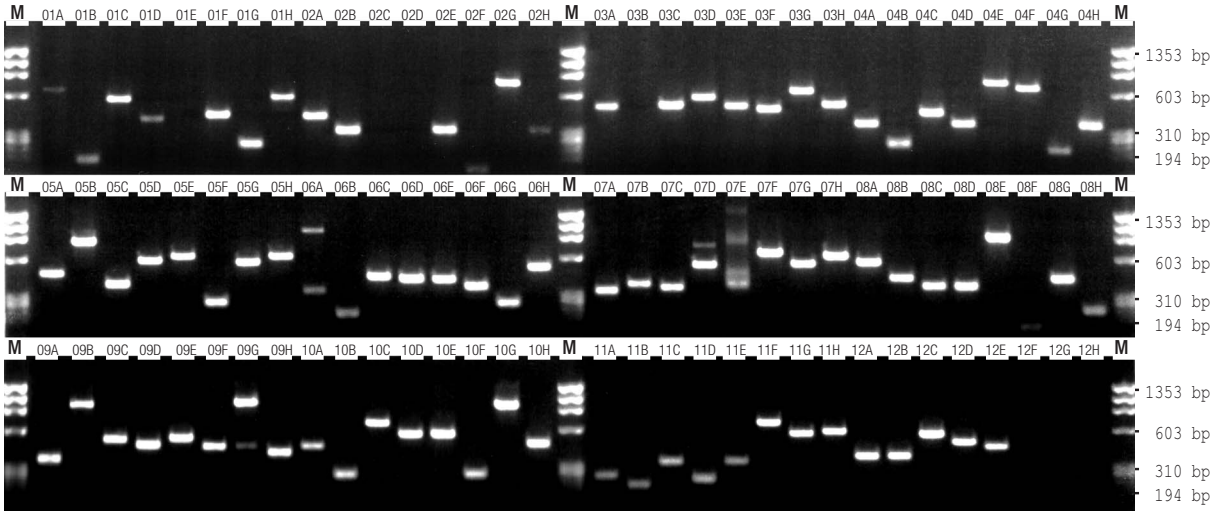

Figure 4.4: Liquid culture PCR. 5 µl of PCR was analyzed on 2 % (w/v) agarose gels and fragment sizes were estimated by comparison to a DNA size marker. M: 0.25 µg of DNA standard ϕX174/*Hae*III (fragment sizes are given at the right). Index 01A to 12H denotes fragment positions in the corresponding 96-well plate: 01 to 12 (column number) and A to H: (row index). The gel corresponding to the third 96-well plate containing clones derived from the β-screen (β3) is shown.

4.1.5. Differential display

In order to assess to what extent the clones represented syringolin-induced transcripts, dot blots were prepared. Groups of 94 PCR products were dot-blotted onto nylon membranes and hybridized to defined amounts of [α-32P]dCTP-labeled probes of equalized radiation levels. Every group was arrayed four times. Hybridization cDNA probes were originating from poly(A)$^+$ RNA previously used for subtraction. Duplicate arrays were hybridized to labeled double-stranded cDNA derived from syringolin-treated test samples or control-treated samples. In addition, remaining duplicate arrays were hybridized to radioactively labeled, forward- and reverse-subtracted cDNA probes in order to achieve enhanced display sensitivity (as proposed by Diatchenko et al., 1999). Representative results are shown in Figure 4.5.

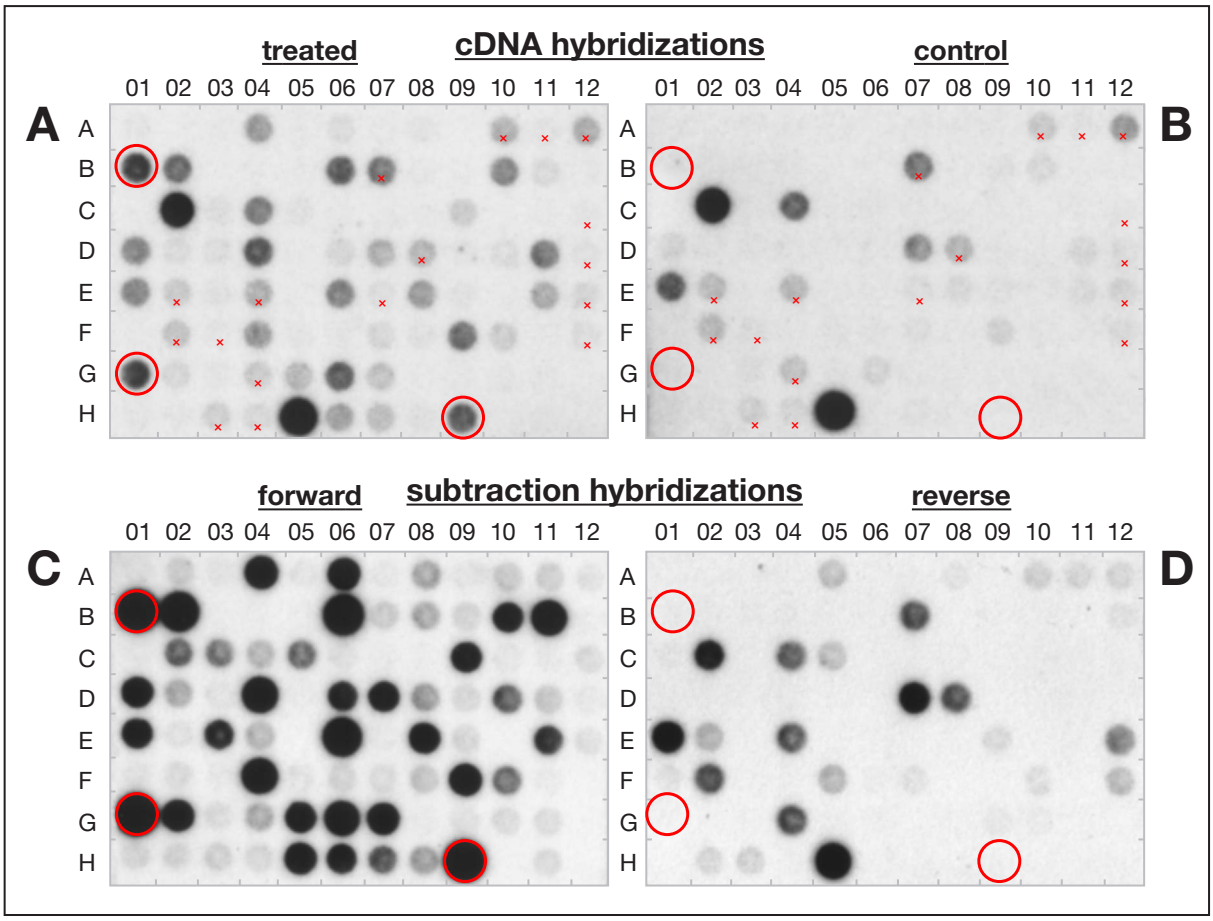

Figure 4.5: Dot blot investigation of differential expression. Duplicate membranes dot-blotted with PCR fragments representing plate one of the β-screen are shown. Membranes were hybridized to different probes of the corresponding time point as follows: (A) test cDNA probe derived from syringolin treated *Bgt*-infected plants. (B) control cDNA probe. (C) forward subtracted probe. (D) reverse subtracted probe. Dots representing DNA fragments corresponding to a wheat homologue of the *Pseudomonas* inducible rice gene *pir7b* are highlighted by red circles. Dots exhibiting equal signals upon hybridization to cDNA probes are marked by an 'x'. Dots G12 and H12: Negative hybridization control. Exposure times to Kodak Biomax MS X-ray films (Kodak, New Haven, USA) were as follows: A and B: 7 d, C and D: 60 h.

While some spots exhibited equal signal strength with both the treatment and the control probe (spots marked with 'x' on Figure 4.5A and B), many showed stronger signals with the treatment probe (e.g. B01 and B02, Figure 4.5A and B). Upon visual inspection of the signals corresponding to the enriched cDNA fragments, data acquisition was accomplished by classifying signal intensities into 5 different classes (illustrated in the Appendix; Table 8.1, p.191).

Upregulation was considered to be indicated when test and control signals were clearly differing in cDNA hybridizations or in the subtraction hybridizations. By this means, 307 out of 498 cDNA fragments were pre-selected as likely representing syringolin-induced genes in a first pass. Corresponding fragments were sequenced. An overview of the whole differential screening process is shown later in Figure 4.6.

Subtraction-derived DNA fragments were named according to their origin and position on storage plates. Only 15 % of sequences carried a poly(A)-tail, indicating that fragments were derived from the entire transcript length. Subsequently, sequence comparison to entries in public DNA databases using blastn (bn), blastx (bx) and tblastx (tbx) search algorithms (Karlin and Altschul, 1990, 1993) resulted in the annotation of 76 % of the candidate sequences. For the remaining 24 %, homology was insignificant.

Low-pass alignment (min. overlap = 20 bp; min. match percentage = 75 %) of the 307 cDNA sequences lead to the assembly of 147 cDNAs into 41 similarity groups (SG) consisting of up to 14 fragments. Examples are listed in Table 4.1 and the complete list is given in the Appendix (Table 8.2).

Table 4.1: Three examples of similarity groups identified by phrap assembly. SG numbers are given on the left of each group. Annotations derived from blast comparisons are indicated. Contigs are separated by horizontal lines. Hybridization classes obtained by reverse northern dot blot hybridization are given in the following order: Forward subtracted probe (fwd), reverse subtracted probe (rev), probe corresponding to syringolin treatment-derived cDNA (syr) and probe corresponding to control cDNA (cont). Sequenced fragment lengths are listed in the last column.

17

frag-ment	signal with probes				seq. length (bp)
	fwd	rev	syr	cont	
ABI-interacting protein					
β2A06	+++	-	+	-	481
β2C08	+++	-	+	-	481
β2G08	+++	-	+	-	799
β3H06	+++	-	+	-	481

03

frag-ment	signal with probes				seq. length (bp)
	fwd	rev	syr	cont	
cytochrome P450					
α1D09	+++	-	+	-	459
α2B01	++	-	(+)	-	459
α1F06	+++	-	(+)	-	327
β1G02	++	-	(+)	-	541

06

frag-ment	signal with probes				seq. length (bp)
	fwd	rev	syr	cont	
enolase (phosphoglycerate dehydratase)					
α2A04	+++	-	+	-	282
α3D01	+++	(+)	+	-	283
α3H09	+++	(+)	+	-	283
β1B02	+++	-	+	-	283
β1E06	+++	-	+	-	283
β2F02	+++	(+)	++	(+)	474
β1H01	(+)	-	(+)	-	270
β2A09	+++	+	++	+	442
β2F11	+++	-	++	-	283

Upon high-pass alignment (min. percentage overlap = 100 bp; min. match percentage = 98 %) similarity groups were subdivided into multiple contigs corresponding to single putative isoenzymes (separated by grey horizontal lines; Table 4.1, SG_03 and 06). By this means, sequences of variable length were assigned to different contigs. (e. g. SG_03). Occasionally, longer fragments were found to contain internal *Rsa*I restriction sites, thus indicating that restriction digestion of the cDNA during subtraction was only partial (SG_17, *β2G08*; SG_06, *β2F02 and β2A09*). As obvious from Table 4.1, comparison of dot

blot hybridization-derived signal information within members of contigs revealed high consistency of the expression data, even between fragments dotted onto different membranes. Subdivision of SGs by high-pass alignment resulted in separation of fragments exhibiting very high similarity (e. g. 100 % sequence identity between *α1D09* and *α2B01*) from sequences with less overall similarity (e. g. 93.5 % sequence identity between *α1D09* and *β1G02*; Table 4.1, SG_03). Still, crosshybridization between members of different contigs was expected to be high because of high local sequence similarities (e. g. 98.1 % sequence identity on 213 bp between *α1D09* and *β1G02*; SG_03).

In a second pass, the 307 pre-selected cDNA fragments were reappraised by integrating data derived from blast analysis, sequence assembly and expression analysis. Based on blast results, numerous fragments were found to exhibit identical putative functions (irrespective of sequence assembly data). Corresponding groups (referred to as functional groups) contained genes present as single copy but also one or multiple similarity groups (data not shown). Again, cDNA fragments were selected for further experiments upon indication for upregulation in either the cDNA hybridizations or the subtraction hybridizations. Similarity groups were represented by only one fragment except if overall sequence comparisons revealed similarities of less than 90 % or if expression data differed significantly. Single copy sequences assigned to functional groups were only selected when upregulation was clearly indicated by cDNA hybridization results. The whole process is illustrated in Figure 4.6.

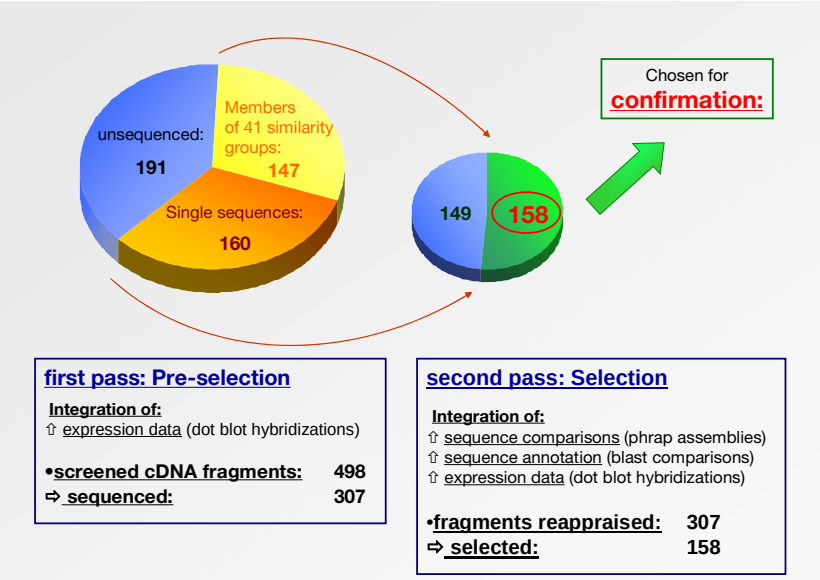

Figure 4.6: Two-pass minimization of redundancy by data integration. 307 cDNA fragments were selected for sequencing in the first pass. Second pass selection by integrating a multitude of information further reduced the number of fragments to 158. Corresponding cDNA fragments were subjected to confirmation by further experiments.

Integration of expression and sequence data scaled down the number of candidate DNA fragments corresponding to induced genes by about 50 % from 307 to 158. The number of fragments assigned to similarity groups was reduced from 147 to 46 and the number of single copy sequences decreased from 160 to 112. Sequences corresponding to the selected cDNA fragments were submitted to the European Bioinformatics Institute (EBI) and can be downloaded (www.ebi.ac.uk/cgi-bin/expasyfetch). A complete list of the 158 cDNAs is presented in Table 4.2.

Table 4.2: List of SSH-derived DNA fragments. cDNA fragments are alphabetically ordered. Annotations are listed in column 2 (updated 2005). Corresponding E-values are given in column 3). Column 4: Accession number. Classified signals derived from hybridizations to forward subtracted (fwd), reverse subtracted (rev), syringolin-treated tissue derived (sylA) and control solution-treated tissue derived (cont) cDNA are shown (columns 5 to 8). PCR fragment sizes (primers *NstPrm1* and *2*) and sequenced fragment lengths are listed in columns 9 and 10 ('m' indicates multiple bands observed by PCR). Checkmarks indicate complete sequencing. Similarity group numbers are listed in column 11. [(1)] Fragments exhibiting clear upregulation upon cDNA hybridizations and subtraction hybridization were marked.

fragment	putative function	E-val	acc. #	signal with probes				PCR	SEQ		SG
				fwd	rev	sylA	contr				
1	2	3	4	5	6	7	8	9	10	11	
α1A03[(1)]	unknown	1.00E-158	AJ888591	+++	-	+		600	**571**	✓	
α1A05	unknown	4.00E-55	AJ888592	+	-	(+)	-	700	**639**		
α1A07	epoxide hydrolase	5.00E-20	AJ888593	++	(+)	-	-	250	**208**	✓	
α1A10[(1)]	polyubiquitin	3.00E-63	AJ888594	+++	++	++	+	500	**480**	✓	**35**
α1A12	DnaJ-1	2.00E-33	AJ888595	+	-	(+)	(+)	300	**300**	✓	
α1B01[(1)]	hsp 23.5	1.00E-133	AJ874072	+++	-	+	-	300	**252**	✓	**01**
α1B08[(1)]	BCS1-like protein / AAA-type ATPase-like protein	1.00E-130	AJ874073	++	(+)	+	(+)	350	**340**	✓	
α1B11	ABA insensitive ABI (protein phosphatase 2C)	8.00E-20	AJ888596	(+)	(+)	-	-	300	**284**	✓	
α1C01	unknown	2.00E-20	AJ888597	++	++	+	(+)	250	**280**		**33**
α1C04[(1)]	cytochrome P450	1.00E-78	AJ888598	+++	+	+	-	750	**794**		**22**
α1C08[(1)]	sucrose synthase 1	2.00E-61	AJ888599	++	(+)	+	-	450	**402**	✓	
α1C12[(1)]	fructose-bisphosphate aldolase	1.00E-141	AJ888600	+++	-	+	-	300	**262**	✓	**02**
α1D03[(1)]	no significant hit	1.00E-03	AJ888601	++	+	+	-	300	**262**	✓	**40**
α1D06[(1)]	alcohol dehydrogenase ADH1	1.00E-131	AJ888602	+++	-	+	-	300	**257**	✓	**14**
α1D08	unknown	8.00E-06	AJ888603	+++	-	+	(+)	200	**198**	✓	**26**
α1D09[(1)]	cytochrome P450	3.00E-67	AJ888604	+++	-	+	-	480	**459**	✓	**03**
α1D10	ferredoxin-dependent glutamate synthase	4.00E-60	AJ888605	+++	+	++	+	m	**334**	✓	
α1E06[(1)]	alternative oxidase	4.00E-87	AJ874074	+++	-	(+)	-	250	**198**	✓	**36**
α1E07[(1)]	hsp 60	5.00E-49	AJ888606	+++	(+)	+	-	350	**337**	✓	
α1E08	NBS-LRR disease resistance protein	3.00E-49	AJ874075	+	-	-	-	900	**630**		
α1E09[(1)]	BRI1-KD interacting protein 130	2.00E-76	AJ888607	++	-	+	-	550	**493**	✓	**31**
α1E11	lysyl-tRNA synthetase	0.00E+00	AJ888608	+++	(+)	-	-	800	**631**		
α1F05[(1)]	unknown	6.00E-97	AJ888609	+++	+	(+)	-	300	**251**	✓	**02**
α1H02[(1)]	hsp 23.6	1.00E-143	AJ874076	+++	(+)	++	-	400	**380**	✓	**32**
α1H06	unknown	3.00E-84	AJ888610	+	-	(+)	-	300	**291**	✓	
α2A03	unknown	2.00E-20	AJ888611	++	+	(+)	-	m	**207**		
α2A05	alcohol dehydrogenase ADH1	1.00E-163	AJ888612	++	-	(+)	-	400	**384**	✓	**39**
α2A06[(1)]	MRP-like ABC transporter	1.00E-161	AJ888613	++	-	+	-	1500	**686**		
α2B04	ligand-gated ion channel 2.8	5.00E-99	AJ888614	+	(+)	-	-	400	**372**	✓	
α2B11[(1)]	NADH dehydrogenase	1.00E-101	AJ874077	+++	+	(+)	-	1400	**625**		

Table 4.2 (continued)

fragment	putative function	E-val	acc. #	signal with probes				PCR	SEQ		SG
				fwd	rev	sylA	contr				
1	2	3	4	5	6	7	8	9	10	11	
α2C02[1]	NADPH-dependent oxidoreductase	3.00E-99	AJ874078	+++	-	(+)	-	300	**250**	✓	
α2C08	glucosyltransferase	1.00E-12	AJ888615	+	(+)	-	-	100	**87**	✓	
α2C11[1]	26S proteasome regulatory subunit	3.00E-62	AJ888616	+++	(+)	(+)	-	400	**375**	✓	**37**
α2D03	similarity to Ser protease	0.00E+00	AJ888617	++	+	(+)	-	m	**634**		
α2D05	no significant hit	2.20E-01	AJ888618	+	(+)	-	-	200	**201**	✓	
α2D07	Probable 26 proteasome complex subunit DSS1/SEM1 family protein	5.00E-35	AJ888619	+	(+)	+	(+)	350	**335**	✓	
α2D10[1]	alanine aminotransferase 2 (glutamic-pyruvic transaminase 2)	0.00E+00	AJ874079	+++	(+)	+	-	600	**592**	✓	
α2E02[1]	MDR-like ABC transporter	0.00E+00	AJ888620	+++	(+)	(+)	-	450	**438**	✓	
α2E05	enoyl-CoA hydratase	7.00E-33	AJ888621	++	+	-	-	650	**610**	✓	**19**
α2E09[1]	unknown	1.00E-51	AJ888622	++	-	(+)	-	250	**193**	✓	
α2E10	unknown	1.00E-173	AJ888623	(+)	(+)	-	-	350	**319**	✓	
α2E11	transmembrane domain / coiled coil-4 domain	1.00E-117	AJ888624	+	(+)	-	-	700	**664**	✓	
α2F04[1]	unknown	0.00E+00	AJ888625	+++	(+)	+	-	500	**468**	✓	
α2G01[1]	enolase 1 (2-phosphoglycerate dehydratase 1)	8.00E-90	AJ888626	+++	-	+	-	200	**182**	✓	**04**
α2H01	unknown, weekly similar to FMIP (Fms-interacting protein)	2.00E-98	AJ888627	+	-	(+)	-	3000	**807**		
α2H02	d-TDP-glucose dehydratase	1.00E-109	AJ874080	+	-	+	-	700	**634**	✓	
α2H03	ABI3-interacting protein 2	1.00E-88	AJ888628	+++	+	+	-	m	**819**		
α2H04[1]	60S ribosomal protein L30	4.00E-41	AJ888629	+	(+)	+	-	400	**382**	✓	
α2H06[1]	P-type ATPase (CA7 gene for)	5.00E-99	AJ888630	+++	+	(+)	-	1000	**829**		
α3A01	glutathione-S-transferase	1.00E-144	AJ888631	+	(+)	-	-	300	**283**	✓	**05**
α3A03	sucrose synthase 1	2.00E-63	AJ888632	+++	(+)	(+)	(+)	450	**398**	✓	**15**
α3A04	PDR-like ABC transporter	1.00E-88	AJ874081	+	(+)	-	-	200	**177**	✓	
α3A05	hsp70-interacting protein	8.00E-35	AJ888633	++	-	-	-	300	**257**	✓	
α3A08	adenylate kinase	1.00E-50	AJ874082	+	-	(+)	(+)	600	**547**	✓	
α3A11	ABC transporter	3.00E-53	AJ888634	+	(+)	-	-	250	**238**	✓	
α3B02[1]	2-oxoglutarate dehydrogenase (E1 subunit)	2.00E-91	AJ874083	++	(+)	(+)	-	900	**805**		
α3B03[1]	UDP-glucose:salicylic acid glucosyltransferase /:anthocyanin 5-O-glucosyltransferase / IAA-glu synthetase	5.00E-49	AJ888635	+++	(+)	(+)	-	500	**434**	✓	
α3B09[1]	hsp 70	4.00E-42	AJ874084	+++	+	(+)	-	350	**313**	✓	
α3C03[1]	prohibitin	1.00E-114	AJ874085	+++	-	+	-	550	**487**	✓	
α3C05	no significant hit	5.40E-01	AJ888637	+	(+)	-	-	350	**293**	✓	
α3C06	hsp 70	4.00E-36	AJ888638	++	+	+	(+)	300	**259**	✓	**21**
α3C11	Pto kinase interactor 1 (Pti1)	1.00E-160	AJ888639	+	(+)	-	-	400	**351**	✓	
α3D05[1]	MRP-like ABC transporter	1.00E-93	AJ888640	+++	(+)	(+)	-	500	**453**	✓	
α3D11	ABC transporter	1.00E-119	AJ888641	++	+	-	-	550	**518**	✓	
α3E08	(alanine) acetyltransferase	2.00E-82	AJ888642	++	-	(+)	(+)	250	**233**	✓	
α3E09[1]	unknown	1.00E-104	AJ888643	+++	-	(+)	-	300	**298**	✓	
α3F01	unknown	2.00E-54	AJ888644	+	(+)	(+)	(+)	400	**431**		
α3F09[1]	cdc 48 homolog E (Transitional endoplasmic reticulum ATPase E)	0.00E+00	AJ888645	++	(+)	++	(+)	850	**799**		
α3F10	ARG1 protein (Altered Response to Gravity)	1.00E-178	AJ888646	+	(+)	-	-	350	**327**	✓	
α3G10	glutathione S-transferase	9.00E-77	AJ888647	+	(+)	(+)	-	200	**153**	✓	**28**
α3G11	unknown	2.00E-17	AJ888648	++	+	(+)	#N/A	300	**243**	✓	
α3H01[1]	MRP-like ABC transporter	5.00E-96	AJ888649	+++	(+)	+	-	400	**356**	✓	**38**
α3H02	no significant hit	#N/A	AJ888650	+	+	+	-	250	**145**		
β1A06[1]	no significant hit	#N/A	AJ874086	+++	-	(+)	-	280	**224**	✓	**26**
β1A07	nuclear coiled-coil protein	0.00E+00	AJ888651	(+)	-	(+)	-	700	**667**	✓	**27**
β1A08	20S proteasome alpha 4 subunit	4.00E-37	AJ888652	+	(+)	(+)	-	500	**451**		**12**
β1A10	unknown	1.00E-107	AJ888653	+	(+)	+	(+)	350	**300**	✓	

Table 4.2 (continued)

fragment	putative function	E-val	acc. #	signal with probes				PCR	SEQ		SG
				fwd	rev	sylA	contr				
1	2	3	4	5	6	7	8	9	10	11	
β1B01[(1)]	pir7b / salicylic acid-binding protein / Ethylene-induced esterase / Polyneuridine aldehyde esterase	2.00E-67	AJ874087	+++	-	++	-	600	**522**		**11**
β1B08	light repressible receptor protein kinase	5.00E-73	AJ888654	+	-	(+)	-	630	**216**		
β1B10[(1)]	pyruvate kinase	0.00E+00	AJ888655	++	-	++	(+)	1000	**934**	✓	**20**
β1C03	26s proteosome regulatory subunit	1.00E-47	AJ888656	+	-	(+)	-	270	**240**	✓	**18**
β1C09[(1)]	hsp 60	5.00E-35	AJ874088	++	-	+	-	600	**541**	✓	
β1D01[(1)]	succinyl-CoA-ligase beta subunit	3.00E-63	AJ874089	++	-	+	(+)	600	**518**	✓	**25**
β1D02	ubiquitin-associated protein (UBA)	5.00E-18	AJ888657	(+)	-	(+)	-	600	**502**		
β1D03	RTNLB30 (reticulon like)	3.00E-39	AJ888658	-	-	(+)	-	375	**351**	✓	
β1D06[(1)]	cytochrome P450	3.00E-47	AJ888659	++	-	(+)	-	450	**382**	✓	**22**
β1D11[(1)]	temperature stress-induced lipocalin / Apolipoprotein D (APOD)	1.00E-142	AJ888660	(+)	-	++	(+)	450	**411**	✓	
β1D12	ubiquitin conjugating enzyme	9.00E-22	AJ888661	(+)	-	(+)	(+)	300	**261**	✓	**23**
β1E11	succinyl-CoA-ligase beta subunit	5.00E-38	AJ874090	+	-	+	(+)	400	**332**	✓	**16**
β1F04[(1)]	voltage-dependent anion channel 1	2.00E-57	AJ888662	+++	-	+	-	850	**854**	✓	**13**
β1F08	26S proteasome RPN9b subunit	1.00E-163	AJ888663	(+)	-	(+)	-	375	**313**	✓	
β1G05[(1)]	20S proteasome alpha 5 subunit	0.00E+00	AJ874091	++	-	+	-	475	**406**	✓	**30**
β1G10	TipC / VPS13 - like protein	1.00E-148	AJ888664	(+)	-	(+)	-	375	**298**	✓	
β1G11	dynamin protein	0.00E+00	AJ888665	(+)	-	(+)	-	850	**802**	✓	
β1H04	eukaryotic translation initiation factor 6 (EIF-6)	2.00E-67	AJ888666	(+)	-	(+)	(+)	325	**305**	✓	
β1H08	glutathione S-transferase	7.00E-81	AJ874092	+	-	(+)	-	200	**180**	✓	
β1H11	citrate synthase	3.00E-59	AJ874093	(+)	-	(+)	-	-	**600**		
β2A02	autophagy / symbiosis-related microtubule associated protein	3.00E-37	AJ888667	+	-	+	+	270	**244**	✓	
β2A06[(1)]	ABI3-interacting protein 2 (abscisic acid insensitive interacting protein)	0.00E+00	AJ888668	+++	-	+	-	500	**481**	✓	**17**
β2A07[(1)]	pir7b / salicylic acid-binding protein / Ethylene-induced esterase / Polyneuridine aldehyde esterase	3.00E-79	AJ874094	+++	-	++	-	500	**451**	✓	**11**
β2A08	phragmoplastin / dynamin-like protein	2.00E-73	AJ888669	++	-	(+)	(+)	700	**640**	✓	
β2A09[(1)]	enolase 2	2.00E-44	AJ888670	+++	+	++	+	500	**442**	✓	**06**
β2B02	ATP-dependent Clp protease	2.00E-53	AJ888671	++	-	+	(+)	575	**525**	✓	
β2B04[(1)]	pyruvate kinase	4.00E-30	AJ888672	+++	(+)	++	-	600	**576**	✓	**41**
β2B06	sucrose synthase 1	7.00E-40	AJ888673	++	(+)	(+)	-	300	**244**	✓	
β2B07[(1)]	no significant hit	#N/A	AJ888674	+++	-	+	-	350	**273**	✓	**26**
β2C03	calreticulin	1.00E-105	AJ874095	+	-	+	+	550	**515**	✓	
β2C04	unknown	1.00E-149	AJ888675	+	-	(+)	-	600	**404**		
β2C05	PHG1A multispanning membrane protein	0.00E+00	AJ888676	+	-	(+)	(+)	550	**492**	✓	
β2C06	pleiotropic regulator PRL1	0.00E+00	AJ888677	+	(+)	+	(+)	750	**648**	✓	
β2C07	20S proteasome beta 6 subunit	2.00E-29	AJ888678	++	(+)	+	+	650	**612**	✓	**34**
β2C10	sorting nexin 1	9.00E-95	AJ888679	+	-	(+)	(+)	600	**534**	✓	
β2D11	heme oxygenase 1	2.00E-34	AJ888680	(+)	-	(+)	(+)	150	**96**	✓	
β2D12	lecithin-cholesterol acyl transferase	1.00E-156	AJ888681	+	+	(+)	-	750	**893**		
β2E03	no significant hit	#N/A	AJ874096	+	-	-	-	800	**811**		
β2E04	DMI1 (does not make infections) protein	0.00E+00	AJ888682	(+)	-	-	-	700	**700**	✓	
β2E06	valyl tRNA synthetase	3.00E-63	AJ888683	+	-	(+)	-	650	**585**	✓	
β2E10	unknown	2.00E-28	AJ888684	+	-	(+)	-	200	**227**	✓	
β2E11	thioredoxin (F-type)	2.00E-24	AJ888685	++	-	+	(+)	400	**300**	✓	
β2F07[(1)]	aspartate aminotransferase (cytoplasmic)	4.00E-82	AJ888686	++	-	+	(+)	700	**633**	✓	
β2F09[(1)]	unknown	6.00E-49	AJ874097	++	(+)	+	(+)	250	**258**	✓	
β2G04	Cf2/Cf5 disease resistance protein	9.00E-59	AJ888687	+	-	-	-	300	**260**	✓	
β2G09	2,3-bisphosphoglycerate-independent phosphoglycerate mutase	1.00E-90	AJ874098	++	(+)	+	+	650	**552**	✓	

Table 4.2 (continued)

fragment	putative function	E-val	acc. #	signal with probes				PCR	SEQ		SG
				fwd	rev	sylA	contr				
1	2	3	4	5	6	7	8	9	10	11	
β2G10[(1)]	unknown	3.00E-66	AJ888688	++	-	(+)	-	350	**296**	✓	
β2G11[(1)]	20S proteasome beta 3 subunit	6.00E-55	AJ888689	++	-	+	(+)	300	**255**	✓	
β2H01[(1)]	epoxide hydrolase	4.00E-69	AJ888690	+++	-	+	-	700	**675**	✓	**10**
β2H03	glucose transport protein fused to Caffeoyl-CoA O-methyltransferase	3.00E-47	AJ874099	(+)	-	(+)	-	320	**286**	✓	
β2H08	T-complex protein 1, theta subunit, TCP-1-theta	1.00E-85	AJ888691	+	-	(+)	(+)	600	**595**	✓	
β3A03	14-3-3 protein homologue (14-3-3a)	3.00E-44	AJ888692	+	-	++	++	500	**547**		
β3A05	Ran	1.00E-138	AJ888693	+	-	+	+	500	**431**	✓	
β3A07	NAC6 domain (NAM protein)	1.00E-67	AJ888694	++	+	(+)	(+)	300	**297**	✓	
β3A08	cytochrome c1	5.00E-25	AJ888695	+	(+)	+	+	600	**547**	✓	
β3A09	unknown	2.00E-49	AJ888696	++	-	(+)	(+)	400	**322**	✓	
β3A12[(1)]	20S proteasome beta 5 subunit	5.00E-64	AJ888697	++	(+)	++	+	400	**338**	✓	
β3B01	unknown	2.00E-46	AJ888698	+	-	(+)	-	200	**142**	✓	**07**
β3B07	similarity to ATP binding protein associated with cell differentiation	6.00E-51	AJ888699	+	-	(+)	-	400	**349**	✓	
β3B10	epoxide hydrolase	2.00E-78	AJ888700	+	-	(+)	-	250	**222**	✓	**10**
β3C01	unknown	9.00E-96	AJ888701	+	-	(+)	(+)	600	**537**	✓	
β3C03[(1)]	sucrase (ferredoxin-like)	6.00E-99	AJ888702	++	-	+	(+)	500	**473**	✓	
β3C08	Ran binding protein-1 (RanBP1)	2.00E-17	AJ888703	++	-	(+)	(+)	400	**338**	✓	
β3C09	unknown	4.00E-33	AJ888704	(+)	-	-	-	500	**480**	✓	
β3C10[(1)]	glyceraldehyde 3-phosphate dehydrogenase (cytosolic)	5.00E-68	AJ874100	+++	+	++	+	750	**661**	✓	**08**
β3C12	unknown	0.00E+00	AJ874101	+	(+)	(+)	(+)	600	**540**	✓	
β3D01	20S proteasome alpha 5 subunit	1.00E-20	AJ888705	+	-	(+)	-	450	**370**	✓	
β3D05[(1)]	glutathione S-transferase	1.00E-152	AJ874102	+++	-	++	-	600	**554**	✓	**29**
β3D11	signal sequence receptor, alpha subunit (SSR-alpha)	2.00E-38	AJ888706	+	-	+	(+)	200	**199**	✓	
β3E03	unknown	1.00E-176	AJ888708	+	-	-	-	500	**470**	✓	
β3E06	unknown	2.00E-67	AJ888709	+	-	(+)	(+)	400	**376**	✓	
β3E08	unknown	4.00E-32	AJ888710	+	-	(+)	(+)	900	**1011**		
β3E09[(1)]	unknown	0.00E+00	AJ874103	++	-	(+)	-	550	**497**	✓	
β3F05	nucleolar GTP-binding protein 1-like	1.00E-109	AJ888711	+	-	-	-	250	**229**	✓	
β3F09	unknown	5.00E-96	AJ888712	+	+	(+)	-	450	**419**	✓	
β3F11	NAM-like (No apical meristem)	0.00E+00	AJ888713	+	-	+	+	700	**684**	✓	
β3G05	aconitate hydratase (cytoplasmic)	4.00E-57	AJ874104	++	-	+	+	600	**528**	✓	
β3G08	ubiquinol-cytochrome C reductase complex 14 kDa protein	2.00E-77	AJ888714	+	+	+	(+)	400	**387**	✓	
β3G10	AAA-metalloprotease FtsH (P. sativum)	1.00E-49	AJ888715	+	-	(+)	(+)	1000	**749**		
β3G11	MAP kinase	2.00E-63	AJ888716	+	-	(+)	(+)	600	**535**	✓	
β3H03[(1)]	20S proteasome beta 2 subunit	2.00E-94	AJ888717	+++	-	+	-	500	**477**	✓	**24**

The largest similarity group identified consisted of 14 fragments with high homology to the syringolin-induced rice gene *Pir7b* (accession #Z34270). Two representatives (*β1B01* and *β2A07*) are listed in Table 4.2. Members of the corresponding group invariably exhibited strong signals on hybridizations with cDNA corresponding to syringolin treated tissue. Signals of three representatives are highlighted in Figure 4.5. Syringolin-induced accumulation of a wheat protein cross reacting to Pir7b-specific antibodies had already been demonstrated earlier (Wäspi et al., 2001). Thus, strong enrichment of corresponding

cDNA fragments demonstrated accuracy of screening and differential display-derived data. This was further supported by the fact that independent subtractions at the earlier α and the later β time point resulted in enrichment of identical cDNA fragments (exemplified by the upper contig of SG_06, Table 4.1).

The cDNA subtraction resulted in strong enrichment of clones representing various genes of the carbohydrate metabolism (notably from glycolysis and tricarboxylic acid cycle), numerous components of the 19S and 20S proteasome subunit, chaperones hsp 60 and hsp 70 and small HSPs, components of detoxification mechanisms (ABC transporters, glutathione S-transferase, or cytochrome P450) and a considerable number of proteins with unknown function. R-genes or associated proteins were represented by Cf2/Cf5-like and RPP8-like *β2G04* and *α1E08*, respectively, and the Pto kinase interactor-like *α3C11*. Genes involved in signaling and signal transduction included receptor kinases (*α1E09* and *β1B08*), protein phosphatase 2C and interacting protein (*α1B11* and *β2A06*), glutamate receptor-like *α2B04*, a MAP kinase (*β3G11*), NAC domain proteins (*β3A07* and *β3F11*), ligand-gated ion channel-like *β2E04* and the pleiotropic regulator *β2C06*. Homologies to components of plant hormonal signal transduction indicated involvement of auxin, abscisic acid and brassinosteroid hormonal signaling. Furthermore, strong upregulation of the cell cycle control gene *CDC48* (*α3F09*; Table 4.2) indicated possible interference with cell cycle progression or cell division. In accordance with earlier experiments (Wäspi et al., 2001), no transcripts corresponding to powdery mildew-induced PR proteins were obtained by SSH and the only fragments corresponding to known PR proteins were all wheat homologues of the syringolin-induced rice *Pir7b* gene (represented by *β1B01* and *β2A07*). Interestingly, SSH also enriched for fragments corresponding to a central component in the induction of animal apoptosis, the voltage-dependent anion channel (represented by *β1F04*), which is located in the outer mitochondrial membrane (Shimizu et al., 2000; Banerjee and Ghosh, 2004).

4.2. SylA-induced differential gene expression

The isolation of sylA responsive genes raised numerous questions with regard to their possible involvement in the onset of HR. Since cDNA is subjected to complex hybridizations during SSH (Figure 4.2), the screening method was expected to preferably enrich for cDNA segments of high sequence specificity. Indeed, of 28 fragments tested for polymorphisms in a cross between wheat varieties Arina and Forno (Paillard et al., 2003), 18 fragments were found to result in 3 or less hybridization bands and additional 5 fragments exhibited less than 6 bands upon southern blot hybridization (T. Schnurbusch, personal

communication). Thus, as judged in consideration of wheat allo-hexaploidy, cDNA fragments obtained by SSH were considered to be suitable for hybridization techniques.

4.2.1. cDNA microarray construction

Detailed analysis of the cDNA fragments obtained from the SSH screening was carried out by cDNA microarray technology. Microarray technology allows for the examination of thousands of genes in one single hybridization experiment and thus offers the opportunity of testing additional genes or cDNAs derived from different screenings. A cDNA microarray was produced according to previously described methods (Eisen and Brown, 1999; Reymond et al., 2000).

4.2.1.1. Array design

The array designed consisted of 1666 DNA spots (probes) interspersed with 382 empty spots spotted with printing buffer only. Probes were composed of three major subsets. Frequently individual DNA fragments were represented in multiple copies and they are therefore described to be present as doublets, triplets or quadruplets in the following.

Subset one: The 158 SSH-derived fragments were represented by 314 doublets and one additional fragment printed five times (319 probes in total). DNA fragments originating from the syringolin screening were named starting with the initials "OA_".

Subset two: 1088 single DNA fragments derived from a cDNA AFLP screen representing wheat genes putatively differentially expressed during attack by the non-host pathogen *Blumeria graminis* f.sp. *hordei* (*Bgh*). This screen was performed by R. Bruggmann in our laboratory and was aimed at cloning cDNAs corresponding to powdery mildew-induced genes in the epidermis. In short, wheat leaves cv. Fidel were heavily infected with *Bgh*. The epidermis of the abaxial side on the primary leaves was manually separated from the remainder of the leaf after 6-9 and 23-26 hours respectively. RNA was extracted from the plant material and subjected to cDNA-AFLP analysis. The 1088 targets of subset two correspond to subcloned DNA fragments originating from 156 polymorphic bands reflecting up- or downregulation of corresponding genes in the infected samples, as identified on polyacrylamide gels (Bruggmann et al., 2005). DNA fragments originating from the non-host screening were named starting with the initials 'RB_'. Some of the cDNA fragments were found to be present in multiple copies and to form contigs upon sequence assembly. For convenience, corresponding contigs were named c### starting from 'c001' instead of 'ctg 1'. Thus, contig 116 was referred to as 'RB_c116' instead of 'ctg 116'.

Subset three: Heterogeneous control subset of 167 probes in total: 69 triplets representing 23 barley ESTs (International *Triticeae* EST Cooperative ITEC) exhibiting little variation of expression in preliminary experiments (F. Pasquer, personal communication). Moreover, 4 wheat induced resistance genes (WIRs, Schweizer et al., 1989), 4 wheat chemically induced genes (WCIs, Goerlach et al., 1996) and 4 additional wheat PR-genes were represented by 36 triplets. In addition, 18 genes represented by 54 triplets plus two probes printed four times corresponded to genes of various origins used as negative hybridization controls, additional housekeeping genes or RNA quality controls (62 probes in total). A list containing all genes of subset 3 is shown in the Appendix (Table 8.3, p.194).

Subset four: Used for development of alternative normalization procedures, the Lucidea Universal ScoreCard (SC) by Amersham Biosciences (Uppsala, Sweden) encompassing 92 quadruplets consisting of 23 artificial genes designed from yeast intergenic regions was spotted. The array design is illustrated in the Appendix (Figure 8.1, p.196).

4.2.1.2. Evaluation of printing device under experimental conditions

Two alternative spotting devices both using contact deposition technology (illustrated in Figure 4.7) were compared for the fabrication of cDNA arrays and tested for their ability to produce functional arrays of appropriate quality in the first stage of the project.

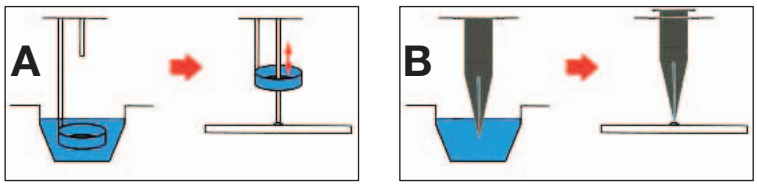

Figure 4.7: Mechanical delivery of probe DNA. A) Spotting solution is taken up in a spotting ring and delivery is carried out by repeated pin piercing (pin-ring technology). B) Spotting solution enters the uptake channel of a microspotting pin and delivery occurs after a single contact with the glass surface.

Microarray series 5 was printed onto epoxy-coated glass slides with the GMS 417 arrayer. The latter functions according to the pin-ring operation method (illustrated in Figure 4.7A). The final spotting solution was buffered at pH 8.5 with 150 mM sodium phosphate. Microarray series 6 was printed onto aldehyde-coated glass slides with an OmniGrid 100 spotting robot. The operation method by microspotting pins is illustrated in Figure 4.7B. The 3 x SSC final spotting solution additionally contained 1.5 M betaine (Diehl et al., 2001). To examine printing reliability and spot morphology, one slide each was hybridized for 1 h at

37°C to Cy3-coupled random 17-mer oligonucleotides. After washing, slides were scanned for fluorescence at a resolution of 10 µm. Representative results are shown in Figure 4.8.

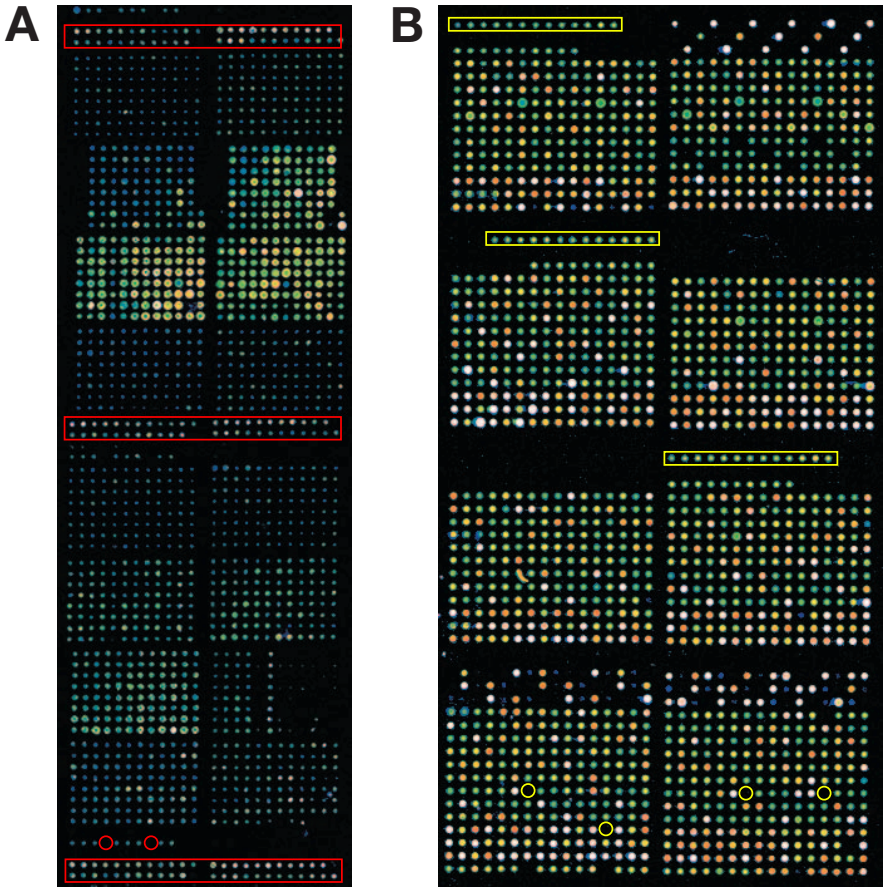

Figure 4.8: Test hybridizations of microarrays. Microarrays were hybridized to a Cy3-labeled random 17-mer oligonucleotide. A) Only half of the array of series 5 that was printed in duplicates is shown. B) The complete array of series 06 is shown. The design is illustrated in the Appendix (Figure 8.1).

Inspection of both arrays revealed remarkable differences between individual spots concerning the amount of DNA linked to the slides as reflected by variable hybridization signals in the random oligo test hybridization (the oligonucleotide was labeled with a fluorescent cyanine dye 3). The phenomenon results in strong differences between sub-groups corresponding to individual 96-well PCR plates on series 5. In addition, DNA spots on series 5 exhibited up to four fold differences in spot diameter complicating downstream data acquisition. However, spot diameter was not clearly correlating with DNA concentration since spots corresponding to the control subset 3 remained small despite high amounts of coupled DNA reflected by strong fluorescence (Figure 4.8A, red boxes). Therefore variable spot size was hypothesized to result from varying salt contents indicating alterations during DNA cleanup. Conversely, variable spot diameters were much less pronounced on series 6.

In addition, a notable amount of doughnut-shaped spots were detected on both series 5 and series 6, resulting from accelerated drying at outer edges under high temperature and low humidity during and after spotting (Lallemant, 2002). Doughnut shaped spot morphology is an undesirable effect negatively influencing downstream data analysis and data reproducibility. Though, the level was found to be much more serious on series 5 where virtually all spots showed either doughnut-shaped or irregular spot morphology. Conversely only 20 % of DNA spots on series 6 exhibited unfavorable morphology and variation effects were found to be less pronounced as compared to series 5 (Figure 4.8A and B). Increased homogeneity on series 6 with respect to both spot size and morphology were ascribed to the presence of 1.5 M betaine in the printing buffer and moderate humidity in the printing chamber. However, due to the absence of a sonication cleaning unit, high concentrations of betaine and elevated viscosity in the printing solution was considered to be hazardous with respect to DNA carry-over or progressive pin contamination and therefore its application was strictly avoided on the GMS 417 arrayer. Unlike spot morphology, steadiness of spotting was found to be better with the GMS 417 arrayer. Proper calibration of the print head and triple deposition of each spot by repetitive delivery of spotting solution by the pin guaranteed proper representation of each spot (exemplified by red circles in Figure 4.8A, empty areas corresponded to spots containing only buffer but no DNA). On series 6, multiple holes corresponding to undelivered spots were observed (exemplified by yellow circles in Figure 4.8B). This resulted from a mechanical problem which can be minimized by optimizing the pin cleaning step of the printing procedure (P. Reymond, personal communication).

In summary, the slower speed in conjunction with elevated heat release during the printing process caused negative effects on spot morphology with the GMS 417 arrayer. On top of this, considerable variations of DNA levels on DNA master plates resulting from evaporation were observed after spotting. Because of this, time consuming manual readjustments of liquid levels were necessary between printing sessions. Alternative comprehensive readjustment by drying DNA to completion at elevated temperature lowers DNA quality when repeated several times and eventually resulted in complete loss due to formation of insoluble aggregates. The overall problems attributed to evaporation on GMS 417 could not be solved by the application of several modifications such as external ventilated cooling of the robotic unit and internal cooling circuit over the printing area as well as improved cooling of DNA master plates by application of an aluminum support. Conversely, the presence of 1.5 M betaine in the printing buffer was shown to greatly improve quality of spot morphology on series 6 and variations of DNA levels on DNA master plates were found to be marginal. Besides, owing to the pin ring technique applied on GMS

417, the requirement of high volumes of DNA for printing was found to markedly complicate and prolong the production of printing master plates containing DNA of adequate concentration for the GMS 417 apparatus. In addition, insufficient cleaning of the pins caused great variation in the amount of spotting solution deposited between individual pins and lead to variations in the amount of DNA coupled to the slides after multiple printing sessions (results not shown). Concerning this, extreme sensitivity of the pins complicating maintenance and repetitive cleaning was found to be a disadvantageous property of pin-ring units.

In consequence, all experiments were performed with microarray series 6 and 7. The latter consisted of 100 additional slides fabricated in a second round of printing onto aldehyde-coated glass slides (Quantifoil Micro Tools GmbH, Jena, Germany) using the OmniGrid 100 spotting robot according to the protocols used for series 6. The layout of both arrays is identical (Figure 8.1, p.196).

4.2.1.3. Evaluation of scanning devices under experimental conditions

After hybridization and subsequent washing steps, microarray slides were scanned for fluorescence at a resolution of 10 µm at the Functional Genomics Centre Zurich (FGCZ). Performance of two different types of microarray scanners was compared.

Scanner A, the GSI Lumonics ScanArray 5000 (PerkinElmer Life Sciences Inc., Boston (MA), USA) uses mobile red (633 nm) and green (543 nm) excitation laser beams and a static slide holder. Geometric beam-splitter optics permit improved collection of emission light. Autofocus is adjusted prior to scanning. The apparatus features a line scan option allowing for balancing adjustment of the two channels by scanning probes in an arbitrary horizontal line (PerkinElmer, 2002). The function was applied at line sections of continuously deposited SC-probes of subset 4 (yellow boxes in Figure 4.8). Equalization variability of fluorescent dye labeling was achieved by separately adjusting the laser power (LP) of each channel prior to scanning of the whole array until corresponding signal intensities were balanced. The photo multiplier tube (PMT) gain was left at 80 %.

Scanner B, the Agilent G2505B microarray scanner (Agilent Technologies Inc., Palo Alto (CA), USA) is equipped with static red (633 nm) and green (532 nm) excitation laser beams and uses a mobile slide holder. A dichroic beam-splitter separates excitation and emission light. Slide scanning occurs from the opposite side and a dynamic auto-focus continuously adjusts for unevenness of microarray slides. In addition, the apparatus features 'dark offset subtraction' providing scans with lower background (Agilent Technologies Inc.,

2003). No line scan function is supported and scanning was carried out at 100 % LP and 100 % PMT gain setting.

Experimental RNA derived from pilot experiments was subjected to fluorescent dye labeling and subsequent microarray hybridization on microarray series 7. Hybridized microarray slides were scanned and data acquisition was carried out with the ImaGene 4.2 software (BioDiscovery Inc, El Segundo (CA), USA). The ratios of signal intensities (I) corresponding to treated and control treated samples (t/c-ratio) were calculated and data normalization was carried out using global locally weighted regression (Lowess) normalization (Quackenbush, 2002). Since normalization of microarray data is additive only for logged intensities, it has become a standard operating procedure to work with logged intensities and usually logarithms base 2 are used (Dudoit et al., 2002). Comparisons between test and control treatment were visualized on MA-plots (Dudoit et al., 2002). In MA-plots, the logarithm base 2 of the intensity ratio $M = \log_2(I_t/I_c)$ (log ratio) is plotted vs. the mean log intensity $A = \frac{1}{2}\log_2(I_t \times I_c)$. Thus, MA-plots show the intensity-dependent log ratios of microarray data. After normalization, data points representing evenly abundant probes (log ratio = 0) are centered vertically about the M = 0 line. Outliers represent differentially expressed genes with M > 0 for induced and M < 0 for repressed genes. Representative results are shown in Figure 4.9.

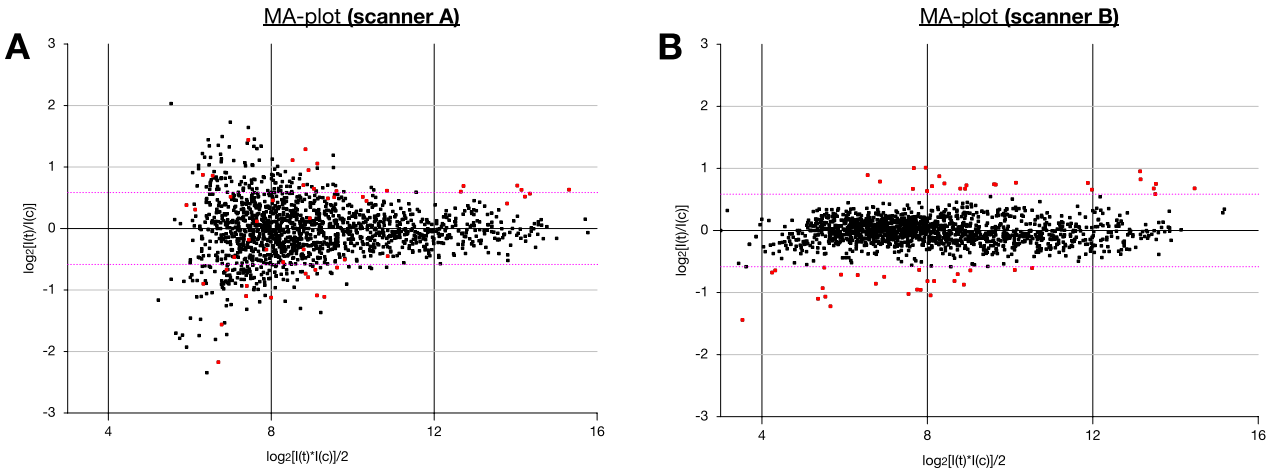

Figure 4.9: MA-plots of one microarray slide (series 7) scanned with scanner A and subsequently with scanner B. Probes exhibiting t/c ratios differing more than 1.5-fold from 1 in the B-scan are labeled in red on both plots. The corresponding threshold limits are indicated by pink dotted lines. Scans were conducted at 60 % LP and 80 % PMT for scanner A and 100% LP and 100% PMT for scanner B.

As obvious in Figure 4.9, data obtained by scanner B were of much higher quality as compared to scanner A. Scanner B exhibited better signal/noise ratios and thus higher

sensitivity in the low signal range. Consequently, at high signal intensities (spots above 9 on the X-axis) putative differentially expressed genes (red dots) identified with scanner B were also over or close to threshold limits in data obtained with scanner A. Yet, at lower intensity (below 9 on the X-axis) the distribution of t/c ratios in the A-scans tended to become random (panel A) whereas homogenous distributions were observed along the whole intensity range in the B-scans (panel B).

Lower sensitivity of scanner A resulted in a spread of expression data towards the lower limit of signal intensity. The convincing performance of scanner B was ascribed to the dynamic autofocus and dark offset function which were both described to lower background levels on the microarray scans (Agilent Technologies Inc., 2003). On the other hand, overall scanning power of scanner B appeared to be considerably lower than the one of scanner A. As a result of this, t/c ratios of the entire array were similarly positioned along the intensity (X) axis (Figure 4.9), despite medium scanning power setting of scanner A and maximum settings of scanner B.

In summary, data of high quality were obtained by scanning with scanner B whereas scanner A allowed only for identification of highly abundant transcripts. Moreover, identification of differentially expressed genes after scanning with scanner B could easily be achieved by application of t/c thresholds (horizontal line on the MA-plot) whereas more sophisticated slice analysis (Yang et al., 2002a) would have been necessary in the case of scanner A. The lacking line scan option in scanner B resulted in less balanced raw data (vertical displacements on MA-plots) but calculative data normalization compensated for shifted baselines (data not shown). Thus, microarray slides of series 7 used in the present work were all scanned with the Agilent G2505B microarray scanner.

4.2.1.4. Generation of a standard normalization strategy meeting the needs of medium-sized microarrays

Normalization of microarray hybridization signals is used to balance treated or control sample-specific variations of biological and technical origin. Normalization of data derived from the present work was intended to balance hybridization signals corresponding to a multitude of different treatments like syringolin application, powdery mildew infection but also comparison of samples derived from different plant tissues (epidermis and mesophyll).

Frequently, t/c ratios of raw data (unnormalized data) are linearly shifted up or down. This is reflected by a vertical displacement of the horizontal baseline on MA-plots. In this case, normalization is achieved by multiplication of signals derived from treated or control

samples by a correction factor. The multitude of publications describing standard normalization procedures usually focus on large arrays representing random gene collections of several ten thousand probes (Quackenbush, 2002; Yang et al., 2002b; Leung and Cavalieri, 2003). Based on their size, these all have two important points in common: First, irrespective of the experiment investigated, only a minor part of probes exhibit differential expression and secondly, the proportion of induced and repressed genes is approximately equal. Standard normalization of microarray data include linear total intensity normalization and Lowess (local weighted regression) normalization (Kepler et al., 2002; Quackenbush, 2002; Yang et al., 2002b; Leung and Cavalieri, 2003).

The applicability of the most popular method, Lowess normalization (implemented in TIGR MIDAS software, Saeed et al., 2003), was tested. In contrast to total intensity normalization methods, Lowess normalization effectuates intensity-dependent regularization and thus bears the capability to even normalize asymmetric distortions of t/c ratios along the intensity (X-axes) scale in MA-plots (reviewed by Quackenbush, 2002; Yang et al., 2002b). Results obtained by normalization of data derived from hybridizations of microarray series 7 to RNA derived from syringolin treated wheat leaves are shown in Figure 4.10. Global Lowess normalization was applied on hybridization data exhibiting slight curvature on the MA-plot (bend is indicated by a red arrow), one-sided differential regulation and considerable displacement of the horizontal t/c baseline Figure 4.10A).

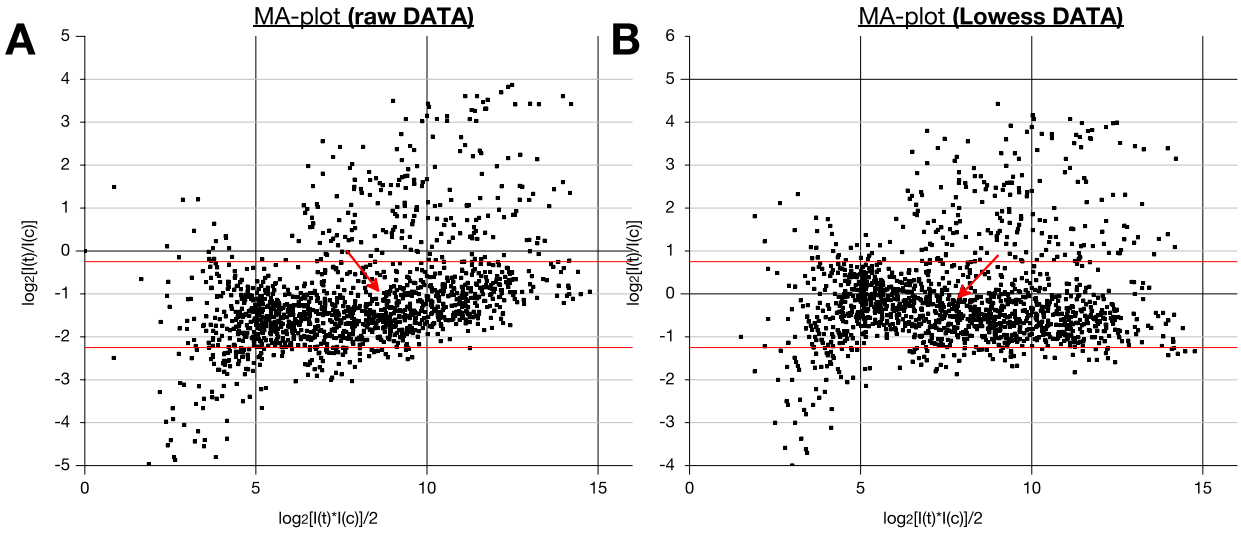

Figure 4.10: MA-plots of microarray series 7 hybridizations to RNA derived from syringolin treated samples. A: Before normalization, B: After global Lowess normalization. Red lines delimit the narrowest cut-off area for the identification of outlying t/c ratios.

Two things were observed after normalization. First, curvature was not removed by Lowess normalization and second, t/c ratios were still clearly repressed by an approximate factor of 1.5 on average Figure 4.10B. Both findings were ascribed to the one-sided distribution of differential expression. On the one hand, numerous induced genes lowered the local average. As a result of this, a new bend (red arrow) was introduced into the data set. This also occurred when no curvature was present in raw data such as in the example in Figure 4.11A (data not shown). Consequently, the range of background fluctuation before and after Lowess normalization remained unchanged (area in between red horizontal lines; Figure 4.10A & B). On the other hand, the same reason caused incomplete normalization of the entire data (the latter was also observed after total intensity normalization, data not shown). Hence, Lowess normalization was found to be unsuitable to be used as standard normalization procedure in the present work.

Fortunately, curvature only occurred rarely and the zero line proceeded horizontally on MA-plots (representative results are shown in Figure 4.11A). However, as shown in the Appendix, Lowess normalization proved to be a powerful tool to balance signal intensity-dependent biases in a few exceptional cases, when t/c ratios were homogenously distributed along the X-axes on MA-plots (Figure 8.2, Appendix).

Satisfying normalization was finally achieved by iterative log(ratio) mean centering (ILMC, implemented in TIGR MIDAS software, Saeed et al., 2003). Representative results are shown in Figure 4.11. Upon ILMC normalization, probes exhibiting differential expression are excluded from the final selection of probes used for calculation of the correction factor.

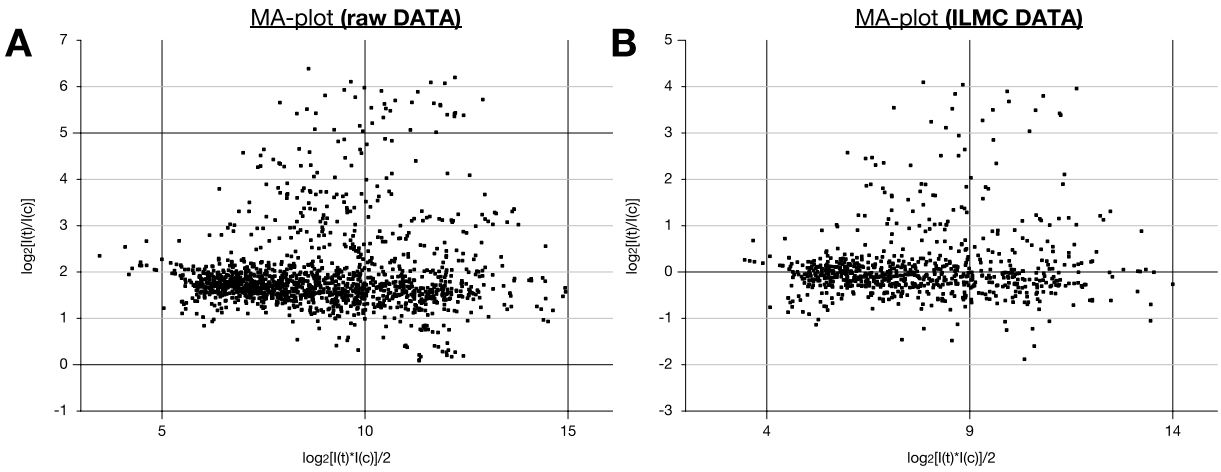

Figure 4.11: MA-plots of microarray series 7 hybridizations to RNA derived from syringolin treated epidermal samples. A: Before normalization, B: After ILMC normalization.

As shown later, the majority of syringolin-induced genes corresponded to SSH-derived probes. These were represented twice on the array. Thus, the efficiency of ILMC normalization was increased by decreasing the impact of multiple spotted probes (decreased redundancy). This was accomplished by averaging the log ratio of corresponding probes prior to ILMC normalization. By this means, several data points representing identical cDNA fragments were reduced to one single data point (details are given in Materials and Methods). Accordingly, MA-plots contained less data points after ILMC normalization Figure 4.11B. As obvious in Figure 4.11B, ILMC normalization perfectly centered the bulk of data points along the zero line on the vertical axis. Before, an approximate threefold displacement resulting from lacking adjustment of scanning power (with the Agilent G2505B microarray scanner) was observed (Figure 4.11A). The example demonstrated that by application of ILMC normalization, t/c ratios could be properly normalized despite one-sided distribution of differential expression. Therefore, the method was used as standard normalization procedure.

Following ILMC normalization, t/c ratios were subjected to additional quality filtering by application of lower and upper signal intensity cutoff limits. The lower limit was calculated on the basis of signal intensities derived from empty spots, sometimes referred to as 'ground' in the literature. The upper limit was set to an empirically defined value (described in Materials and Methods). Intensity values exceeding cutoff limits were set equal to the cutoff value. As shown in Figure 4.12, application of cutoff limits (blue dots) corrected variability at the lower and upper end of the signal intensity.

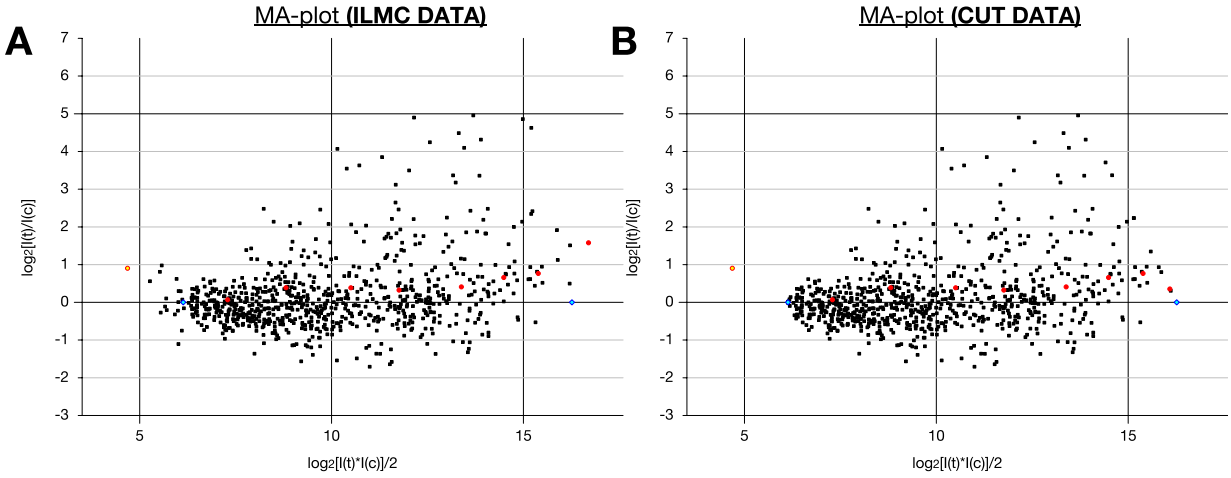

Figure 4.12: MA-plots of microarray series 7 hybridizations to RNA derived from syringolin treated epidermal samples. A: Before cutoff application, B: After cutoff application. Red dots: Average values of the SC calibration control spots (subset four). Yellow dot: Data corresponding to the median log intensities of empty control spots. Blue spots: High and low cutoff limits.

In addition, biases derived from slight curvature occasionally obtained by dye-specific biases at the lower end or saturated scanning at the upper end of signal intensity were effectively dampened. The latter was demonstrated by the correction of an outlying member of the SC control probes (red dots) at high signal intensity (Figure 4.12A) down to baseline levels (Figure 4.12B). Note that target RNA of the SC control probes (red dots) was spiked into experimental RNA samples before labeling. Thus, depending on the accuracy of measurement and pipetting, signals corresponding to SC control probes were not necessarily normalized by normalization of signals corresponding to experimental probes. Still, SC control probes were found to be useful to survey deviations of log ratios resulting from technical biases.

In summary, combining averaging of multiple spotted probes, ILMC normalization and cut off application allowed for efficient normalization of microarray data obtained with microarray slides of series 7. In contrast, one-sided distribution of log ratios rendered Lowess normalization impossible. With respect to this, monitoring progression of log ratios along the intensity scale supported by the SC control probes normally revealed linearity. Occasional curvature was efficiently dampened by cut off application.

As a standard procedure, triplicate biological replication was carried out in downstream experiments to statistically identify true alterations of gene regulation. To further prevent identification of false positives, target cDNA was labeled alternately using either fluorescent dye one or dye two for the test or control cDNA, respectively (flip-dye or dye-swap experiments). Subsequently, one-sample t-test statistics were applied (Dudoit et al., 2002). Genes were considered to be differentially expressed if log ratios varied from 0 with a probability of error of less than five percent ($p < 0.05$) based on the T-distribution (Materials and Methods). In addition, lower threshold levels for t/c ratios were set to 1.5-fold difference between control and treated samples for multiple spotted probes and to 2-fold difference for single spotted probes.

4.2.1.5. Indirect labeling method

Fluorescent probe labeling for microarray hybridization was carried out following a two step procedure involving separate coupling of N-hydroxysuccinimidyl ester activated dyes to aminoallyl dUTP. Aminoallyl dUTP was incorporated during preceding cDNA synthesis (Randolph and Waggoner, 1997; Hughes et al., 2001) (Figure 4.13).

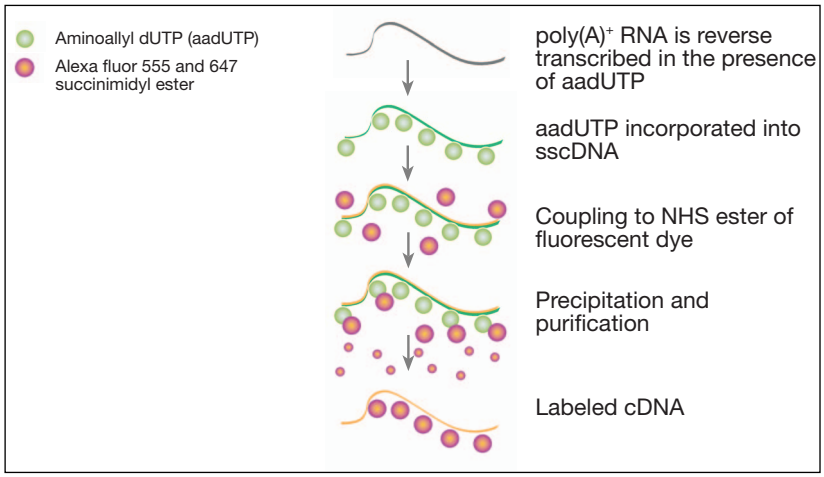

Figure 4.13: Simplified illustration of indirect cDNA labeling protocol (Lallemant, 2002, modified).

Labeling was carried out with fluorescent dyes Alexa Fluor 555 (AF_{555}) and Alexa Fluor 647 (AF_{647}) (Molecular Probes Inc., Eugene (OR), USA). Alexa Fluor dyes were favored over cyanine dyes mainly because of high photo-stability (microarray slides could be scanned several weeks after hybridization without loss of signal intensity). In addition, they had been reported to be less affected by coupling-derived absorption shifts and unfavorable quenching (Molecular Probes, 2004).

In one step labeling protocols (direct labeling), incorporation of dUTP previously coupled to fluorescent dyes into cDNA during reverse transcription directly yields labeled cDNA. In contrast, coupling of dUTP to fluorescent dyes is carried out in a separate step in the indirect two step labeling procedure as shown in Figure 4.13. Two step labeling was reported to be more efficient and to guarantee uniformity of labeling with different dyes (Lallemant, 2002).

To quantify incorporation and coupling efficiency, the amount of dye coupled to cDNA can be described as the number of nucleotides coupled to fluorescent dye in relation to the total number of nucleotides present in the probe (base/dye ratio). Details for computation of base/dye ratios are given in the Appendix (chapt. 8.4). In our hands, two step labeling resulted in high average base/dye ratios (bdr) of up to 26, indicating that every 26^{th} nucleotide of a given cDNA fragment in the probe was an uridine successfully coupled

to the respective dye. Conversely, incorporation efficiencies of direct labeling tested in earlier experiments were found to be significantly lower (Rémy Bruggmann, personal communication). Starting from 2 µg of poly(A)$^+$ RNA, average cDNA yield was found to be 2.03 µg. Thus, RT-PCR in the presence of aminoallyl dUTP was found to be very efficient.

Unexpectedly, coupling efficiency was found to vary between different fluorescent dyes. Average bdr for AF_{555} was 26 whereas coupling to AF_{647} was less efficient and showed a bdr of only 41. These findings were similar to base/dye ratios derived from earlier experiments carried out with cyanine dyes (Amersham Biosciences, Uppsala, Sweden) cy3 and cy5 (data not shown). With respect to syringolin treatment, most of the probes were expected to exhibit upregulation rather than downregulation. Thus, control samples were coupled to AF_{555} by default in order to minimize identification of false positives caused by variable labeling efficiencies.

Altogether, two step labeling with fluorescent succinimidyl ester activated Alexa Fluor dyes yielded probes of high intensity which proved to be very robust against photo bleaching. Variable coupling efficiency between different dyes found for Alexa Fluor as well as cyanine dyes were hypothesized to be caused by different shelf life and stability of succinimidyl ester activated dyes. No further investments in order to obtain dyes of high coupling activity were carried out. However, bdr up to 66 were found to still result in good hybridization intensity and high signal / background ratios. Thus, upper threshold limits for bdr were set to 66 and no additional efforts were put into further balancing of coupling efficiency.

4.2.1.6. Labeling of antisense-RNA vs. poly(A)$^+$ RNA

RNA amplification efficiency

Large amounts of 2 µg of poly(A)$^+$ RNA required for two step labeling were found to complicate microarray investigations of peeled epidermal tissue, where sample material for RNA isolation was limited. Commonly, enrichment of poly(A)$^+$ RNA was done with 400 µg of total RNA and yielded 0.81 % corresponding to 3.2 µg of high quality poly(A)$^+$ RNA on average. Thus, linear RNA amplification based on *in vitro* transcription using T7 RNA polymerase (Van Gelder et al., 1990) became an optional standard component of probe preparation for cDNA microarray experiments. The method is also applied for standard RNA labeling in custom oligo gene chip technology (Affymetrix, Santa Clara (CA), USA). Briefly, reverse transcription of oligo(dT)-primed RNA into sscDNA is followed by second strand

synthesis. Featured by the presence of a T7 promoter site 3-prime of the oligo(dT), dscDNA then serves as template for *in vitro* transcription by T7 RNA polymerase. *In vitro* transcription results in the production of thousands of antisense RNA (aRNA) copies of each mRNA present in the sample. On average, amplification of 2 µg of total RNA yielded 80 µg of aRNA. Assumed that mRNA account for about 2 % of total RNA, linear RNA amplification by T7 RNA polymerase allowed for 2000-fold amplification of mRNA. Subsequently, 2 µg of aRNA was used for two step cDNA labeling following standard protocols established previously for poly(A)$^+$ RNA.

SylA-induced differential transcription detected by labeling of poly(A)$^+$ RNA and aRNA

To compare the two labeling methods under experimental conditions, total RNA was subjected to microarray analysis by labeling of poly(A)$^+$ RNA or aRNA. The total RNA was extracted in the course of investigations of sylA responsiveness described in chapt. 4.2.2. Syringolin was sprayed onto nine day-old leaves of *Bgt*-infected and uninfected wheat. Leaves were collected 24 hours after syringolin treatment (hat).

Data derived from poly(A)$^+$ RNA preparation encompassed two biological repetitions in total. One of which was labeled with fluorescent dyes in reciprocal direction (dye swap). In order to minimize experimental variation, t/c ratios were subjected to global SD-normalization (scale normalization by Yang et al., 2002b). Genes were considered to be differentially regulated when ratios were above threshold levels of 2 and below 0.5 respectively.

Data derived from aRNA preparation encompassed the same biological repetitions plus one additional repetition (three repetitions in total). Ranking of altered gene expression was done according to standard procedures based on t-test statistics (as described in chapt. 4.2.1.4). Comparison of average t/c-ratios between aRNA and poly(A)$^+$ RNA experiments was carried out. MA-plots illustrating distributions of hybridizations corresponding to uninfected plants are shown in Figure 4.14.

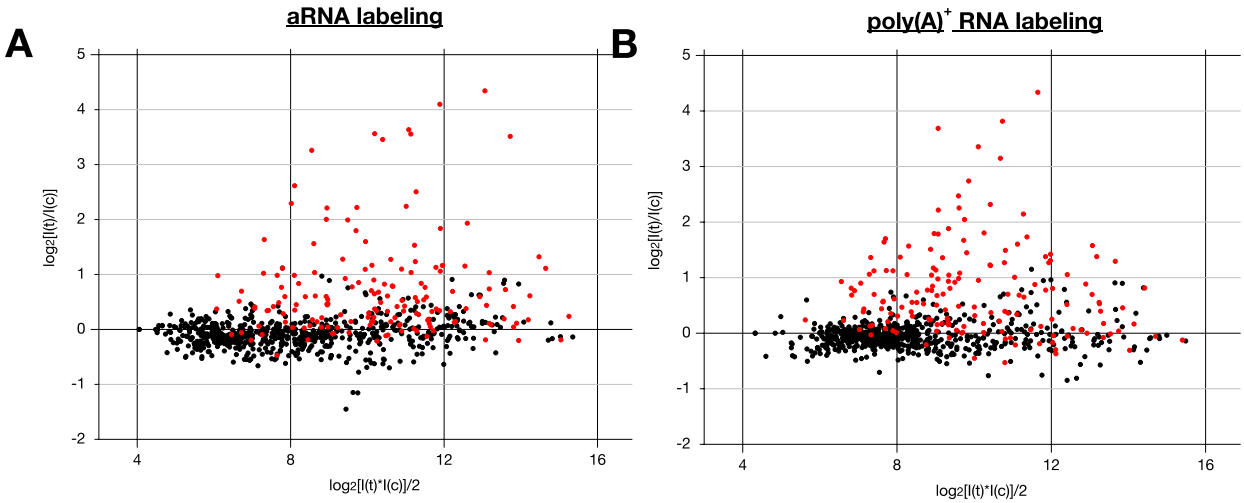

Figure 4.14: MA-plots representing average ratios of microarray slides hybridized to three biological repetitions using amplified RNA (A) and two repetitions using poly(A)$^+$ RNA (B) for labeling. Both experiments represent uninfected wheat leaves (cv. Fidel) treated with sylA and harvested 24 hat. Red dots: Probes corresponding to SSH-derived subset one are highlighted.

As obvious in Figure 4.14, both RNA preparations resulted in similar gene induction patterns. However, direct comparison of average t/c-ratios revealed that genes identified to be differentially regulated fell into three groups. Group one consisted of genes identified by both labeling methods (referred to as common genes). Group two contained genes identified only with targets obtained by RNA amplification (referred to as aRNA genes) and group three contained the genes identified exclusively with targets obtained by enrichment of poly(A)$^+$ RNA (referred to as poly(A)$^+$ RNA genes). A comprehensive list of all genes identified by either method is given in Table 4.3. Of 67 genes totally identified, only 46 % were common genes whereas the rest was assigned to poly(A)$^+$ RNA or aRNA genes. The findings are illustrated in Figure 4.15.

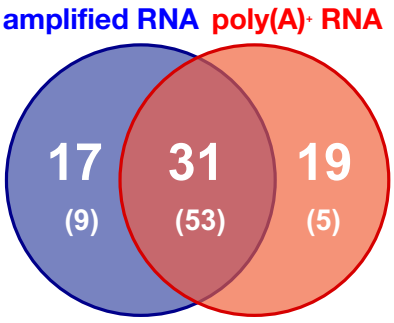

Figure 4.15: Venn diagram showing the distribution of detected differentially expressed genes between microarrays hybridized to targets derived from amplified or poly(A)$^+$ RNA. The numbers of probes identified to be differentially expressed by aRNA, poly(A)$^+$ RNA or both preparations are given (criteria are described above). By assigning differential expression solely by transgression of t/c ratio limit factor of 1.5, a higher percentage of probes was assigned to the common genes (numbers in brackets).

Inspection of common genes revealed that next to genes showing identical induction on both types of hybridization, some showed stronger response on the amplified RNA hybridizations whereas ratios of others were pronounced on poly(A)$^+$ RNA hybridizations. Subgroups were distinguished when highest t/c ratios differed for a factor of more than 2-fold between the two preparation methods. Subgroups were separated by a horizontal line in Table 4.3. Balanced ratios were found for the probes of rows 1-11 whereas probes of rows 12-22 showed higher ratios in the poly(A)$^+$ RNA preparations and ratios in rows 23-31 were higher in the aRNA preparations. Occasionally, as for example in the case of *OA_a1D08* (row 23) or *OA_b2A07* (row 30), t/c ratios considerably differed for factors of more than 4-fold.

Upon inspection of the poly(A)$^+$ RNA genes, two subgroups could be distinguished. On the majority of 14 genes (rows 32-45), induction was also indicated on aRNA hybridizations (t/c ratios above 1.5-fold limit), however it was found not to be statistically significant (p-values above 0.05% upon one-sample t-test). In the minor group, absolutely no indication for differential expression was found by aRNA hybridization (t/c ratio below 1.5-fold limit). Likewise, numerous genes belonging to aRNA genes were found to display elevated ratios also on poly(A)$^+$ RNA hybridizations, however ratios were low (between 1.5 and 2.0; Table 4.3, rows 51-57). When genes with a small t/c ratio (above 1.5) were also considered as being differentially expressed, a much higher number of 79 % fell into the common genes group detected by both types of RNA preparation (numbers in brackets on Figure 4.15).

Irrespective of the type of RNA preparation, t/c ratios were found to be reduced on hybridizations with probes derived from infected samples as compared to probes derived from uninfected wheat leaves. Average reduction of 1.505-fold on experiments of aRNA hybridization was found to be nearly identical to an average reduction of 1.513 on experiments hybridized to labeled poly(A)$^+$ RNA. Thus, despite the fact that t/c ratios varied between the two RNA preparation methods, relative proportions remained almost unchanged, as was found in the common genes (examples are fragments *OA_a2G01*; row 17, *OA_b1F09*; row 18 or *OA_b1A06*; row 26, Table 4.3).

Table 4.3: t/c ratios of gene sets identified by hybridization of 2-step cDNA-labeled aRNA (three repetitions) and poly(A)$^+$ RNA (two repetitions) respectively. Average t/c ratio are given in columns 5 to 8**.** Bold t/c ratios in columns 5 & 6: t/c threshold =1.5 and p≤0.5. Bold t/c ratios in columns 7 & 8: t/c threshold = 2.0. The three groups of common genes, poly(A)+ RNA genes and aRNA genes were labeled (underlined headings). Subgroups were separated by horizontal lines.

		Putative function & [Blast hit]	access. no#	E-val	syringolin A, 24 hat			
					aRNA		poly(A)$^+$	
	EST ID				-	Bgt	-	Bgt
1		2	3	4	5	6	7	8
		Common identified:						
1	***OA_a2C11***	26S proteasome regulatory subunit [AP004778]	AJ888616	3.E-62	**2.4**	1.5	**2.2**	1.8
2	***OA_a2E02***	ABC transporter (MDR-like) [Ta.9295]	AJ888620	0.E+00	**1.7**	1.2	**2.1**	1.5
3	***OA_a3B09***	hsp 70 [P37900]	AJ874084	4.E-42	**2.9**	1.5	**2.1**	1.7
4	***OA_a3C03***	prohibitin [AF236371]	AJ874085	1.E-114	**2.4**	1.2	**3.0**	1.9
5	***OA_b1F08***	26S proteasome RPN9b subunit [Ta.1348]	AJ888663	1.E-163	**1.8**	1.4	**2.3**	1.6
6	***OA_b1G05***	20S proteasome alpha 5 subunit [CD936318]	AJ874091	0.E+00	**3.8**	1.5	**3.0**	1.8
7	***OA_b2F07***	aspartate aminotransferase (cytoplasmic) [P37833]	AJ888686	4.E-82	**2.2**	1.4	**2.1**	1.3
8	***OA_b2F09***	unknown [Ta.12787]	AJ874097	6.E-49	**2.0**	1.3	**2.2**	1.4
9	***OA_b3A12***	20S proteasome beta 5 subunit [BJ219720]	AJ888697	5.E-64	**1.7**	1.1	**2.5**	1.4
10	***OA_b3B10***	epoxide hydrolase [Ta.26236]	AJ888700	2.E-78	**3.5**	**2.0**	**3.1**	1.8
11	***OA_b3H03***	20S proteasome beta 2 subunit [BE494850]	AJ888717	2.E-94	**2.2**	1.2	**2.4**	1.5
12	***OA_a1A03***	unknown [Hv.10128]	AJ888591	1.E-158	**2.1**	1.6	**5.0**	**2.4**
13	***OA_a1C12***	fructose-bisphosphate aldolase [CD907979]	AJ888600	1.E-141	**1.6**	1.2	**3.0**	1.7
14	***OA_a1D09***	cytochrome P450 [AF321867]	AJ888604	3.E-67	**1.5**	1.0	**5.5**	**2.4**
15	***OA_a1H02***	hsp 23.6 [Ta.214]	AJ874076	1.E-143	**3.0**	**1.9**	**8.9**	**3.7**
16	***OA_a2C02***	NADPH-dependent oxidoreductase [CA736677]	AJ874078	1.E-120	**2.2**	1.5	#N/A	**2.5**
17	***OA_a2G01***	enolase 1 (2-phosphoglycerate dehydratase 1) [CD454849]	AJ888626	8.E-90	**4.9**	**3.0**	**12.9**	**8.2**
18	***OA_a3A01***	glutathione-S-transferase/glutaredoxin [BE405126]	AJ888631	1.E-144	**1.6**	1.3	**2.7**	**2.0**
19	***OA_b1F04***	voltage-dependent anion channel 1 [X77733]	AJ888662	2.E-57	**6.1**	**3.0**	**14.1**	**6.7**
20	***OA_b2B07***	no significant hit	AJ888674	#N/A	**11.7**	**7.8**	**20.2**	**9.3**
21	***OA_b2E04***	DMI1 protein [CA027230]	AJ888682	0.E+00	**2.0**	1.4	**4.8**	**2.4**
22	***OA_b3E03***	unknown [BQ789018]	AJ888708	1.E-176	**2.0**	1.5	**3.4**	**2.5**
23	***OA_a1D08***	unknown [D22421]	AJ888603	8.E-06	**12.4**	**7.5**	**2.9**	1.8
24	***OA_a1E07***	hsp 60 [L21006]	AJ888606	5.E-49	**4.6**	**2.2**	**2.2**	1.4
25	***OA_a2A05***	alcohol dehydrogenase ADH1 [CD868456]	AJ888612	1.E-163	**4.7**	2.0	**2.1**	1.3
26	***OA_b1A06***	no significant hit	AJ874086	#N/A	**11.8**	**8.4**	**3.3**	**2.0**
27	***OA_b1B01***	pir7b / salicylic acid-binding protein / Ethylene-induced esterase [Q43360]	AJ874087	2.E-67	**17.1**	**9.5**	**10.2**	**5.2**
28	***OA_b1C09***	hsp 60 [AC027038]	AJ874088	5.E-35	**5.7**	**2.3**	**2.2**	1.8
29	***OA_b1D06***	cytochrome P450 [AP002839]	AJ888659	3.E-47	**9.6**	**5.1**	**4.6**	1.8
30	***OA_b2A07***	pir7b / salicylic acid-binding protein / Ethylene-induced esterase [CB864680]	AJ874094	3.E-79	**20.2**	**10.5**	**3.2**	**2.2**
31	***OA_b3D05***	glutathione S-transferase [CN013161]	AJ874102	1.E-152	**11.4**	**9.4**	#N/A	**3.0**
		unique to poly(A)$^+$						
32	***OA_a1B01***	hsp 23.5 [Ta.203]	AJ874072	1.E-133	1.5	1.3	**3.5**	1.9
33	***OA_b1A08***	20S proteasome alpha 4 subunit [O04861]	AJ888652	4.E-37	1.6	1.0	**2.1**	1.2
34	***OA_b1G10***	TipC / VPS13 - like protein [Ta.8446]	AJ888664	1.E-148	1.7	1.1	**2.6**	1.8

Table 4.3 (continued)

	EST ID	Putative function & [Blast hit]	access. no#	E-val	syringolin A, 24 hat aRNA -	aRNA Bgt	poly(A)+ -	poly(A)+ Bgt
1	2		3	4	5	6	7	8
35	***OA_b2B04***	pyruvate kinase [AY090539]	AJ888672	4.E-30	1.7	1.2	**2.5**	1.4
36	***OA_b2G11***	20S proteasome beta 3 subunit [CD866745]	AJ888689	6.E-55	1.9	1.4	**3.3**	1.8
37	***OA_b3C12***	unknown [Ta.27220]	AJ874101	0.E+00	1.5	1.3	**2.0**	1.4
38	***OA_b3D01***	20S proteasome alpha 5 subunit [Q9LSU1]	AJ888705	1.E-20	2.1	1.4	**4.4**	**2.0**
39	***OA_b3E09***	unknown [BU100203]	AJ874103	0.E+00	1.5	1.1	**3.5**	**2.7**
40	***OA_b1B10***	pyruvate kinase-like protein [AY090539]	AJ888655	1.E-151	2.5	1.2	**2.4**	1.6
41	***OA_b1C03***	26s proteosome regulatory subunit [CA602939]	AJ888656	1.E-47	2.0	1.3	**2.6**	2.0
42	***OA_b1D01***	succinyl-CoA-ligase beta subunit [AY180975]	AJ874089	3.E-63	2.4	1.6	**2.6**	1.7
43	***OA_b1E11***	succinyl-CoA-ligase beta subunit [AY180975]	AJ874090	5.E-38	2.1	1.4	**2.7**	1.7
44	***OA_b1H11***	citrate synthase [AP000367]	AJ874093	3.E-59	2.2	1.3	**2.6**	2.0
45	***OA_b2C07***	20S proteasome beta 6 subunit [O64464]	AJ888678	2.E-29	2.0	1.2	**2.1**	1.3
46	***OA_a2D10***	alanine aminotransferase 2 [CF133158]	AJ874079	0.E+00	1.4	1.2	**2.8**	1.6
47	***OA_a2F04***	unknown [CK215536]	AJ888625	0.E+00	1.3	1.1	**2.3**	1.8
48	***OA_b1H08***	glutathione S-transferase [CA719629]	AJ874092	7.E-81	1.3	1.2	**2.3**	1.4
49	***OA_b2E06***	valyl tRNA synthetase [AC084023]	AJ888683	3.E-63	1.4	1.1	**3.7**	1.7
50	***OA_b2G10***	unknown [BJ291998]	AJ888688	3.E-66	1.3	1.2	**2.6**	1.6
		unique to aRNA						
51	***OA_a1C08***	sucrose synthase 1 [CK209269]	AJ888599	2.E-61	**2.2**	1.2	1.6	1.1
52	***OA_a1D06***	alcohol dehydrogenase ADH1 [BJ307901]	AJ888602	1.E-131	**4.6**	2.3	1.8	1.1
53	***OA_a1E06***	alternative oxidase [AF174004]	AJ874074	4.E-87	4.0	**2.2**	1.9	1.3
54	***OA_a2E09***	unknown [CN013234]	AJ888622	1.E-51	**3.1**	1.5	1.6	1.1
55	***OA_a3B02***	2-oxoglutarate dehydrogenase (E1 subunit) [AP005199]	AJ874083	2.E-91	**1.8**	1.4	1.9	1.4
56	***OA_b1B08***	light repressible receptor protein kinase (Putative integral membrane protein) [BE517637]	AJ888654	5.E-73	**2.9**	1.6	1.9	1.3
57	***RB_96.2***	B12D protein [BQ170981]	AJ888727	1.E-31	**2.2**	**1.6**	1.7	1.2
58	***OA_a1E08***	NBS-LRR disease resistance protein [AJ507096]	AJ874075	3.E-49	**4.0**	**2.2**	1.4	1.2
59	***OA_a2B04***	ligand-gated ion channel 2.8 [BQ659530]	AJ888614	5.E-99	**11.0**	**5.0**	1.0	1.1
60	***OA_a2D05***	no significant hit [CX630958]	AJ888618	2.E-01	**2.0**	1.5	1.0	1.0
61	***OA_b2H01***	epoxide hydrolase [Ta.26236]	AJ888690	4.E-69	**3.6**	**2.2**	0.9	1.0
62	***OA_b3C01***	unknown [BE488635]	AJ888701	9.E-96	**1.8**	1.1	1.5	1.1
63	***OA_b3F05***	nucleolar GTP-binding protein 1-like [BI751677]	AJ888711	1.E-109	**1.9**	1.2	1.4	1.1
64	***RB_39.2***	Ripening-related protein-like [CD872650]	AJ888725	5.E-67	**0.7**	0.7	0.8	1.0
65	***RB_c001***	gigantea mRNA [BG909229]	AJ873936 AJ873963	1.E-117	**0.4**	1.0	0.8	0.9
66	***RB_c048***	Putative immediate-early salicylate-induced glucosyltransferase [Ta.23340]	AJ874027	2.E-29	**0.4**	1.1	1.0	1.0
67	***RB_c116***	28S ribosomal RNA gene (fungal) [AY064705]	AJ888238	4.E-71	1.0	**2.1**	0.8	0.9

Interestingly, t/c ratios of certain genes were found to be similar between the two preparation methods (rows 1-11) whereas others were varying (rows 12-31). This indicated that variability between individual t/c ratios upon RNA amplification were caused by technical peculiarities acting in a gene-specific manner. Thus, gene specificity resulted in a consistent increase or decrease and therefore relative t/c ratios (between different

treatments) resulting from either RNA preparation method remained unchanged. Differences between the gene sets identified by the two RNA preparation techniques were most likely caused by varying efficiencies for the enrichment by either method. Indeed, when signal intensities of probes uniquely identified by one type of RNA preparation were categorized within corresponding hybridization results of the entire array, average ranking of the poly(A)$^+$ RNA genes was found to be higher in the poly(A)$^+$ RNA hybridizations than in the aRNA hybridizations (72 % as compared to 48 %). Conversely average ranking of the aRNA genes was found to be higher in the aRNA hybridizations than in the poly(A)$^+$ RNA hybridizations (66 % as compared to 55 %). The comparisons were based on 15 genes showing absolutely no indication for differential expression on the opposite hybridization (data not shown). Occasionally, t/c ratios obtained by the two RNA preparation methods varied for high factors of more than 10 (e.g. *OA_a2B04*, Table 4.3, row 59)

The whole analysis revealed that both types of RNA preparations were equally sensitive resulting in the identification of equal numbers of regulated genes (48 and 50 respectively). Identified sets of genes by either type or RNA were not identical. Still, differential expression of 61 % of genes identified uniquely by one type of RNA preparation was also indicated (although weak) in the hybridizations of the other type of preparation. Thus, it was concluded that the real set of overlapping genes corresponded to 79 % rather than 46 %. The discrepancy was assumed to have one main cause: The 24 hat time point used for these evaluations was found to be away from peak induction by syringolin treatment in experiments described below (chapt. 4.2.2.2). As a result of this, t/c ratios of many genes were considered to be around detection limits of both RNA preparation methods.

Altogether, both RNA preparation methods were considered to be effective for future microarray hybridization experiments. They both were considered to deliver true indication for differential expression of identified genes. Yet, small amounts of only 2 µg of total RNA (or even less) sufficient as starting material were found to be a great advantage of linear amplification. Because gene sets identified by either method were not totally identical, all experiments described below were carried out with aRNA unless otherwise stated. By this means, variability resulting from technical biases was considered to by avoided. It is worthwhile to note that apart from gene *OA_b3C12* of unknown function (Table 4.3, row 37), all poly(A)$^+$ RNA genes were found to be differentially regulated at earlier time points in experiments described below (chapt 4.2.2.2 and 4.2.4.1).

4.2.2. Investigation of syringolin-induced transcription in the presence and absence of powdery mildew on wheat

Syringolin treatment was shown to be accompanied by the induction of genes in the host plant (chapt. 4.1). SSH screening for upregulated transcripts in powdery mildew-infected wheat treated with syringolin yielded 158 cDNA fragments corresponding to putatively activated genes. Indicative for true upregulation, a high percentage was found to display clear differential signals on dot-blotted membranes hybridized to radioactively labeled cDNA probes. Sequence analysis by blast searches in public DNA databases revealed that the vast majority of the cloned cDNA fragments clearly corresponded to transcripts of plant origin (blasts of some fragments did not return significant hits and therefore their origin remains unclear as yet).

Following our hypothesis, genes responding to syringolin in the host plant were expected roughly to fall into two different classes: (I) Syringolin genes: Syringolin-induced genes not contributing to the onset of HR and (II), HR genes: Syringolin-induced genes triggering or accompanying HR in colonized cells. However, present information did not allow drawing any conclusion on hypothesized HR specific regulation of certain genes. Therefore, next to the confirmation of syringolin-mediated regulation, getting insight into underlying mechanisms leading to this local cell death event was a major objective of the work.

Two different approaches to dissect between globally induced and infection site-specific induced upregulated genes were followed: First, gene induction was to be monitored in the presence and absence of powdery mildew on the plant (core experiment A; ceA, chapt. 4.2.2.2). Genes accompanying succession of HR in attacked cells were expected to be induced only in the presence, but not in the absence of *Bgt.* At the same time, induction by syringolin would be confirmed on several biological repetitions. In addition, the curative effect of syringolin was molecularly compared to the one of the fungicide cyprodinil (chapt. 4.2.3). Cyprodinil (cyp) was previously shown to effectively kill powdery mildew and prevent infected leaves from being overgrown by the fungus (Wäspi et al., 2001). The experimental setup is illustrated in Figure 4.16.

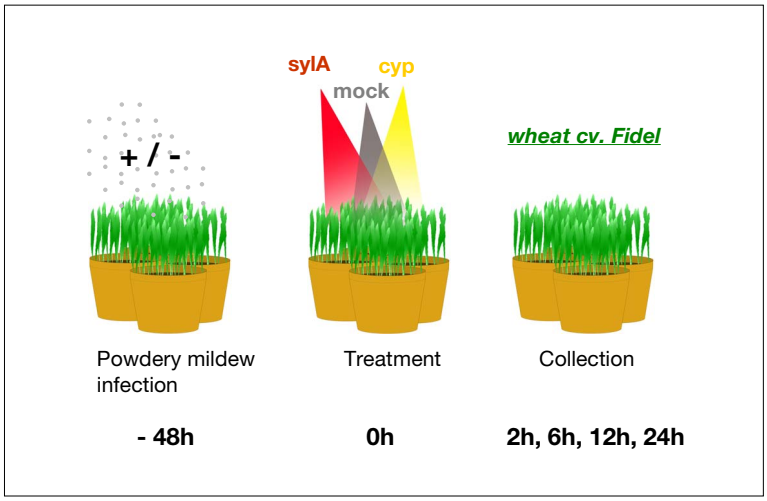

Figure 4.16: Experimental setup of core experiment A and cyprodinil treatment. Treatment was carried out on infected and uninfected plants. Leaf material was harvested at different time points after treatment.

4.2.2.1. Pilot experiments

Candidate genes hypothesized to be upregulated by the application of syringolin were derived from screening in a time frame of 2 h to 24 h after treatment with the agent (chapt 4.1). In order to get basal information about global timing of the transcriptional response to sylA, pilot experiments were carried out at the edges of the time frame 2 h and 24 h after syringolin application (hat).

Seven day-old seedlings of winter wheat (*Triticum aestivum* cv. Fidel) were infected at high spore density on the primary leaf with a highly virulent Swiss field isolate of wheat powdery mildew (*Blumeria graminis* f.sp. *tritici*). Forty-eight h after infection, the plants were sprayed with a 100 µM solution of syringolin A or a control solution. In addition, syringolin treatment was carried out on uninfected plants. Primary leaves were harvested at 2 h and 24 h after syringolin treatment and total RNA was extracted. Starting from poly(A)$^+$ RNA, microarray hybridization was carried out as described in Materials and Methods. All experiments were repeated twice. MA-plots representing average intensities as observed in the 2 experiments are shown in Figure 4.17.

As obvious from Figure 4.17B, numerous SSH-derived OA-genes were found to be upregulated at 24 hat. However, despite a clear displacement of expression ratios, approximately 50 % out of the subset of induced genes showed only weak induction of less than 2 fold. At the early side of induction, only marginal transcriptional changes were observed at 2 hat (Figure 4.17A). Genes found to be induced early are described later and listed in Table 4.9 (p.97).

Investigating differential expression in the absence of powdery mildew indicated elevated gene activation at the 24 hat time point. Visually, this resulted in an increased spread of data points in Figure 4.17D as compared to B. In the absence of powdery mildew on wheat, more genes were transcriptionally upregulated than in infected wheat. Thus,

despite the fact that screening for upregulated transcripts was carried out in the presence of powdery mildew on plants, the enrichment apparently targeted more transcripts generally induced by the compound.

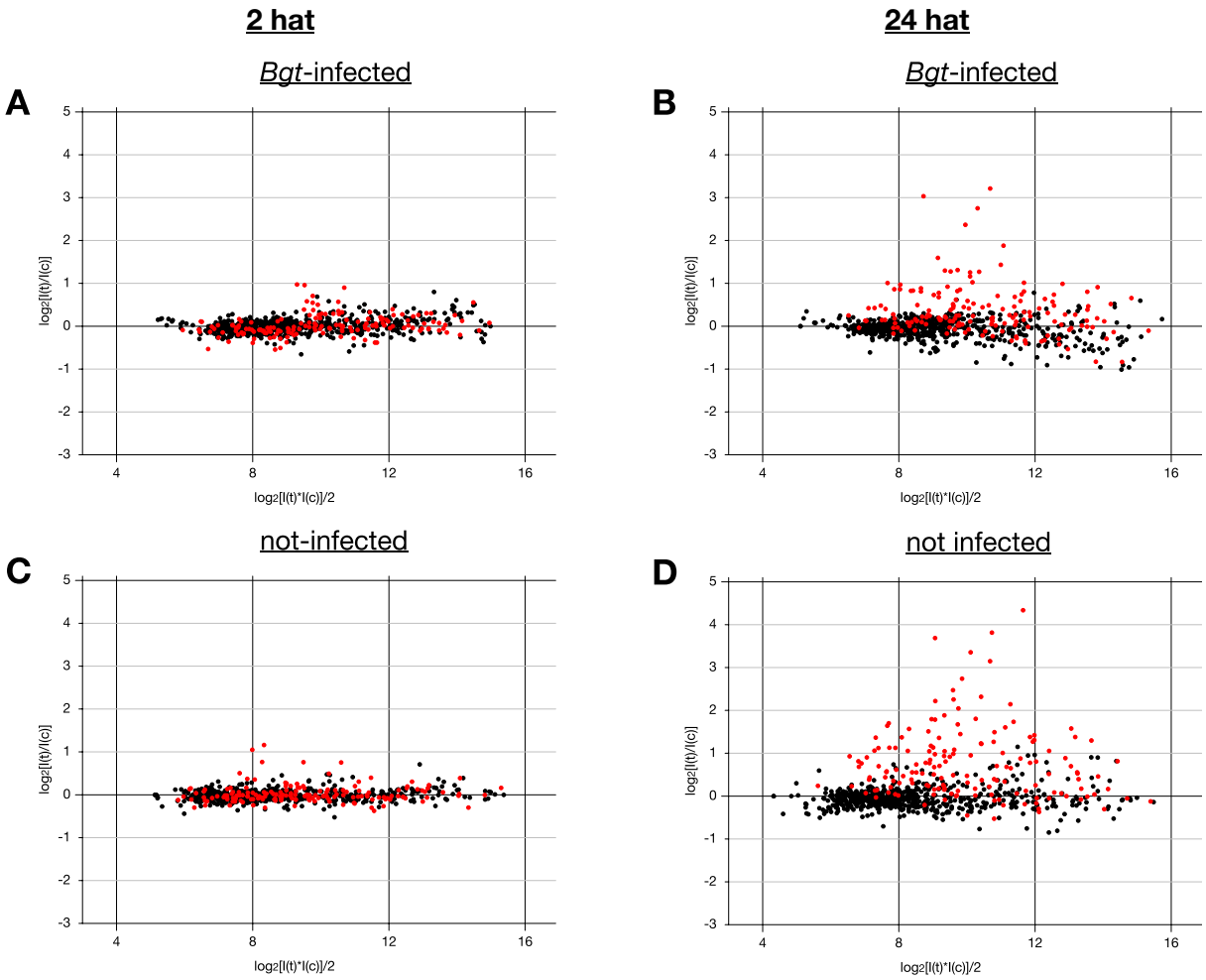

Figure 4.17: MA-plots visualizing average hybridization intensity ratios of 2 independent pilot experiments. Infected plants were treated with 100 µM syringolin and collection of primary leaves was done at 2 hat (A) and 24 hat (B). MA-plots corresponding to samples of uninfected plants collected at 2 hat (C) and 24 hat (D) are shown on the bottom. Red dots: Genes corresponding to OA-transcripts derived from SSH-screening on syringolin-treated plants are highlighted. Black dots: Genes corresponding to microarray subset 2 and 3 are shown (subset 4 is not shown). Microarray probe-labeling was done with polyA$^+$ RNA (dye-swap labeling was applied in the second experiment).

Together with the previous findings that nearly 50 % of syringolin-induced SSH genes were observed to be induced at the α time point (2 and 6 hat; chapt. 4.1.5), the above results indicated that a peak induction occurred between 6 and 24 hours after syringolin treatment. In addition, weak expression changes at early time points indicated that separate screening at the earlier α time point and the later β time point both yielded transcripts of

only a single overlapping induction peak. Consequently, core experiments were carried out at 12 and 24 hours after the application of syringolin.

4.2.2.2. Core experiment A (ceA)

Core experiments were carried out encompassing 3 independent biological repetitions. One experiment was labeled the opposite way (flip-dye experiment; chapt. 4.2.1.4). *Bgt*-infected and uninfected nine-day-old seedlings of *T .aestivum* cv. Fidel were sprayed with a 100 µM solution of sylA or control solution at 48 hours after the infection. Primary leaves were harvested at 12 h and 24 h after syringolin treatment and total RNA was extracted (illustrated in Figure 4.16). Following RNA amplification, microarray hybridization was carried out as described (Materials and Methods). MA-plots representing average intensities of infected plants are shown in Figure 4.18.

Comparing MA-plots corresponding to *Bgt*-infected samples revealed that significantly more genes were found to be activated at 12 hat as compared to 24 hat (Figure 4.18A and B). As observed previously (chapter 4.2.2.1), the transcriptional response to syringolin comprised predominantly genes derived from SSH-screening (red dots).

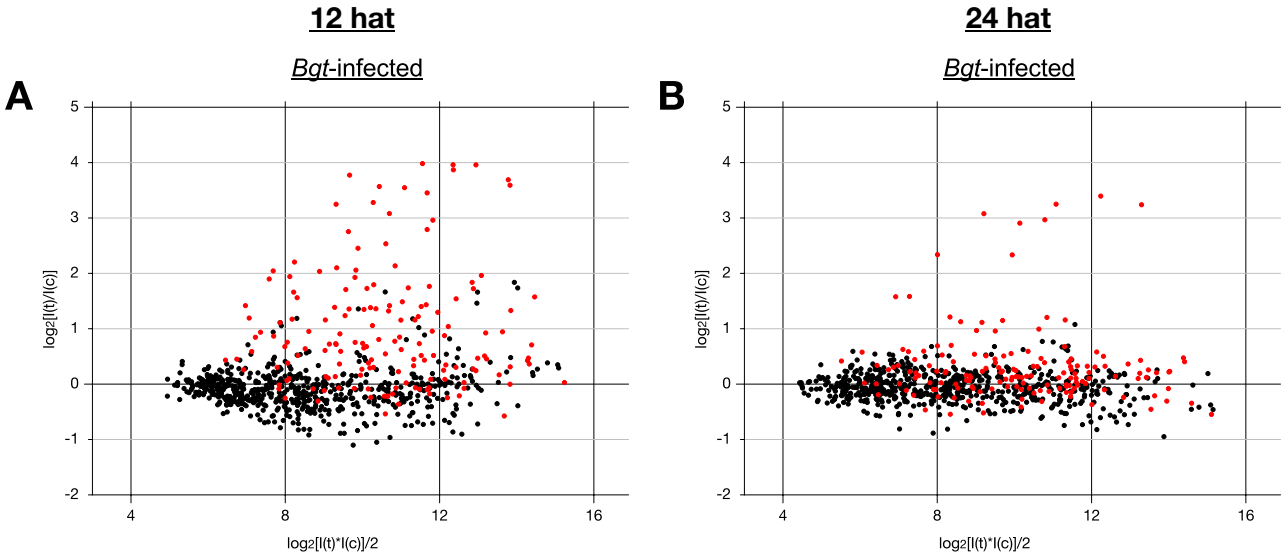

Figure 4.18: MA-plots visualizing average t/c ratios of three independent biological repetitions. Leaf material was collected at 12 hat (A) and 24 hat (B) from *Bgt*-infected plants sprayed with 100 µM sylA. Red dots: Genes corresponding to *OA*-transcripts derived from SSH-screening. Black dots: Genes corresponding to the cDNA AFLP-derived subset two and the control gene subset three are shown (the calibration control subset four is not shown).

Direct comparisons of t/c ratios revealed that none of the genes exhibited stronger induction at 24 hat than at 12 hat. On average, induction ratios in the absence of the fungus

was 1.9-fold reduced in the later time point (as judged for all genes induced at 12 hat). In order to identify genes specifically induced in the presence of *Bgt*, data derived from infected plant material was compared to data corresponding to uninfected wheat. MA-plots are shown in Figure 4.19.

Like in the presence of powdery mildew, significantly more genes were found to be upregulated at 12 hat when the pathogen was absent from the plants (Figure 4.19). Similarly, t/c ratios were found to be reduced at 24 hat as compared to 12 hat (2.3-fold reduction on average). As already indicated earlier (chapt. 4.2.2.1), syringolin treatment resulted in the induction of an elevated number of genes when plants were not previously infected with *Bgt*. As obvious by comparison of corresponding MA-plots from Figure 4.18 and Figure 4.19, the phenomenon occurred at both early and the late time points.

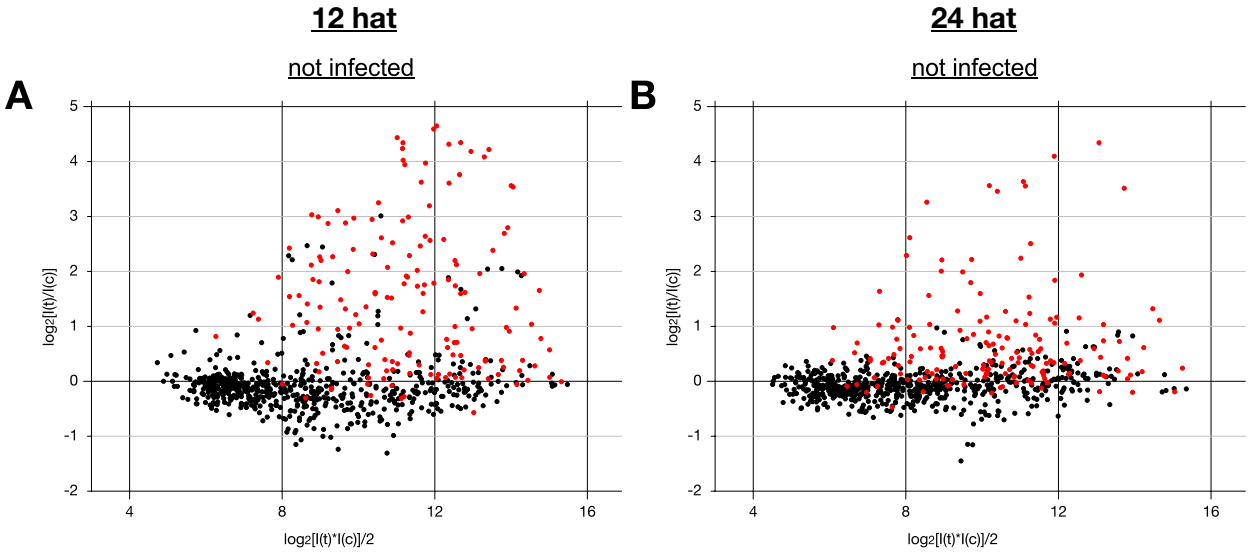

Figure 4.19: MA-plots visualizing average t/c ratios of three biological repetitions. Uninfected leaf material was collected at 12 hat (A) and 24 hat (B) after spraying with 100 µM sylA. Red dots: Genes corresponding to *OA*-transcripts derived from SSH-screening. Black dots: Genes corresponding to the cDNA AFLP-derived subset two and the control gene subset three are shown (the calibration control subset four is not shown).

To simplify matters, genes found to be significantly induced in at least one time point in data derived form either pre-infected or uninfected plants were listed in a single table. Significance was assigned by one-sample t-test statistics at a probability of error of less than five percent ($p < 0.05$), as described in chapt. 4.2.1.4. Results are presented in Table 4.4. Upon analysis of syringolin-induced transcriptional up- and downregulation in whole leaf material, 117 genes were identified to be regulated. Of these, the majority was found to be upregulated and only 6 genes (all of which members of the cDNA-AFLP-derived *RB* selection) were found to be slightly downregulated (rows 38, 39, 61, 79, 82, 84). Apart from

one exception (*RB_c116*; row 99), all genes were of plant origin as indicated by blast comparisons (origins of 4 genes were unpredictable).

Of all upregulated genes, 81% were members of the SSH-derived OA selection. Sorting regulated genes into functional groups revealed that the collection consisted of a large proportion of genes belonging to the carbohydrate metabolism (rows 19-44). A second group of remarkable size was assigned to ubiquitin-dependent protein catabolism (rows 1-12). All but four sequences were found to return significant blast hits with E-values smaller than 1.0E-10. Still, molecular and biological function of more than 20 % remained unknown. Induction of diverse functional groups and individual genes are described in chapter 4.2.5.

Table 4.4: t/c-ratios of syringolinA-induced differentially expressed genes. All experiments of ceA were repeated three times (the average t/c ratio is shown). Bold t/c ratios: P-value smaller than 5 % as assigned by one-sample t-test. Fragments forming contigs identified after data normalization are separated by horizontal lines. #N/A denotes that corresponding data were not available. Fragments are grouped according to biological and molecular function GO terms (Ashburner et al., 2000). IDs corresponding to probes detected exclusively in ceA (but not in the later core experiment B) were marked with a superscript 'A'.

	Putative function & [Blast hit]	EST ID	access. no#	E-val	ceA ($p < 0.05$) sylA on whole leaves			
					Bgt-infected		uninfected	
					12 hat	24 hat	12 hat	24 hat
	1	2	3	4	5	6	7	8
	Ubiquitin-dependent protein catabolism							
1	26S proteasome RPN9b subunit [Ta.1348]	***OA_b1F08***	AJ888663	1.00E-163	**2.2**	1.4	**4.0**	**1.8**
2	26S proteasome regulatory subunit [AP004778]	***OA_a2C11***	AJ888616	3.00E-62	**5.5**	1.5	**12.3**	**2.4**
3	26s proteasome regulatory subunit [CA602939]	***OA_b1C03***	AJ888656	1.00E-47	**2.7**	1.3	**5.4**	2.0
4	26s proteasome regulatory subunit [BJ287131]	***RB_226.4***	AJ888721	1.00E-44	1.6	1.2	**2.5**	1.9
5	20S proteasome alpha 4 subunit [O04861]	***OA_b1A08^A***	AJ888652	4.00E-37	1.1	1.0	**1.7**	1.6
6	20S proteasome alpha 5 subunit [CD936318]	***OA_b1G05***	AJ874091	0.00E+00	**3.9**	1.5	**6.9**	**3.8**
7	20S proteasome alpha 5 subunit [Q9LSU1]	***OA_b3D01***	AJ888705	1.00E-20	**2.6**	1.4	**5.5**	2.1
8	20S proteasome beta 2 subunit [BE494850]	***OA_b3H03***	AJ888717	2.00E-94	**1.7**	1.2	**2.9**	**2.3**
9	20S proteasome beta 3 subunit [CD866745]	***OA_b2G11***	AJ888689	6.00E-55	**2.6**	1.4	**4.2**	1.9
10	20S proteasome beta 5 subunit [BJ219720]	***OA_b3A12***	AJ888697	5.00E-64	**1.7**	1.1	**3.0**	**1.7**
11	20S proteasome beta 6 subunit [O64464]	***OA_b2C07^A***	AJ888678	2.00E-29	1.9	1.2	**2.0**	2.0
12	ubiquitin-associated protein (UBA) [AP004079]	***OA_b1D02^A***	AJ888657	5.00E-18	1.9	1.4	**2.5**	2.2
	Chaperones							
13	hsp 23.5 [Ta.203]	***OA_a1B01***	AJ874072	1.00E-133	**3.8**	1.3	**7.4**	1.5
14	hsp 23.6 [Ta.214]	***OA_a1H02***	AJ874076	1.00E-143	**3.5**	**1.9**	**7.9**	**3.0**
15	hsp 60 [L21006]	***OA_a1E07***	AJ888606	5.00E-49	**9.7**	**2.2**	**18.8**	**4.6**
16	hsp 60 [AC027038]	***OA_b1C09***	AJ874088	5.00E-35	**7.8**	**2.3**	**13.6**	**5.7**

Table 4.4 (continued)

	Putative function & [Blast hit]	EST ID	access. no#	E-val	ceA ($p < 0.05$) sylA on whole leaves *Bgt*-infected 12 hat	*Bgt*-infected 24 hat	uninfected 12 hat	uninfected 24 hat
	1	2	3	4	5	6	7	8
17	hsp 70 [P37900]	***OA_a3B09***	AJ874084	4.00E-42	**4.4**	1.5	**9.1**	**2.9**
18	hsp 70 [AF479058]	***OA_a3C06***	AJ888638	4.00E-36	1.3	0.8	**1.7**	0.9
	Carbohydrate metabolism (regulation)							
19	alcohol dehydrogenase ADH1 [BJ307901]	***OA_a1D06***	AJ888602	1.00E-131	**9.5**	2.3	**20.2**	**4.6**
20	alcohol dehydrogenase ADH1 [CD868456]	***OA_a2A05***	AJ888612	1.00E-163	**11.7**	2.0	**20.3**	**4.7**
21	phosphatases pleiotropic regulator PRL1 [Ta.6105]	***OA_b2C06***	AJ888677	0.00E+00	**1.7**	1.1	**2.0**	1.5
	Carbohydrate metabolism (TCA)							
22	2-oxoglutarate dehydrogenase (E1 subunit) [AP005199]	***OA_a3B02***	AJ874083	2.00E-91	**2.7**	1.4	**3.7**	**1.8**
23	succinyl-CoA-ligase beta subunit [AY180975]	***OA_b1D01***	AJ874089	3.00E-63	**2.3**	1.6	**3.5**	2.4
24	succinyl-CoA-ligase beta subunit [AY180975]	***OA_b1E11***	AJ874090	5.00E-38	**2.2**	1.4	**3.3**	2.1
25	citrate synthase [AP000367]	***OA_b1H11***	AJ874093	3.00E-59	**2.5**	1.3	**3.3**	2.2
26	aconitate hydratase (cytoplasmic) [BJ230524]	***OA_b3G05***	AJ874104	4.00E-57	1.5	1.1	**2.0**	1.4
	Carbohydrate metabolism (glycolysis)							
27	glyceraldehyde-3-phosphate dehydrogenase (Arabidopsis)	***GapC***	#N/A	#N/A	**2.8**	1.1	**4.1**	1.6
28	glyceraldehyde-3-phosphate dehydrogenase (cytosolic, wheat) [AF251217]	***OA_G3PDH Rsa***	AJ890249	1.00E-133	**3.3**	1.2	**3.8**	1.9
29	glyceraldehyde-3-phosphate dehydrogenase (cytosolic) (barley)	***BE437891***	BE437891	1.00E-67	**3.6**	1.1	**4.0**	1.8
30	glyceraldehyde-3-phosphate dehydrogenase (cytosolic, barley)	***BE437899***	BE437899	4.00E-81	**3.2**	1.1	**4.2**	1.6
31	glyceraldehyde 3-phosphate dehydrogenase (cytosolic) [P08477]	***OA_b3C10***	AJ874100	5.00E-68	**3.6**	1.3	**5.2**	1.6
32	fructose-bisphosphate aldolase [CD907979]	***OA_a1C12***	AJ888600	1.00E-141	**2.6**	1.2	**4.9**	**1.6**
33	enolase 1 (2-phosphoglycerate dehydratase 1) [CD454849]	***OA_a2G01***	AJ888626	8.00E-90	**4.6**	**3.0**	**7.3**	**4.9**
34	enolase 2 [P42895]	***OA_b2A09^A***	AJ888670	2.00E-44	1.5	0.9	**2.4**	1.5
35	pyruvate kinase-like protein [AY090539]	***OA_b1B10***	AJ888655	1.00E-151	**3.0**	1.2	3.1	2.5
36	pyruvate kinase [AY090539]	***OA_b2B04***	AJ888672	4.00E-30	2.9	1.2	**4.6**	1.7
37	2,3-bisphosphoglycerate-independent phosphoglycerate mutase [AP003255]	***OA_b2G09***	AJ874098	1.00E-90	**2.5**	1.3	**4.1**	1.5
38	fructose-1,6-bisphosphatase [CD894371]	***RB_97.3^A***	AJ888728	4.00E-40	**0.5**	0.8	**0.5**	0.9
	Carbohydrate metabolism (hexose metabolism)							
39	apospory-associated protein C [CA655323]	***RB_265.2^A***	AJ888723	3.00E-29	0.6	0.8	**0.5**	0.8
40	sucrose synthase 1 [CK209269]	***OA_a1C08***	AJ888599	2.00E-61	**3.3**	1.3	**6.5**	**2.2**
41	sucrose synthase 1 [P31922]	***OA_a3A03***	AJ888632	2.00E-63	**3.3**	1.2	**6.2**	1.6
42	sucrose synthase 1 [AF412038]	***OA_b2B06***	AJ888673	7.00E-40	**1.9**	0.9	**2.8**	1.0
43	sucrase (ferredoxin-like) [BQ458888]	***OA_b3C03***	AJ888702	6.00E-99	**1.8**	1.3	**3.4**	1.3
44	sucrase (ferredoxin-like) [Hv.12867]	***RB_c020^A***	AJ888720	6.00E-12	1.2	0.9	**2.3**	1.0

Table 4.4 (continued)

	Putative function & [Blast hit]	EST ID	access. no#	E-val	ceA ($p < 0.05$) sylA on whole leaves *Bgt*-infected 12 hat	*Bgt*-infected 24 hat	uninfected 12 hat	uninfected 24 hat
	1	2	3	4	5	6	7	8
	Lipid metabolism							
45	lecithin-cholesterol acyl transferase [CK157509]	***OA_b2D12***	AJ888681	1.00E-156	1.5	0.8	**2.3**	1.1
	Response to abiotic stimulus							
46	MDR-like ABC transporter [Ta.9295]	***OA_a2E02***	AJ888620	0.00E+00	**2.3**	1.2	**4.8**	**1.7**
47	MRP-like ABC transporter [BT009369]	***OA_a3D05***	AJ888640	1.00E-93	1.3	0.9	**2.1**	1.0
48	MRP-like ABC transporter [CA736782]	***OA_a3H01***	AJ888649	5.00E-96	**2.2**	1.1	**3.6**	1.0
49	glutathione-S-transferase/glutaredoxin [BE405126]	***OA_a3A01***	AJ888631	1.00E-144	**2.3**	1.3	**3.7**	**1.6**
50	glutathione S-transferase [CK217249]	***OA_a3G10***	AJ888647	9.00E-77	**1.7**	1.0	**3.1**	1.0
51	glutathione S-transferase [CA719629]	***OA_b1H08***	AJ874092	7.00E-81	**1.6**	1.2	**1.9**	1.3
52	glutathione S-transferase [CN013161]	***OA_b3D05***	AJ874102	1.00E-152	**12.9**	**9.4**	**11.8**	**11.4**
53	glutathione S-transferase [CK205115]	***RB_c017***	AJ873967 AJ873968	4.00E-25	**2.6**	1.5	**8.1**	1.9
54	cytochrome P450 [AF321867]	***OA_a1D09***	AJ888604	3.00E-67	2.4	1.0	**5.0**	**1.5**
55	cytochrome P450 [AP002839]	***OA_b1D06***	AJ888659	3.00E-47	**13.7**	**5.1**	**21.6**	**9.6**
56	cytochrome P450 [AP002839]	***OA_a1C04***	AJ888598	1.00E-78	1.7	0.8	**3.1**	1.0
57	temperature stress-induced lipocalin / Apolipoprotein D (APOD) [AY077702]	***OA_b1D11***	AJ888660	1.00E-142	2.5	1.2	**3.9**	1.7
	Response to biotic stimulus							
58	DMI1 (does not make infections) protein [CA027230]	***OA_b2E04***	AJ888682	0.00E+00	**2.9**	1.4	**4.6**	**2.0**
59	NBS-LRR disease resistance protein [AJ507096]	***OA_a1E08***	AJ874075	3.00E-49	**4.2**	**2.2**	**9.5**	**4.0**
	Response to endogenous stimulus							
60	ABI3-interacting protein 2 (abscisic acid insensitive interacting protein) [Ta.6216]	***OA_b2A06***	AJ888668	0.00E+00	1.6	0.7	**3.8**	1.2
61	Putative immediate-early salicylate-induced glucosyltransferase [Ta.23340]	***RB_c048[A]***	AJ874027	2.00E-29	1.3	1.2	0.8	**0.5**
	Signal transduction							
62	ligand-gated ion channel 2.8 [BQ659530]	***OA_a2B04***	AJ888614	5.00E-99	**15.8**	**5.0**	**25.0**	**11.0**
63	light repressible receptor protein kinase (Putative integral membrane protein) [BE517637]	***OA_b1B08***	AJ888654	5.00E-73	**4.1**	1.6	**8.6**	**3.0**
	Cell growth / maintenance (Cell cycle)							
64	prohibitin [AF236371]	***OA_a3C03***	AJ874085	1.00E-114	**2.8**	1.2	**5.9**	**2.4**
65	cell division control protein 48 homolog E (Transitional endoplasmic reticulum ATPase E) [Ta.28850]	***OA_a3F09***	AJ888645	0.00E+00	**2.1**	1.1	**2.9**	1.3
66	cell division control protein 48 homolog D (Transitional endoplasmic reticulum ATPase D) [BJ220165]	***RB_169.8***	AJ888718	2.00E-72	1.5	0.9	**2.2**	1.0
	Respiration							
67	BCS1-like protein / AAA-type ATPase-like protein [Ta.11182]	***OA_a1B08***	AJ874073	1.00E-130	**2.5**	1.5	**7.6**	1.4
68	alternative oxidase [AF174004]	***OA_a1E06***	AJ874074	4.00E-87	**8.4**	**2.2**	**16.3**	4.0
69	NADH dehydrogenase [BT009120]	***OA_a2B11***	AJ874077	1.00E-101	**6.9**	1.4	**12.2**	1.3

Table 4.4 (continued)

	Putative function & [Blast hit]	EST ID	access. no#	E-val	ceA ($p < 0.05$) sylA on whole leaves *Bgt*-infected 12 hat	*Bgt*-infected 24 hat	uninfected 12 hat	uninfected 24 hat
	1	2	3	4	5	6	7	8
	Aminoacid metabolism							
70	alanine aminotransferase 2 (glutamic-pyruvic transaminase 2) [CF133158]	***OA_a2D10***	AJ874079	0.00E+00	**3.3**	1.2	**5.7**	1.4
71	aspartate aminotransferase (cytoplasmic) [P37833]	***OA_b2F07[A]***	AJ888686	4.00E-82	1.6	1.4	1.5	**2.2**
	Protein metabolism							
72	lysyl-tRNA synthetase [BI480436]	***OA_a1E11***	AJ888608	0.00E+00	3.8	1.3	**7.7**	1.7
73	60S ribosomal protein L30 [AJ417524]	***OA_a2H04***	AJ888629	4.00E-41	1.6	1.1	**2.6**	1.5
74	(alanine) acetyltransferase [BE420036]	***OA_a3E08***	AJ888642	2.00E-82	**1.8**	1.3	**2.6**	1.4
75	valyl tRNA synthetase [AC084023]	***OA_b2E06***	AJ888683	3.00E-63	**1.9**	1.1	**3.0**	1.4
	Transport							
76	P-type ATPase (CA7 gene for) [AJ310846]	***OA_a2H06***	AJ888630	5.00E-99	2.1	1.3	**3.1**	1.3
77	voltage-dependent anion channel 1 [X77733]	***OA_b1F04***	AJ888662	2.00E-57	**6.7**	**3.0**	**15.4**	**6.1**
78	TipC / VPS13 - like protein [Ta.8446]	***OA_b1G10***	AJ888664	1.00E-148	1.8	1.1	**3.4**	1.7
79	Aquaporin PIP1 [BJ284089]	***RB_34.4[A]***	AJ888724	4.00E-22	0.5	0.7	**0.4**	0.8
80	harpin induced gene homolog (wheat)	***BE419039[A]***	BE419039	#N/A	1.5	1.1	**1.7**	0.9
	Development							
81	24 kDa seed maturation protein [CK202154]	***OA_b1D03[A]***	AJ888658	2.00E-52	1.1	1.0	**1.5**	1.1
82	gigantea mRNA [BG909229]	***RB_c001[A]***	AJ873936 AJ873963 AJ873964	1.00E-117	0.7	1.0	0.4	**0.4**
83	embryo-abundant protein [Ta.8017]	***RB_c118***	AJ873998 AJ873999	8.00E-16	**3.2**	1.2	**5.0**	0.8
84	Ripening-related protein-like [CD872650]	***RB_39.2[A]***	AJ888725	5.00E-67	0.8	0.7	**0.5**	**0.7**
85	Ripening-related protein-like	***RB_39A.1[A]***	#N/A	#N/A	0.8	0.7	**0.5**	0.7
86	B12D protein [BQ170981]	***RB_96.2[A]***	AJ888727	1.00E-31	**2.3**	**1.6**	**4.9**	**2.2**
	Hydrolase							
87	pir7b / salicylic acid-binding protein / Ethylene-induced esterase / Polyneuridine aldehyde esterase [Q43360]	***OA_b1B01***	AJ874087	2.00E-67	**15.5**	**9.5**	**16.9**	**17.1**
88	pir7b / salicylic acid-binding protein / Ethylene-induced esterase / Polyneuridine aldehyde esterase [CB864680]	***OA_b2A07***	AJ874094	3.00E-79	**12.0**	**10.5**	**11.6**	**20.2**
89	epoxide hydrolase [Ta.26236]	***OA_b2H01***	AJ888690	4.00E-69	**14.6**	**2.2**	**18.6**	**3.6**
90	epoxide hydrolase [Ta.26236]	***OA_b3B10***	AJ888700	2.00E-78	**5.8**	**2.0**	**15.7**	**3.5**
	Various							
91	NADPH-dependent oxidoreductase [CA682777]	***OA_a2C02***	AJ874078	3.00E-99	4.3	1.5	**7.8**	**2.2**
92	glucosyltransferase [CD490938]	***OA_a2C08***	AJ888615	1.00E-12	**1.9**	1.2	**2.9**	1.0
93	adenylate kinase (ATP-AMP transphosphorylase) [D10334]	***OA_a3A08[A]***	AJ874082	1.00E-50	1.4	1.3	**1.9**	1.4
94	nucleolar GTP-binding protein 1-like [BI751677]	***OA_b3F05[A]***	AJ888711	1.00E-109	1.3	1.2	1.3	**1.9**

Table 4.4 (continued)

	Putative function & [Blast hit]	EST ID	access. no#	E-val	ceA ($p < 0.05$) sylA on whole leaves *Bgt*-infected 12 hat	*Bgt*-infected 24 hat	uninfected 12 hat	uninfected 24 hat
	1	2	3	4	5	6	7	8
95	monooxygenase [CD452994]	***RB_53.1***	AJ888726	8.00E-85	**2.1**	1.0	**5.5**	1.3
96		***RB_53.3***	#N/A	#N/A	1.5	0.9	**3.5**	1.2
97		***RB_53.6***	#N/A	#N/A	**2.2**	1.2	**5.4**	1.4
98		***RB_53.7***	#N/A	#N/A	1.9	1.0	**4.6**	1.3
	Fungal							
99	fungal 28S ribosomal RNA [AY064705]	***RB_c116[A]***	AJ888238	4.00E-71	**2.0**	**2.1**	1.4	1.0
	Unknown							
100	unknown [Hv.10128]	***OA_a1A03***	AJ888591	1.00E-158	**3.3**	1.6	**6.1**	**2.1**
101	unknown [D22421]	***OA_a1D08***	AJ888603	8.00E-06	**10.9**	**7.5**	**19.9**	**12.4**
102	no significant hit	***OA_b1A06***	AJ874086	#N/A	**11.9**	**8.4**	**24.1**	**11.8**
103	no significant hit	***OA_b2B07***	AJ888674	#N/A	**15.5**	**7.8**	**18.2**	**11.7**
104	unknown [CN011234]	***OA_a1H06***	AJ888610	3.00E-84	1.7	1.0	**3.5**	1.3
105	unknown [CN013234]	***OA_a2E09***	AJ888622	1.00E-51	**4.1**	1.5	**8.2**	**3.1**
106	unknown [BQ579520]	***OA_a2E10***	AJ888623	1.00E-173	1.2	0.9	**2.0**	1.3
107	unknown [CK215536]	***OA_a2F04***	AJ888625	0.00E+00	**2.2**	1.1	**3.6**	1.3
108	unknown fused to ABI3-interacting protein 2 [BQ789184]	***OA_a2H03***	AJ888628	1.00E-88	**1.9**	1.0	**3.0**	1.1
109	unknown [BQ768185]	***OA_a3E09***	AJ888643	1.00E-104	2.6	1.2	**5.3**	1.4
110	nuclear coiled-coil protein [Ta.16935]	***OA_b1A07[A]***	AJ888651	0.00E+00	1.3	1.1	**2.1**	1.5
111	unknown [Ta.8833]	***OA_b2C04***	AJ888675	1.00E-149	**2.7**	1.3	**4.4**	2.1
112	unknown [Ta.12787]	***OA_b2F09***	AJ874097	6.00E-49	**3.4**	1.3	**6.0**	**2.1**
113	unknown [BJ291998]	***OA_b2G10***	AJ888688	3.00E-66	**1.8**	1.2	**4.3**	1.3
114	unknown [BQ789018]	***OA_b3E03***	AJ888708	1.00E-176	**3.2**	1.5	**4.8**	**2.0**
115	unknown [BU100203]	***OA_b3E09***	AJ874103	0.00E+00	1.6	1.1	**2.7**	1.5
116	unknown [AW448695]	***RB_240.4[A]***	AJ888722	2.00E-55	1.4	1.1	**2.4**	1.6
117		***RB_240.5[A]***	#N/A	#N/A	1.3	1.1	**2.3**	1.6
118	unknown [AK103640]	***OA_a2H01[A]***	AJ888627	2.00E-98	1.2	0.9	**1.8**	1.4
119	unknown [CK160653]	***OA_b3B01[A]***	AJ888698	2.00E-46	1.1	1.0	**1.6**	1.2
120	unknown [BE488635]	***OA_b3C01[A]***	AJ888701	9.00E-96	0.9	1.1	0.8	**1.8**
121	no significant hit [CX630958]	***OA_a2D05***	AJ888618	2.20E-01	**3.7**	1.5	**7.9**	**2.0**
122	no significant hit [Str.21194]	***OA_a3C05***	AJ888637	5.40E-01	1.2	0.9	**2.4**	1.3
123	no significant hit	***RB_17.2***	#N/A	#N/A	**1.9**	1.0	**3.2**	1.3
124	no significant hit	***RB_17.3***	AJ888719	#N/A	**2.3**	1.1	**3.7**	1.5

Comparison of t/c-ratios corresponding to infected and uninfected samples revealed a general tendency of elevated induction ratios in the absence of the fungus. On average, induction ratios were found to be 1.6 (± 0.5)-fold higher at 12 hat when plants were not previously infected with *Bgt*. The only exceptions found to exhibit reciprocal proportions

were probes *OA_b2A07* and *RB_c116* (Table 4.4; rows 88 & 99). Yet, t/c ratios of *OA_b2A07*, a wheat homologue of the rice pir7b esterase were only very slightly elevated in the presence of *Bgt* and the effect was restricted to the earlier 12 hat time point whereas the t/c ratio of infected samples at 24 hat was reduced 2-fold again. Conversely, t/c ratios of *RB_c116* were two-fold elevated in the presence of *Bgt* at both, 12 hat and 24 hat time point. Based on blast analysis *RB_c116* was found to correspond to 28S rRNA of fungal origin. As a possible cause for seeming upregulation, a normalization bias originating from elevated amounts of fungal RNA in control treatment samples was taken into consideration. Indeed the effect was expected to result in over-correction towards positive log ratios (chapt. 5.1.2, p.122). Actually, MA-plots corresponding to leaf material collected at 12 hat rather indicated slight over-correction towards negative log ratios (Figure 4.18A and Figure 4.19A), a fact that was hypothesized to result from slight over correction by ILMC. Moreover, the array totally contained 10 fragments corresponding to fungal transcripts but *RB_c116* was the only one exhibiting elevated expression upon syringolin treatment (data not shown). Consequently, the stronger signals derived from syringolin-treated samples in the case of *RB_c116* were considered to reflect biological action rather than a technical bias.

Illustrative for the overall decrease of t/c ratios in the presence of *Bgt*, syringolin treatment resulted in a clear down-shift of the OA-subset on MA-plots visualizing direct comparisons of *Bgt*-infected and uninfected samples (Figure 4.20). Investigation of microarray hybridization results showing gene regulation at 72 hours after infection (hai) revealed numerous genes being upregulated in response to powdery mildew infection. Upregulation was mainly restricted to genes of the RB-subset and control genes and downregulation occurred sparsely. Conversely, two major differences were observed when infected and uninfected plants were sprayed with syringolin 48 hours after inoculation. First, as a result from induction by syringolin application, the whole OA-subset was shifted to the right on the X-axes. Second, the OA-subset was shifted down on the Y-axes resulting from reduced induction in the presence of the fungus (Figure 4.20B).

As possible causes for reduced transcriptional responsiveness in the presence of powdery mildew, different factors were accounted to contribute to the reduction of t/c ratios. Theoretical considerations included various scenarios of fungus-mediated inhibition of syringolin responses (chapt 5.2, p.123). Since it could not be excluded that the presence of *Bgt* on the leaf surface decreased syringolin accessibility of plant tissue, mathematical compensation for such an effect was attempted by global standard deviation (SD) regularization (scale normalization by Yang et al., 2002b).

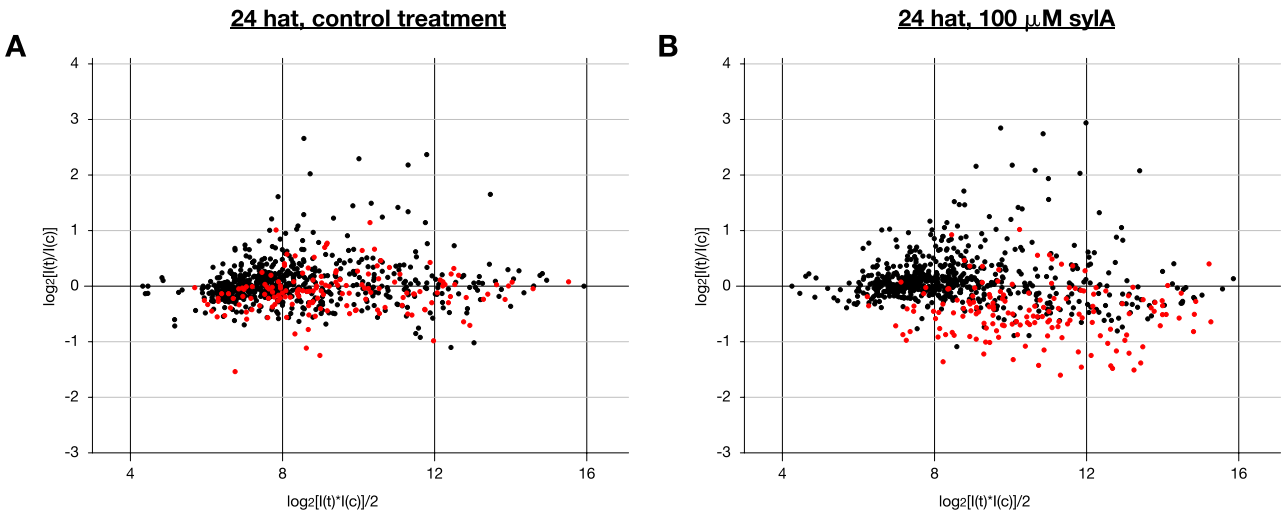

Figure 4.20: Effect of infection on syringolin action. Infected and uninfected wheat leaves were collected at 72 hai and subjected to microarray investigation. Leaves were sprayed with control solution (A) or 100 µM sylA (B) at 48 hai. Data correspond to a single-pass experiment hybridized to target cDNA derived from poly(A)$^+$ RNA. Red dots: Genes corresponding to *OA*-transcripts derived from SSH-screening. Black dots: Genes corresponding to the cDNA AFLP-derived subset two and the control gene subset three are shown (the calibration control subset four is not shown).

After SD regularization, average t/c ratios between infected and uninfected samples were found to be more constant and were reduced by a factor of only 1.2 on average instead of 1.6 at the 12 hat time point of ceA (data not shown). Genes exhibiting t/c ratios differing more than 1.5-fold between infected and uninfected experiments after global SD normalization are listed in the Appendix (Table 8.4). Based on that, five genes were identified to exhibit increased transcription activity in the presence of *Bgt.* Next to *OA_b2A07* and *RB_c116* identified previously, the list contained the second wheat homologue of *Pir7b* (*OA_b1B01*), a glutathione S-transferase (GST; *OA_b3D05*) and one fragment of unknown function (*OA_b2B07*). Except for *RB_c116*, elevated induction in the presence of *Bgt* was restricted to 12 hat and t/c ratios were similar at the later 24 hat time point.

The finding of the glutathione-S-transferase (GST) fragment *OA_b3D05* was opposed to the presence of other GSTs in the opposite group, exhibiting more than 1.5-fold higher induction in the absence of *Bgt* (*OA_a3G10,* row 12 and *RB_c017,* row 13; Table 8.4). Interestingly, *OA_b3D05* was also found to exhibit epidermis-specific induction 24 hours after infection with barley powdery mildew (Bruggmann et al., 2005). The two wheat *pir7b* homologues showed 82 % and 80 % sequence identity to the rice *Pir7b* for *OA_b1B01* and *OA_b2A07* respectively, and 93 % identity to each other and they both aligned to the central region of the rice mRNA. An alignment is shown in the Appendix (Figure 8.4, p.214). The *Pseudomonas*-induced gene *Pir7b* (accession #Z34270) is an indicator for the action of

syringolin on rice (Wäspi et al., 1998a). It encodes an esterase with activity towards naphthol AS-esters but nothing is known about its biological function. In addition, *OA_b2B07*, a cDNA fragment of unknown function was identified. On the other hand, 20 genes were still found to exhibit more than 1.5-fold stronger induction in the absence of *Bgt* after SD-regularization, indicating that powdery mildew infection indeed dampened syringolin action.

To sum-up, investigation of transcriptional induction of genes represented on microarray series 7 by syringolin revealed that a large proportion of genes obtained by SSH-screening exhibited responsiveness. Yet, apart from two exceptions, none of the genes was induced stronger in the presence of *Bgt*. Moreover, t/c ratios were found to be significantly reduced when plants were infected with powdery mildew prior to syringolin treatment as compared to sylA treatment of uninfected plants. It was concluded that the response to syringolin in *Bgt*-infected wheat leaves was diminished by some global effect and SD-regularization did not allow to mathematically compensate completely.

4.2.3. Cyprodinil impact on host gene transcription

As shown previously, spray application of the contact fungicide Cyprodinil (cyp) effectively killed powdery mildew on wheat leaves (Wäspi et al., 2001). In contrast to treatment with sylA, cyp treatment did not provoke autofluorescence of infected cells (shown in chapt. 3.3). However, in both cases disappearance of the parasite and thus disappearance of virulence factors interfering with the host transcriptome was hypothesized to result in re-induction/-suppression of transcripts in order to re-establish status quo by the infected cell. With the aim of being able to distinguish putative candidates involved in induction of HR from re-induced transcripts, cyprodinil experiments were carried out in parallel to ceA.

Bgt-infected and uninfected nine-day-old seedlings of *T .aestivum* cv. Fidel were sprayed with a 200 ppm solution of cyp or control solution at 48 hours after the infection. Primary leaves were harvested at 12 h and 24 h after treatment. Three biological repetitions including dye-swaps were carried out only in one case where pre-infected leaves were harvested at 12 hat. For the rest, data correspond to single experiments. Genes found to be significantly induced as judged by one-sample t-test statistics at a probability of error of less than five percent ($p < 0.05$) in the pre-infected sample at 12 hat are listed in Table 4.5.

Table 4.5: Genes regulated by application of 200 ppm cyprodinil (p < 0.05). Time point 12 hat pre-infected with *Bgt* was repeated three times (column 5). The average t/c ratio is shown and fields are green colored Bold t/c ratios: P-value smaller than 5 % as assigned by one-sample t-test. Other t/c ratios correspond to single-pass experiments (columns 6-8). Biological and molecular function GO terms (Ashburner et al., 2000) are listed in column 9.

	Putative function & [Blast hit]	EST ID	access. no#	E-val	Cyprodinil, whole leaf *Bgt*-infected 12 hat	*Bgt*-infected 24 hat	uninfected 12 hat	uninfected 24 hat	GO
	1	2	3	4	5	6	7	8	9
	Cyp-induced genes also regulated by sylA								
1	sucrose synthase 1 [CK209269]	***OA_a1C08***	AJ888599	2.00E-61	**2.1**	2.5	2.5	2.6	Carbohydrate metabolism
2	unknown [D22421]	***OA_a1D08***	AJ888603	8.00E-06	**2.0**	1.6	2.0	1.4	Unknown
3	PDR-like ABC transporter [CD881196]	***OA_a3A04***	AJ874081	1.00E-88	**4.6**	3.8	5.0	4.2	Response to abiotic stimulus
4	glutathione S-transferase [CK205115]	***RB_c017***	AJ873967 AJ873968	4.00E-25	**2.8**	2.6	2.7	2.3	Response to abiotic stimulus
5	embryo-abundant protein [Ta.8017]	***RB_c118***	AJ873998 AJ873999	8.00E-16	**1.5**	1.2	1.3	0.7	Development
	Cyp-induced genes not regulated by sylA								
6	WIR2 (thaumatin-like protein)	***X58394***	X58394	#N/A	**1.6**	2.1	1.2	0.9	Response to external stimulus
7	peptide transporter protein [AJ495773]	***RB_c021***	AJ873978 AJ874008 AJ874009	1.00E-33	**1.7**	1.8	1.6	1.7	Transport
8	unknown [#N/A]	***RB_c037***	AJ874025 AJ874026	2.10E+00	**2.1**	2.6	1.6	2.1	unknown
9	similar to WAK4 (wall-associated kinase) [Q9LWG6]	***RB_c052***	AJ874036 AJ874037	1.00E-08	**2.4**	2.7	2.4	2.5	Cell elongation
10	beta-1,3-endoglucanase [Y18212]	***RB_c091***	AJ874012	1.00E-100	**1.6**	1.7	1.2	1.3	Response to external stimulus

As evident from Table 4.5, only a small set encompassing 10 genes was shown to be reproducibly induced by cyprodinil. t/c ratios were found to be relatively small. Five of the genes were also induced by syringolin (Table 4.4, rows 40, 53, 83 & 101; Table 4.7, row 42). The products of the two genes *OA_a3A04* and *RB_c017* exhibited homology to an ABC transporter and a GST, enzymes known to be involved in the detoxification of xenobiotics (Edwards et al., 2000; Martinoia et al., 2002; Windsor et al., 2003; Reade et al., 2004). A third cDNA fragment (*OA_a1C08*) exhibited homology to sucrose synthase and no clear function was known for fragments *OA_a1D08* and *RB_c118*. Five genes found to be transcriptionally induced by the fungicide were not responding to sylA treatment (Table 4.5, rows 6-10). In conclusion it was found that the syringolin-specific gene set was largely unaffected by the application of the contact fungicide cyprodinil.

4.2.4. Tissue specificity of syringolin-induced transcription

Activity of syringolin in powdery mildew-infected wheat leaves was described to occur in a translaminar manner (Wäspi et al., 2001). This could either be explained by the generation of a signal translocated to the opposite side of the leaf. Alternatively, syringolin could be physically translocated to the opposite side and directly induce transcriptional changes. Either way, it was likely that the general response to syringolin occurred ubiquitous in virtually all cells along the cross section of the leaf. Conversely, syringolin mediated cell death was shown to be restricted to *Bgt*-infected epidermal cells (chapt. 3.3, Figure 3.11). Therefore manual separation of epidermis and mesophyll by stripping off epidermis from *Bgt*-infected syringolin-treated leaves was used to display putative epidermis specific syringolin action on genes involved in the accomplishment of HR. In addition, enrichment of epidermal transcripts by stripping off epidermis from the remainder of the leaves may also lower the detection limit of transcriptional changes restricted to colonized epidermal cells.

4.2.4.1. Core experiment B (ceB)

Bgt-infected nine day-old seedlings of *T .aestivum* cv. Fidel) were sprayed with a 100 µM solution of syringolin A or control solution at 48 hours after the infection. Primary leaves were harvested and the abaxial epidermis was immediately peeled off the remainder of the leaf. Epidermis and remaining leaf tissue was stored separately and subsequently subjected to RNA isolation. For simplicity, samples of stripped abaxial epidermis were referred to as 'epidermis samples' and remaining leaf samples containing less epidermal tissue were referred to as 'mesophyll samples'. Epidermis stripping was carried out during two collection periods from 1.5 to 8 hat (referred to as -08 hat) and from 24 to 32 hat (referred to as -32 hat). The experimental setup is illustrated in Figure 4.21.

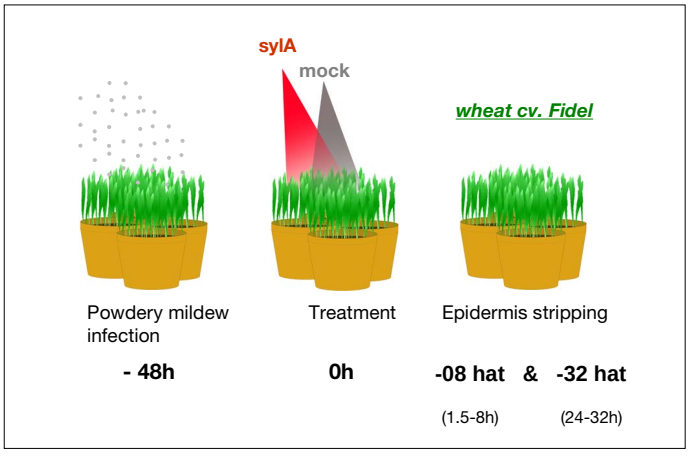

Figure 4.21: Experimental setup of core experiment B. Treatment was carried out on infected plants. Epidermis stripping was carried out during the earlier -08 hat and the later -32 hat period. Epidermis and mesophyll samples were frozen separately.

Relating signal intensities of probes of interest to signals derived from probes exclusively expressed in the mesophyll had already been proven to allow for the identification of epidermis specific gene expression (Bruggmann et al., 2005). The gene encoding ribulose bisphosphate carboxylase (rubisco) was used as a standard and was represented by eight different probes on the microarray. A specificity factor called epidermis specificity factor (ϵ_s) was calculated as described in Figure 4.22. ϵ_s-factors describe the allocation of the signal to the epidermis and the mesophyll.

$$\varepsilon_s = \frac{I_{x_{epi}}}{\rho_{epi}} \Big/ \frac{I_{x_{mes}}}{\rho_{mes}}$$

$I_{x_{epi}}$ = Spot intensity in the epidermal sample of an arbitary gene.

$I_{x_{mes}}$ = Spot intensity in the mesophyll sample of an arbitary gene.

ρ_{epi} = Average rubisco intensity in the epidermal sample

ρ_{mes} = Average rubisco intensity in the mesophyll sample

Figure 4.22: Equation used for calculation of the epidermis specificity factor (ϵ_s).

Estimations of cell type proportions (Appendix, p.200) indicated that the stripping of the epidermis resulted in a 10-fold enrichment of epidermal tissue in epidermis samples. In order to properly interpret results corresponding to ϵ_s, several variables such as epidermis, infected cells and stomata cells proportions had to be determined (Appendix, chapt. 8.5.1, 8.5.2 and 8.5.3) to simulate resulting ϵ_s-factors under different conditions (data not shown). By this means, it was found that arbitrary genes expressed exclusively in the mesophyll would exhibit ϵ_s around 0.9. Lower ϵ_s than 0.9 denoted exotic genes exhibiting higher expression in the adaxial part of the leaf and ϵ_s values as low as 0.0 were found to be theoretically possible. Balanced expression between epidermis and mesophyll was found to result in ϵ_s of 1.75 (Appendix, chapt. 8.7, p.200). Conversely, ϵ_s, higher than 2.0 strongly indicated expression of corresponding genes in the abaxial epidermis. With respect to the mesophyll, simulations revealed that mesophyll specificity was indicated at a narrow range of ϵ_s-factors between 0.9 and 1.3. In addition, ϵ_s-factors were assessed for reliability by one-sample t-test. High reliability was indicated if log ratios differed from 0 with a probability of error of less than five percent ($p < 0.05$). Resulting average ϵ_s-factors of a selection of probes used as controls to monitor ϵ_s reliability is presented in Table 4.6.

Table 4.6: Control genes demonstrating significance of ϵ_s-factors. All experiments of ceB were repeated three times (the average ϵ_s is shown). ϵ_s was calculated by comparison of data corresponding to syringolin-treated epidermis and mesophyll (columns 5 & 6). Bold ϵ_s-factors: ϵ_s exceeding threshold limit of 2.0 and exhibiting p-values smaller than 5 % as assigned by one-sample t-test. #N/A denotes that corresponding data were not available. Different types of control genes were grouped together: Fungal probes were derived from AFLP cloning (subset 2), *TaGLP4* was described to be specifically expressed in the epidermis (Schweizer et al., 1999a), *Bgh*-specific non-host PR genes were also derived from AFLP cloning (subset 2) and rubisco standards were members of control probes (subset 3) with the exception of *OA_b3E01*.

	Putative function & [Blast hit]	EST ID	access. no#	E-val	ceB (p < 0.05) sylA-treated infected leaves -08 hat ϵ_S	-32 hat ϵ_S
	1	2	3	4	5	6
	fungal probes					
1	cDNA clone D01275 similar to retinal short-chain (*Bgh*) [AW792581]	***RB_43A.5***	AJ888230	1.00E-107	2.9	**4.3**
2	cDNA clone D01017 similar to s-adenosylmethionine synthetase (*Bgh*) [AW792123]	***RB_96.1***	AJ888231	8.00E-86	3.3	**3.3**
3	glyceraldehyde 3-phosphate dehydrogenase (*Bgh*) [X99732]	***RB_c122***	AJ888233	1.00E-71	2.2	**3.0**
4	cDNA clone C00255 (*Bgh*) [AW788184]	***RB_c010***	AJ888234	3.00E-68	2.0	2.4
5	T4 cDNA library under conditions of nitrogen deprivation (*Botrytis cinerea*) [AL115778]	***RB_c082***	AJ888237	1.00E-11	3.0	**5.7**
	control PR-gene					
6	TaGLP4 (germin-like protein)	***AJ237942***	AJ237942	#N/A	**7.9**	**6.3**
	Bgh-*specific non-host PR genes*					
7	chromosome 1 YAC yUP8H12 complete sequence, *A. thaliana* [CA662411]	***RB_74.2***	AJ885880	4.00E-11	**2.9**	**4.7**
8	lectin-like protein kinase, *O. sativa [Q7XIH4]*	***RB_78.2***	AJ885881	6.00E-14	2.0	**4.0**
9	ethylene-responsive small GTP-binding protein, Lycopersicon esculentum [U38471]	***RB_339.8***	AJ874032	3.00E-37	**2.0**	**2.1**
10	NAD- dependent formate dehydrogenase, mitochondrial precursor, *H. vulgare* [D88272]	***RB_c045***	AJ874031 AJ874060 AJ874064	1.00E-63	**2.2**	**4.2**
11	Putative VAMP-associated protein, *A. thaliana* [Q9SHC8]	***RB_c099***	AJ873983	2.00E-15	**6.1**	**8.2**
12	Polyphosphoinositide binding protein Ssh1p, *Glycine max* [AF024651]	***RB_c107***	AJ873985	4.00E-51	**5.9**	**7.9**
	mesophyll-specific rubisco standards					
13	ribulose-bisphosphate carboxylase small subunit (barley)	***BE437451***	BE437451	#N/A	1.1	1.0
14	ribulose-bisphosphate carboxylase small subunit (barley)	***BE437892***	BE437892	#N/A	1.1	1.1
15	rubisco 3' end (wheat)	***RUB_3prime***	#N/A	#N/A	0.8	0.8
16	rubisco 5' end (wheat)	***RUB_5prime_2***	#N/A	#N/A	1.1	1.2
17	rubisco middle part (wheat)	***RUB_5prime_3prime***	#N/A	#N/A	1.2	1.1
18	rubisco (small subunit) [AB042066]	***OA_b3E01***	AJ888707	4.00E-55	0.8	0.9

Genes used as controls for ϵ_s (Table 4.6) were selected not to exhibit altered expression upon syringolin treatment (data not shown). Fungal probes derived form *Bgh* (rows 1-5) were found to crosshybridize also with the wheat powdery mildew (*Bgt*) and expectedly exhibited epidermis specificity higher than two. The wheat germin-like *TaGLP4*

(row 6) was described to exhibit strong induction upon infection with the wheat powdery mildew up to three days after infection (dpi). The induction was found to be located in the epidermis (Schweizer et al., 1999a). As shown in Table 4.6, the corresponding probe also exhibited high ϵ_s values at the early and late time point (around 56 and 80 hai) in the infected samples sprayed with syringolin (columns 5 & 6). Furthermore, several novel PR-genes from wheat exhibiting epidermis specific expression at 24 h after infection with the nonhost barley powdery mildew (*Bgh*) were identified recently (rows 7-12, Bruggmann et al., 2005). Of those, numerous were found to exhibit strong epidermis specificity also at the later time points after infection with the compatible wheat powdery mildew (*Bgt*). Conversely, the probes used as references corresponding to rubisco (rows 13 to 18) exhibited average ϵ_s-factors of 1 and variation was found to be low. In summary, ϵ_s-factors of control genes presented in Table 4.6 were found to be reliable indicators of tissue-specific gene expression.

In order to investigate syringolin responsiveness in ceB, average t/c ratios between corresponding samples treated with syringolin or control solution were calculated. Induction of gene transcription was judged for reliability by one-sample t-test (chapter 4.2.1.4). Significance was assigned at a probability of error of less than five percent ($p < 0.05$). Genes found to be significantly induced at one time point at least, in data derived form either mesophyll or epidermis samples, are listed in a single table. For the sake of completeness, the table was extended to additionally contain genes identified in ceA which were not found to exhibit significant gene regulation in ceB. The results are listed in Table 4.7 (below).

Investigation of gene regulation in epidermis and mesophyll samples derived from syringolin treatment of *Bgt*-infected wheat resulted in the identification of 101 probes. Thereof, 80 % belonged to the SSH-derived *OA*-subset one. Comparison to the gene set identified in ceA (Table 4.4) revealed that 81 % of the genes identified previously also showed significant regulation in ceB (shown later in Figure 4.24).

Table 4.7: t/c-ratios of syringolinA-induced differentially expressed genes in epidermis and mesophyll (derived from *Bgt*-infected wheat leaves). All experiments of ceB were repeated three times (the average t/c ratio is shown). Bold t/c ratios: ($p < 0.05$) as assigned by one-sample t-test. Fragments forming contigs identified after data normalization are separated by horizontal lines. #N/A denotes that corresponding data were not available. Fragments are grouped according to biological and molecular function GO terms (Ashburner et al., 2000). Average ϵ_s calculated by comparison of data corresponding to syringolin-treated epidermis and mesophyll are printed in red (columns 7 & 10). ϵ_s values found to be reliable ($p < 0.05$) according to t-test statistics were printed in bold letters when exceeding a threshold limit of 2.0. Probes detected exclusively in ceA were appended and corresponding IDs were marked with a superscript 'A' followed by the row number indicating relative positions in Table 4.4. IDs corresponding to probes detected in ceB only were marked with a superscript 'B'. Probes exhibiting higher epidermal t/c ratios at the early time point are highlighted by an arrow (⇦).

	Putative function & [Blast hit]	EST ID	access. no#	E-val	ceB ($p < 0.05$) sylA on epidermis and mesophyll (*Bgt* infected leaves) -08 hat epi	-08 hat mes	-08 hat ϵ_S	-32 hat epi	-32 hat mes	-32 hat ϵ_S	
	1	2	3	4	5	6	7	8	9	10	
	Ubiquitin-dependent protein catabolism										
1	polyubiquitin [X69422]	***OA_a1A10^B***	AJ888594	3.00E-63	1.6	**1.7**	1.3	1.0	1.1	1.5	
2	26S proteasome RPN9b subunit [Ta.1348]	***OA_b1F08***	AJ888663	1.00E-163	**2.6**	**2.7**	1.1	**1.8**	1.3	**2.9**	
3	26S proteasome regulatory subunit [AP004778]	***OA_a2C11***	AJ888616	3.00E-62	**15.9**	**15.1**	1.4	**3.9**	**2.5**	**3.5**	⇦
4	26s proteosome regulatory subunit [CA602939]	***OA_b1C03***	AJ888656	1.00E-47	**4.8**	**4.9**	1.5	2.3	**1.5**	**3.2**	
5	26s proteasome regulatory subunit [BJ287131]	***RB_226.4***	AJ888721	1.00E-44	**1.5**	1.5	1.2	1.5	1.2	**2.8**	⇦
6	20S proteasome alpha 5 subunit [CD936318]	***OA_b1G05***	AJ874091	0.00E+00	**2.9**	**2.9**	0.8	**2.1**	1.3	2.0	
7	20S proteasome alpha 5 subunit [Q9LSU1]	***OA_b3D01***	AJ888705	1.00E-20	**2.4**	**2.3**	1.3	**1.8**	1.2	**2.6**	⇦
8	20S proteasome beta 2 subunit [BE494850]	***OA_b3H03***	AJ888717	2.00E-94	1.4	**1.6**	0.9	1.4	1.1	1.7	
9	20S proteasome beta 3 subunit [CD866745]	***OA_b2G11***	AJ888689	6.00E-55	**2.0**	**2.2**	1.1	1.7	1.2	2.2	
10	20S proteasome beta 5 subunit [BJ219720]	***OA_b3A12***	AJ888697	5.00E-64	**2.0**	**1.8**	1.3	1.4	1.1	1.9	⇦
	Chaperones										
11	hsp 23.5 [Ta.203]	***OA_a1B01***	AJ874072	1.00E-133	**4.5**	**5.4**	1.1	2.3	1.4	3.3	
12	hsp 23.6 [Ta.214]	***OA_a1H02***	AJ874076	1.00E-143	**5.6**	**7.6**	1.2	**3.5**	**2.7**	**2.5**	
13	hsp 60 [L21006]	***OA_a1E07***	AJ888606	5.00E-49	**18.9**	**25.7**	0.7	**4.6**	3.5	2.0	
14	hsp 60 [AC027038]	***OA_b1C09***	AJ874088	5.00E-35	**11.0**	**14.2**	1.6	**5.4**	**5.1**	**4.7**	
15	hsp 70 [P37900]	***OA_a3B09***	AJ874084	4.00E-42	**7.1**	**10.1**	0.9	**2.7**	**2.3**	**3.1**	
16	hsp 70 [AF479058]	***OA_a3C06***	AJ888638	4.00E-36	**1.7**	1.4	1.5	0.9	1.0	2.1	⇦
	Carbohydrate metabolism (regulation)										
17	alcohol dehydrogenase ADH1 [BJ307901]	***OA_a1D06***	AJ888602	1.00E-131	**12.5**	**14.4**	0.9	3.9	**2.7**	4.5	
18	alcohol dehydrogenase ADH1 [CD868456]	***OA_a2A05***	AJ888612	1.00E-163	**13.6**	**18.0**	1.0	2.4	2.3	3.3	
19	pleiotropic regulator PRL1 [Ta.6105]	***OA_b2C06***	AJ888677	0.00E+00	**1.7**	**1.6**	1.1	1.2	1.0	2.2	⇦

Table 4.7 (continued)

	Putative function & [Blast hit]	EST ID	access. no#	E-val	ceB ($p < 0.05$) sylA on epidermis and mesophyll (*Bgt* infected leaves) -08 hat epi	-08 hat mes	-08 hat ϵ_S	-32 hat epi	-32 hat mes	-32 hat ϵ_S	
	1	2	3	4	5	6	7	8	9	10	
	Carbohydrate metabolism (TCA)										
20	2-oxoglutarate dehydrogenase (E1 subunit) [AP005199]	***OA_a3B02***	AJ874083	2.00E-91	**4.8**	**3.7**	1.4	**1.9**	1.1	2.7	⇦
21	succinyl-CoA-ligase beta subunit [AY180975]	***OA_b1D01***	AJ874089	3.00E-63	**1.9**	**2.2**	1.2	**1.6**	1.4	2.5	
22	succinyl-CoA-ligase beta subunit [AY180975]	***OA_b1E11***	AJ874090	5.00E-38	**1.9**	**2.3**	1.2	**1.5**	1.2	**2.5**	
23	citrate synthase [AP000367]	***OA_b1H11***	AJ874093	3.00E-59	**1.8**	**2.4**	1.3	**1.7**	1.5	**2.6**	
24	aconitate hydratase (cytoplasmic) [BJ230524]	***OA_b3G05***	AJ874104	4.00E-57	1.4	**1.7**	1.8	1.2	1.1	**2.9**	
	Carbohydrate metabolism (glycolysis)										
25	glyceraldehyde-3-phosphate dehydrogenase (cytosolic, wheat) [AF251217]	***GapC***	0	#N/A	**2.3**	**2.7**	1.1	1.4	1.4	1.5	
26	glyceraldehyde-3-phosphate dehydrogenase (cytosolic, wheat) [AF251217]	***OA_G3PDH Rsa***	AJ890249	1.00E-133	**3.0**	**3.4**	1.4	**1.5**	1.5	1.9	
27	glyceraldehyde-3-phosphate dehydrogenase (cytosolic, wheat) [AF251217]	***BE437891***	BE437891	1.00E-67	**3.1**	**3.3**	1.3	**1.8**	**1.6**	2.0	
28	glyceraldehyde-3-phosphate dehydrogenase (cytosolic, wheat) [AF251217]	***BE437899***	BE437899	4.00E-81	**3.2**	**3.9**	1.2	**1.6**	**1.5**	1.9	
29	glyceraldehyde 3-phosphate dehydrogenase (cytosolic) [P08477]	***OA_b3C10***	AJ874100	5.00E-68	**3.2**	**4.1**	1.2	**1.6**	1.3	**2.3**	
30	fructose-bisphosphate aldolase [CD907979]	***OA_a1C12***	AJ888600	1.00E-141	**3.0**	**3.5**	1.2	1.7	1.5	**2.3**	
31	enolase 1 (2-phosphoglycerate dehydratase 1) [CD454849]	***OA_a2G01***	AJ888626	8.00E-90	**4.9**	**5.7**	1.2	**4.8**	**2.9**	3.6	
32	pyruvate kinase [Hv.2627]	***OA_b1B10***	AJ888655	0.00E+00	**2.7**	1.5	1.4	1.4	1.3	1.5	⇦
33	pyruvate kinase [AY090539]	***OA_b2B04***	AJ888672	4.00E-30	2.5	**2.6**	1.9	1.5	1.3	**2.2**	
34	2,3-bisphosphoglycerate-independent phosphoglycerate mutase [AP003255]	***OA_b2G09***	AJ874098	1.00E-90	**3.1**	**2.5**	1.1	2.1	1.4	2.4	⇦
	Carbohydrate metabolism (hexose metabolism)										
35	sucrose synthase 1 [CK209269]	***OA_a1C08***	AJ888599	2.00E-61	**2.4**	**3.6**	1.2	1.1	1.1	2.5	
36	sucrose synthase 1 [P31922]	***OA_a3A03***	AJ888632	2.00E-63	**2.0**	**3.6**	0.6	1.1	1.1	1.6	
37	sucrose synthase 1 [AF412038]	***OA_b2B06***	AJ888673	7.00E-40	1.4	**1.7**	0.9	1.0	0.9	1.2	
38	sucrase (ferredoxin-like) [BQ458888]	***OA_b3C03***	AJ888702	6.00E-99	**1.9**	**2.2**	1.0	1.3	1.1	**2.1**	
	Lipid metabolism										
39	lecithin-cholesterol acyl transferase [CK157509]	***OA_b2D12***	AJ888681	1.00E-156	**1.6**	1.7	1.2	1.2	1.2	1.9	
	Response to abiotic stimulus										
40	MRP-like ABC transporter [CA733405]	***OA_a2A06^{B}***	AJ888613	1.00E-161	**2.4**	**2.5**	0.8	1.0	0.9	1.4	
41	MDR-like ABC transporter [Ta.9295]	***OA_a2E02***	AJ888620	0.00E+00	**4.1**	**3.9**	1.6	1.5	1.3	**2.6**	⇦
42	PDR-like ABC transporter [CD881196]	***OA_a3A04^{B}***	AJ874081	1.00E-88	1.5	**1.8**	1.0	**1.7**	1.2	3.0	
43	MRP-like ABC transporter [BT009369]	***OA_a3D05***	AJ888640	1.00E-93	**2.7**	**2.4**	1.5	1.0	1.0	1.8	⇦
44	MRP-like ABC transporter [CA736782]	***OA_a3H01***	AJ888649	5.00E-96	**5.3**	**4.3**	1.3	1.5	1.1	2.1	⇦
45	glutathione-S-transferase/glutaredoxin [BE405126]	***OA_a3A01***	AJ888631	1.00E-144	**2.9**	**2.7**	1.1	1.5	1.1	2.4	⇦

Table 4.7 (continued)

	Putative function & [Blast hit]	EST ID	access. no#	E-val	ceB ($p < 0.05$) sylA on epidermis and mesophyll (*Bgt* infected leaves) -08 hat epi	-08 hat mes	-08 hat ϵ_S	-32 hat epi	-32 hat mes	-32 hat ϵ_S	
	1	2	3	4	5	6	7	8	9	10	
46	glutathione S-transferase [CK217249]	***OA_a3G10***	AJ888647	9.00E-77	**2.0**	**2.7**	0.9	1.0	0.9	1.6	
47	glutathione S-transferase [CA719629]	***OA_b1H08***	AJ874092	7.00E-81	1.3	**1.6**	1.0	1.2	0.9	2.1	
48	glutathione S-transferase [CN013161]	***OA_b3D05***	AJ874102	1.00E-152	**9.2**	**9.3**	1.5	**9.1**	**13.7**	3.0	
49	glutathione S-transferase [CK205115]	***RB_c017***	AJ873967 AJ873968	4.00E-25	**2.9**	**3.3**	1.1	1.9	1.5	4.7	
50	cytochrome P450 [AF321867]	***OA_a1D09***	AJ888604	3.00E-67	**2.5**	2.7	1.1	1.2	1.0	1.9	
51	cytochrome P450 [AP002839]	***OA_b1D06***	AJ888659	3.00E-47	**12.9**	**16.0**	0.9	**6.0**	**3.3**	3.1	
52	cytochrome P450 [AP002839]	***OA_a1C04***	AJ888598	1.00E-78	**2.6**	**3.3**	1.0	1.4	0.9	2.0	
53	temperature stress-induced lipocalin / Apolipoprotein D (APOD) [AY077702]	***OA_b1D11***	AJ888660	1.00E-142	**3.1**	**2.1**	1.0	**1.7**	1.4	1.2	⇦
	Response to biotic stimulus										
54	DMI1 (does not make infections) protein [CA027230]	***OA_b2E04***	AJ888682	0.00E+00	**2.4**	**2.2**	1.1	1.8	**1.6**	2.3	⇦
55	NBS-LRR disease resistance protein [AJ507096]	***OA_a1E08***	AJ874075	3.00E-49	**6.1**	**4.5**	1.6	**5.4**	**2.7**	**3.9**	⇦
	Response to endogenous stimulus										
56	UDP-glucose:salicylic acid glucosyltransferase /:anthocyanin 5-O-glucosyltransferase / IAA-glu synthetase [AL606590]	***OA_a3B03^B***	AJ888635	5.00E-49	**2.1**	**2.4**	1.0	1.0	1.0	1.6	
57	ABI3-interacting protein 2 (abscisic acid insensitive interacting protein) [Ta.6216]	***OA_b2A06***	AJ888668	0.00E+00	**2.3**	**2.6**	1.1	1.2	1.0	1.6	
	Signal transduction										
58	ABA insensitive ABI (protein phosphatase 2C) [CL594560]	***OA_a1B11^B***	AJ888596	8.00E-20	1.5	**1.7**	1.2	1.0	1.1	1.9	
59	ligand-gated ion channel 2.8 [BQ659530]	***OA_a2B04***	AJ888614	5.00E-99	**10.4**	**12.6**	0.8	**4.4**	**3.1**	2.5	
60	light repressible receptor protein kinase (Putative integral membrane protein) [BE517637]	***OA_b1B08***	AJ888654	5.00E-73	**3.0**	**3.3**	0.8	**2.9**	**2.1**	**2.2**	
	Cell growth / maintenance (Cell cycle)										
61	prohibitin [AF236371]	***OA_a3C03***	AJ874085	1.00E-114	**3.5**	**3.3**	1.3	1.9	1.4	**2.4**	⇦
62	cell division control protein 48 homolog E (Transitional endoplasmic reticulum ATPase E) [Ta.28850]	***OA_a3F09***	AJ888645	0.00E+00	**2.3**	**2.5**	0.6	1.3	1.0	1.3	
63	cell division control protein 48 homolog D (Transitional endoplasmic reticulum ATPase D) [BJ220165]	***RB_169.8***	AJ888718	2.00E-72	1.8	**2.1**	1.4	1.3	1.0	**2.0**	
	Respiration										
64	BCS1-like protein / AAA-type ATPase-like protein [Ta.11182]	***OA_a1B08***	AJ874073	1.00E-130	**2.8**	**4.4**	1.2	**1.6**	1.1	3.3	
65	alternative oxidase [AF174004]	***OA_a1E06***	AJ874074	4.00E-87	**10.3**	**16.1**	1.0	**3.8**	**4.4**	3.0	
66	NADH dehydrogenase [BT009120]	***OA_a2B11***	AJ874077	1.00E-101	**3.8**	**4.7**	0.7	1.8	1.5	**2.2**	
	Aminoacid metabolism										
67	alanine aminotransferase 2 (glutamic-pyruvic transaminase 2) [CF133158]	***OA_a2D10***	AJ874079	0.00E+00	**3.8**	**3.9**	0.8	1.4	1.3	1.5	
	Protein metabolism										
68	lysyl-tRNA synthetase [BI480436]	***OA_a1E11***	AJ888608	0.00E+00	**8.2**	**8.1**	1.1	1.7	1.4	**2.3**	⇦

Table 4.7 (continued)

	Putative function & [Blast hit]	EST ID	access. no#	E-val	ceB ($p < 0.05$) sylA on epidermis and mesophyll (*Bgt* infected leaves) -08 hat epi	-08 hat mes	-08 hat ϵ_S	-32 hat epi	-32 hat mes	-32 hat ϵ_S	
	1	2	3	4	5	6	7	8	9	10	
69	60S ribosomal protein L30 [AJ417524]	***OA_a2H04***	AJ888629	4.00E-41	**2.3**	**2.4**	1.1	1.2	1.1	2.0	
70	(alanine) acetyltransferase [BE420036]	***OA_a3E08***	AJ888642	2.00E-82	**2.0**	**2.5**	1.0	1.1	1.1	2.3	
71	valyl tRNA synthetase [AC084023]	***OA_b2E06***	AJ888683	3.00E-63	**5.7**	**3.6**	2.1	1.3	0.9	2.6	⇦
	Transport										
72	P-type ATPase (CA7 gene) [AJ310846]	***OA_a2H06***	AJ888630	5.00E-99	**2.9**	**3.4**	0.8	1.4	1.2	2.0	
73	voltage-dependent anion channel 1 [X77733]	***OA_b1F04***	AJ888662	2.00E-57	**13.3**	**11.2**	1.5	**6.2**	**3.8**	**4.5**	⇦
74	TipC / VPS13 - like protein [Ta.8446]	***OA_b1G10***	AJ888664	1.00E-148	**2.0**	**1.9**	1.9	1.4	1.2	**4.1**	⇦
	Development										
75	embryo-abundant protein [Ta.8017]	***RB_c118***	AJ873998 AJ873999	8.00E-16	**4.7**	**5.0**	1.0	**2.2**	1.3	3.0	
	Hydrolase										
76	pir7b / salicylic acid-binding protein / Ethylene-induced esterase / Polyneuridine aldehyde esterase [Q43360]	***OA_b1B01***	AJ874087	2.00E-67	**17.0**	**17.9**	1.4	**14.7**	**17.2**	1.7	
77	pir7b / salicylic acid-binding protein / Ethylene-induced esterase / Polyneuridine aldehyde esterase [CB864680]	***OA_b2A07***	AJ874094	3.00E-79	**13.5**	**11.7**	1.5	**10.7**	**15.2**	1.9	⇦
78	epoxide hydrolase [Ta.26236]	***OA_b2H01***	AJ888690	4.00E-69	**7.8**	**6.2**	1.2	**2.9**	1.4	2.7	⇦
79	epoxide hydrolase [Ta.26236]	***OA_b3B10***	AJ888700	2.00E-78	**10.9**	**11.2**	1.4	4.6	**1.9**	4.2	
	various										
80	NADPH-dependent oxidoreductase [CA682777]	***OA_a2C02***	AJ874078	3.00E-99	**4.2**	**4.9**	1.2	**2.1**	1.5	**2.9**	
81	glucosyltransferase [CD490938]	***OA_a2C08***	AJ888615	1.00E-12	**5.5**	**6.5**	0.7	1.3	0.9	**2.4**	
82	monooxygenase [CD452994]	***RB_53.1***	AJ888726	8.00E-85	**4.1**	3.6	1.8	2.3	1.1	3.2	⇦
83	#N/A	***RB_53.3***	#N/A	#N/A	**3.2**	3.6	1.5	1.8	1.0	2.8	
84	#N/A	***RB_53.6***	#N/A	#N/A	**4.4**	**3.4**	1.4	2.5	1.2	2.9	⇦
85	#N/A	***RB_53.7***	#N/A	#N/A	**3.7**	**2.9**	1.1	2.2	1.0	2.8	⇦
	unknown										
86	unknown [Hv.10128]	***OA_a1A03***	AJ888591	1.00E-158	**3.9**	**4.6**	1.6	1.8	**1.6**	**3.1**	
87	no significant hit [BG415498]	***OA_a1D03^B***	AJ888601	1.00E-03	2.1	**2.4**	0.8	1.0	1.0	1.5	
88	unknown [D22421]	***OA_a1D08***	AJ888603	8.00E-06	**10.1**	**12.0**	1.3	**7.4**	**6.1**	3.2	
89	unknown [BE445384]	***OA_a1F05^B***	AJ888609	6.00E-97	**6.0**	**5.7**	1.1	1.9	1.3	1.8	⇦
90	unknown [CN011234]	***OA_a1H06***	AJ888610	3.00E-84	**2.2**	**2.2**	1.3	1.2	1.1	1.9	⇦
91	unknown [CN013234]	***OA_a2E09***	AJ888622	1.00E-51	**10.0**	**11.6**	1.2	3.7	**1.7**	**4.5**	
92	unknown [BQ579520]	***OA_a2E10***	AJ888623	1.00E-173	**2.0**	**2.2**	1.1	1.1	0.9	1.9	
93	unknown [CK215536]	***OA_a2F04***	AJ888625	0.00E+00	4.4	**3.7**	1.8	1.4	1.1	3.3	⇦
94	unknown fused to ABI3-interacting protein 2 [BQ789184]	***OA_a2H03***	AJ888628	1.00E-88	**2.7**	**2.5**	1.1	1.4	1.2	2.2	⇦
95	unknown [BQ768185]	***OA_a3E09***	AJ888643	1.00E-104	4.1	**4.8**	1.6	1.8	1.3	2.3	
96	no significant hit	***OA_b1A06***	AJ874086	#N/A	**15.4**	**16.7**	1.3	**11.4**	**11.4**	3.8	

Table 4.7 (continued)

	Putative function & [Blast hit]	EST ID	access. no#	E-val	ceB ($p < 0.05$) sylA on epidermis and mesophyll (*Bgt* infected leaves) -08 hat epi	-08 hat mes	-08 hat ϵ_S	-32 hat epi	-32 hat mes	-32 hat ϵ_S	
	1	2	3	4	5	6	7	8	9	10	
97	no significant hit	***OA_b2B07***	AJ888674	#N/A	**15.3**	**21.2**	1.0	**14.2**	**14.2**	2.1	
98	unknown [Ta.8833]	***OA_b2C04***	AJ888675	1.00E-149	**2.6**	**2.5**	1.6	1.8	1.3	3.3	⇦
99	unknown [Ta.12787]	***OA_b2F09***	AJ874097	6.00E-49	**4.2**	**3.8**	1.3	2.6	**1.6**	2.7	⇦
100	unknown [BJ291998]	***OA_b2G10***	AJ888688	3.00E-66	**2.4**	**2.6**	1.2	1.4	1.1	2.3	
101	unknown [BQ789018]	***OA_b3E03***	AJ888708	1.00E-176	**2.5**	**2.6**	1.1	**2.2**	1.4	1.7	
102	unknown [BU100203]	***OA_b3E09***	AJ874103	0.00E+00	**1.7**	**1.8**	1.2	1.3	1.1	1.8	
103	no significant hit [CX630958]	***OA_a2D05***	AJ888618	2.20E-01	**6.0**	**7.6**	1.0	1.8	1.2	2.4	
104	no significant hit [Str.21194]	***OA_a3C05***	AJ888637	5.40E-01	**2.4**	**2.5**	1.2	1.3	1.2	2.0	
105	#N/A	***RB_17.2***	#N/A	#N/A	**1.7**	**2.1**	1.5	1.3	1.2	**3.4**	
106	fructose 1-,6-biphosphate aldolase [CD903437]	***RB_17.3***	AJ888719	9.00E-11	**1.9**	**2.7**	1.2	1.2	1.3	2.7	
	ceA only										
107	harpin induced gene homolog (wheat)	***BE419039^{A80}***	BE419039	#N/A	1.5	1.5	2.0	1.3	1.4	**3.2**	
108	unknown, weekly similar to FMIP (Fms-interacting protein) [AK103640]	***OA_a2H01^{A118}***	AJ888627	2.00E-98	1.4	1.3	1.2	1.4	1.3	1.5	
109	adenylate kinase (ATP-AMP transphosphorylase) [D10334]	***OA_a3A08^{A93}***	AJ874082	1.00E-50	1.2	1.4	1.3	1.3	1.0	**3.2**	
110	nuclear coiled-coil protein [Ta.16935]	***OA_b1A07^{A110}***	AJ888651	0.00E+00	1.3	1.4	1.6	1.2	1.0	2.8	
111	20S proteasome alpha 4 subunit [O04861]	***OA_b1A08^{A5}***	AJ888652	4.00E-37	1.3	1.2	1.9	1.2	1.0	1.7	
112	ubiquitin-associated protein (UBA) [AP004079]	***OA_b1D02^{A12}***	AJ888657	5.00E-18	1.8	1.6	1.5	1.5	1.2	3.0	
113	RTNLB30 (reticulon like) [AY164945]	***OA_b1D03^{A81}***	AJ888658	3.00E-39	1.2	1.2	0.9	1.1	0.9	2.1	
114	enolase 2 [P42895]	***OA_b2A09^{A34}***	AJ888670	2.00E-44	1.7	1.3	0.5	1.2	1.0	0.7	
115	20S proteasome beta 6 subunit [O64464]	***OA_b2C07^{A11}***	AJ888678	2.00E-29	1.4	1.4	0.9	1.4	1.3	1.3	
116	aspartate aminotransferase (cytoplasmic) [P37833]	***OA_b2F07^{A71}***	AJ888686	4.00E-82	1.2	1.1	1.5	1.0	1.2	2.0	
117	unknown [CK160653]	***OA_b3B01^{A119}***	AJ888698	2.00E-46	1.1	1.2	1.0	1.0	1.1	1.2	
118	unknown [BE488635]	***OA_b3C01^{A120}***	AJ888701	9.00E-96	0.9	0.9	0.7	1.0	1.1	0.7	
119	nucleolar GTP-binding protein 1-like [BI751677]	***OA_b3F05^{A94}***	AJ888711	1.00E-109	1.2	1.2	1.0	1.2	1.0	1.7	
120	unknown [AW448695]	***RB_240.4^{A116}***	AJ888722	2.00E-55	1.5	1.5	1.1	1.2	0.9	2.0	
121	#N/A	***RB_240.5^{A117}***	#N/A	#N/A	1.1	1.4	1.0	1.3	1.1	1.7	
122	apospory-associated protein C [CA655323]	***RB_265.2^{A39}***	AJ888723	3.00E-29	0.7	0.7	1.3	0.7	0.8	2.3	
123	Aquaporin PIP1 [BJ284089]	***RB_34.4^{A79}***	AJ888724	4.00E-22	0.6	0.7	0.7	0.6	0.8	1.1	
124	Ripening-related protein-like [CD872650]	***RB_39.2^{A84}***	AJ888725	5.00E-67	0.7	1.0	1.2	0.7	0.8	2.3	
125	#N/A	***RB_39A.1^{A85}***	#N/A	#N/A	0.7	0.8	1.4	0.7	0.8	2.4	
126	B12D protein [BQ170981]	***RB_96.2^{A86}***	AJ888727	1.00E-31	1.8	1.7	2.3	2.2	**1.9**	**4.0**	
127	fructose-1,6-bisphosphatase [CD894371]	***RB_97.3^{A38}***	AJ888728	4.00E-40	1.0	0.7	1.2	0.8	0.9	0.6	
128	gigantea mRNA [BG909229]	***RB_c001^{A82}***	AJ873936 AJ873963 AJ873964	1.00E-117	0.8	0.6	**2.9**	1.1	1.0	**5.5**	

Table 4.7 (continued)

	Putative function & [Blast hit]	EST ID	access. no#	E-val	ceB ($p < 0.05$) sylA on epidermis and mesophyll (*Bgt* infected leaves) -08 hat epi	-08 hat mes	-08 hat ϵ_s	-32 hat epi	-32 hat mes	-32 hat ϵ_s
	1	2	3	4	5	6	7	8	9	10
129	sucrase [Hv.12867]	***RB_c020^{A44}***	AJ888720	6.00E-12	1.3	1.3	1.0	1.0	1.1	1.4
130	Putative immediate-early salicylate-induced glucosyltransferase [Ta.23340]	***RB_c048^{A61}***	AJ874027	2.00E-29	0.9	0.9	0.6	1.6	1.2	0.9
131	28S ribosomal RNA gene [AY064705]	***RB_c116^{A95}***	AJ888238	4.00E-71	2.2	1.6	**2.8**	2.3	1.6	**6.5**

In accordance to observations in ceA, t/c ratios of syringolin-induced genes were found to be 1.8-fold less elevated on average at the late time point as compared to the early time point also in ceB (visualized in Figure 4.23B). The only exceptions were a putative GST (*OA_b3D05*; Table 4.7, row 48) and one wheat homologue of *Pir7b* (*OA_ b2A07*; row 77). Investigations of ϵ_s-factors revealed that the vast majority of genes did not show epidermis specific expression at the -08 hat time point. In fact, average ϵ_s-factors of genes regulated by syringolin were found to be 1.19 in the early time point. Conversely, average ϵ_s-factors at the late time point were 2.28 and thus they were clearly above threshold limits of 2. The situation is illustrated in Figure 4.23A.

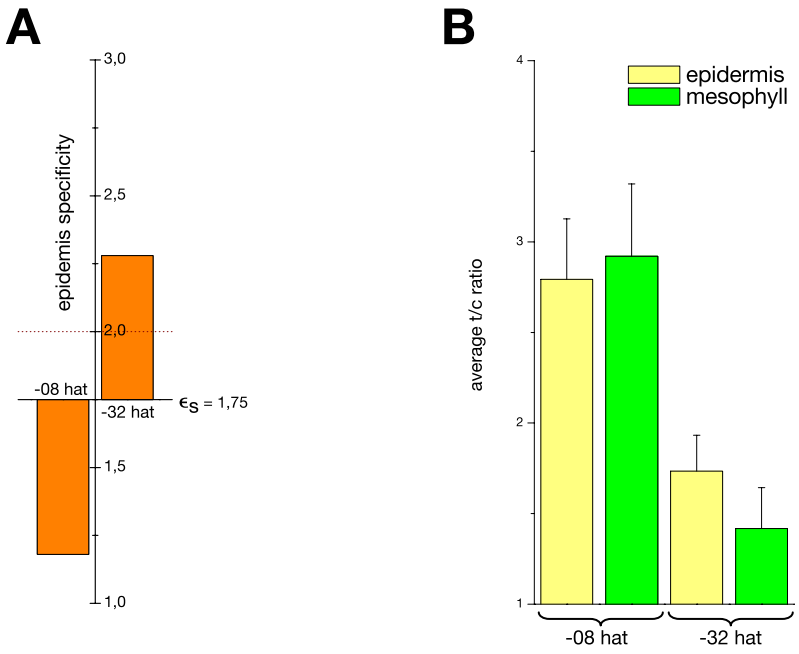

Figure 4.23: Column plots illustrating trends observed in core experiment B (note that all plants investigated in ceB had previously been infected with *Bgt*). A: Average ϵ_s-factors are shown. The X-axes was positioned at ϵ_s=1.75, the average rubisco proportion indicating balanced expression between epidermis and mesophyll. B: Average t/c ratios of genes regulated by syringolin are shown (deviations are indicated by standard error bars). ϵ_s-factors were determined for syringolin-treated plants.

It was concluded that induced transcription of genes observed up to 8 hat occurred ubiquitously or even augmented in the mesophyll. Of the sylA-responsive probes, only one fragment (*OA_b2E06*) was found to exhibit an ϵ_s-factor higher than two at the early time point (Table 4.7, row 71). Blastx comparison to public databases revealed that *OA_b2E06* with a length of 588 bp showed 80 % amino acid identity (in 145 aa) to a putative valyl tRNA synthetase from rice (accession #AC084023). On the other hand, 69 fragments exhibited epidermis-specific expression at the late time point (Table 4.7). Apart from one exception (*OA_b3D05*; Table 4.7, row 48), all of them were induced stronger at the earlier -08 hat time point. Thus, induction of transcription observed at -08 hat was largely reduced and numerous genes were found to exhibit epidermis-specific transcription at -32 hat (e.g. *OA_a3B09* or *OA_a1E06*, Table 4.7, rows 15 & 65).

At first glance, the finding that at the early time point t/c ratios were sometimes found to be elevated in the epidermis as compared to the mesophyll whereas ϵ_s-factors indicated ubiquitous or mesophyll-specific expression was surprising (e.g. rows 20, 32 or 34 in Table 4.7, columns 5-7). Simulations of ϵ_s-factors under different situations revealed that a high background expression in the mesophyll combined with low epidermal expression would mask a significant (e.g. 10-fold) epidermis-specific induction. The ϵ_s-factor eventually would not exceed neutral levels of 1.75. Actually, separate calculation of ϵ_s-factors in control-treated leaves (data not shown) revealed low ϵ_s values of 1.1, 0.8 and 1.0 at -08 hat in the three cases mentioned above. High background expression might either reflect natural tissue-specificity or result from tissue-specific pathogen related pre-induction (studied in chapt. 4.2.6).

The fact that many genes exhibited t/c ratios not significantly different from 1 but at the same time had ϵ_s values greater than 2 in the -32 hat time point was unexpected. The most plausible explanation is that at this time point the syringolin-induced transient gene expression is back to normal levels and genes exhibiting ϵ_s values > 2 show an epidermis-specific background expression. This was for example the case for *OA_a1A03*, *OA_a1C08* and *OA_a2E02* (Table 4.7, rows 86, 35 & 41), where ϵ_s-factors in control-treated leaves were found to be 2.5, 2.3 and 2.0 (data not shown).

However, in 35 cases epidermis specificity at 32 hat was observed also for genes still significantly induced ($p < 0.05$) at this time point. Often, epidermis specificity changed from mesophyll specificity at -08 hat to epidermis specificity at -32 hat. This was accompanied by a switch from higher t/c ratios at -08 hat in the mesophyll to lower t/c ratios at -32 hat as compared to the epidermis. The situation was reflected in switched proportions of average t/c ratios (Figure 4.23B). In the case of *OA_a1H02*, *OA_a1E07* and *OA_b1D06* (Table 4.7, rows 12, 13 & 51), ϵ_s-factors at -32 hat in control-treated leaves were

found to be 1.8, 1.5 and 1.6 (clearly below 2, not shown). It was concluded that the initial ubiquitous induction of transcription by sylA treatment had changed into a weaker but more epidermis-specific induction at the later time point (Figure 4.23A & B). A faster decay of the transcriptional response in the mesophyll could be explained by hampered accessibility of inner tissues as compared to epidermal outer tissues to sylA after spray application. Alternatively, sylA treatment could trigger prolonged or persistent gene transcription in epidermal or powdery mildew-infected cells whereas the transcriptional response in the mesophyll would be shorter (studied in chapt. 4.2.7).

Taken together, analysis of epidermis specificity revealed that the strong induction of investigated genes around 8 hat by syringolin predominantly occurred in an ubiquitous manner in the whole wheat leaf (Figure 4.23A). At the -32 hat time point, the situation had changed due to a slower decay of induced transcription in the epidermis as compared to the mesophyll. High mesophyll-specific expression in ϵ_s-factors of control-treated leaves indicated that epidermis specificity might have been masked in some instances. Yet, evaluation of epidermis specific induction on the basis of t/c ratios alone revealed that only 5 genes exhibited more than 1.3-fold higher t/c ratios in the epidermis as compared to the mesophyll at -08 hat. The corresponding fragments *OA_a3B02*, *OA_b1D11*, *OA_b1B10*, *OA_a1E08*, and *OA_b2E06* are listed in Table 4.7 (rows 8, 13, 32, 55 & 71). Interestingly, highest induction ratio was found in the case of an NBS-LRR resistance gene homolog (*OA_a1E08*, accession #AJ874075) which simultaneously exhibited highest epidermis specificity in the late time point.

4.2.4.2. Examination of data derived from ceA and ceB

Examination of the two sets of genes identified in ceA and ceB revealed a total number of 124 genes (listed in Table 4.7) exhibiting significant responsiveness to syringolin treatment in one or both experiments. Apart form one exception (*OA_a1E09*), these contained all 59 SSH-derived cDNA fragments exhibiting clear syringolin responsiveness as judged by dot blot hybridization signals (fragments marked with [(1)] in Table 4.2, chapter 4.1.5). *OA_a1E09*, a putative brassinosteroid receptor interacting protein exhibited statistically significant induction at the early time point of ceB but the average t/c ratio of 1.491 was slightly below threshold limits (data not shown).

Upon comparison of data derived from ceA and ceB, 94 of the 124 genes (76 %) were found to be significantly regulated in both experiments whereas 30 genes were identified in only one of the two experiments. The findings are illustrated in Figure 4.24.

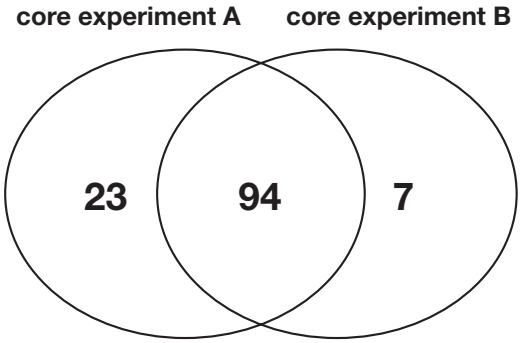

Figure 4.24: Venn diagram showing the distribution of differentially expressed genes between core experiment A and core experiment B.

As obvious by the larger number of 23 ceA-specific genes (marked with [(A)] in Table 4.4 and Table 4.7), stripping of epidermis and thus enhancement of epidermis- and mesophyll-derived signals in the corresponding samples did not result in identification of a higher number of differentially regulated genes in ceB. With respect to this, two aspects had to be taken into consideration: At first, sampling in ceB was carried out at earlier and later time points as compared to ceA (-08 hat and -32 hat in ceB compared to 12 hat and 24 hat in ceA). Second, all samples of ceB had been infected with *Bgt* which was shown previously to significantly decrease t/c ratios upon treatment with syringolin (chapt. 4.2.2.2). Indeed, most of the genes identified in ceA exhibited differential expression only in the absence of the fungus. In addition, t/c ratios were consistently low. It was concluded that corresponding genes were induced stronger around 12 hat.

Genes identified exclusively in ceB were of particular interest since stripping off epidermis from the remainder of the leaves was hypothesized to lower the detection limit of transcriptional changes restricted to colonized epidermal cells. Seven genes (all derived from screening at the early α time point) were found to be exclusively induced in ceB. In 4 cases, t/c ratios were above 2 but not significant ($p > 0.05$) in ceA (e.g. *OA_a3A04*, Table 4.7, row 42). In the case of *OA_a1A10, OA_a1B11 and OA_a1D03* (Table 4.7, row 1, 50 & 87), no indication for induction was found in ceA (data not shown). Since induction was always observed at the early -08 hat time point, corresponding genes were considered to be transiently upregulated before 12 hat.

In summary, investigations of ceA and ceB resulted in the confirmation of transcriptional up- or downregulation of 124 genes by sylA treatment of wheat. The set consisted of 103 SSH-derived OA-fragments of microarray subset one, 16 cDNA AFLP-derived RB-fragments of subset two and 5 control fragments of subset three. Unexpectedly, none of them was found to clearly exhibit pronounced syringolin responsiveness only in the presence of *Bgt,* nor was any of them shown to be exclusively expressed in the epidermis.

4.2.5. Genes induced by syringolin (overview)

4.2.5.1. Control genes

As described in chapt. 4.2.1.1, microarray series 6 and 7 contained a set of probes (subset three) corresponding to housekeeping genes as well as probes corresponding to PR genes known to be transcriptionally induced during wheat-powdery mildew interaction. In addition, several newly identified probes involved in the wheat response to *Bgh* infection were present among the cDNA AFLP-derived collection of probes corresponding to subset two (Bruggmann et al., 2005).

Indicative for proper normalization, many of the putative housekeeping genes such as wheat α-tubulin (#AJ890248) or barley and rice actin (#BE437261 & #X16280) exhibited constitutive expression which was the case for the majority of genes corresponding to subset two and three in ceA and ceB (Figure 4.18 & Figure 4.19, p.63). Yet, it was surprising to find transcriptional upregulation of some prominent housekeeping genes such as the SSH-derived cDNA fragment *OA_a1A10* encoding ubiquitin (Table 4.7, row 1) or several probes encoding G3PDHs (Table 4.4, rows 27-31). As discussed later, both genes were found to be transcriptionally induced in the context of a defined plant response which involved ubiquitin-dependent protein catabolism and glycolysis (chapt. 5.3).

In accordance to previous investigations by Wäspi et. al (2001), none of the PR genes including the *WIR* and *WCI* genes represented in subset three (Appendix, Table 8.3) was transcriptionally induced upon syringolin treatment of infected and uninfected wheat leaves within the first 32 hat monitored in ceA and ceB. The finding that syringolin application in wheat does not induce accumulation of PR-gene transcripts could even be extended to numerous additional genes encoding β-1,3-endoglucanase (*TaGLUC2*, #Y18212), germin-like protein 4 (*TaGLP4,* #AJ237942), PR-1 protein (*RB_c072*, #AJ874038 & #AJ874039) and phenylalanine ammonia-lyase (RB_c011, # AJ873947; RB_c101, #AJ873941 & #AJ873961 and RB_c115, #AJ874042). The only exception exhibiting weak transcript accumulation encoded a wheat homologue of the harpin induced Hin1 (#BE419039, Table 4.4, row 80) which is a PR protein that was recently found to carry a WHy domain (water stress and hypersensitive response (Ciccarelli and Bork, 2005). Transcriptional induction of *Hin1* in response to infiltration with *P. syringae* is dependent on the presence of a functional *hrp* gene cluster but can also occur in a race-specific manner as found for the Pto/AvrPto interaction (Gopalan et al., 1996).

In this place it should be mentioned that apart from the WCI genes, all the genes mentioned above were found to be transcriptionally upregulated after 24 hai upon infiltration of wheat cv. Fidel with 10 mM $MgCl_2$ containing 10^9 cfu/ml of *Pseudomonas syringae* pv. *syringae* B301D-R, the strain which was commonly used for purification of syringolin (preliminary results). Strongest inductions were observed for *TaGLP4, WIR3, PAL* and *Hin1* (results based on a single experiment; not shown).

To sum up, the lack of syringolin dependent induction of PR genes in wheat described previously (Wäspi et al., 2001) was confirmed and expanded to additional PR genes. By showing that the corresponding PR genes were also responsive to *Pseudomonas* infiltration in wheat, the difference in the syringolin mode of action between wheat and rice, where homologous PR-genes are induced in response to sylA treatment (Wäspi et al., 1998a) was reinforced. In addition cloning and confirmation of strong transcript accumulation of wheat homologs of the syringolin-induced rice Pir7b esterase confirmed previous results (Wäspi et al., 2001) and demonstrated reliability of the present work (Table 4.4, rows 87 & 88). Besides, microarray comparison of wheat infiltrated with the wild type *P. syringae* pv. *syringae* B301D-R and a mutant strain which does not accumulate syringolin (Amrein et al., 2004) allowed for the identification of additional marker genes expressed exclusively in the presence of syringolin (preliminary results). Next to transcripts corresponding to the wheat homologs of Pir7b (*OA_b1B01* & *OA_b2A07*), this included transcripts encoding sHsps (*OA_a1B01* & *OA_a1H02*), a putative ligand-gated ion channel (*OA_a2B04*), VDAC1 (*OA_b1F04*) and two proteins of unknown function (*OA_a2D05* & *OA_a2E09*).

4.2.5.2. Biological processes

Genes confirmed to be induced by sylA application in ceA and ceB were grouped according to biological and molecular function GO terms (Ashburner et al., 2000) with emphasis on biological functions. An overview is presented in Figure 4.25 and prevalent groups are briefly described below. Altogether, four large groups of genes were identified. The first group contained 12 members of the 26S proteasome core and lid particle including three regulatory particles, a putative E3 enzyme and ubiquitin which were all assigned to the ubiquitin-dependent protein catabolism.

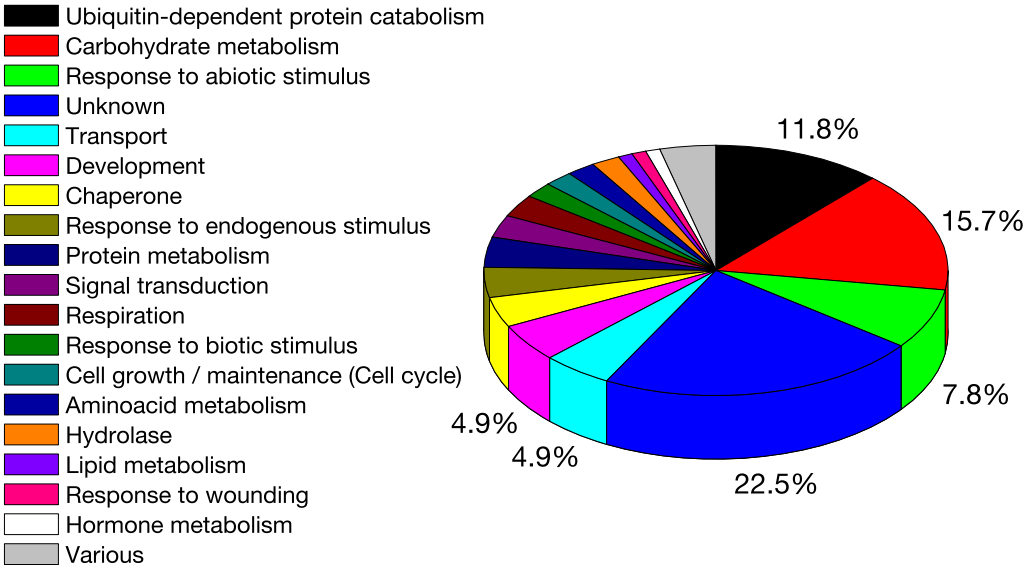

Figure 4.25: Pie graph illustrating proportions of functional groups involved in the sylA-response of the cDNA collection tested. Fragments are grouped according to biological and molecular function GO terms (Ashburner et al., 2000). For the calculations, genes present in more than one copy were only counted once.

The largest group with known biological function encompassed enzymes functioning in carbohydrate metabolism. This included two major enzymes of sucrose breakdown, five enzymes of glycolysis including pyruvate kinase, three enzymes of the tricarboxylic acid cycle (TCA) and alcohol dehydrogenase 1 (ADH1) which is involved in fermentation. In addition this group contained PRL1 which is a regulator of glucose and hormone responses. Notably, no enzyme participating in other pathways such as pentose phosphate pathway or phenylpropanoid metabolism was found to be involved.

The third group corresponded to genes which are known to be involved in detoxification (partially represented by 'response to abiotic stimulus' in Figure 4.25). This group included numerous ABC transporters, GSTs and cytochrome P450s. In addition, this group might also include the two hydrolases epoxide hydrolase and Pir7b esterase assigned to 'hydrolases' as well as monooxygenase and glucosyltransferase.

The fourth and biggest group encompassed more than 20 % of the genes and exhibited high similarity to EST and genomic sequences of unknown function. Only three fragments (*OA_a1D08*, *OA_a2D05* & *OA_a3C05*; #AJ888603, #AJ888618 & #AJ888637) were not found to have significant homology to known sequences in public databases.

Next to these four major groups, a fifth large group might be defined by the name 'mitochondrial'. This group would contain all chaperones since the two sHsps are both located to the mitochondria and the other two chaperones, Hsp 60 and Hsp 70, both were

found to correspond to mitochondrial isoforms. Furthermore, prohibitin which was assigned to 'cell growth' may also have mitochondrial chaperone activity (Nijtmans et al., 2000). In addition, the group would contain alternative oxidase, external rotenone insensitive NAD(P)H dehydrogenase, and BCS-1 which were assigned to 'respiration' as well as the voltage dependent anion channel 1. Together, this distinct group would encompass 8.6 % of all genes.

Additional genes of interest included two putative regulators of ABA signaling (protein phosphatase 2C and AIP2, Table 4.4, row 60 & Table 4.7, row 58), DMI1 (Table 4.4, row 58), which is required for symbiotic rhizobial interactions in leguminous plants (Endre et al., 2002) and a gene encoding a ligand gated ion channel which exhibited strong transcript accumulation upon syringolin treatment (Table 4.4, row 62). Furthermore, an NBS-LRR resistance gene which showed some homology to the Arabidopsis *RPP8* and a putative receptor-like kinase were strongly induced upon syringolin treatment (Table 4.4, rows 59 & 63).

This compilation given above demonstrates that syringolin appears to exhibit cytotoxic activity as reflected by the numerous enzymes with detoxifying activity. The fact that the induced chaperones were all found to be located to the mitochondria and the simultaneous induction of alternative respiration components points to an activity which might be targeted to the mitochondria. The large group of genes participating in carbohydrate metabolism indicates that the plant might undergo remarkable metabolic changes after syringolin treatment. Possible involvement of fermentation as indicated by ADH1 was unexpected. Simultaneously, many cDNA fragments corresponding to syringolin-responsive genes encoded components or regulators of the 26S proteasome indicative for large metabolic reorganizations. Interestingly, two fragments indicated involvement of ABA signaling. Possible implications in the context of syringolin action on powdery mildew infected wheat were discussed in chapt. 5.3.

4.2.6. Background induction by *Bgt* infection

In order to investigate if and to what extent fungal pre-induction contributed to the generally lower t/c ratios when sylA was applied to infected plants as compared to uninfected ones, RNA derived from previously infected and non-infected samples was directly compared by microarray hybridization following the RNA amplification protocol. The information given is based on only a single repetition of ceB. MA-plots corresponding to epidermal and mesophyll tissue of infected and uninfected wheat leaves at the -08 hat time

point are shown in Figure 4.26. A list of genes exhibiting induction ratios greater than 2 is given in the Appendix (Table 8.7).

Indeed, numerous genes were found to be differentially expressed in response to *Bgt*-infection later than 48 hours after inoculation. As expected, highest t/c ratios were observed for DNA fragments corresponding to fungal RNA in epidermal tissue (Figure 4.26A, *RB_c122*, *RB_c082* and *RB_c116*). The high t/c ratios were caused by the absence of the fungus in the control samples and thus they were not related to transcriptional regulation (e.g. *RB_c116*, Table 8.7, p.204, row 90). Consequently, corresponding genes exhibited no or much smaller t/c ratios in the mesophyll experiment (Figure 4.26B). Furthermore, all the wheat WIR and additional PR genes showed induction in epidermal and mesophyll-derived data (*WIR2*, *WIR3* and *TaGLP4* and *TaGLUC2* are marked in Figure 4.26).

Strong epidermis-specific downregulation of transcripts hybridizing to a barley protein kinase (accession #BE437646) was observed. Interestingly, downregulation of the large subunits of the mesophyll-specific ribulose-bisphosphate carboxylase (rubisco) was observed in both tissues (yellow dots in Figure 4.26A & B). The same phenomenon was observed in total leaf experiments at 24 h (but not at 8 h) after *Bgh* and *Bgt* infection (e.g. Table 8.13, p. 221, rows 23-25). For the SSH-genes of subset one, only low to moderate background induction by *Bgt* infection was observed (red dots in Figure 4.26). Strongest induction was observed for *OA_a3A04* and *OA_a1B08* exhibiting homology to PDR-like ABC transporters and a BCS1-like protein, respectively. In both cases, epidermal specificity was indicated by a significantly lower induction ratio in mesophyll samples (Table 8.7, p.204, rows 21 & 30). In correlation to this, epidermis specific induction after 24 h following infection with the incompatible barley powdery mildew was described for both genes (Bruggmann et al., 2005).

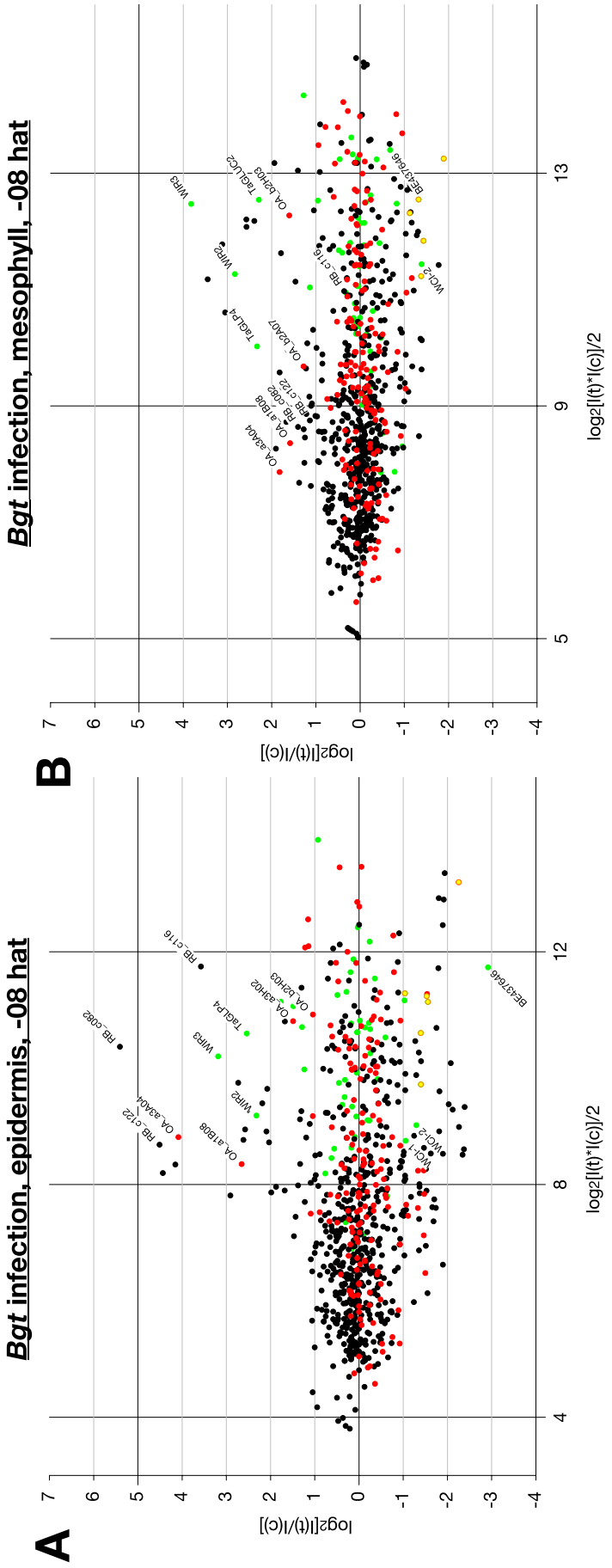

Figure 4.26: MA-plots visualizing background induction by *Bgt* in tissues enriched for epidermis (A) or mesophyll (B) during a time interval of 1 to 8 hours after treatment with control solution. Data were derived from direct comparison of RNA corresponding to epidermis of *Bgt*-infected (t) and uninfected (c) wheat leaves sprayed with mock solution (48 hai, ceB). Epidermis was separated from the remainder of the leaf and collected at 1 to 8 hat. Data were subjected to Lowess normalization (chapt. 4.2.1.4 & 8.8). Red dots: Probes corresponding to subset one (SSH-derived *OA*-fragments). Black dots correspond to subset two (cDNA AFLP-derived RB-clones). Green dots: Control probes corresponding to subset three (including WIR and WCI genes). Yellow dots: Ribulose bisphosphate carboxylase.

In ceA and ceB, several genes were identified to exhibit unusual expression in response to sylA treatment. For example *OA_a1E08* exhibiting homology to resistance genes was found to exhibit higher t/c ratios in the epidermis at both time points of ceB. To monitor responsiveness of genes with putative relevance in regard to the eradication of *Bgt* by treatment with syringolin, data of corresponding probes were assembled in Table 4.8.

In ceA (chapt. 4.2.2.2), five genes were found to exhibit exceptionally high t/c ratios in the presence of *Bgt*. Two of them, the *Pir7b*-like *OA_b2A07* (Table 4.8, row 7) and the GST *OA_b3D05* (row 9) showed weak induction of transcription by fungal infection at the corresponding time points. Interestingly, *OA_b2A07* exhibited mesophyll specific induction whereas induction of *OA_b3D05* was elevated in the epidermis. As mentioned above, in the case of the fungal *RB_c116,* high t/c ratios primarily confirmed fungal origin of the corresponding transcript. For the *Pir7b*-like *OA_b1B01* and the unknown *OA_b2B07*, no responsiveness to *Bgt* infection was indicated (rows 3 and 7).

Table 4.8: Selection of genes exhibiting aberrant transcriptional induction in ceA or ceB and their regulation by *Bgt*-infection at -08 and -32 hat following control treatment. Data were derived from one single experiment of ceB (Figure 4.26). Bold ratios: Ratios exceeding threshold limit of 2. 'no' denotes that corresponding genes did not exhibit variable expression of more than 2-fold difference. Genes described elsewhere to be epidermally induced by barley powdery mildew attack are marked with $^{'Bgh'}$, genes found to be ubiquitously induced by *Bgh* are marked with $^{'bgh'}$ (Bruggmann et al., 2005).

	Putative function & [Blast hit]	EST ID	access. no#	E-val	ceB (p < 0.05) stripped & *Bgt*-infected leaves treated with control solution - 08 hat epi	- 08 hat mes	- 32 hat epi	- 32 hat mes
	1	2	3	4	5	6	7	8
1	NBS-LRR disease resistance protein [AJ507096]	***OA_a1E08^{bgh}***	AJ874075	3.00E-49	*no*	*no*	*no*	*no*
2	2-oxoglutarate dehydrogenase (E1 subunit) [AP005199]	***OA_a3B02^{bgh}***	AJ874083	2.00E-91	*no*	*no*	*no*	*no*
3	pir7b [Q43360]	***OA_b1B01^{bgh}***	AJ874087	2.00E-67	*no*	*no*	*no*	*no*
4	pyruvate kinase [Hv.2627]	***OA_b1B10***	AJ888655	0.00E+00	*no*	*no*	*no*	*no*
5	temperature stress-induced lipocalin / Apolipoprotein D [AY077702]	***OA_b1D11***	AJ888660	1.00E-142	1.6	1.9	1.6	**2.5**
6	pir7b [CB864680]	***OA_b2A07^{bgh}***	AJ874094	3.00E-79	1.2	**2.4**	1.1	**2.3**
7	no significant hit	***OA_b2B07***	AJ888674	#N/A	*no*	*no*	*no*	*no*
8	valyl tRNA synthetase [AC084023]	***OA_b2E06***	AJ888683	3.00E-63	*no*	*no*	*no*	*no*
9	glutathione S-transferase [CN013161]	***OA_b3D05^{Bgh}***	AJ874102	1.00E-152	1.9	1.4	**2.1**	1.4
10	B12D protein [BQ170981]	***RB_96.2^{Bgh}***	AJ888727	1.00E-31	**2.8**	1.2	**3.2**	1.2
11	gigantea mRNA [BG909229]	***RB_c001^{Bgh}***	AJ873936 AJ873963 AJ873964	1.00E-117	**6.6**	**3.4**	1.9	**2.3**

In ceB (chapt. 4.2.4.1), the valyl tRNA synthetase *OA_b2E06* was found to exhibit epidermis specific expression according to ϵ_s-factors (Table 4.7, row 71). No regulation of transcription was indicated by *Bgt* infection (Table 4.8, row 8). It was therefore concluded that epidermis specificity was likely to directly result from syringolin treatment in this case.

On the other hand, epidermis specificity was sometimes observed for genes exhibiting t/c ratios close to 1. Prominent examples are *RB_96.2*, and *RB_c001* which both exhibited high ϵ_s-factors already at the early -08 hat time point (Table 4.7, rows 126 & 128). Indeed, both genes were found to exhibit epidermis specific induction upon infection with *Bgt* (Table 4.8, rows 10 & 11).

For the five cDNA fragments *OA_a1E08, OA_a3B02, OA_b1B10, OA_b1D11* and *OA_b2E06*, induction of transcription was found to be elevated in the epidermis as compared to the mesophyll (chapt. 4.2.4.1, p.85). Of these, *Bgt*-responsiveness was indicated in mesophyll samples for the lipocalin-like *OA_b1D11* (Table 4.8, row 5) but not for the rest of genes. (rows 1, 2, 4 & 5). Thus, epidermis specificity was found to result from sylA treatment and not from pre-induction by *Bgt* infection.

In conclusion, responsiveness of syringolin-induced genes to *Bgt* infection at the time points of interest was found to be low (indicated by low overall deviation of the SSH-derived OA-cDNA fragments from zero (Figure 4.26). Anyhow, 18 % of the 124 genes responding to syringolin treatment (Table 4.7) were also found to be differentially regulated by the *Bgt*-infection alone (corresponding genes were marked with an arrow in Table 8.7, p.204). Thus, regulation of transcription by infection with wheat powdery mildew 48 h before sylA treatment was found to interfere with syringolin responsiveness of individual genes. Yet, pre-induction or -repression of only 18 % of syringolin responsive genes did not explain the overall reduced t/c ratios observed in the *Bgt*-infected samples in ceA (chapt. 4.2.2.2)

4.2.7. Investigation of timing of syringolin induction

Most of the genes regulated by syringolin exhibited differential expression predominantly at the early time points in both ceA and ceB, respectively and thus they were termed 'early induced' genes. (Table 4.4 & Table 4.7). In a few cases, transcriptional induction was still found to be high also at 24 hat and -32 hat. Thirteen genes emerged from filtering of the syringolin responsive genes collection (Table 4.7) for weak decay of t/c ratios (less than 2.5-fold) and significant induction at the later time points (higher than 3-fold). Corresponding genes are listed separately in the Appendix (Table 8.8).

Conversely, only limited data was available at the early side of induction. As found by pilot experiments (chapt. 4.2.2.1) low or only little differential expression was observed at the earliest (2 hat) time points investigated (Figure 4.17A & C). Yet, average ratio deviation from zero was found to be low as well (below 1.1-fold induction and repression). Thus, also small changes as low as 1.5-fold of transcription gained increasing attention and were considered to be valuable indications for relevant differential expression. In the course of pilot experiments, syringolin treatment of infected and uninfected plants and collection of whole leaf material at the 2 hat time point was carried out twice and corresponding RNA was subjected to microarray analysis following the poly(A)$^+$-labeling protocol. Probes of the second experiment were labeled reciprocally (dye swap). Average t/c ratios were visualized on MA-plots shown in Figure 4.27 (next page).

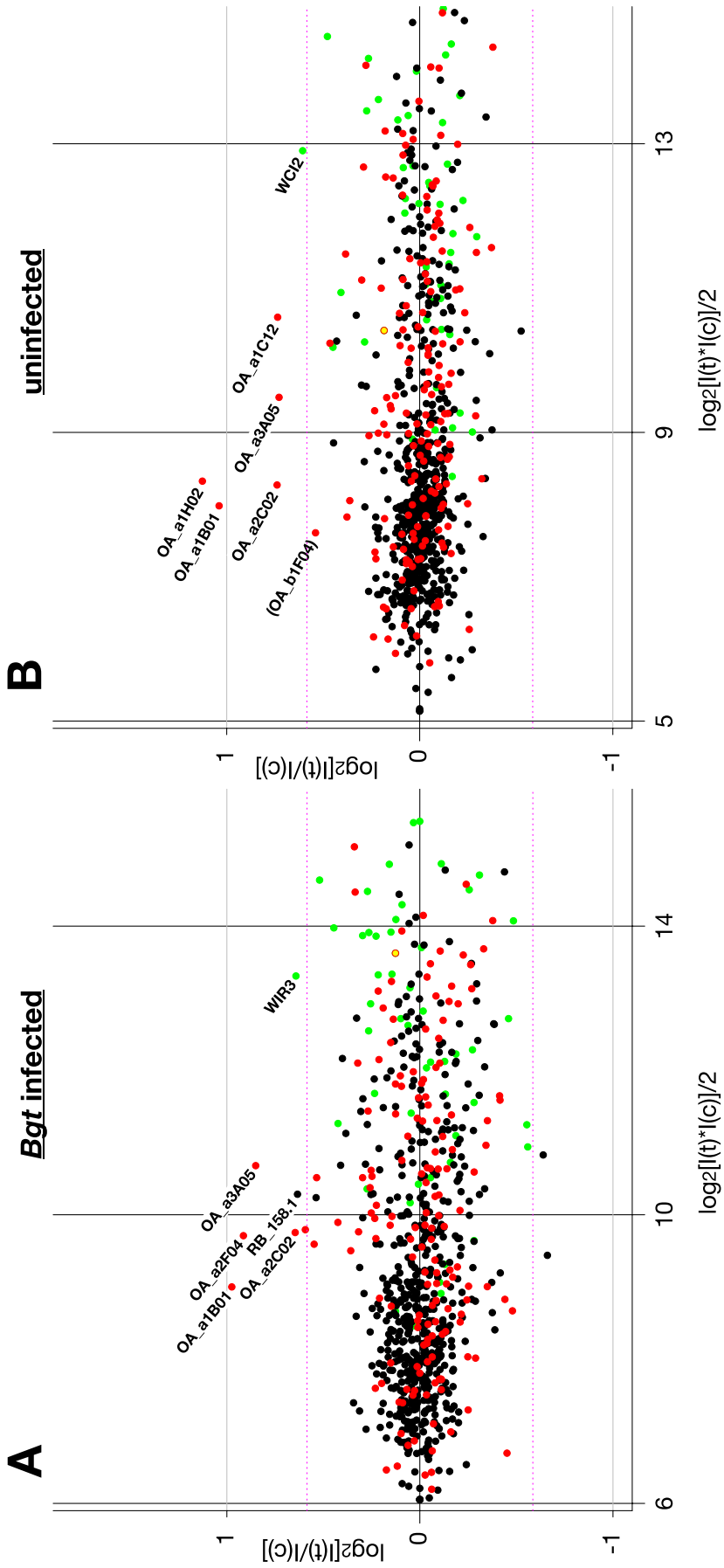

Figure 4.27: MA-plots visualizing microarray experiments corresponding to total leaf material collected 2 hours after syringolin treatment. Plants were infected (A) or uninfected with *Bgt* 48 h before treatment (B). Data was derived from pilot experiments and labeling was done according to the poly(A)$^+$ RNA method (chapt. 4.2.1.5). Two biological repetitions were carried out and average t/c ratios were calculated. Red dots: Probes corresponding to subset one (SSH-derived OA-fragments). Black dots correspond to subset two (cDNA AFLP-derived RB-clones). Green dots: Control targets corresponding to the control gene subset three (including WIR and WCI genes). Yellow dot (panel A): *WCI2* (accession #U32428). Yellow dot (panel B): *WIR3* (accession #X56011). Pink line: Threshold level of 1.5-fold induction / repression.

A number of genes was identified to reproducibly exhibit t/c ratios greater than 1.3-fold in both repetitions and an average t/c ratio greater than 1.5-fold. Corresponding genes and average t/c ratios were listed in Table 4.9. The transcripts listed in rows 3, 6, 8, and 9 were not found to exhibit increased abundance at later time points and thus, they were considered to be upregulated only transiently around 2 hours after syringolin treatment.

Table 4.9: Genes exhibiting differential expression after syringolin treatment at 2 hat. Experiments were repeated twice (the average t/c ratio is shown). Bold t/c ratios**:** t/c ratios greater than 1.3-fold in both repetitions and average t/c ratio greater than 1.5-fold. Criteria were fulfilled by genes of rows 1-9.

	Putative function & [Blast hit]	EST ID	access. no#	E-val	Syringolin 2 hat *Bgt*	Syringolin 2 hat -
	1	2	3	4	5	6
	regulated in both situations					
1	hsp 23.5 [Ta.203]	***OA_a1B01***	AJ874072	1.00E-133	**2.0**	**2.1**
2	NADPH-dependent oxidoreductase [CA682777]	***OA_a2C02***	AJ874078	3.00E-99	**1.6**	**1.7**
3	hsp70-interacting protein [CA719392]	***OA_a3A05***	AJ888633	8.00E-35	**1.8**	**1.7**
	***regulated in the ABSENCE of* Bgt**					
4	hsp 23.6 [Ta.214]	***OA_a1H02***	AJ874076	1.00E-143	1.5	**2.2**
5	fructose-bisphosphate aldolase [CD907979]	***OA_a1C12***	AJ888600	1.00E-141	1.4	**1.7**
6	WCI-2 (lipoxygenase) (wheat)	***U32428***	U32428	#N/A	1.1	**1.5**
	***regulated in the PRESENCE of* Bgt**					
7	unknown [CK215536]	***OA_a2F04***	AJ888625	0.00E+00	**1.9**	1.0
8	Wir3 (peroxidase) (wheat)	***X56011***	X56011	#N/A	**1.6**	1.1
9	BAC OSJNBa0059E14, (*O. sativa*)	***RB_158.1***	#N/A	#N/A	**1.6**	1.2

In summary, syringolin was found to result in peak induction at around 8 hours after treatment while earliest transcriptional regulation was detected at 2 hat. Levels of most transcripts were back to nearly neutral values at 24 hat with the exceptions of transcripts listed in the Appendix (Table 8.8).

4.3. SylA-responsive genes in nonhost and race-specific resistance

4.3.1. Investigation of HR during nonhost and race-specific resistance of wheat to *Blumeria graminis*

As shown in Figure 3.3, incompatible interactions of wheat and powdery mildew can result in HR of attacked cells. The phenomenon is accompanied by the induction of whole cell autofluorescence (AF) and in sylA-treated leaves, the latter directly correlated with cell death (Wäspi et al., 2001). Preliminary investigations revealed that whole cell AF was a more sensitive indication for cell death than in vitro staining of collapsed cells with Trypan blue (not shown).

To test the involvement of sylA-responsive genes in an appropriate natural system involving high proportions of cells committing HR, different interactions between powdery mildew and wheat were investigated. Differences with respect to timing and proportions of cells committing HR as reflected by whole cell autofluorescence were investigated during incompatible interactions of wheat with the nonhost pathogen *Bgh* and race-specific resistance to avirulent isolates of *Bgt*.

Wheat leaves were placed on plates containing phytagar and infected with different isolates of powdery mildew. After collection, the plant material was destained by immersion in highly concentrated chloral hydrate. Fungal structures were stained with coomassie blue and plant-pathogen interactions were investigated by bright field and incident fluorescent light microscopy. The ability of the pathogen to colonize attacked epidermal cells is reflected by the penetration efficiency (PE). Penetration efficiencies were calculated according to the equation shown below.

$$PE = \frac{HAU}{APP + HAU}$$

***PE**: Penetration efficiency* ***HAU**: Interacting cells containing haustoria* ***APP**: Interacting cells containing only appressoria*

Results are listed in the Appendix (Table 8.11) and illustrated in Figure 4.28. The nonhost wheat cv. Fidel was found to be 100 % resistant to the attack by *Bgh* (PE = 0 %). The resistance was found be caused by HR in 67 % of the interacting cells. This was reflected by the occurrence of whole cell AF as scored at two days after the infection (dpi).

Conversely, PE of the virulent strain of *Bgt* was found to be 26 %. In contrast to the incompatible interaction, unsuccessful penetration attempts did not cause HR in the majority of the cases (reflected by the low proportion of HR, Figure 4.28).

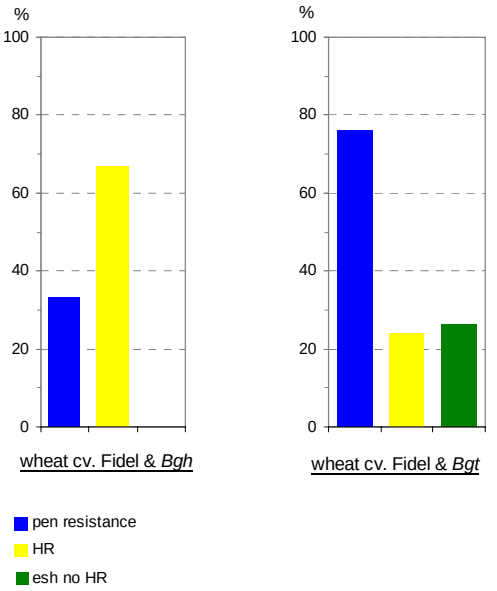

Figure 4.28: Nonhost Resistance: Proportions of cells exhibiting HR during incompatible interactions with wheat and *Blumeria graminis*. Interactions on 10 leaves were scored at 2 dpi. The percentage of cells exhibiting whole cell AF is labeled with HR resistance. The percentage of cells exhibiting no or only local autofluorescence is labeled with pen resistance. No colonized cells containing haustoria or elongating secondary hyphae (esh) were observed (labeled with 'esh no HR'). Left graph: Nonhost interaction. Right graph: Compatible interaction.

An even higher proportion of nearly 80 % of whole cell AF was observed upon interaction with another wheat cultivar (Kanzler, Table 8.11). In both nonhost interactions, extensive AF was already observed at 1 dpi (data not shown). In the case of wheat cv. Kanzler, whole cell AF occasionally was observed also in epidermal cells adjacent to attacked cells (not shown). Frequently, a strong local autofluorescence at the site of attempted penetration indicated formation of a papilla. A typical interaction is shown in Figure 4.29.

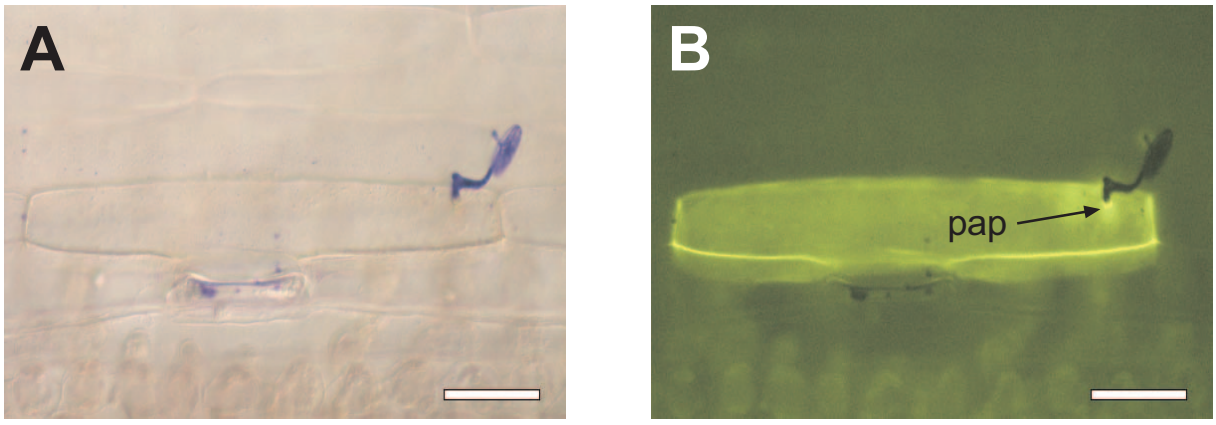

Figure 4.29: Nonhost interaction between wheat and *Blumeria graminis* f.sp. *hordei*. Fungal growth was stopped at the early penetration stage and a papilla was formed by the plant (pap). The interaction was captured at 2 dpi. Leaves were destained in chloral hydrate and fungal structures

were stained with coomassie blue. A: Bright field microscopy. B: Blue light incident fluorescence microscopy (excitation filter 450-490 nm; bypass filter 515-565 nm). Scale bar: 50 µm.

In wheat, race-specific resistance to *Bgt* is conferred by the *Pm* resistance genes (Chen and Chelkowski, 1999; Huang et al., 2004). Ten alleles were identified at the *Pm3* locus on the short arm of chromosome 1A and *Pm3b* derived from wheat cv. Chul has been physically mapped and cloned recently (Yahiaoui et al., 2004).

Induction of autofluorescence during race-specific incompatibility interactions was investigated in wheat cv. Michigan Amber (MA), the donor line of the *Pm3f* allele (N. Yahiaoui, personal communication). Wheat cv. MA was infected with virulent and avirulent Swiss field isolates of *Bgt*. The virulent isolate (referred to as *BgtVir*) corresponded to *Bgt* used in previous experiments (chapt. 4.1 & 4.2). Two avirulent isolates were used (*BgtAvr2* and *BgtAvr3)*.

Unlike the nonhost interaction, microscopical examination of incompatible interactions between wheat cv. MA and *BgtAvr2* frequently revealed the presence of fungal prehaustorial structures inside fluorescing attacked cells. A typical example is shown in Figure 4.30. Consequently, fluorescing cells harboring prehaustorial structures were recorded separately in investigations of race-specific resistance.

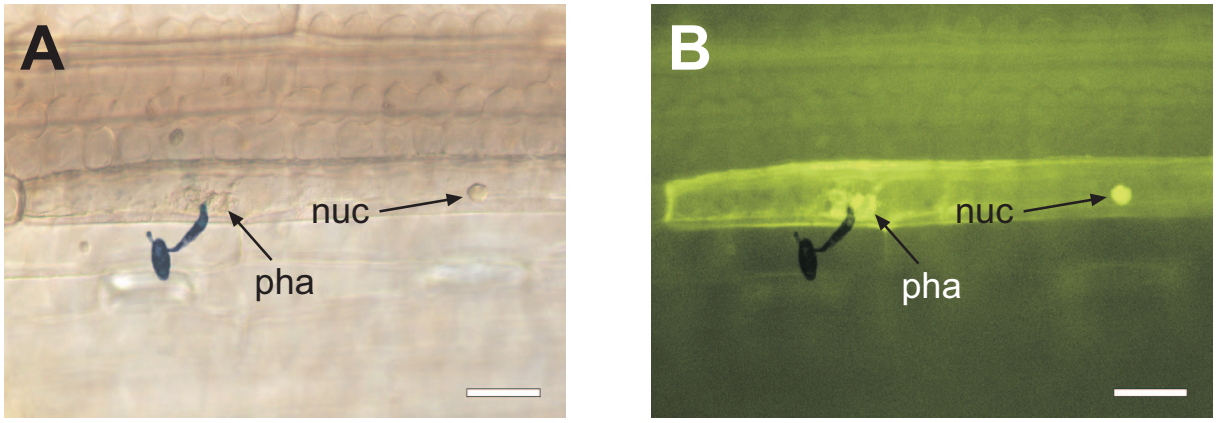

Figure 4.30: Incompatible race-specific interaction between wheat cv MA and *BgtAvr2*. Fungal growth was stopped at a late penetration stage and the formation of fungal prehaustorial structures is visible (pha). The position of the plant cell nucleus is indicated by arrows (nuc). The interaction was captured at 2 dpi. Leaves were destained in chloral hydrate and fungal structures were stained with coomassie blue. A: Bright field microscopy. B: Blue light incident fluorescence microscopy (excitation filter 450-490 nm; bypass filter 515-565 nm). Scale bar: 50 µm.

Results describing race-specific interactions between wheat cv. MA and different *Bgt* isolates are listed in the Appendix (Table 8.12) and illustrated in Figure 4.31. Cultivar MA was found to be highly resistant against *BgtAvr2* (only 1 % PE) and *BgtAvr3* (2 % PE) whereas *BgtVir* was found to be highly virulent (56 % PE). Interestingly, the resistance

against the avirulent races involved different proportions of cells exhibiting autofluorescence. Whereas resistance against *BgtAvr2* involved autofluorescence in more than 90 % of all interactions, the percentage was 32 % in the case of *BgtAvr3* (Figure 4.31, left and middle graph). In contrast to the incompatible nonhost interaction described above, whole cell AF occurred later in the incompatible race-specific interactions and it was not observed at 24 h after the infection (data not shown). More than 75 % of the attacked cells exhibiting AF harbored prehaustorial structures in the interaction with both avirulent isolates. In the compatible interaction, resistance was predominantly caused by penetration (pen) resistance. Unlike the incompatible interactions, no prehaustorial structures were observed in attacked cells exhibiting whole cell AF after infection with the virulent isolate (Figure 4.31, right graph).

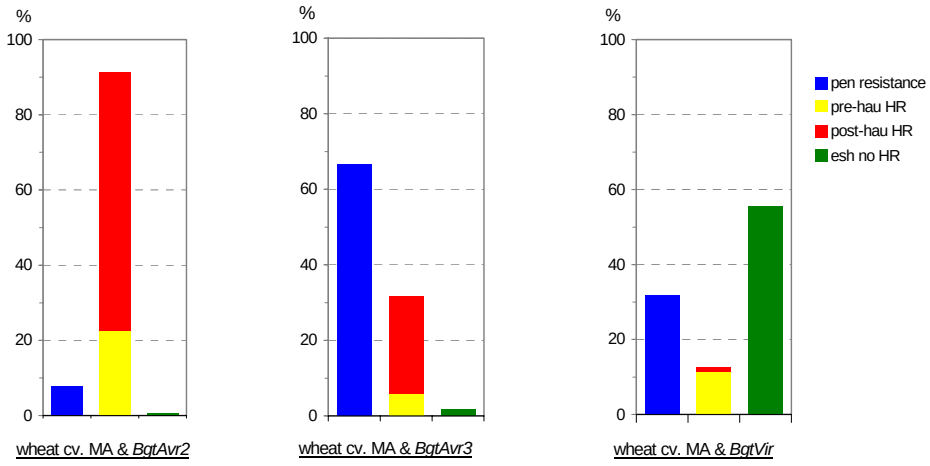

Figure 4.31: Race-specific resistance: Proportions of cells exhibiting HR during incompatible interactions with wheat and *Blumeria graminis*. Interactions on 2 leaves were scored at 2 dpi. The percentage of cells exhibiting whole cell AF lacking prehaustorial structures is labeled with 'pre-hau HR'. Whole cell AF in the presence of pre-haustorial structures is labeled with 'post-hau HR'. The percentage of cells exhibiting no or only local autofluorescence is labeled with pen resistance. Colonized cells containing haustoria or esh were labeled with 'esh no HR'. Left and middle graph: Race-specific resistance. Right graph: Compatible interaction.

In summary, it was found that nonhost and *Pm3* race-specific resistance of wheat to powdery mildew was frequently accompanied by remarkable proportions of HR. Whereas HR was initiated during earlier penetration stages in nonhost resistance, initiation predominantly occurred at later haustorium formation stages in the race-specific resistance interactions. This coincided with the fact that whole cell AF was visible at 24 hai in the nonhost interaction but not in the *Pm3* race-specific interaction. Since penetration of attacked cells by the fungus takes place at 10 to 12 hai, whereas the haustorium is formed at 18 to 24 hai (Figure 3.3), it was concluded that the occurrence of autofluorescence

followed initiation of HR in a time interval of about 8 to 10 h. Whereas defense occurred at later time points with *BgtAvr*2, resistance of wheat cv. MA to *BgtAvr3* was strongly based on penetration resistance. This indicated that the quality of recognition of an avirulence gene product by the resistant plant cell might influence the speed by which corresponding cells defend themselves.

In conclusion, the interaction of wheat cv. MA and powdery mildew isolate *BgtAvr2* was considered to be a promising system to study possible participation of sylA-responsive genes in the onset of the hypersensitive response.

4.3.2. Functional characterization of selected genes

In order to efficiently test biological functions of candidate genes during the interaction of powdery mildew and the host plant, transient epidermal single cell transformation by bombardment with DNA-coated particles was successfully applied on wheat leaves and allowed for the characterization of several PR-genes (Schweizer et al., 1999b). The system was further improved to study loss of gene function by specific induction of RNA interference via transformation with either double stranded RNA (dsRNA) or hairpin loop expression vectors (Schweizer et al., 2000).

Transient transformation of wheat only offers a small time frame for subsequent infection with powdery mildew due to considerable induction of basal resistance in bombarded leaves (P. Schweizer, personal communication). Thus, the incompatible *Pm3* race-specific interaction was considered to be well suitable for current investigations due to the late induction of HR observed in previous experiments (chapt. 4.3.1). Simultaneously to microarray experiments, a system allowing to investigate the involvement of candidate gene expression during onset of HR in the wheat cv. MA was tested. Upon biolistic transformation of wheat cv. MA epidermal cells with a marker vector carrying the *GUS* gene under the control of the maize ubiquitin promoter (pUbiGUS), bombarded leaves were frequently found to be highly susceptible against the nominal avirulent isolate *BgtAvr2* (data not shown). The phenomenon was hypothesized to be of technical origin and to be related with the less robust morphology of wheat cv. MA as compared to other cultivars like Fidel or CC. Indeed, the problem could be solved in later experiments by increasing the humidity to 90 % relative humidity during incubation of infected leaves (data not shown). This indicated that in the transient assay system, wheat cv. MA was more sensitive to drought as compared to the other cultivars and that dry conditions eventually result in a complete collapse of the plant defense. Total control over humidity was found to be possible by incubation in fully controlled climate chambers only. High humidity with simultaneous strict avoidance of formation of condensate were critical factors to create favorable growth conditions for the pathogen and physiological environmental conditions for the plant leaves at the same time.

Alternatively, the possibility to induce HR in the robust but susceptible wheat cv. Fidel was assessed. Heterologous expression of the wheat *Pm3b* resistance gene allele in the susceptible *T. aestivum* cv. Chancellor (CC) had been described to protect transformed cells from subsequent infection with a wheat powdery mildew isolate avirulent for *Pm3b* expressing plants (Yahiaoui et al., 2004). For simplicity, the corresponding *Bgt* isolate was

referred to as *BgtAvr1.* As observed 44 hai, blocked colonization of a near-isogenic wheat line for *Pm3b* in the genetic background of CC with *BgtAvr1* was accompanied by HR in 54% of the infected cells (Yahiaoui et al., 2004).

To induce HR-related resistance in wheat cv. Fidel, epidermal cells were transformed with the pGY1 expression vector carrying the wild type allele of *Pm3b* under the control of the 35SCaMV promoter (referred to as pPm3b). As negative control, leaves were either transformed with the empty pGY1 expression vector or with pGY1 carrying a mutant allele for *Pm3b (*pM23*)*. The corresponding DNA sequence contained a single-base deletion causing premature abortion of transcription (Yahiaoui et al., 2004). To microscopically detect transformed cells, leaves were co-bombarded with a marker vector carrying the *GUS* gene under the control of the maize ubiquitin promoter (pUbiGUS). Three hours after bombardment, leaves were infected at high spore density with *BgtAvr1*. Staining for GUS activity and fungal structures was performed 48 hours after transformation. Transformed epidermal cells interacting with powdery mildew (iaGUS cells) were microscopically investigated and scored for modes of interaction. Examples of compatible and incompatible interactions are shown in Figure 4.32.

PEs were calculated for the interacting GUS-positive cells (iaGUS). Colonization by the pathogen was considered to be successful upon the presence of a mature haustorium which usually was accompanied by the formation of secondary elongating hyphae on the leaf surface. Upon simultaneous attack of individual cells by multiple fungal appressoria, the interaction was judged with regard to the final outcome. Since the presence of only one single haustorium would already have resulted in colonization by the fungus, corresponding cells were considered to be susceptible.

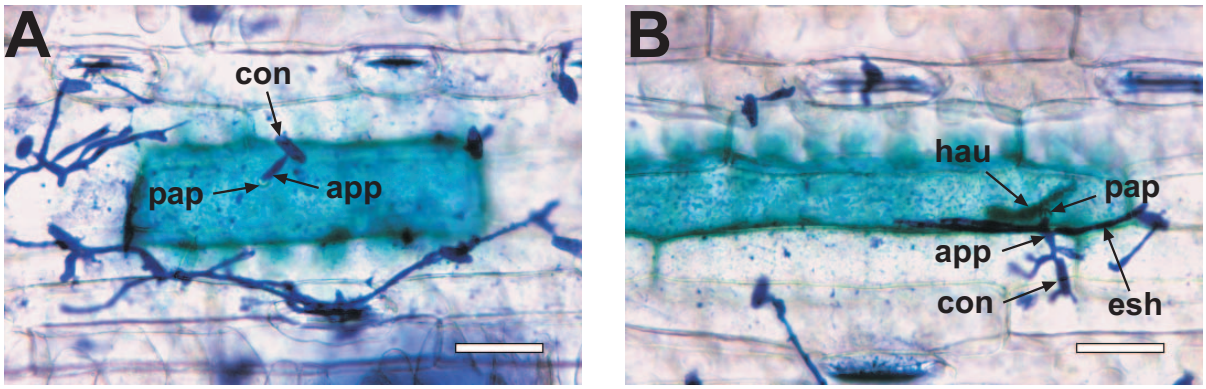

Figure 4.32: Interaction of transformed epidermal wheat cells with *Blumeria graminis* f.sp. *tritici* at 40 hai. After landing, fungal conidia (con) form appressorial germ tubes (app). In incompatible interactions (A), penetration is often stopped by the formation of cell wall appositions called papillae (pap) by the host cell. In the compatible interaction (B) papillae are sometimes formed but broken through and the formation of haustorial feeding structures (hau) is initiated. In the course of the proceeding colonization, elongating secondary hyphae (esh) start to overgrow the whole leaf surface. Scale bar: 50 µm.

In addition, a few transformations were carried out with a pGY1 expression vector carrying the *Pm3f* allele (pPm3f) derived from wheat cv. Michigan Amber (Yahiaoui, personal communication). Results are shown in Figure 4.33.

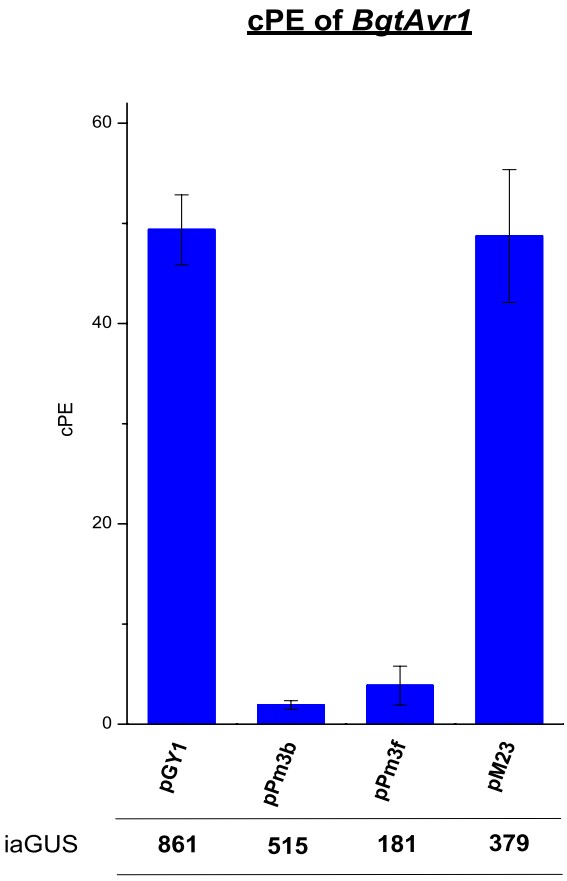

Figure 4.33: Effect of *Pm3b* and *Pm3f* overexpression in wheat cv. Fidel on the penetration efficiency of *BgtAvr1*. cPE was related to the number of interacting GUS cells in the control transformation with the empty expression vector. Average values were calculated. Experiments were repeated 7 times for pGY1 and pPm3b, twice for pPm3f and 3-times for pM23. Standard error bars are given. iaGUS denotes the total number of interacting GUS cells scored.

It was found that overexpression of the functional resistance genes caused two effects. First, successful colonization of epidermal cells was drastically reduced as compared to the control treatment. Second, also the number of GUS-expressing cells was reduced when leaves were bombarded with the expression vector carrying the resistance genes. As compared to transformation with the empty pGY1, reduction to 55 % of GUS expressing cells was observed upon transformation with pPm3b as well as with pPm3f. A similar but slightly stronger effect had already been observed upon transient transformation of wheat cv. CC and it was ascribed to result from suppressed *GUS* transcription due to induction of HR (Yahiaoui et al., 2004). Thus, for the calculation of the penetration efficiency, the number of cells containing fungal haustoria after individual transformations was always related to the total number of interacting GUS-expressing cells of the pGY1 control transformation. The corresponding (control) penetration efficiency was referred to as cPE.

As obvious in Figure 4.33, cells transformed with the empty control vector were highly susceptible to *BgtAvr1* and penetration resulted in the formation of the haustorial

feeding structure in 49 % of all cases. Upon overexpression of transcripts corresponding to the *Pm3b* allele, cPE was strongly reduced to 1.9 %. Reduced cPE was also observed after transformation with pPm3f but cPE was still at 3.9 % on average. Conversely, no reduction of cPE was observed upon heterologous expression of the mutant *Pm3b* allele (pM23) and average cPE remained at 49 %.

It was concluded that incompatible race-specific interaction with *Bgt* in wheat cv. Fidel could successfully be generated by transient overexpression of the resistance genes *Pm3* alleles b and f. Reduced numbers of GUS-expressing cells upon co-bombardment with pPm3b and pPm3f indicated that like in the near-isogenic Chul/8*CC wheat lines, the resistance reaction of wheat cv. Fidel was also associated with a certain percentage of HR in attacked cells.

Based on early results of ongoing microarray experiments, several genes were selected for investigations of functional involvement in *Pm3b*-related HR. Selection was predominantly based on epidermis specificity observed at late time points after sylA treatment in ceB. Loss of gene function of relevant genes was expected to hamper the onset of the hypersensitive response and to re-induce susceptibility against *BgtAvr1* of wheat cv. Fidel cells expressing transcripts of *Pm3b*.

Numerous DNA fragments obtained by PCR of SSH-derived cDNA fragments were cloned into RNAi expression vectors. Two different vectors both allowing for hairpin loop expression were used. pJP26 corresponds to pGY1 carrying the second intron of a wheat resistance gene analog (accession #AY270159) in the middle of the multiple cloning site (MCS). pJP26 mediated expression of *TaGLP4* hairpin transcripts efficiently induced RNAi in transformed wheat epidermal cells (Christensen et al., 2004). pIPKTA30N (Douchkov et al., 2005) was kindly provided by P. Schweizer (IPK Gatersleben, Germany). It corresponded to a modified version of pJP26 converted into a destination vector for site-specific recombination cloning with the Gateway cloning system (Invitrogen BV, Groningen, The Netherlands).

In 11 cases, PCR fragments were obtained with gene-specific primers. Constructs were generated by two directed cloning steps of sense and antisense orientated DNA copies into pJP26. Corresponding constructs were referred to as foldback constructs (p_FB). Details are given in Materials and Methods. Alternatively, 19 hairpin loop expression constructs were obtained by Gateway cloning. cDNA fragments were PCR-amplified with universal primers specific for the SSH-derived adapter sequences present at the 5' and the 3' ends of corresponding cDNAs. The PCR fragments were cloned into appropriate entry vectors and recombined into the pIPKTA30N destination vector in a single step.

Corresponding constructs were referred to as IPK constructs (p_IPK). All constructs were verified by sequencing. A list is presented in Table 4.10.

Table 4.10: Constructs created for gene-specific inhibition of expression by induction of RNAi in a transient expression system. Constructs created with pJP26 were referred to as FB constructs. Constructs created with pIPKTA30N were referred to as IPK constructs. All constructs were assigned to pools for simultaneous testing of multiple genes (column 4). Asterisks in column 1 indicate that corresponding constructs were renamed after sequencing and original names are listed in the Appendix (p.219).

Construct ID	putative function	cDNA accession#	pool
1	2	3	4
pOA_a1E06_FB	alternative oxidase	AJ874074	1
pOA_a2C11_FB	26S proteasome regulatory subunit	AJ888616	1
pOA_a3B03_FB	UDP-glucose:salicylic acid glucosyltransferase	AJ888635	1
pOA_a3C11_FB	NADPH-dependent oxidoreductase	AJ888639	2
pOA_a3F09_FB	cdc 48	AJ888645	2
pOA_a3G10_FB	glutathione S-transferase	AJ888647	2
pOA_b2A02_FB	autophagy / symbiosis-related microtubule associated protein	AJ888667	3
pOA_b2A06_FB	ABI3-interacting protein 2 (abscisic acid insensitive interacting protein)	AJ888668	3
pOA_b3F11_FB	NAM-like (No apical meristem)	AJ888713	3
pOA_a3H01_FB	MRP-like ABC transporter	AJ888649	4
pOA_a1H02_FB	small heat shock protein Hsp23.6	AJ874076	4
pOA_b3C08_IPK*	Ran binding protein-1	AJ888703	4
pOA_a1B08_IPK	BCS1-like protein / AAA-type ATPase-like protein	AJ874073	5
pOA_a1D06_IPK	alcohol dehydrogenase ADH1	AJ888602	5
pOA_a1D08_IPK	no significant hit	AJ888603	5
pOA_a2E09_IPK	unknown	AJ888622	6
pOA_a2F04_IPK	unknown	AJ888625	6
pOA_a3B09_IPK	hsp70	AJ874084	6
pOA_b1E11_IPK	succinyl-CoA-ligase beta subunit	AJ874090	7
pOA_b1F08_IPK	26S proteasome subunit-like protein	AJ888663	7
pOA_b2E06_IPK	valyl tRNA synthetase	AJ888683	7
pOA_a3A04_IPK*	PDR-like ABC transporter	AJ874081	8
pOA_a3C03_IPK	prohibitin	AJ874085	8
pOA_b1G11_IPK	dynamin protein	AJ888665	8
pOA_b1G10_IPK*	TipC / VPS13 - like protein	AJ888664	9
pOA_a2A05_IPK	alcohol dehydrogenase ADH1	AJ888612	9
pOA_b1D01_IPK	succinyl-CoA-ligase beta subunit	AJ874089	9

Table 4.10 (continued)

Construct ID	putative function	cDNA accession#	pool
1	2	3	4
pOA_a1D09_IPK*	cytochrome P450	AJ888604	10
pOA_b3C03_IPK*	sucrase	AJ888702	10
pOA_b2G09_IPK*	2,3-bisphosphoglycerate-independent phosphoglycerate mutase	AJ874098	10

Suppression of transcriptional induction was simultaneously monitored for three constructs by transformation with pooled DNA. Corresponding pool numbers are listed in Table 4.10, column 4. As negative control, leaves were transformed with the empty hairpin transcript expression vector or with the empty pGY1 vector. To detect transformed cells, leaves were co-bombarded with the pUbiGUS plasmid. In terms of a medium scale screening, transformation with each pool was carried out once. To confirm results, transformation was repeated in six cases. All transformations were carried out with identical total amounts of DNA and control transformations were performed with either the empty expression vector (pGY1) or the empty RNAi expression vectors (pJP26 and pIPKTA30N). Details are given in Materials and Methods. Results are shown in Figure 4.34. On average, 271 interacting GUS cells were evaluated for each control and reference transformation (blue bars in Figure 4.34). For the test pools, the average number of interacting GUS cells was 174 for each transformation. As compared to the control transformation with the empty expression vector only, transformation with pPm3b reduced cPE from 53 % to 2 %. In control transformations with the empty RNAi expression vectors, cPE was slightly higher. In particular for the pJP26 control, cPE was elevated to 6 %.

As obvious in Figure 4.34, none of the transformations with the test pools resulted in a significant increase of cPE as compared to the control transformations with the empty RNAi expression vectors. Strikingly, transformation with pool 05 reproducibly resulted in a decrease of cPE. Thus, members of pool 05 were subjected to separate transformation with single constructs in the absence of the resistance gene *Pm3b*. However, repetition of the experiment with the individual construct did not confirm the first result.

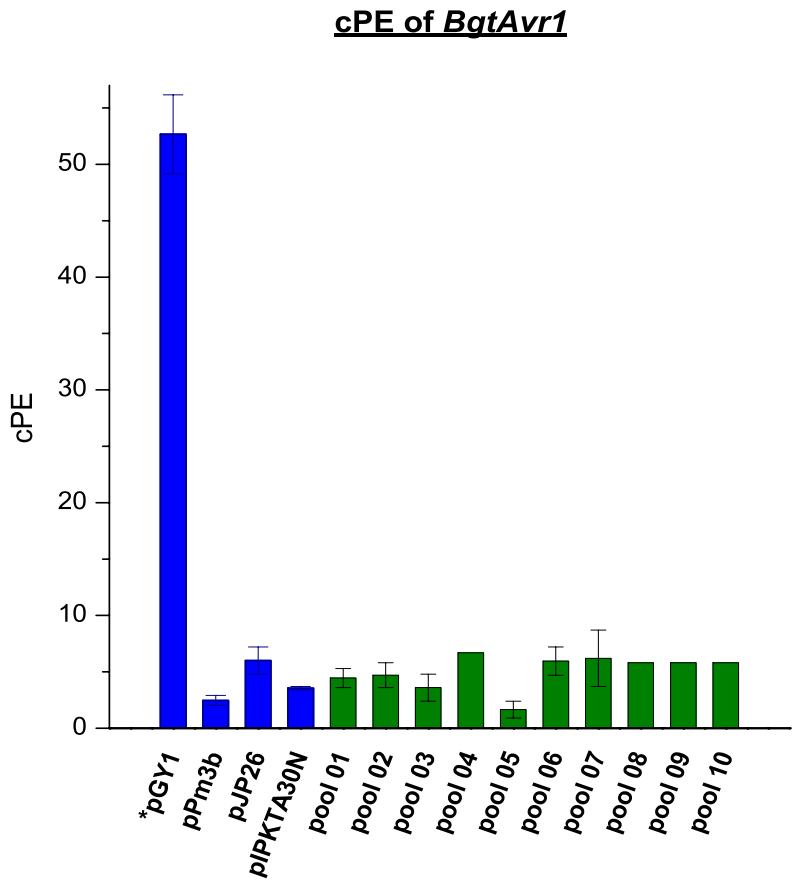

Figure 4.34: Effect of co-bombardment with pooled RNAi-inducing constructs on resistance conferred by *Pm3b* overexpression in *BgtAvr1*-infected wheat cv. Fidel. cPE was related to the number of interacting GUS cells in the control transformation with the empty expression vector pGY1. Average values were calculated. No repetition was carried out for pool 04, 08, 09 and 10. Upon repetition, standard error bars are indicated. Except for the control transformation (pGY1 marked with an asterisk), all transformations were carried out with identical amounts of pPm3b DNA.

Besides, a significantly elevated number of iaGUS cells was observed for pool 08 (1.5-fold above average) but due to a low relative proportion of haustorium formation in iaGUS cells, the former finding was not reflected in the cPE data presented in Figure 4.34. Yet, separate transformation with the corresponding single constructs in the presence and absence of the resistance gene *Pm3b* did not confirm these observations. In contrast, transformations in the absence of *Pm3b* even indicated a decrease in PE upon RNAi-mediated silencing in the case of *OA_a3A04* (data not shown). The two probes *OA_a1B08* and *OA_a3A04* (pools 5 & 8) were both found to be induced in the epidermis upon infection with the *Bgh* nonhost pathogen (Bruggmann et al., 2005). With regard to that, it was hypothesized that expression of the corresponding transcripts might be required for colonization of the host plant.

To test this, induction of RNAi by transient expression in wheat epidermal cells in the absence of pPm3b and subsequent challenge inoculation with *BgtAvr1* was repeated five times and the results are presented in Table 4.11.

Table 4.11: Effect of silencing (RNAi) on the penetration efficiency of *Blumeria graminis* f.sp. *tritici.* To visualize transformed cells, wheat cv. Fidel leaves were co-bombarded with pUbiGUS. The penetration efficiency (PE %) was calculated in relation to the number of interacting GUS-positive cells of the corresponding transformation (standard errors are given). The relative PE reflects the relation between PE of the pGY1-control transformation and transformation with corresponding test constructs. Average values are listed and standard errors are given behind. Experiments were repeated five times and total numbers of interacting GUS-positive cells are listed.

Transgene	Series	PE(%)	rel.PE (%)	rep	iaGUS
pGY1	1	43 ± 1.5	100	5	360
pOA_a3A04_IPK	1	43 ± 4.8	103 ± 14.7	5	397
pGY1	2	40 ± 1.4	100	5	253
pOA_a1B08_IPK	2	40 ± 4.5	99 ± 11.5	5	312

As obvious, no change of PE was observed and average rel. PE were found to be 103% and 99%, respectively. Thus, none of the 30 genes tested for the ability to induce elevated susceptibility of Pm3b expressing epidermal cells against *BgtAvr1* showed a clear effect upon medium scale screening of pools of three silencing constructs.

4.3.3. Activation of transcription during incompatible and compatible interactions

To investigate the involvement of sylA responsive genes during nonhost and race-specific resistance of two wheat cultivars to powdery mildew, eight day-old plants were heavily infected with various isolates of *Blumeria graminis*. The experimental setup based on the results presented in chapt. 4.3.1. Wheat cv. MA was infected with the two avirulent isolates *BgtAvr2* and *BgtAvr3*, the virulent isolate *BgtVir* and the nonhost pathogen *Bgh*. In addition, wheat cv. Kanzler was infected with the nonhost pathogen *Bgh* and the virulent wheat powdery mildew isolate *BgtVir*. Plant material was harvested at 8 and 24 hai. RNA was extracted and subjected to microarray analysis following the poly(A)$^+$ RNA labeling protocol on microarray slides series 7. The experiment was carried out once (single-pass experiment). In addition to standard normalization procedures (chapt. 4.2.1.4), all data derived from the same collection time point was subjected to global SD-normalization (scale normalization by Yang et al., 2002b) as implemented in TIGR MIDAS software (Saeed et al.,

2003). By this means, variability derived from variations of infection densities were minimized. Representative MA-plots are shown in Figure 4.35.

As obvious, differential transcription was very pronounced at 24 hai and included extensive up as well as down regulation of gene transcription (Figure 4.35B, D and F). At the earlier time point, differential transcription was mainly manifested by upregulation and strongest responses to powdery mildew infection were observed for *WIR* genes (Figure 4.35A, C and E; the control gene subset three is visualized by green dots). Altogether, a very distinct pattern arose after infection with powdery mildew as compared to sylA treatment (e.g. Figure 4.19A & B), where upregulation was restricted to mainly the SSH-derived probes of the SSH-derived *OA*-fragments of subset one. Here, the response to *Blumeria* infection expectedly also included numerous genes of the cDNA AFLP-derived subset two and the control gene subset three. Interestingly, it also involved many genes of the sylA-responsive subset one (red spots; Figure 4.35). Moreover, the responses in the susceptible and race-specific as well as nonhost resistant interactions were found to be quite alike as visually judged by the MA-plots in Figure 4.35.

A list of probes exhibiting more than two-fold up or downregulation in any of the treatments is presented in the Appendix (Table 8.13). It encompassed a total number of 263 probes, 70 of which corresponded to *OA*-probes. With regard to the induction of HR in *Bgt*-infected cells by syringolin treatment, the main interest here was to identify genes exhibiting pronounced differential expression in incompatible interactions involving high percentages of HR. The latter included interaction of wheat cv. MA and *BgtAvr2* and wheat cv. Kanzler with *Bgh* (chapt. 4.3.1). Thus, expression data were filtered for genes exhibiting more than 2-fold elevated or decreased expression in either the interaction with *BgtAvr2* or *Bgh* as compared to the interaction with *BgtVir*.

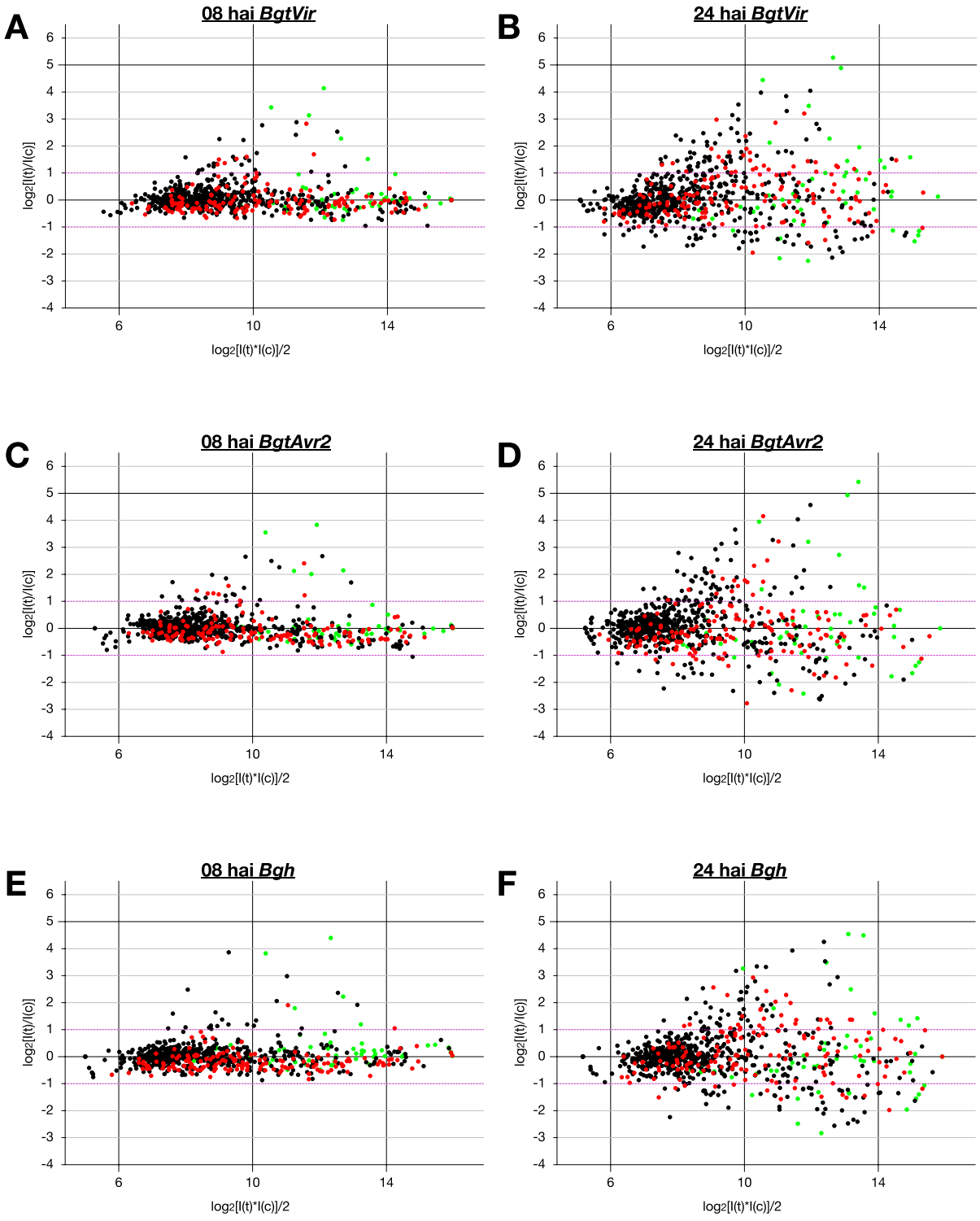

Figure 4.35: MA-plots of single experiments demonstrating induction of transcription in response to *Blumeria* infection. Leaf material was collected at 08 hai (A, C and E) and 24 hat (B, D and F) from wheat cv. MA heavily infected with different *Blumeria* isolates (indicated at the top of each MA-plot). Red dots: Genes corresponding to *OA*-transcripts derived from SSH-screening on syringolin-treated plants. Black dots: *RB*-genes corresponding to microarray subset 2. Green dots: Genes corresponding to the control subset 3 (subset 4 is not shown). Pink line: Threshold limit of 2-fold induction/repression.

The main attention was focused on genes exhibiting elevated induction in the HR-related interactions. Thirteen genes including 5 *OA*-genes, 7 *RB*-genes and *WCI2* belonging to the control subset three were identified. The strongest effect was observed for *OA_a2F04* exhibiting 10-fold elevated expression after infection with *BgtAvr2* as compared to *BgtVir* (Table 8.13, row 46, columns 11 and 12). Expression of genes exhibiting similar patterns was clustered by the multiple *k*-medians clustering (Soukas et al., 2000) on the basis of Pearson distance metrics (Saeed et al., 2003). Expression graphs are illustrated in Figure 4.36.

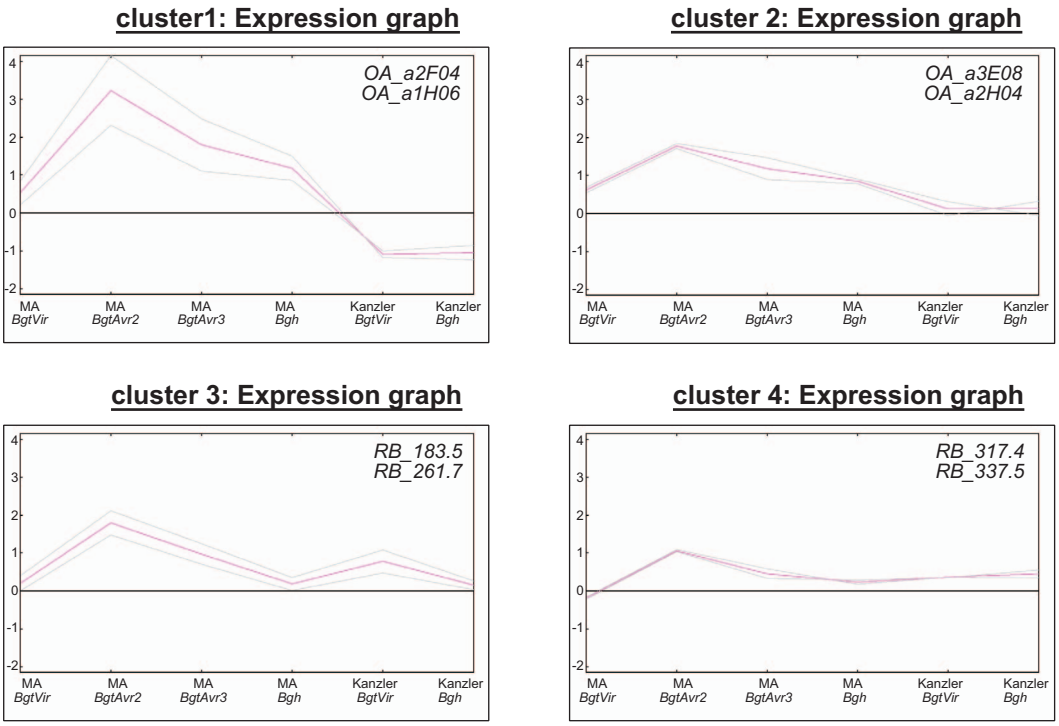

Figure 4.36: Expression graphs of genes exhibiting elevated expression at 24 hai in the incompatible race-specific interaction. Graphs of totally 8 genes are shown. Log base 2 ratios of individual genes were plotted (y-axes) and the different interactions were arranged along the x-axes. Grey lines connect log ratios of individual genes. The red line corresponds to the centroid graph (mean expression levels). The wheat cultivar is indicated at the bottom (Michigan Amber and Kanzler) and the pathogen isolates are given just below.

The expression pattern of the two genes exhibiting strongest induction in the wheat cv. MA interaction with *BgtAvr2* clustered together (Figure 4.36, cluster 1). Both genes encoded proteins of unknown function. The expression pattern of cluster 2 was found to be very similar, except that genes of cluster 1 appeared to be downregulated in wheat cv. Kanzler. *OA_a2H04* encoded a putative 60S ribosomal protein L30 and *OA_a3E08* exhibited high similarity to alanine acetyltransferases. t/c ratios are listed in Table 8.13 on p.221 (columns 37, 46, 47 & 56). All four *OA*-probes were found to be upregulated by sylA treatment (Table 4.7). Apart from *OA_a2H04*, the genes showed *Bgt*-specific upregulation of

transcription at 8 hai (Table 8.13). Interestingly, the relation between t/c ratios derived from *BgtAvr2* and *BgtAvr3* infection was found to be reversed at the earlier time point.

Unlike genes of clusters 1 and 2, none of the genes assigned to clusters 3 and 4 was found to exhibit sylA responsiveness in ceA and ceB. Putative function of encoded proteins was known only in the case of RB_317.4 exhibiting weak similarity to a 14-3-3-like protein. Corresponding t/c ratios were listed in Table 8.13 (row 210 for *RB_183.5*, row 226 for *RB_261.7*, row 245 for *RB_317.4* and row 251 for RB_337.5).

For the race-specific incompatibility between wheat cv. MA and *BgtAvr2*, only *WCI-2* (Table 8.13, row 16) was found to exhibit elevated expression at 08 hai. Interestingly, expression of the gene which exhibited sylA responsiveness only very early (Table 4.9, p.97) was found to be very different between the interactions to the two avirulent isolates (Table 8.13, columns 6 & 7) and the expression was found to be 10-fold downregulated at 24 hai in interactions with wheat cv. Kanzler (columns 15 & 16).

Altogether, transcription profiling of wheat-powdery mildew interactions only revealed small overlaps of gene transcription with the response to sylA treatment. Only 16 % of all sylA-responsive probes which included genes encoding G3PDH, sHsps, prohibitin or NADH dehydrogenase showed similar responses upon infection with powdery mildew (t/c ratios higher than 3). Only three genes, enolase 2, lecithin-cholesterol acyl transferase and epoxide hydrolase showed reverted transcription. Yet, the identification of genes exhibiting pronounced transcriptional induction in the interaction with *BgtAvr2* was interesting. In this respect, cluster 1 (Figure 4.36) containing *OA_a2F04* which showed 18-fold induction with *BgtAvr2,* only 6-fold induction with *BgtAvr3* and only 2-fold induction with *BgtVir* (Table 8.13, row 46) gained particular attention since elevated transcript accumulation at 24 hai coincided with the hypothesized time point of HR induction in the respective interaction (chapt. 4.3.1).

5. Discussion

5.1. Technical aspects

5.1.1. Suppression subtractive hybridization

Suppression subtractive hybridization (SSH) according to Diatchenko et al. (1999) was carried out in order to identify gene transcript accumulation in syringolin-treated wheat leaves infected with *Bgt*. SSH combined with differential screening by reverse northern dot blot hybridization and sequence analysis yielded 158 different candidate genes out of 498 cDNA fragments screened (chapt 4.1). Of these, 103 cDNA fragments encoding proteins of a broad functional range were confirmed to be differentially expressed by microarray analysis. This remarkable change in the wheat transcriptome is in accordance with earlier findings in syringolin-treated wheat leaves 10 hours after application (Wäspi et al., 2001). The identification of a wheat homolog of the rice *Pir7b* gene proved the reliability of the technique and confirmed data obtained by in vitro translation of RNA derived from sylA-treated wheat leaves (Wäspi et al., 2001).

Enrichment by SSH is based on DNA hybridization kinetics and its efficiency greatly depends on the number of target sequences (transcripts of higher relative abundance) within the test samples and the strength of transcriptional induction (Diatchenko et al., 1999). Accordingly, the large and complex transcriptome resulting from the allo-hexaploid nature of wheat causes lower relative abundance of accumulating transcripts and may significantly lower subtraction efficiency. However, the yield of 103 different cDNA fragments demonstrates that the method can also be very successfully applied to wheat. Still, with regard to the high number of different genes obtained by SSH, it is speculated that the collection might represent only prominent representatives of a larger set of transcripts induced in the course of large changes in the wheat transcriptome after syringolin application.

As a result from stringent selection by hybridizations during SSH, the obtained cDNA fragments were found to be highly specific and of 28 fragments tested, more than 60 % were found to give rise to 3 or fewer bands on wheat southern blots (T. Schnurbusch, personal communication). Seven cDNA fragments including the ones encoding an NADPH-dependent oxidoreductase (*OA_a2C02*), Hsp23.6 (*OA_a1H02*), and an MRP-like ABC transporter (*OA_a3D05*) exhibited polymorphic bands between wheat varieties Arina and Forno and were mapped during construction of a genetic linkage map in wheat (Paillard et

al., 2003). High DNA sequence specificity also rendered the SSH-fragments particularly suitable for subsequent investigations by cDNA microarray hybridization experiments.

A high average size of 550 bp of the cDNA fragments obtained by SSH was found to by very advantageous for blast analysis and sequence alignment. Sequence annotation played a key role in the present work. The marked increase during the past years of wheat EST sequence information available in public databases allowed to assign putative gene functions with increasing probability in the progression of the study. Still, the function of more than 20 % remained unknown. Assigning functions via highly similar but longer or overlapping EST sequences was very time consuming and frequently required blasting of sequences obtained by previous blasting of *OA* cDNA sequences (blastblasts). In this respect, the EST contigs assembled by the National Center for Biotechnology Information (NCBI, Bethesda (MD), USA) in the UniGene database proved to be a helpful tool. At present, the UniGene database contains 34'606 EST entries derived from wheat (*Triticum aestivum*). Yet it was also found that contigs sometimes contained EST sequences derived from two different transcripts. For example *OA_a2C02* encoding an NADPH-dependent oxidoreductase shows high sequence similarity (98% of 254 nt) to members of a UniGene cluster (accession #Ta.3448). In this cluster, EST fragments assigned to NADPH-dependent oxidoreductases are linked to the function of PRL1-interacting factor N via one single EST (accession #CA736677). The latter exhibits high similarity to NADPH-dependent oxidoreductases at the 5' end and to PRL1-interacting factor N at the 3' end but none of the fragments was overlapping, indicating that *CA736677* might represent a fusion between two different transcripts.

Reverse dot blot hybridization (macroarray analysis) provided important information about syringolin responsiveness. Sequencing efforts were reduced since constitutively expressed fragments could be omitted from further analyses. Interpretation of signals derived from hybridizations to labeled cDNA or subtracted cDNA pools allowed to identify 59 genes upregulated with high probability (indicated with [(1)] in Table 4.2, p.36). Of these, transcriptional upregulation was confirmed by microarray for all but one fragment, demonstrating that data obtained by a single repetition of semi-quantitative macroarray analysis without application of computational normalization were of high reliability.

Furthermore, reduction of redundant sequences by aligning homologous sequences obtained by SSH contributed to elevated accuracy of ILMC normalization during later microarray experiments and also simplified the biological interpretation of microarray results.

The reverse subtraction would provide information on syringolin-induced downregulation of gene transcription. Yet, massive hyphal growth generally occurring after successful penetration (from 48 hai on) was hypothesized to cause a disequilibrium of fungal transcripts between control solution-treated and sylA-treated samples and to favor isolation of random fungal transcripts in the reverse subtraction. Indeed, dots exhibiting equal signals upon hybridization to cDNA probes frequently showed stronger signals upon hybridization to forward subtracted as compared to reverse subtracted cDNA probes (Figure 4.5, p.33, e.g. dot B07 or E04). Hence, the reverse subtracted cDNA pool was not subjected to further investigations.

A beneficial feature of SSH is the equalization acting on high and low abundant differentially regulated transcripts. The effect is based on the second order kinetics of hybridization and increases the possibility of isolating low abundant transcripts, which are often found to fulfill regulatory functions during signal transduction (Diatchenko et al., 1999). The equalization effect became obvious in the case of dots A04 and A06, whose corresponding transcripts finally were both similarly abundant in the forward subtracted pool (Figure 4.5, p.33). With regard to fungal transcripts, equalization would allow to isolate differentially regulated fungal transcripts although they are of much lower abundance than transcripts derived from wheat. Thus, the fact that none of the cloned transcripts returned significant homology values to fungal transcripts upon blast searches strongly indicates that the response to syringolin accompanying eradication of the fungus occurs primarily on the plant but not (or less) on the fungal side.

5.1.2. cDNA microarray hybridization analysis

Many advances were made in the microarray technology within the past years and resulted in a variety of different equipment and protocols presently available. Microarrays are used for expression profiling under various conditions or during development and alternative applications include comparative genomic hybridization, genotyping or mutation detection (reviewed by Holloway et al., 2002).

Basically, microarray technology includes two different versions varying in the type of DNA which is used as probes. Oligonucleotides present on gene chips from Affymetrix (Santa Clara (CA), USA) are synthesized in situ. This technique requires detailed knowledge about the DNA sequences corresponding to the genes of interest. In contrast, cDNA microarrays consist of several thousand cDNA probes spotted onto modified glass slides. The great advantage of cDNA microarrays is that probes can be spotted without sequence

knowledge. The first glass slide microarrays were produced in P. Brown's laboratory at Stanford University (Schena et al., 1995).

The comparison of two different spotting protocols and contact deposition devices revealed large differences in the quality of slides produced depending on the equipment and printing protocols used. Most importantly, addition of 1.5 % betaine guaranteed homogeneity with respect to both spot diameter and spot morphology, respectively. Betaine strongly increased viscosity of the printing solution and was also reported to increase binding efficiency on poly-lysine coated glass slides (Diehl et al., 2001). The addition of betaine into the spotting solution solved problems related to evaporation of spotting solution during the printing process (freshly printed microarray slides could be stored for several days before blocking). Conversely, cooling of the printing chamber did not show a positive effect. Since the GMS 417 arrayer is equipped with a pin wash station lacking sonication cleaning, the risk of DNA carry-over made the use of betaine impossible in this case. The advantages of low evaporation in the DNA master plates should not be underestimated since the major effort in the fabrication of cDNA microarrays is put into the amplification and purification of the probes. Low evaporation strongly facilitates the reuse of probes in subsequent printing sessions.

Another aspect which is related to the process of cDNA amplification is the minimum probe volume required for printing. A high volume of 50 µl necessary to guarantee proper filling of the pin ring in the case of GMS 417 was opposed to only 10 µl sufficient for printing with OmniGrid 100. In order to achieve appropriate DNA concentrations for printing, probe amplification required two parallel PCR reactions which were combined during subsequent purification in the case of GMS 417. This not only doubled the work but also increased the risk of cross-contamination of probes during combination.

Taken together, the requirement of very low amounts of printing solution together with the possibility to add betaine to the printing solution are considered as key criteria for the selection of a suitable printing device for medium and large size microarrays (more than 500 probes) for future experiments. The use of betaine essentially renders climatisation of the printing chamber unnecessary. The opportunity of duplicate or triplicate printing strongly increases reliability of microarray data. In the present case, this was not possible due to limited loading capacity of the printing pins used in combination with the OmniGrid 100. This handicap can be overcome by using alternative types of printing pins such as the bubble uptake channel tips (TeleChem International, Sunnyvale (CA), USA).

Alternative devices work with non-contact deposition like ink jet spotting or PiezoTip technology. For example the Piezorray system (PerkinElmer Life Sciences Inc., Boston (MA), USA) is supposed to deliver spots of high uniformity. It allows printing buffers of high viscosity, and it is equipped with an ultrasonic washing device. Thus it would allow the use of betaine and might therefore be an interesting alternative to the OmniGrid 100. A very favorable feature of Piezorray is an automated detection system for missing spots which is coupled with post printing error correction. Missing spots were a great disadvantage of OmniGrid 100 in microarray series 6 as well as series 7. They required large efforts of visual inspection of every single slide and the information had to be integrated into downstream processing of the data in order to avoid averaging over present and absent spots.

The choice of reliable scanning devices significantly increased the quality of microarray data and was a central prerequisite enabling proper interpretation. The high signal to noise ratios obtained by the Agilent G2505B scanner also allowed for identification of differential expression at low signal intensities (Figure 4.9, p.46). Similar results were obtained upon methodological investigations by Francois and co-workers (2003). They found that a microarray scanner equipped with dynamic autofocus provided high inter-slide correlation, more linear signal responses and thus was found to be more reliable than an equivalent apparatus without dynamic autofocus and mobile optics (Francois et al., 2003). However, after disabling the dark offset function, the Agilent scanner exhibited higher signal biases as compared to an apparatus of another brand (Bengtsson et al., 2004). Thus, high quality and linearity obtained by scanning with the Agilent G2505 apparatus is ascribed mainly to dark offset subtraction improving the accuracy of generated data (Agilent Technologies Inc., 2003). On the other hand, low scanning power made originally intended multiple scanning at various power settings impossible (data not shown). The strategy was intended to widen the dynamic range of scanning at low and high signal intensities and the scanning power was adjusted with the help of the SC calibration control spots using the line-scan option of the ScanArray 5000. Due to low signal to noise ratios of this scanner, these attempts were without success. The same strategy was also suggested recently by Bengtsson et al. (2004), in order to extend the dynamical range of the data. Increasing the dynamic range of scanning might become particularly necessary with regard to improved sensitivity obtained by novel microarray substrates. Thus, the ideal scanner would successively scan with increasing laser power and intensities of individual spots would be automatically extracted from the scan of optimal linearity for both channels. Subsequently, proper relative signal proportions between all spots of the array would have to be reestablished by calculation.

Indirect labeling of DNA yielded targets of high specificity (bdr up to 26). Significantly lower coupling efficiency of AF_{555} as compared to AF_{647} were assigned to variable reactivity of the two fluorescent dyes. With regard to homogenous labeling it is important to realize that the strength of signals obtained by scanning differently labeled targets also strongly depends on the quantum yield (the ratio of the amount of light emitted to the amount of light absorbed) and extinction coefficient. Accordingly, targets equally labeled with different fluorescent dyes may exhibit clearly different fluorescence intensities. Hence, no further efforts to obtain equal coupling efficiencies were undertaken.

Recently, a microparticle labeling method using gold particles instead of fluorescent dyes was reported to provide more than 50-fold higher sensitivity by Francois et al. (2003). Thus this might be a promising alternative in order to achieve enhanced sensitivity at low signal intensities. The technique is based on resonance light scattering and whole systems including reader and image analysis software are commercially available (e.g. the HiLight array system by Qiagen AG, Hombrechtikon, Switzerland).

Within the past years, various investigations describing sensitivity of microarray investigations with regard to different target materials such as total RNA, poly(A)$^+$ RNA or aRNA have been published (Baugh et al., 2001; Pabon et al., 2001; Feldman et al., 2002; Polacek et al., 2003). Traditional labeling requires 10-100 µg of total RNA or 2-5 µg of mRNA, whereas amplification according to Van Gelder and Eberwine (1990) can lower starting amounts of total RNA to 2 ng (Baugh et al., 2001). In our hands, a single round of amplification resulted in a 2000-fold amplification of mRNA. In general, amplification was reported to increase sensitivity and higher numbers of differentially expressed genes were detected upon amplification. The data presented in chapt. 4.2.1.6 show that aRNA and poly(A)$^+$ RNA labeling are equivalent methods for the preparation of target DNA. The differences of gene sets identified by the two methods were related to a bias acting in a gene specific manner which equally alters the relative abundance of individual transcripts in RNA preparations derived from treated and control samples. Accordingly, the relations between sylA-induced accumulation of transcripts in the presence and absence of *Bgt* were the same when comparing genes identified by both labeling methods. However, it is fundamental to recognize that t/c ratios derived from different labeling methods may differ significantly. Thus, calculation of t/c ratios from data obtained by different hybridization and labeling methods is forbidden. Theses findings are highly consistent with those obtained by recent systematic comparison between aRNA, mRNA and total RNA microarray hybridizations (Li et al., 2004). The authors reported that all three methods provide reliable data and low false positive rates. In the context of hepatocarcinogenesis, from which the

target RNA was derived, they also found that genes of high importance described in the literature are frequently identified with only one of the three different types of RNA.
These findings indicate that there is no RNA preparation method of choice with regard to increased sensitivity. Yet, since RNA amplification is sometimes required in order to obtain sufficient starting material, it is suggested that ideally all RNA preparations should be done according to the same aRNA protocol and that sensitivity of microarray should rather be increased by technical advances such as for example microparticle labeling mentioned above. By this means, the compatibility of data derived from different laboratories would be increased.

The use of housekeeping genes as standards for microarray normalization occasionally can introduce new sources of error. In our case, upregulation of *G3PDH* transcription was already indicated during SSH and confirmed by microarray analysis. Another example is the elevated abundance of transcripts corresponding to ubiquitin. Similarly, Hückelhoven et al. (2001) observed transient decreases in the expression of actin in powdery mildew-infected barley. It was therefore proposed by Lee et al. (2002) that expression of every gene should be considered as context dependent. However, this largely complicated normalization of microarray data in the present case since a high proportion of genes was found to be upregulated (e.g. Figure 4.19, p.64) which could only be compensated by ILMC (chapt. 4.2.1.4.). Visualization of data by using MA-plots (Dudoit et al., 2002) proved to be a valuable tool not only to monitor correct normalization but also to interpret the results in a biological context. Unbalanced distribution of induction ratios had the major drawback that common smoothing normalization methods such as Lowess (Quackenbush, 2002) could not be applied (chapt. 4.2.1.4.). As shown below, this may have become a critical limitation since comparison of hybridization signals corresponding to samples with different content of biological material (e.g. higher and lower proportions of fungal tissue) may result in systematic dependence of intensity which would not be normalized by global normalization such as ILMC. Figure 5.1 illustrates a simulation of a high background signal derived from large amounts of fungal tissue in the control sample. Data correspond to *Bgt*-infected epidermal wheat tissue at 12 hat (Figure 5.1A). In Figure 5.1B, a constant (low) value simulating background signals derived from crosshybridization with fungal target DNA was added to all signals of the control data. In both cases, t/c ratios were normalized by ILMC. As obvious, t/c ratios were markedly shifted upwards after normalization in Figure 5.1B.

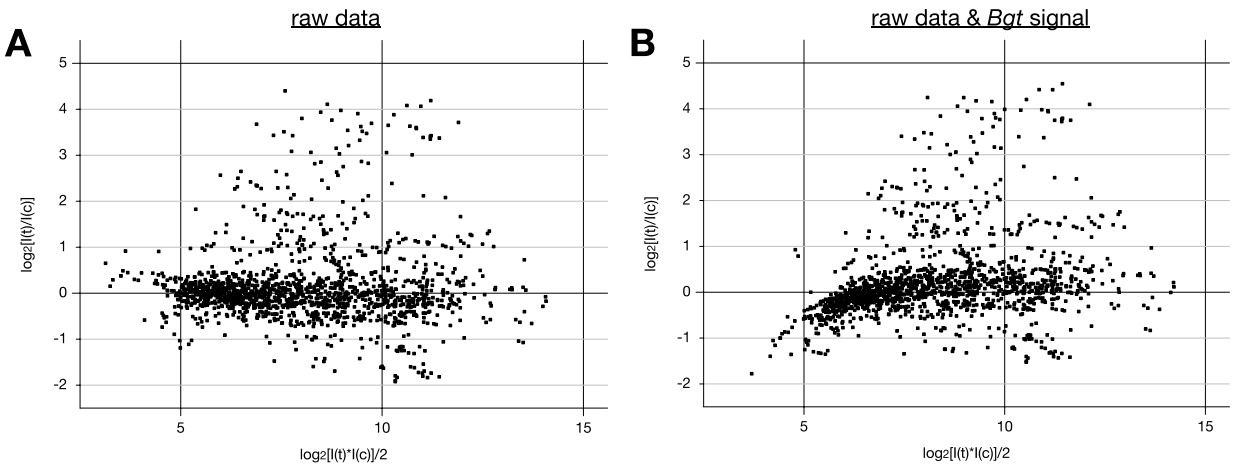

Figure 5.1: MA-plots visualizing simulation of *Bgt*-background. A: Raw microarray data derived from a syringolin treatment experiment after ILMC normalization. B: Simulation of a *Bgt*-background effect by addition of a low signal to control signals of the same data followed by ILMC normalization.

Fortunately, since usually both samples (control and treated) were either infected or uninfected, no such effects were observed upon comparisons of syringolin- and mock-treated samples although interruption of fungal growth by syringolin treatment may have lead to a certain degree of imbalance. The only exception occurred upon investigation of the effects of fungal pre-induction of gene transcription (Figure 8.2, p.203). As predicted, a high degree of fungal background in the treated sample as compared to no fungal background in the control sample shifts up t/c ratios of weakly expressed genes. In practice, this rather caused a tilt than a bend of the data set on MA-plots. Luckily t/c ratios were nearly homogenously distributed along the y-axes which allowed for Lowess normalization in these exceptional cases.

Taken together, it was found that analysis by medium scale microarrays can be highly challenging especially with regard to proper normalization. Open software such as TIGR MIDAS (Saeed et al., 2003) allowing to test different normalization strategies were found to be valuable tools. Visualization of the data is considered to be a must and is highly recommended also for analyses with large scale microarrays, especially in the case of experiments involving mixed DNA targets. In conclusion, large numbers of randomly selected probes significantly simplify microarray data analysis which might be circumscribed by 'the bigger, the better'. In general, cDNA and oligonucleotide arrays have been described to give similar reproducible results and differences observed in inter-lab comparisons of identical platforms appear to be a bigger problem when comparing microarray data (Petersen et al., 2005; Wang et al., 2005). Still, due to the highly increased amount of DNA sequences available from public databases there is trend away from cDNA microarrays to commercially fabricated oligonucleotide arrays.

5.2. Transcript profiling in syringolin-treated wheat

Microarray comparisons between powdery mildew-infected and uninfected syringolin-treated wheat as well as transcript profiling in epidermal and mesophyll tissue was carried out in order to identify genes transcriptionally involved in the localized induction of HR in *Bgt*-infected epidermal cells. Surprisingly, only a single cDNA fragment (*RB_c116*; Table 4.4, row 99) exhibited a transcriptional expression pattern as it was expected for putative genes involved in the sylA-induced localized HR. Interestingly, the fragment was not derived from the SSH screening for sylA-induced genes and it encoded 28S rRNA of fungal origin. A similar phenomenon was reported recently by Fleischmann & Liu (2001) who were surprised to find frequent representation of 25S rRNA upon differential display in the course of studies of hyphal transformation in *Candida albicans*. Subsequent investigations revealed that this was due to polyadenylation of rRNA which resulted in efficient reverse transcription with poly(T)$^+$ primers upon differential display (Fleischmann and Liu, 2001). The fact that this transient effect was also observed for 18S rRNA lead to the hypothesis that it might play a role in the polymorphic behavior of *C. albicans* (Fleischmann et al., 2004). In *Saccaromyces cerevisiae*, polyadenylation of rRNA is hypothesized to be part of a quality control mechanism of noncoding RNAs which involves activity of riboexonuclease Rrp6p (Kuai et al., 2004).

In contrast to *RB_c116* and to our surprise, all genes transcriptionally induced by sylA exhibited weaker responsiveness in the presence of *Bgt* (chapt. 4.2.2.2). As demonstrated by investigating pre-induction/-repression by fungal infection (chapt. 4.2.6), the phenomenon could not be generally ascribed to interference with *Bgt*-induced transcriptional changes since only a small proportion of sylA-responsive genes was found to exhibit significant transcriptional regulation upon *Bgt* infection. Anyhow, in some instances like for example *RB_96.2* or *RB_c001* encoding a B12D protein and a wheat homologue of gigantea, tissue specific pre-induction by powdery mildew infection explained epidermis specific expression observed in ceB (Table 8.7, rows 21 & 50). Since targets prepared from infected samples might contain variable amounts of fungal RNA which in turn might alter individual t/c ratios by crosshybridization, it was hypothesized that this might be a source for the differences observed in ceA in the presence of *Bgt*. Yet, theoretical considerations indicated that the effect would rather cause elevated induction ratios in *Bgt*-infected samples after sylA treatment (p.122).

Alternatively, it could be argued that immediate cell death of a significant amount of infected cells would alter the signal intensities derived from treated and control samples. However this situation would result in a reduced RNA yield upon RNA extraction and imbalances would subsequently be corrected by adjusting RNA levels during target labeling and by subsequent ILMC normalization.

Consequently, the repressed responsiveness to syringolin in the presence of *Bgt* was considered most likely to be caused by inhibitory fungal activity on the plant cellular perception and/or signal transduction in response to syringolin treatment. Under the assumption that nearly all cells of the wheat leaf respond to syringolin treatment, estimations indicated that approximately 50 % would have to be blocked for transcriptional upregulation of sylA-responsive genes in order to observe the 1.6-fold difference described in chapt. 4.2.2.2. This high proportion appears to be contradictory to the low proportion of less than 1 % infected cells in a typical experiment (Appendix, p.198). In this respect, the ability of powdery mildew to not only control host cell metabolism or viability of infected but also of neighboring cells in a translaminar fashion is impressively demonstrated by the green island effect (as illustrated in Schulze-Lefert and Vogel, 2000). Still, with regard to the small size of fungal colonies and the absence of secondary infections during the time points of investigation (illustrated in Figure 3.11, p.24), the discrepancy between low percentage of infected cells and large average difference of t/c ratios in the presence and absence of *Bgt* on sylA-treated wheat leaves was considered to be high.

In this respect it should be mentioned that a dose effect which might originate from the spreading fungal network might also have an impact on dampened transcriptional induction. Concretely, the fungal hyphae might promote formation of droplets of the sprayed material enhancing run-off along the plant surface. This may be caused by the water repellent properties of hydrophobins, which are known to be synthesized by many filamentous fungi (Whiteford and Spanu, 2002). Accordingly the protective activity of syringolin was found to be strongly dependent on the concentration since treatment of infected wheat with 10 µM solutions of sylA was ineffective and did not prevent fungal colonization as judged macroscopically (not shown).

It was concluded that the plant response to syringolin likely is suppressed by powdery mildew. Yet, a dose effect mediated by the fungal hyphae cannot be entirely excluded to contribute to the decreased responsiveness to syringolin treatment. The reduction of t/c ratios in the presence of *Bgt* might also result from a combination of both mechanisms.

Since ribulose bisphosphate carboxylase is expressed exclusively in photosynthetic active cells mainly present in the mesophyll, comparison of rubisco-relations of single genes between epidermis and mesophyll samples allowed to discriminate whether individual genes exhibited higher expression in epidermal samples than rubisco. On the basis of this, ϵ_s factors were calculated for individual genes. Balanced expression between epidermis and mesophyll was found to result in ϵ_s factors of 1.75 and upper threshold levels of 2.0 had already been used previously for the identification of epidermis specific gene expression (Bruggmann et al., 2005).

In line with the absence of *Bgt*-dependent transcript accumulation after sylA treatment, no statistically significant epidermis specific induction was observed for the syringolin-responsive genes in *Bgt*-infected wheat leaves at the -08 hat time point (with the exception of *RB_c116* encoding the fungal 28S rRNA; Table 4.7, row 131). In other words, no indication for differential regulation of transcription which might be related to the epidermis and *Bgt* infection specific induction of HR by the plant was observed by microarray analysis during the time interval of 2 to 32 hours after treatment with syringolin. For some genes, significant epidermis specific expression at -32 hat was found to be due to natural or *Bgt*-induced epidermis specific expression (chapt. 4.2.4.1, p.84). In addition, uneven distribution of sylA within the leaf was hypothesized to be a plausible cause of sudden epidermis specific induction at the late time point, where t/c ratios were found to be lower than at the earlier -08 hat time point. This was related to the observation that ϵ_s factors, which on average showed mesophyll specificity at the early time point, did not just raise back to neutral levels (like in control-treated samples; not shown) at the late time point but even climbed up to a clearly epidermis specific average value of 2.28 (Figure 4.23A & B, p.83). A faster decay of transcription in the inner part of the leaf would be related to the fact that syringolin may have to be translocated from the leaf surface to the mesophyll, which might cause lower sylA concentrations in the mesophyll. With respect to this, it is not clear how exactly the very hydrophilic syringolin would enter the leaf. It might be speculated that sylA might either be absorbed through stomatal openings or alternatively that it might even traverse the cuticula through small aqueous pores (Schlegel et al., 2005).

Thus, calculation of epidermis specificity which already previously was found to be a useful tool (Bruggmann et al., 2005) also produced reliable data in the present work as demonstrated in the case of a number of control genes (Table 4.6, p.76) The results consolidated the findings of ceA. Yet, the aforementioned situation demonstrates that the presence of multiple factors influencing epidermis specificity can markedly complicate interpretation of the results. In addition the efficiency of translocation and distribution of bio-agents plays an important role.

Taken together, the ability of syringolin to selectively induce HR of *Bgt*-infected epidermal cells was found not to be correlated with transcriptional upregulation of putative HR-related genes. Instead, the cellular response to syringolin treatment was even found to be negatively controlled by *Bgt*. However, plants were found to strongly respond to sylA treatment by the transcriptional induction of genes covering a broad range of biological functions (chapt. 5.3).

Induction of RNAi by biolistic transformation of vectors carrying foldback constructs has been shown to efficiently inhibit transcript accumulation of targeted genes and thus was proven to be a helpful tool for investigations in plant-powdery mildew interactions (Schweizer et al., 2000). Investigations with the help of RNAi hold the indisputable advantage that even fragments of cDNAs are sufficient to target transcript accumulation of corresponding genes. In the present work, a test system was introduced in parallel to ongoing microarray analysis in order to investigate effects of RNAi of candidate genes on the induction of *Pm3b*-related HR. No indication of an inhibitory effect on the onset of HR was observed upon inhibition of transcript accumulation in the case of 30 genes tested by biolistic transformation (chapt. 4.3.2).

In general, inhibition of transcript accumulation by RNAi in wheat faces two major problems. First, due to allo-hexaploidy, wheat possesses a great potential to compensate for the suppression of individual genes by homologous genes which might mask effects of silenced gene activity. Second, transient expression in the presence of powdery mildew only offers a small time frame of maximally 4 h after bombardment for infection with the pathogen because of significant induction of basal resistance (P. Schweizer, personal communication). These limitations do not exist in diploid barley. On the other hand, since data derived from transcript profiling indicate that sylA-induced gene transcription may additively contribute to the induction of HR (described below), it appears to be necessary to obtain full length cDNAs in order to carry out tests by transient overexpression, an experimental variant which does not face the problems of RNAi described above.

As already mentioned in chapt. 4.3.2, the initial difficulties which required the switch to the artificial test system, where the R-gene was co-transformed into susceptible wheat cv. Fidel, were solved in the meantime. Since R-proteins appear to act in a dose-dependent manner (Bieri et al., 2004; Holt et al., 2005), it is considered to be crucial for future experiments to be carried out in a resistant genetic background which would guarantee appropriate expression levels of the corresponding R-protein.

5.3. Syringolin-induced gene transcription

Syringolin was found to induce accumulation of transcripts of a broad range of functions. Possible effects and properties of some of these genes are discussed in the following.

5.3.1. Ubiquitin/26S-proteasome pathway

The Ubiquitin/26S-proteasome pathway is an elaborate regulatory mechanism which controls selective protein breakdown and appears to be particularly important in plants (reviewed by Sommer et al., 2001; Vierstra, 2003). In the ubiquitin/26S proteasome system, selected proteins are coupled to ubiquitin which targets them for degradation by the 26S proteasome. In plants, the proteasome is involved in the control of plant growth, development and defense (Tör et al., 2003; Moon et al., 2004).

In the ubiquitin conjugation cascade, ubiquitin (Ub) is recruited by E1 (Ub-activating enzyme) and transferred to E2 (Ub-conjugating enzyme). E3 (Ub-protein ligase) recruits the substrate and initiates conjugation of ubiquitin to a free lysyl group and a chain of multiple Ubs is usually built by several rounds of conjugation. Five types of E3 units are known to date and there are more than 1200 components known in the *Arabidopsis* genome (Vierstra, 2003). The most prominent are the SCF (Skip1-cullin-F-box) type complexes with 694 members and the Ring/U-box type complexes with almost 400 members, including the COP1 (constitutively photomorphogenic 1) complex (Vierstra, 2003). Since in animals, most targets of SCF complexes have to be phosphorylated, it is hypothesized that many plant protein kinases modulate target recognition by kinase activity. Ubiquitin-protein ligases are the most abundant components of the Ub/26S-proteasome pathway and they are thought to be responsible for tightly controlled specific protein degradation. The SCF complex shows high flexibility and can form a plethora of distinct subtypes as it can be composed of different cullin and SKP subunits.

The 26S proteasome is a large multisubunit ATP-dependent protease controlling proteolytic degradation of ubiquitylated intracellular proteins. The *Arabidopsis* 26S proteasome has been isolated recently (Yang et al., 2004). Like the animal counterpart, it consists of a cylinder-shaped 20S proteolytic core (CP) and two 19S regulatory cap particles (RP). The 20S core particle carries two copies each of seven different α and β subunits arranged in four $\alpha_7\beta_7\beta_7\alpha_7$ stacked rings. The RP confers substrate specificity and is subdivided into lid and base, both parts consisting of nine AAA-ATPase (RPT) and non-

ATPase subunits (RPN). An illustration is shown in Figure 5.2. The lid is evolutionary related and highly homologous to the COP9/signalosome (CSN).

Involvement of the Ub/26S proteasome pathway was recently found to be an important aspect of plant defense and proteins interacting with E3 ubiquitin ligases may mediate altered specificity of the 26S proteasome (reviewed by Tör et al., 2003). For example, the barley RAR1 regulator of race specific resistance interacts with SGT1 (suppressor of G-two allele of skp1) which associates with SCF complexes. The stability of the *Arabidopsis* RPM1 resistance protein which is degraded upon initiation of HR in incompatible interactions with *P. syringae* (Boyes et al., 1998) is dependent on RAR1 (a model is illustrated in Figure 3.8, p.19). Based on the fact that plant SGT1 is required for the resistance conferred by numerous R proteins, it is hypothesized that targeting of R proteins by SGT1-SCF complexes regulates plant resistance (Vierstra, 2003).

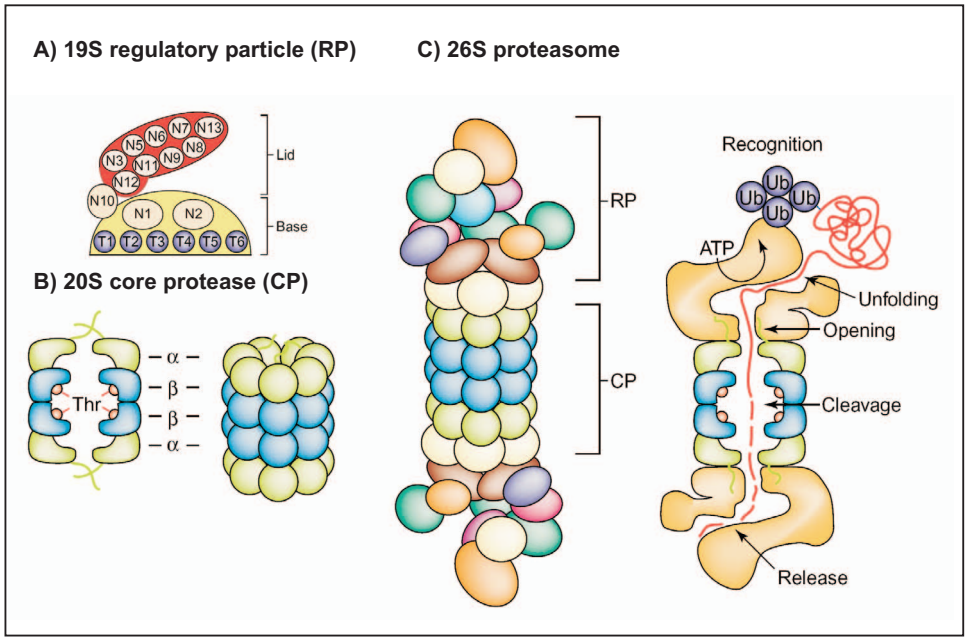

Figure 5.2: Organization and structure of the 26S proteasome: A: Organization of the regulatory particle (RP) with its Lid and Base sub-particles. B: Organization of the core protease (CP). The N-terminal threonine residues that form the protease active sites in the β1, β2, and β5 subunits are indicated. Abbreviations: N, RP non-ATPase subunits; T, RP AAA-ATPase subunits. C: Proposed structure and sequence of events that lead to the degradation of a ubiquitylated protein by the 26S holoprotease. (Vierstra, 2003, modified).

Interestingly, syringolin was found to induce accumulation of numerous transcripts encoding proteasome subunits. Accumulation was confirmed by microarray analysis for three different α and four β subunits including β_2 and β_5, two of three active site subunits in the 20S core protease. Regulatory particles included *RPT4a* and *RPN9b* and two AAA-ATPase like putative regulatory subunits (*OA_a2C11* and *OA_b1C03*). Highest t/c ratios were found for *OA_a2C11*, one of the uncharacterized putative regulatory subunits. RPT4 is

located in the base of the RP and is thought to be involved in unfolding or target proteins (Vierstra, 2003). RPN9 is a non-ATPase subunit involved in the assembly of the lid of the yeast RP (Takeuchi et al., 1999).

One fragment (*OA_b1D02*) which was found to accumulate at 12 hat exhibited homology to Ub associated proteins. The ubiquitin associated (UBA) domain is found in many E2 and E3 enzymes and *Arabidopsis* SnRKs (Snf1-related protein kinases) and thus, *OA_b1D02* might have a regulatory function on the proteasome specificity.

A hypothesized increase of the 26S proteasome level resulting from upregulation of the CP and RP components is thought to reflect a higher demand for protein degradation via the ubiquitination pathway after sylA treatment. Indeed, syringolin application also caused a transient increase in ubiquitin transcript abundance (*OA_a1A10*). In animals, abundance of the proteasome was recently found to be transcriptionally regulated via an autoregulatory feedback mechanism (Meiners et al., 2003). Indicative for the presence of similar mechanisms in plants, transcription of *Arabidopsis* 26S proteasome subunits was upregulated in mutant lines expressing diminished levels of RPN10 or RPN12a (Yang et al., 2004). Yet, the proteasome is not only a large multisubunit of fixed composition and for example the integration of alternative β subunits in specialized mammalian cells alters catalytic activity of the CP. Since plants contain gene pairs for most of the CP and RP subunits, it was hypothesized that they might assemble multiple types of 26S proteasomes exhibiting variable properties (Yang et al., 2004).

Interestingly, *OA_b2F09* which is transcriptionally upregulated at 12 and 24 hat was found be related to the human proteasome (prosome, macropain) activator subunit 4 (PSME4). *OA_b2F09* exhibited 93 % sequence identity (of 81 aa) with a wheat hypothetical protein (accession #Ta_12787). *Ta_12787* in turn showed 80 % sequence identity (of 221 aa) to a rice PSME4-like protein (accession #BAD53980) and 50 % similarity (of 205 aa) to the human PSME4 (synonym PA200) corresponding to the KIAA0077 gene (accession #BAA07526). PA200 had been demonstrated to induce proteasome activity in a unique manner for it activates hydrolysis of peptides (but not proteins). Activation of peptide hydrolysis was ATP-independent and was mainly targeted on the peptidylglutamyl peptidase activity of the 20S proteasome (Ustrell et al., 2002). Recently, PA200 was found to bind to the end of the CP. It activates the CP by opening the axial gate of the α-rings (Ortega et al., 2005).

Within the past years, the regulatory role of proteolysis in many aspects of life including developmental and hormonal processes as well as plant resistance has gained increasing attention (reviewed by Tör et al., 2003; Moon et al., 2004). Investigations of Bieri et al. (2004) have shown that plant defense mediated by *Mla* resistance genes under the

control of RAR1 or SGT1 is dependent on the abundance of the R-proteins. As already described in chapt 3.2.1, the stability of numerous resistance genes appears to be controlled by factors such as SGT1 which are able to associate with E3 ubiquitin ligase complexes and by this means may directly target R-proteins for degradation by the proteasome (Figure 3.8). Thus it is tempting to speculate that the transcriptional upregulation of nearly the complete proteasome and numerous regulatory factors might be directly associated with induction and regulation of plant defense mechanisms or hypersensitive response.

In addition, it cannot be excluded that the transcriptional upregulation of proteasome components might also be required for direct degradation of syringolin. The upregulation might either reflect the demand for more or alternate protease activity. Yet, degradation of syringolin via the ubiquitination pathway would require prior modification in order to provide a free internal lysyl ϵ-NH_2 group for ubiquitination. With respect to a putative recycling of syringolin components, it is interesting to find syringolin-induced upregulation of lysyl and valyl tRNA synthetase transcripts (*OA_a1E11* and *OA_b2E06*). The cloning of only these two tRNA synthetases is intriguing with regard to the fact that syringolin is most likely synthesized from two valins and one lysine by the nonribosomal syringolin synthetase (Amrein et al., 2004). The valyl tRNA synthetase was the only syringolin responsive probe which showed epidermis specific expression at the early time point ($\epsilon_s > 2$; Table 4.7, row 71 on p.81).

5.3.2. Detoxification

Eighteen cDNA fragments functionally assigned to detoxification were confirmed to exhibit transcriptional induction upon sylA treatment. Investigation of the transcriptional plant response during detoxification with the help of large microarrays is still at the beginning. Recently, Bearson et al. (2005) studied the transcriptional detoxification response of *Arabidopsis* to treatment with the allelochemical BOA (Benzoxazolin-2(3*H*)-one) which involves accumulation of transcripts corresponding to ABC transporters, cytochrome P450s, GSTs, glucosyl transferases but also transcription factors and receptor kinases. The authors briefly reviewed the plant response to xenobiotics which basically consists of four different phases: Phase I involves modification by hydrolases, cytochrome P450s and peroxidases facilitating formation of conjugates by glucosyl transferases and GSTs in phase II. ABC transporters recognize xenobiotic conjugates resulting in vacuolar sequestration or exocytosis in phase III. Occasionally, less well characterized further modifications constitute phase IV. Baerson et al. (2005) discovered striking overlaps between gene activation by

BOA and a number of additional xenobiotics indicating the presence of chemosensory mechanisms which coordinately upregulate transcription of whole batteries of detoxifying enzymes.

In the present issue, syringolin was found to upregulate transcription of genes encoding two putative epoxide hydrolases (*OA_b2H01* & *OA_b3B10*; Table 4.4, rows 89 & 90), one monooxygenase (*RB_53.1*; Table 4.4, rows 95-98), three cytochrome P450 (*OA_a1D09*, *OA_b1D06* & *OA_a1C04*; Table 4.4, rows 54-56), five GSTs (*OA_a3A01*, *OA_a3G10*, *OA_b1H08*, *OA_b3D05* & *RB_c017*; Table 4.4, rows 49-53), two glucosyltransferases (*OA_a2C08* & *OA_a3B03*; Table 4.4, row 92 & Table 4.7, row 56) and five ABC transporters (*OA_a2A06*, *OA_a2E02*, *OA_a3A04*, *OA_a3D05* & *OA_a3H01*; Table 4.4, rows 46-48 & Table 4.7, rows 40 & 42). In addition, the collection of cDNA fragments exhibiting transcriptional activation by syringolin also contained two wheat homologs of the rice *Pir7b* (*OA_b1B01* & *OA_b2A07*; Table 4.4, rows 87-88) encoding a syringolin-induced esterase of the α/β hydrolase fold enzyme family with a hypothesized detoxifying biological activity (Wäspi et al., 1998b). The large functional groups of cDNA fragments usually contained one representative which exhibited exceptionally strong transcript accumulation upon sylA treatment. This was the case for *OA_b1D06* encoding a cytochrome P450 (Table 4.4, row 55) and *OA_b3D05* encoding a GST (Table 4.4, row 52) whereas the ABC transporters all exhibited weak to moderate transient transcript accumulation (Table 4.7, rows 40-45).

In the case of *OA_b2H01* (accession #AJ888690), tblastx analysis revealed 76 % identity (of 275 aa) to a putative epoxide hydrolase from *Arabidopsis* (accession #AC002343). *OA_b2H01* and *OA_b3B10* (accession #AJ888700) both exhibited high homology to the same wheat EST contig (accession #Ta.26236). However, the two fragments of the microarray subset one were not overlapping and it remained unclear whether they were corresponding to the same gene or whether they represented different members of a gene family (an alignment to *Ta.26236* is shown in the Appendix (p.216). In mammals epoxide hydrolases are involved in the metabolism of a wide range of drugs and other xenobiotics. Their substrate, epoxides, mainly arise from oxidations of unsaturated carbon-carbon bonds by the cytochrome P450 monooxygenase system (Seidegard and Ekstrom, 1997; Fretland and Omiecinski, 2000). In addition, plant epoxide hydrolases were also reported to be induced by auxin and upon stress (Kiyosue et al., 1994), in response to pathogen attack (Guo et al., 1998) and they are also involved in the biosynthesis of cutin (Heredia, 2003). *Ta.26236* in turn exhibited strongest homology (74 % sequence identity of 278 aa) to a rice CGI-58-like protein (accession # Q650U5). Like epoxide hydrolases, CGI-

58 belongs to the large family of α/β hydrolase fold enzymes (Nardini and Dijkstra, 1999; Holmquist, 2000). In mammals, CGI-58 was found to be located at the surfaces of lipid droplets in the cytoplasm and its role in lipid metabolism and triacylglycerol turnover is being investigated (Subramanian et al., 2004).

Clearly, general classification of GSTs and ABC transporters into detoxification activity is a strong simplification which is based on the fact that apart from some exceptions, little information is presently available in wheat on individual isoenzymes of the two functional groups which encompass large enzyme families. Yet, the large relative size of the collection of cDNA fragments corresponding to enzymes with possible detoxifying activity anticipates that many of them effectively do participate in detoxification. However, it has to be mentioned that ABC transporters are also involved in plant growth and development (reviewed by Martinoia et al., 2002). In *Arabidopsis* it was shown that an MDR type ABC transporter is involved in the control of hypocotyl cell elongation (Sidler et al., 1998) whereas an MRP type ABC transporter recently was found to be required for ABA related control of transpiration via stomatal opening (Klein et al., 2003). Likewise, besides their importance in detoxification of electrophilic herbicides, GSTs, which are excessively abundant in crops, may also be involved in transport of plant hormones and oxidative stress tolerance (reviewed by Edwards et al., 2000). Interestingly, a barley homologue of the WIR5 GST showed similar expression patterns like the *Mlo* transcript which accumulates in response to powdery mildew infection, elicitor- or herbicide treatment and wounding (Piffanelli et al., 2002).

Comparing the wheat response to syringolin treatment with the one observed upon nonhost interaction with barley powdery mildew (Bruggmann et al., 2005) revealed only partial overlaps between the gene sets activated. For example, epoxide hydrolase or monooxygenase were not activated upon *Bgh* infection (Bruggmann et al., 2005). In the case of Pir7b, weak accumulation of corresponding transcripts was observed upon *Bgh* infection. This was also found for a different *Pir7*-like cDNA fragment (*RB_c058*; accession #AJ873957, #AJ873958 & #AJ873959) which in turn did not exhibit transcriptional activation upon sylA treatment (not shown). The same situation was true for *RB_c070* (accession #AJ874023) encoding a cytochrome P450.

Interestingly, the two cDNA fragments *OA_b3D05* and *OA_a3A04* encoding a GST and a PDR-like ABC transporter belonged to those transcripts which exhibited strongest epidermis specificity upon transcriptional induction by *Bgh* infection (Bruggmann et al., 2005). This may indicate that they directly participate in the plant nonhost resistance reaction, more precisely in the aspect of defense which is localized to the epidermal cell

layer. Intriguingly, transcripts encoding the WIR5 GST (Schweizer et al., 1989) were not accumulating upon syringolin treatment (chapt. 4.2.5.1). Whereas *OA_b3D05* simultaneously exhibited strongest transcriptional induction upon sylA treatment of all GSTs present on the microarray, transcriptional induction of *OA_a3A04* was hardly detectable and was not statistically significant in ceA, probably due to variations resulting from interference with fungal pre-induction (Table 4.7, row 42). In addition, *OA_a3A04* also exhibited strongest responsiveness to treatment with the fungicide cyprodinil (Table 4.5, row 3). Thus, the PDR type ABC transporter encoded by *OA_a3A04* appears to hold an exceptional position within the fragments identified by SSH. Yet, suppression of transcript accumulation by transient RNAi did not affect penetration efficiency of wheat powdery mildew (Table 4.11). It might be noteworthy that PDR5-like ABC transporters may be required for excretion of secondary metabolites during plant defense (reviewed by Martinoia et al., 2002). In contrast to *OA_a3A04*, the rest of ABC transporters transcriptionally induced by sylA was not found to exhibit activation upon *Bgh* infection (Bruggmann et al., 2005).

The large number of putative detoxifying enzymes indicates that sylA exhibits phytotoxic activity in wheat, although no defects are observed macroscopically in seven day-old seedlings sprayed with up to 400 µM solutions of syringolin (not shown). Alméras et al. (2003) studied gene activation by cytotoxic reactive electrophile species (RES; in that case compounds with α,β-unsaturated carbonyl groups) in *Arabidopsis*. They observe interesting parallels between RES and *Pseudomonas*-induced gene induction. Interestingly, syringolin also harbors an electrophilic region encompassing C1, C2 and C3 of 5-methyl-4-amino-2-hexenoic acid. Like sylA on wheat, RES treatment of *Arabidopsis* causes transcriptional activation of genes encoding GSTs, cytochrome P450s, or epoxide hydrolase. Yet, in contrast to the plant response to RES described by Alméras et al (2003), none of the defense-related PR genes of the present microarray (which are also transcriptionally induced upon infiltration with *Pseudomonas syringae*; not shown) is found to be activated upon sylA treatment. The only exception is weak accumulation of transcripts corresponding to a wheat homologue of Hin (accession #BE419039; Table 4.4, row 80). In addition, general overlaps between transcriptional regulation upon syringolin treatment and plant pathogen interaction are found to be weak (chapt. 4.3.3). Thus, despite the presence of an electrophilic region, syringolin appears to posses the potential of triggering an innate response in the plant different from the one generally induced by RES.

5.3.3. Chaperones

Transcripts of several heat shock proteins (Hsps) are found to accumulate upon sylA treatment. The list includes *Hsp60* and *Hsp70*, the small heat shock proteins *Hsp23.5* and *Hsp23.6,* and the co-chaperone *HspBP1*.

Heat shock proteins function as molecular chaperones. They are involved in protein folding and re-folding or degradation of denatured proteins. Some but not all of them are induced in response to heat (Wang et al., 2004). The heat response is regulated by heat shock transcription factors (HSFs, reviewed by Pirkkala et al., 2001). In plants, Hsps are induced in response to a wide range of environmental impacts and thus they may be particularly important for the re-establishment of cellular homoeostasis.

Heat shock proteins of mammals are able to enforce cell survival by interaction with various key components of apoptosis which results in inhibition of caspase activity (Xanthoudakis and Nicholson, 2000; Beere, 2004; Gupta and Knowlton, 2005). Hsp70 can negatively regulate the mitochondrial pathway of apoptosis by inhibiting pro-apoptotic Bax translocation to the mitochondria or by preventing assembly of the apoptosome via direct interaction with Apaf-1 (the components are illustrated in Figure 3.6, p.13). It also prevents cleavage of Bid with functions between the mitochondrial and the death receptor pathway. Hsp70 can also exhibit anti-apoptotic activity in the death receptor pathway for example by interactions during Fas receptor downstream signaling. In addition, Hsps mediate induction of apoptosis at the top of the signaling cascade for example by Hsp70-mediated retention of JNK (c-Jun NH_2-terminal kinase) in its inactive dephosphorylated form (Beere, 2004). The cytosolic Hsp60 appears to have anti- as well as pro-apoptotic activity. Complexed with additional proteins, it can enforce execution of apoptosis by enhancement of pro-caspase 3 activation whereas Hsp60 complexes with Bax inhibit Bax-induced release of cytochrome *c* from the mitochondria and thus prevent induction of apoptosis (Gupta and Knowlton, 2005). Following the regulatory activity of the chaperone network in animals, similar mechanisms may exist in plants. Yet, the present knowledge is still limited and further research is required in order to clarify the role of plant chaperones as mediators of signaling.

Hsp70 is forming a complex with the co-chaperones DnaJ and GrpE in bacteria (Knippers, 1997). The co-chaperones are required for substrate binding by Hsp70, which is coupled to its ATPase activity. Interestingly, a plant DnaJ homologue (*OA_a1A12*) was found by SSH but it did not exhibit transcriptional responsiveness to sylA treatment upon microarray investigation. A second transcript (*OA_a3A05*) was found to transiently accumulate at 2 hat (Table 4.9, p.97). Blast analysis revealed 100 % identity (of 32 aa) to a wheat cDNA (accession #CV771079) exhibiting high similarity to a rice Hsp70-interacting-

like protein (accession #AC093018). Indeed, *CV771079* exhibited moderate similarity (49 % similarity of 181 aa) with the human Hsp70 binding protein HspBP1 (accession # AF187859). The yeast homolog of HspBP1 was described recently to function as a nucleotide exchange factor required for Hsp70-mediated protein folding at 37°C (Shomura et al., 2005). Hsp70 family chaperones are expressed in various compartments but the one that was strongly induced by sylA exhibited strongest similarity to mitochondrial forms, in particular to the DnaK-like form located in the mitochondrial matrix.

Similarly, both fragments corresponding to Hsp60 (chaperonins) were mitochondrial isoforms and belong to the group I chaperonins. The bacterial forms of this group consist of two family members (chaperonin 60 and chaperonin 10) which function together. It is thought that this also holds true for the organellar forms (Wang et al., 2004).

Hsp90 inter alia appears to be required for the proteasome assembly and maintenance (Imai et al., 2003). Thus, with regard to the observed upregulation of proteasomal transcripts, the absence of Hsp90-like cDNA fragments in the collection obtained by SSH is surprising.

The most abundant group of Hsps in plants are the small Hsps which are subdivided into 6 different classes according to their subcellular localization (Scharf et al., 2001). They posses the ability to prevent aggregation of non-native proteins and by this means facilitate refolding by other chaperones.

OA_a1H02 exhibited 91 % sequence identity (of 93 aa) to a wheat EST (accession #BG604320) which in turn showed 92 % identity (of 107 aa) to the wheat small heat shock protein Hsp23.6 (accession #Q9ZP24). Similarly, *OA_a1B01* exhibited 99 % DNA sequence identity (of 251 bp) to a wheat EST (accession #CD907952), which was part of an EST contig encoding small heat shock protein Hsp23.5 (accession #Ta.203). The two representatives of small heat shock proteins (sHsps) belong to the mitochondrial class M but are encoded in the nucleus. As most organelle-specific sHsps they are thought to be unique to the plant kingdom (Scharf et al., 2001).

The plant sHsps may play an important role in stress tolerance. In tomato chloroplasts, sHsps were found to retain electron transport during heat stress by protecting PSII (Heckathorn et al., 1998). Similarly, mitochondrial sHsps were demonstrated to protect the NADH:ubiquinone oxidoreductase (Complex I) electron transport under saline stress conditions in maize (Hamilton and Heckathorn, 2001). The authors suggested that the damage to the Complex I electron transport upon NaCl stress occurs by oxidative stress and they hypothesized that sHsps may exhibit antioxidative activity.

The fragments *OA_a1B01* and *OA_a3A05* corresponding to Hsp23.5 and Hsp70-interacting protein were both found to accumulate at 2 hours after syringolin treatment (Table 4.9, p.97). Thus they belong to the earliest transcriptional response of wheat to treatment with syringolin observed in this study, indicating that heat shock proteins may play an important role in the plant response to sylA. Intriguingly, most Hsps cloned by SSH were mitochondrial forms. As reflected by their strong induction, accumulation of Hsps appears to be particularly important in the mitochondria (Table 4.4, p.65; Rows 13-17). Based on the protective activity of mitochondrial sHsps observed by Hamilton et al., (2001), it might be speculated that mitochondria are particular targets of syringolin action.

5.3.4. Mitochondria

Mitochondria are polymorphic organelles harboring the respiratory electron transfer chain responsible for the mobilization of energy in the form of ATP in plants and animals (Buchanan et al., 2001). It has been widely accepted that they evolved from prokaryotic origin. Mitochondria are strictly compartmentalized semiautonomous cell components containing a DNA genome (mtDNA) encoding rRNA, tRNA and some proteins of the electron transfer chain. The large inner membrane (IMM) folds into cristae and separates the mitochondrial matrix from the intermembrane space. A strong electrochemical proton gradient across the IMM is generated by the electron transfer chain and drives phosphorylation of ADP to ATP by the F_0F_1-ATP synthase. The organelle is enclosed by the outer membrane (OMM) which separates the intermembrane space from the cytosol (Buchanan et al., 2001).

Remarkably, a number of proteins encoded by SSH-derived cDNA fragments are located in the mitochondria in vivo. Next to the Hsps already mentioned, this includes the voltage dependent anion channel (VDAC; *OA_b1F04*), prohibitin (*OA_a3C03*), alternative oxidase 1(AOX, *OA_a1E06*), external rotenone insensitive NAD(P)H dehydrogenase-like *OA_a2B11* or the BCS1-like (bc_1 synthesis) *OA_a1B08*. Of these, strongest accumulation was observed for the VDAC and AOX (Table 4.4, rows: 64, 67-69 & 77). Like in the case of the two sHsps, transcriptional upregulation of VDAC transcripts was detected as early as 2 hat (Figure 4.27B, p.96) and was still clearly detectable at 48 hat (Table 8.9, p.212; rows 1, 25 & 34).

Accumulation of transcripts corresponding to the VDAC gained particular attention because of its involvement in the mitochondrial pathway of animal apoptosis (introduced on p.13). The VDAC (synonym porin) is encoded in the nucleus and the protein is located in the OMM where it forms a membrane channel, a cylinder with hydrophilic interior (Benz, 1994).

It is permeable to nonelectrolytes of molecular masses less than 8 kDa (Colombini, 1980; Zalman et al., 1980). However, permeability to anions is depending on the electrical membrane potential (Rostovtseva and Colombini, 1997). The VDAC was subject to extensive investigation over the past 30 years for it is consolidating two large fields of interest: Participation in the regulation of apoptosis in mammals via interaction with pro- and anti-apoptotic factors such as Bax or Bcl-x(L) (Shimizu et al., 2000; Banerjee and Ghosh, 2004) or formation of the permeability transition pore complex (PTPC) (Crompton et al., 2002) and control of mitochondrial homeostasis and metabolism with respect to variable permeability to ATP (Lemeshko, 2002; Lemeshko and Lemeshko, 2004). Possible implications of the VDAC as therapeutic target for initiation of cell death have been discussed recently (Granville and Gottlieb, 2003).

Mitochondrial membrane permeabilization (MMP) is a central event during initiation of apoptosis. It causes protein permeability of the OMM and dissipation of the mitochondrial transmembrane potential ($\Delta\Psi_m$) at the IMM (Ferri and Kroemer, 2001). The exact role of the VDAC in the release of apoptogenic factors from the intermembrane space to the cytosol which is under the control of pro- and anti-apoptotic members of the Bcl-2 protein family is still controversial (reviewed by Ferri and Kroemer, 2001; Bras et al., 2005). Members of the Bcl-2 family are able to form membrane channels and tBid-induced oligomerization of Bax within the outer mitochondrial membrane causes release of apoptogenic factors and cell death. In addition to that, release of cytochrome *c* may be mediated by opening of the VDAC. It was found that pro-apoptotic Bax can induce release of cytochrome *c* by interaction with the VDAC antagonized by the activity of Bcl-X_L (Shimizu et al., 1999; Shimizu et al., 2000).

Since MMP is an important aspect of animal apoptosis, transcriptional upregulation of the VDAC might increase the capability of mitochondria to release apoptogenic factors into the cytosol. However, regulatory effects reported from the VDAC so far depend on conformational changes and protein interactions whereas altered transcription is less characterized. With respect to this, it has been found that the abundance of transcripts encoding components of another channel of the outer mitochondrial membrane, the TOM complex channel, were increased in *S. cerevisiae* mitochondria depleted of the VDAC channel (Kmita et al., 2004). Thus, abundance of outer mitochondrial membrane channels might be under transcriptional control and depend on the physiological situation.

The VDAC can interact with the adenine nucleotide translocase (ANT) at a 1:1 ratio to form contact sites between the IMM and the OMM. These junctional complexes include additional proteins such as creatine kinase, hexokinase or cyclophilin-D (reviewed by Crompton et al., 2002). Binding of creatine kinase by the ANT in the intermembrane space

contributes to efficient distribution of energy via the synthesis of highly diffusible creatine phosphate from ATP and creatine, which subsequently is released into the cytosol. Association of the VDAC with hexokinases bypasses the low permeability of ATP by bringing together sites of ATP production and usage (Crompton et al., 2002). The role of cyclophilin-D (CyP-D) is less well understood. It was hypothesized that the peptidylprolyl *cis-trans*-isomerase activity of CyP-D might mediate a conformational change of the VDAC/ANT/CyP-D complex into the PTPC (discussed by Crompton et al., 2002). In mammals, mitochondrial permeability transition occurs at pathological states of low cellular ATP and high Ca^{2+}, caused by anoxia, ischemia (reduced blood supply) and reperfusion (restoration of blood flow). Rapizzi et al. (2002) found that the human VDAC positively regulates mitochondrial Ca^{2+} accumulation and by this means might be involved in tuning of mitochondrial Ca^{2+} signals upon mitochondrial apoptosis. Accordingly, they observed higher susceptibility of VDAC-overexpressing cells against apoptosis induced by the sphingolipid ceramide (Rapizzi et al., 2002).

Since the VDAC is 10x less-abundant than the ANT (Crompton et al., 2002), transcriptional upregulation of the VDAC might also increase the number of VDAC/ANT complexes formed between the IMM and the OMM. V. & S. Lemeshko (2002; 2004) investigated the formation of an outer mitochondrial membrane potential and possible regulatory mechanisms of the VDAC conformation which is closed at high electrical potentials. They found that the VDAC may behave like a biological transistor which was hypothesized to be part of a basic concept of cellular energy metabolism regulation. According to their model, an increase of VDAC channels which is observed in malignant tumor cells would result in closing of the VDAC. Consequently, ATP release from the mitochondria to the cytosol would be suppressed, which might mimic a respiratory defect (Lemeshko, 2002).

By aerobic respiration, plants and animals are able to mobilize energy by oxidation of organic substrates to CO_2 and H_2O. A large amount of reducing power in the form of NADH and $FADH_2$, which is produced during glycolysis and in the tricarboxylic acid (TCA) cycle, is converted to energy in the form of ATP by oxidative phosphorylation at the IMM (Buchanan et al., 2001). The electron transfer chain at the IMM consists of four redox centers (complex I through IV) and the final reduction of oxygen to water is coupled to the stepwise generation of an electrochemical gradient across the IMM. This proton motive force drives the phosphorylation of ADP to ATP by the F_0F_1-ATP synthase. Electrons are shuttled from one complex to the other by ubiquinol and cytochrome *c* (cytochrome *c* pathway). As illustrated in Figure 5.3, plant mitochondria contain additional components next to the universal electron transfer chain such as alternative NAD(P)H dehydrogenases at both sides

of the IMM (Rasmusson et al., 2004) and the alternative oxidase (Millenaar and Lambers, 2003).

Control of the respiratory activity (respiratory control) is dependent on the availability of ADP and P_i and a large proton gradient limits the electron flow through the electron transfer chain (Buchanan et al., 2001). The unique energy-wasting nonphosphorylating bypasses in plants are presently viewed to allow for rapid adaptation to adverse environmental conditions (Buchanan et al., 2001; Millenaar and Lambers, 2003; Rasmusson et al., 2004).

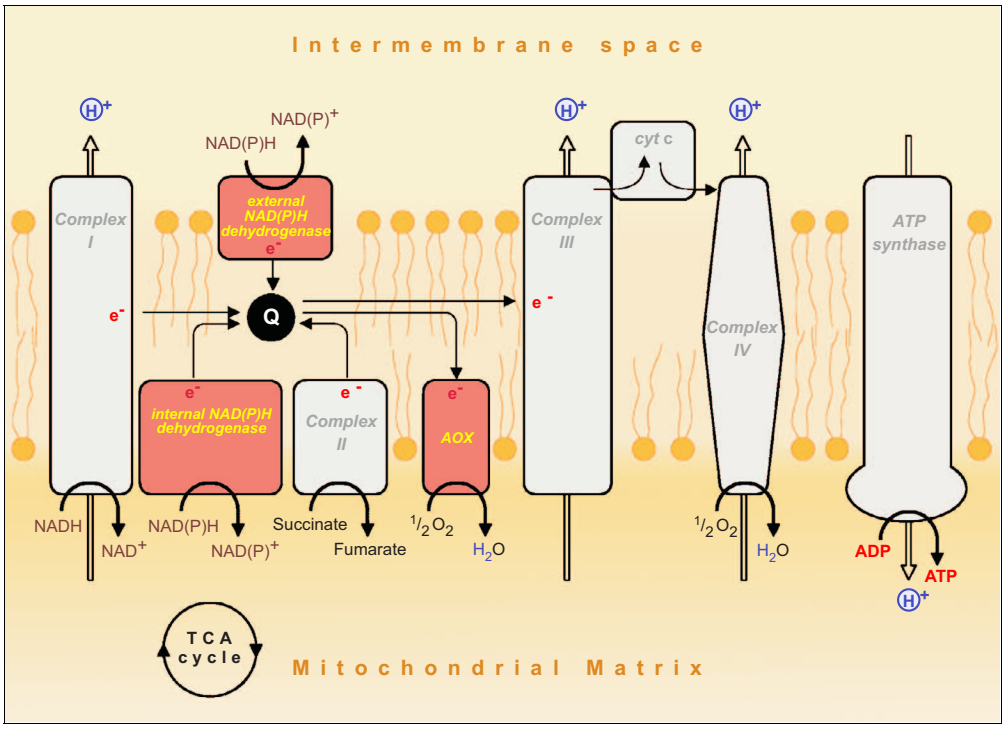

Figure 5.3: Organization of the plant electron transfer chain at the IMM. Q: Ubiquinol, AOX: Alternative oxidase, TCA cycle: Tricarboxylic acid cycle, complex I: NADH dehydrogenase, complex II: succinate dehydrogenase, complex III and IV: Part of the cytochrome pathway, cyt *c*: Cytochrome *c*, grey components: Cytochrome *c* pathway, red components: Alternative components of plant mitochondria. (Millenaar and Lambers, 2003, modified).

Synthesis of the AOX is induced under various conditions such as oxidative stress, herbicide treatment or inhibition of the electron transfer (Buchanan et al., 2001). The alternative oxidase competes for ubiquinol with the cytochrome *c* pathway. Due to the fact that the activity is not coupled to proton pumping, this allows for ATP/ADP ratio-independent NAD(P)H oxidation. Linking of alternative NAD(P)H dehydrogenase activity (*OA_a2B11*) with the alternative oxidase (*OA_a1E06*) results in oxygen reduction without proton pumping or ATP generation (Rasmusson et al., 2004). Autooxidation of ubiquinol during overreduction of the electron transfer chain can result in the formation of reactive

oxygen intermediates (ROIs). With respect to this, AOX activity may balance ubiquinone reduction and function as an electron valve which reduces ROI formation and permits oxidative respiration when the electron transfer chain is impaired (Buchanan et al., 2001). Accordingly, AOX activity is considered to have a protective nature and to prevent cell death alongside with ROI-scavenging enzymes (Maxwell et al., 1999; Lam et al., 2001). Silencing of AOX transcription by antisense expression of AOX in transgenic tobacco cells results in ROI accumulation and increases susceptibility to chemically induced mitochondria dependent and independent cell death (Maxwell et al., 1999; Robson and Vanlerberghe, 2002). Conversely, overexpression significantly decreases transcription of ROI-scavenging enzymes or ROI-sensitive PR-1 and transgenic tobacco plants exhibit reduced lesion size in response to TMV (Maxwell et al., 1999; Ordog et al., 2002).

OA_a2B11 exhibited sequence similarities with external NADH dehydrogenases. A second sylA-responsive fragment (*OA_a2C02*) showed similarity to NAD(P)H-dependent oxidoreductases but no precise function could be assigned by blast comparison. Alternative NAD(P)H dehydrogenases which are found at both sides of the IMM are insensitive to the dehydrogenase inhibitor rotenone and their exact physiological role is still unclear (Rasmusson et al., 2004). Their function is thought to be related to the one of the AOX. It has been hypothesized that external NAD(P)H dehydrogenases may regulate the reduction state of cytoplasmic NAD(P)H (Rasmusson et al., 2004). An increase of AOX and alternative NADH dehydrogenase activity in tobacco cells under phosphate-limited conditions was interpreted to reflect a coordinated response of nonphosphorylating pathways which relieves respiratory control restriction (Rasmusson et al., 2004). At low ADP concentration, amino acid metabolism via the TCA cycle is impaired since NAD^+ reduction via the cytochrome *c* pathway is under respiratory control. Under these conditions, the alternative pathways would permit continuation of the TCA cycle (Millenaar and Lambers, 2003).

Prohibitin (*OA_a3C03*), which was observed in mitochondrial fractions of tobacco leaves is a highly conserved multifunctional protein of about 280 aa found in plants, yeast and animals (Snedden and Fromm, 1997). In human, prohibitin was first identified to block G1/S phase cell cycle transition (Roskams et al., 1993). Transcription of yeast prohibitin is transiently increased during diauxic shift (shift from anaerobic fermentation of glucose to aerobic respiration of ethanol) and the protein was found to form oligomeric complexes in the IMM where it is hypothesized to exhibit chaperone-like functions and might be involved in the assembly of respiratory chain enzymes (Nijtmans et al., 2000). In mammals, prohibitin is a target for ubiquitination which directs sperm mitochondria for degradation by the 26S proteasome (Thompson et al., 2003). Recent investigations in mammals revealed that prohibitin is a potential tumor suppressor protein which similarly modulates Rb/E2F and p53

regulatory pathways (Fusaro et al., 2003). Prohibitin overexpression protects from camptothecin-induced apoptosis (Fusaro et al., 2002). The protein was found to interact with the pro-apoptotic E2F1 and p53 in the nucleus and upon induction of apoptosis migrates to the mitochondria where it co-localizes with p53 and might mediate apoptotic signaling (Fusaro et al., 2003). Its anti-apoptotic properties also attracts attention with regard to potential involvement in chemoresistance, a severe problem for chemotherapy during cancer treatment (Fraser et al., 2003).

The plant BCS1 family (bc_1 synthesis) of AAA-type ATPases represented by *OA_a1B08* is larger than the animal and fungal family and the plant members form a separate cluster within the whole BCS1 group (Frickey and Lupas, 2004). Yeast BCS1 is located at the IMM where it exhibits chaperone activity during assembly of the respiratory chain complex III (Cruciat et al., 1999).

Taken together, the high proportion of mitochondrial proteins and their putative biological functions indicate that the action of syringolin in wheat directly or indirectly affects mitochondrial integrity. This might be of importance with respect to the central role of mitochondria in the regulation and induction of apoptosis (Ferri and Kroemer, 2001; Bras et al., 2005). Interpretation of the mitochondrial response leads to the hypothesis that sylA activity impairs oxidative phosphorylation and by this means might have strong effects on the availability of ATP in the cell. The mechanism by which syringolin might affect oxidative respiration is not known. A respiratory defect might theoretically be caused by direct inhibition of components of the electron transfer chain or alternatively could also be mimicked by elevated expression of the VDAC (as speculated by Lemeshko, 2002).

The fact that HR as indicated by whole cell autofluorescence exclusively occurs in the presence and not in the absence of *Bgt* on sylA-treated leaves (data not shown) demonstrates that wheat epidermal cells successfully counteract sylA-induced instabilities under normal conditions. In line with that, products of genes transcriptionally induced after sylA treatment exhibit protective functions like maintenance of NAD(P)H oxidation, minimization of ROI formation, chaperone activity for newly synthesized mitochondrial proteins or putative direct anti-apoptotic activity like in the case of prohibitin.

The fungal elicitor harpin is a ribosomally synthesized protein of about 400 aa secreted into the apoplast via the type III secretion system (TTSS) by several Gram-negative plant pathogenic bacteria like *Erwinia amylovora* or *P. syringae* (reviewed in Li et al., 2005a). The protein, which has the ability to form ion-conductive channels and at high concentrations induces HR and SAR in some nonhost plants has been hypothesized to be required as part of the TTSS for the interaction of the pathogen with the host plant (Li et al., 2005a). The rapid HR induced in *Arabidopsis* suspension cells by harpin derived from *P.*

syringae was recently found to resemble apoptosis triggered via the mitochondrial pathway (Krause and Durner, 2004). Transcripts corresponding to sHsps and AOX only accumulate transiently (around 2-4 hat) and disappear after cytochrome *c* has been released into the cytosol (between 1-3 hat). Apparently, transcription of proteins with protective function is repressed in plant cells undergoing harpin-induced cell death.

In contrast to harpin treatment, sylA-induced accumulation of transcripts encoding protective proteins in wheat is observed up to 24 hat (Table 4.4, rows 14-17, 64, 68 & 77). Some of them (*Hsp23.6*, *Hsp60* and *VDAC1*) were even found to exhibit extended induction when compared to the rest of sylA-responsive genes.

5.3.5. Carbohydrate metabolism

As already mentioned in chapt. 4.2.5.2, a large portion of sylA-responsive genes encoded proteins of the carbohydrate metabolism. Upregulated transcription was exclusively found for enzymes involved catabolic processes like sucrose break down, glycolysis, tricarboxylic acid cycle (TCA) or fermentation. An overview is presented in Figure 5.4. Enzymatic functions frequently were represented by more than one distinct cDNA fragment indicative either for the cloning of more than one isoenzyme or of different regions of the same enzyme. In plants, sucrose synthase and invertase (Table 4.4, rows 40-44) are both responsible for sucrose degradation. The reason for the presence of two different enzymes for sucrose breakdown is not entirely clear and often both are found to be expressed in the same tissue (Buchanan et al., 2001).

Five enzymes identified to be upregulated by sylA treatment participate in glycolysis. The cytosolic NAD^+-dependent glyceraldehyde-3-phosphate dehydrogenase and enolase are the two enzymes which deliver high-energy compounds allowing ATP generation during the energy-conserving reactions of glycolysis. Significant transcriptional induction was observed for an enolase 1-like fragment (*OA_a2G01*). Interestingly, an enolase 2-like cDNA fragment (*OA_b2A09*) was also cloned by SSH but t/c ratios were only slightly above 2 and investigation of epidermis specificity indicated strong mesophyll specific expression (Table 4.4, rows 33 & 34 and Table 4.7, rows 31 & 114). In animals, pyruvate kinase activity is positively regulated by the product of the reaction mediated by the glycolysis key regulatory enzyme phosphofructokinase (Stryer, 1988).

This 'top down' regulatory mechanism is absent in plants, where a negative feedback regulation by phosphoenolpyruvate (PEP) strongly inhibits PFK activity (Buchanan et al., 2001). With respect to this, transcriptional upregulation of pyruvate kinase (Table 4.4, rows 35 & 36) which catalyzes the almost irreversible energy-conserving conversion of PEP to pyruvate was considered to be key regulatory event for carbohydrate catabolism by glycolysis following sylA treatment of wheat leaves.

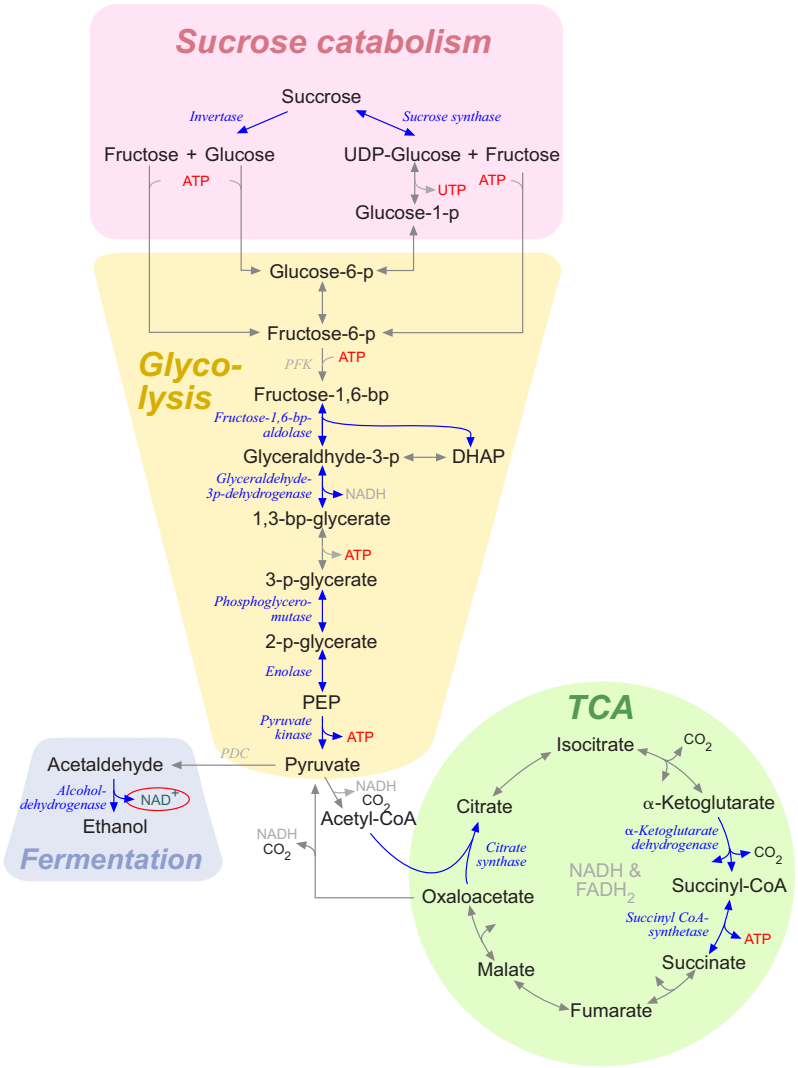

Figure 5.4: Carbohydrate metabolism. Participating enzymes upregulated by sylA treatment and corresponding reactions are labeled in blue. Additional relevant enzymes are written in grey italic letters. Abbreviations: DHAP: Di-hydroxyacetone phosphate, PEP: Phosphoenolpyruvate, p: phospho or phosphate, bp: bisphosphate, TCA: Tri-carboxylic acid cycle, PFK: Phosphofructokinase (not cloned), PDC: Pyruvate de-carboxylase (cloned, not confirmed). Reactions were drawn according to Buchanan et al. (2001).

Microarray analysis also revealed the transcriptional upregulation of three enzymes participating in the tricarboxylic acid cycle (TCA), the following step of energy production under aerobic conditions located in mitochondria. Citrate synthase and α-ketoglutarate dehydrogenase catalyze the irreversible steps of the TCA (Figure 5.4) and are responsible for the negative regulatory control of ATP on the TCA turnover in animals (Stryer, 1988). Since the α-ketoglutarate dehydrogenase complex is also negatively regulated by succinyl-

CoA, transcriptional upregulation of succinyl-CoA ligase (syn. succinyl-CoA synthetase) might have a positive regulatory effect on the turnover of the TCA.

Interestingly, a putative aconitate hydratase (aconitase) was also slightly upregulated in response to sylA-treatment (Table 4.4, row 26). The cDNA fragment exhibited highest sequence similarity to cytoplasmic isoforms and thus it does not participate in the TCA. This cytoplasmic isoform rather might participate in plastidial amino acid transamination reactions or ammonia assimilation by providing cytoplasmic α-ketoglutarate (Buchanan et al., 2001). A putative cytoplasmic isoform of the aspartate aminotransferase (*OA_b2F07*), which plays a key role in plant metabolism, exhibited transcriptional upregulation at 24 hat (Table 4.4, row 71). The enzyme, which catalyzes the reversible interconversion of glutamate and oxaloacetate to α-ketoglutarate and aspartate, is involved in nitrogen assimilation and intracellular transfer of carbon, nitrogen and reducing equivalents (Buchanan et al., 2001).

Strong transcriptional induction of alcohol dehydrogenase 1 (*OA_a1D06* and *OA_a2A05*) indicative for the induction of fermentative catabolic activity displays an important aspect of sylA-action on wheat. Fermentation permits regeneration of NAD^+ for the maintenance of ATP generation by glycolysis under low oxygen concentrations (reviewed in Buchanan et al., 2001; Geigenberger, 2003). The pathway from pyruvate to acetaldehyde and ethanol involves the activity of pyruvate decarboxylase (PDC) and alcohol dehydrogenase (Figure 5.4). The *Arabidopsis* PDC1 was reported recently to exclusively protect from anoxic stress (Kürsteiner et al., 2003). In accordance, SSH also resulted in enrichment for a PDC-like fragment (*β1G07*) and reverse northern dot blot hybridization indicated sylA-induced transcriptional upregulation (Figure 4.5, p.33). However, since sequence analysis revealed that *β1G07* corresponded to a fusion between two different cDNAs (data not shown), the corresponding fragment was not represented on the microarray. Conversely, none of the SSH fragments showed similarity to lactate dehydrogenase, the enzyme which catalyzes the second fermentation pathway from pyruvate to lactate described in plants (Buchanan et al., 2001). Glycolytic fermentation also results in accumulation of minor products such as alanine and γ-aminobutyrate (Buchanan et al., 2001). The formation of these products from pyruvate and α-ketoglutarate might counteract cytosolic acidification during anoxia (Geigenberger, 2003). Synthesis of alanine from pyruvate is catalyzed by alanine aminotransferase, the second transaminase obtained by SSH (*OA_a2D10*) which exhibited stronger transcriptional induction as compared to the other transaminase (Table 4.4, row 70). Alanine accumulation is hypothesized to significantly contribute to anoxia stress tolerance (Ricoult et al., 2005). Since aspartate aminotransferase

(*OA_b2F07*) is involved in the synthesis of γ-aminobutyrate, it is likely that both enzymes are transcriptionally upregulated in the context of fermentation.

The observed transcript accumulations tempted to speculate about possible consequences of elevated enzymatic activity resulting from activation of corresponding genes, being aware that the control of metabolic pathways also largely involves post-transcriptional and -translational regulatory levels (Buchanan et al., 2001). It was found that syringolin application in wheat may induce sucrose breakdown via the glycolytic pathway and involve alcoholic fermentation. The transcriptional activation of these pathways appeared to be specific, since no cDNA fragment corresponding to enzymes of related metabolic pathways was obtained by SSH. The overall picture is only partially similar to the one observed during interaction of *Arabidopsis* with *P. syringae* pv. *tomato* (Scheideler et al., 2002). The authors reported a biphasic switch to defense metabolism at 7 hai and back to housekeeping metabolism at 24 hai, which also affected genes of glycolysis and TCA but additionally involved the pentose phosphate pathway and aromatic amino acid biosynthesis. This involvement of bioenergetic pathways in plant defense was explained by a transiently increased demand for energy and biosynthetic capacity and preceded increased transcription of stress-responsive genes (Scheideler et al., 2002). Likewise, transcription of many genes involved in the response of wheat to sylA treatment was shifted back to normal levels at 24 hat. Yet some, like sucrose synthase, enolase or alcohol dehydrogenase, were still clearly transcriptionally upregulated at 24 hat (Table 4.4; rows: 40, 33 & 145 - 146). In addition, despite the upregulation of many stress-related transcripts (chapt. 5.3.3 & chapt. 5.3.2), no transcriptional regulation of PR-genes or phenylalanine ammonia-lyase, which is required for flavonoid and isoflavonoid synthesis (Dixon, 2001), was observed within the first 24 hat (chapt. 4.2.5.1). Thus, it is speculated that the metabolic transition by glycolytic enzymes after sylA treatment at least partially reflects a specific response independent from defense mechanisms rather than a global change accompanying or preceding the induction of the plant defense machinery.

Analysis of the putative carbohydrate metabolic changes induced by syringolin revealed remarkable similarities to protein accumulation observed under anoxic conditions, including sucrose synthase, enolase, alcohol dehydrogenase, G3PDH and fructose bisphosphate aldolase (Buchanan et al., 2001). Low oxygen strongly affects ATP production by oxidative phosphorylation. Resulting from flooding or water logging, it is a cause of yield losses of agronomically important crop plants (Drew, 1997; Subbaiah and Sachs, 2003) and therefore variable tolerance of different plant species to low oxygen also gained attention in plant breeding. Transition from oxic to anoxic metabolism under unfavorable conditions

involves a first phase of reduced ATP consumption followed by a second phase of exclusive ATP production by fermentation (reviewed by Geigenberger, 2003). Inhibition of glycolysis is followed by stimulation which finally results in direction of sucrose or glucose to glycolysis (known as Pasteur effect). Whereas transcription of alcohol dehydrogenase gradually increases with decreasing O_2 concentrations, the final switch to glycolytic fermentation as reflected by stimulation of glycolysis only occurs at O_2 contents of 1 % and less (Geigenberger, 2003).

Under anoxic conditions, wheat seedlings are completely inhibited in growth (Biemelt et al., 1998; Emel'yanov et al., 2003). Low oxygen concentrations have broad inhibiting effects on the whole plant metabolism and result in rapid shutdown of sucrose, amino acid, protein and lipid biosynthesis (Geigenberger, 2003). A large number of proteins disappear from two-dimensional gel patterns within the first one hour after transition to low oxygen (Sachs et al., 1980). Moreover, hypoxia in potato tubers prevents transcription and translation of wound response genes such as PAL, which might explain increased susceptibility against bacterial soft rot under low oxygen conditions (Butler et al., 1990). Transcriptional downregulation of lignin and flavonoid biosynthetic pathways under hypoxic conditions was also reported by Liu et al. (2005). Klok et al. (2002) found that the transition to low-oxygen metabolism consists of an early phase (up to 0.5 h) of transcriptional gene regulation of a small set of genes including transcription factors and metabolic enzymes which is followed by regulation of a different and large set of genes including enzymes involved in metabolism but also receptor kinases involved in signal transduction. Transcriptionally upregulated enzymes involved in metabolism included typical well known anaerobic proteins (ANPs) such as ADH1, sucrose synthase or PDC, many of which were also found to be upregulated after sylA treatment. Likewise, a remarkable number of enzymes with detoxifying properties such as glutathione-S transferase, epoxide hydrolase, monooxygenase and ABC transporters was transcriptionally upregulated in both situations hypoxia, and sylA-treatment, respectively (Klok et al., 2002, & chapt. 5.3.2.).

With regard to the inhibitory effect of hypoxia on various metabolic pathways it might be speculated that the global transient upregulation of the whole proteasome machinery after sylA treatment might be related to extensive protein breakdown or altered expression in response to anoxia. Yet, Butler et al. (1990) did not find indications for increased protein turnover under hypoxic conditions in potato. In addition, no transcriptional upregulation of the 26S proteasome was found upon recent transcript profiling experiments in *Arabidopsis* (Klok et al., 2002; Liu et al., 2005). However, Klok and coworkers reported accumulation of ubiquitin which might denote elevated proteolytic activity. Apart from the two studies, there is little information about global transcriptional changes under hypoxic conditions at

present. Moreover, the present data found in the literature are not fully consistent and partially contradictory, which is explained by the fact that they were derived from different plant material (Liu et al., 2005). It should also be mentioned that the degree of oxygen deficiency may play a fundamental role in particular with respect to putative proteasome activity, which is an ATP-consuming process and therefore might be suppressed under pre-anoxic conditions. In the case of the study carried out by Liu et al (2005), it was found that the treatment was not sufficient to induce transcription of the *SAG12* gene, which is induced by flooding.

Like in the case of reperfusion in animals, re-aeration of plants results in ROI formation and is a critical phase for plants previously kept under hypoxic conditions (Geigenberger, 2003). The deleterious effects of re-aeration are counteracted by superoxide dismutase (SOD) activity and the activity of the ascorbate-gluathione cycle and appear to be more severe when plants were kept under anoxic conditions (Biemelt et al., 1998; Biemelt et al., 2000).

To test if the putative anoxia response of wheat to sylA treatment also causes growth inhibition, wheat seeds were planted onto growth medium containing phytagar and 2 µM sylA. After germination, sylA-treated seedlings formed primary roots of a length of 2 to 3 cm but further growth was completely suppressed (Figure 5.5B).

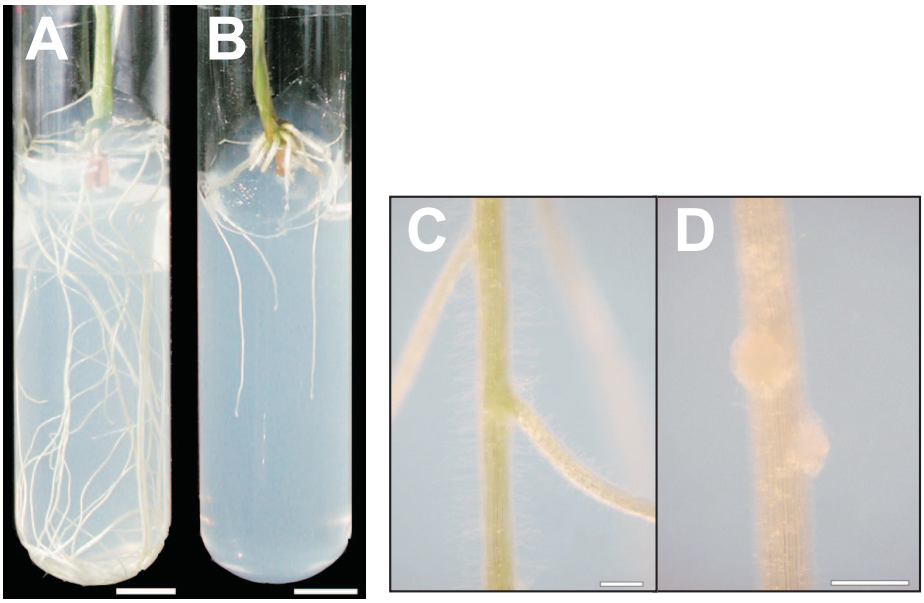

Figure 5.5: SylA-induced root growth inhibition in wheat: Seeds were either placed on pure growth medium containing phytagar (A & C) or on growth medium supplied with 2 µM sylA (B & D). A & B: Macroscopic effect (scale bar = 1 cm), C & D: close up (scale bar = 1 mm). Pictures were taken 2 weeks after sowing.

Adventitious roots were induced but did not grow into the medium and lateral roots were restricted to the formation of primordia (Figure 5.5.D). Meanwhile, no growth inhibitory effect was observed for the shoots when sylA was added to the growth medium (not shown). Roots of plants transferred to soil after 2 weeks of growth on synthetic medium completely recovered from previous negative growth effects of sylA and after 1 month of growth in soil, no difference was obvious when compared to control plants (not shown).

If syringolin induces an anoxia-like response in wheat, it would be interesting to find out more about the mechanism by which the response is induced. The present knowledge about possible mechanisms involved in the transition to anoxic metabolism was outlined by Geigenberger (2003). Crucially, the coordinated changes in metabolism and inhibition of respiration under hypoxic conditions appears to be controlled by an oxygen-sensing system which involves the electron transfer chain but is not dependent on the adenylate energy status (ATP/ADP ratio) (Geigenberger, 2003). The transcriptional activation of ANPs like ADH1 is mediated by the AtMYB2 transcription factor which binds an anaerobic response element (ARE) in the promoter region of the corresponding genes (reviewed in Klok et al., 2002; Geigenberger, 2003; Liu et al., 2005). Interestingly, the AtMYB2 transcription is not only induced by low oxygen but also by drought stress and ABA (Hoeren et al., 1998). The mechanism by which respiration is suppressed upon low oxygen is yet unknown. (Geigenberger, 2003). It was hypothesized that the inhibition of ATP-consuming processes involves Snf1-related protein kinase SnRK1 (Geigenberger, 2003). Three SSH-derived cDNA fragments which correspond to genes transcriptionally induced by sylA treatment may possibly be related to anoxic signaling. These are PRL1 (*OA_b2C06*), PP2C (*OA_a1B11*) and ABI3-interacting protein 2 (*OA_b2A06*).

cDNA fragment *OA_b2C06* was found to share 82 % amino acid sequence identity (of 140 aa) to an mRNA corresponding to the *Arabidopsis* PRL1 protein (accession #X82825) upon tblastx comparison searches. The protein encoded at the pleiotropic regulatory locus 1 (PRL1) was found to belong to the WD-repeat family of proteins (Nemeth et al., 1998; Yu et al., 2000) to which also the G-protein β subunit belongs (Garcia-Higuera et al., 1996). PRL1 was shown to function as a pleiotropic regulator of glucose and hormone responses in *Arabidopsis* (Nemeth et al., 1998). It consolidates effects on the reaction to diverse plant hormones such as cytokinin, ethylene, abscisic acid and auxin (Nemeth et al., 1998). Salchert et al. (1998) proposed a model outlining connections between glucose and steroid signaling via PRL1. A recessive mutation in the PRL1 locus inhibits root elongation in *Arabidopsis* and spontaneous initiation of side roots demonstrating enhanced auxin sensitivity of mutant plants (Nemeth et al., 1998). PRL1 was shown to interact with and

downregulate activity of SnRKs (Snf1-related protein kinases), *Arabidopsis* homologs of the yeast key regulator of glucose signaling Snf1 (sucrose non-fermenting; a serine/threonine kinase) (Bhalerao et al., 1999). Farras et al. (2001) found that the *Arabidopsis* ortholog of SKP1 (S-phase kinase-associated protein 1) and AtCUL1, which are subunits of the E3 ubiquitin ligase SCF^{TIR}, associate with the corresponding SnRK and the α4/PAD 20S proteasomal subunit, indicating that SnRKs may be required for phosphorylation of SCF^{TIR} substrates. The binding of PRL1 to the SnRK in turn competes with the association of the SCF complex and by this means PRL1 may negatively regulate the activity of the E3 ubiquitin ligase (Figure 5.6).

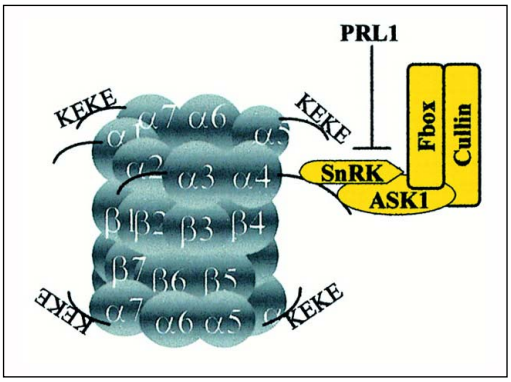

Figure 5.6: Interaction of SCF with the proteasome and association of SnRK. The SnRK inhibitor PRL1 competes association of SnRK with the SCF complex by binding to the same binding domain like ASK1 (= *Arabidopsis* homologue of SKP1). (Farras et al., 2001).

Obviously, PRL1 functions in a complex network of SnRK-mediated regulation of ubiquitin ligases consolidating hormonal regulation and direction of proteasome specificity. It is therefore difficult to interpret sylA-induced upregulation of PRL1 because accumulation of the protein may alter balanced control of proteasome specificity which in turn may have complex effects on plant growth and metabolism. Accordingly, the exact role of the protein has not yet been elucidated. Nevertheless, the relation of PRL1 to carbohydrate signaling and its regulatory capacity indicates that it might play a key role in the induction of the anoxia-like plant metabolism which is observed after sylA-application.

Intriguingly, SCF-type ubiquitin ligases are also found to be important in R-gene related plant resistance responses (Sullivan et al., 2003). The *Arabidopsis* homologue of SKP1 (SKP1/ASK1) is part of the E3 ubiquitin ligase SCF^{TIR1} which contains the *Arabidopsis* homologue of Cdc53 (AtCUL1) and the F-box protein TIR1 and is required for the plant response to auxin (Gray et al., 1999). SCF^{TIR} interacts with the COP9 signalosome which resembles the lid of the 26S proteasome (Schwechheimer et al., 2001) and mediates the plant auxin response and disease resistance (Schwechheimer et al., 2001; Liu et al., 2002). SGT1 (suppressor of G-two allele of SKP1) is required for the resistance conferred by various R-genes in *Arabidopsis* and barley and also interacts with COP9 and SKP1 (Azevedo et al., 2002; Liu et al., 2002). Based on this, Nishimura and Sommerville (2002)

proposed a model for the role of an SCF-SGT1-COP9 supra-complex in plant resistance (Figure 3.8, p.19). With regard to this, it could be speculated further that if SKP1/ASK1 association with SnRK was also required for the function of the E3 SCF ubiquitin ligase within the supra-complex, accumulation of PRL1 might negatively regulate its activity and thereby suppress R-gene mediated plant defense or COP9-related auxin signaling. Latest results indicate a dual role of SGT1 which implies antagonistic destabilization of R-proteins by interacting with RAR1 and HSP90 and requirement for induction of HR probably via SCF-related ubiquitin-mediated proteolysis of a negative regulator (Takahashi et al., 2003; Zhang et al., 2004b; Holt et al., 2005). Thus, PRL1 might exhibit direct anti-apoptotic activity by inhibiting the required E3 ubiquitin ligase activity of SCF^{TIR}.

Notably, Snf1 kinase activity was also shown to be inactivated by mammalian protein phosphatases PP2A and PP2C and also by the plant homolog of PP2C encoded at the *ABI1* locus (MacKintosh, 1998). A gene encoding a protein phosphatase 2C (PP2C) showed transcriptional upregulation by syringolin in the early time point in ceB (*OA_a1B11*). Plants contain a large family of the okadaic acid-insensitive Mg^{2+}-dependent PP2Cs which are key players in signal transduction processes (reviewed by Sheng, 2003). The subfamily ABI1 and ABI2 (ABA insensitive) is involved in signal perception of the plant hormone abscisic acid (ABA) and ABI1 and ABI2 are thought to act as negative feedback regulators in the signal transduction (Merlot et al., 2001). Transcripts corresponding to ABI1 and ABI2 accumulate in response to ABA (Leung et al., 1997).

ABA enhances seed dormancy and is involved in drought stress responses regulating transpiration by reducing water loss via rapid induction of stomata closure in vegetative tissues (Buchanan et al., 2001). In this respect it might be noteworthy that the probes corresponding to a PIP1-like aquaporin (*RB_34.4*) and a ripening-related protein (*RB_39.2*) displayed transcriptional downregulation after sylA treatment (Table 4.4, rows, 79 & 84). Hypoxia-sensitive wheat seedlings show strong ABA accumulation under anoxic conditions whereas hypoxia-tolerant rice seedlings accumulate less ABA but high levels of ethylene, which was hypothesized to explain the ability of rice to grow under anoxic conditions (Emel'yanov et al., 2003). ABA was found to counteract ROI-induced cell death in barley aleurone cell layers by inducing transcription of genes encoding ROI scavenging enzymes and probably stimulates the alternative electron transport pathway at the mitochondria (Fath et al., 2002). A cell death-suppressing role was also observed in developing barley anthers (Wang et al., 1999). With respect to cell cycle control, ABA inhibits G1-S phase transition by transcriptional upregulation of cyclin-dependent kinase inhibitors (Buchanan et al., 2001; Francis and Sorrell, 2001).

Next to ABI1 and ABI2, additional genes including three transcription factors (ABI3, ABI4 and ABI5) involved in ABA signal transduction were identified by mutation screening (for review, see Brady et al., 2003). A current model of ABA signal transduction is shown below in Figure 5.7. *OA_b2A06* encodes ABI3-interacting protein 2 (AIP2) and is transcriptionally induced at 12 hat by sylA treatment (Table 4.4, row 60). AIP2 is a Ring/U-box type E3 ubiquitin ligase which regulates ABA signaling by targeting ABI3 to the 26S proteasome (Zhang et al., 2005).

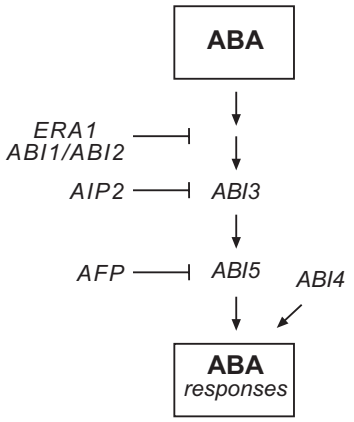

Figure 5.7: Model for ABA signaling in seed germination. ABI1/ABI2 phosphatases and ERA1 farnesyl transferase are negative regulators of ABA signaling. AIP2 promotes ABI3 degradation in ABA signaling. ABI5, which is negatively regulated by AFP (ABI five interacting protein), acts downstream of ABI3. ABI4 acts positively downstream in ABA signaling pathway. Arrows: Activation, Bars: Inhibition. (Zhang et al., 2005).

The *Arabidopsis* ABI3 transcription factor is the ortholog of the maize VP1 (VIVIPAROUS1) and is thought to regulate developmental transitions (Suzuki et al., 2001; Zhang et al., 2005). It is involved in seed development, plastid differentiation, lateral root formation and flowering time regulation (Brady et al., 2003; Zhang et al., 2005). ABI3 contains two DNA binding domains, one of which is also present on auxin response factors (ARFs) and insensitivity to auxin-induced lateral root formation in VP1-overexpressing plants indicates that the transcription factor represents an interaction point for auxin and ABA signaling (Suzuki et al., 2001; Zhang et al., 2005). *ABI3* transcripts are abundant in seeds and usually absent after germination but accumulation in vegetative tissue occurs in response to ABA upon post-germination growth arrest (Zhang et al., 2005). *AIP2* transcripts also accumulate in the presence of ABA and the AIP2 protein is thought to negatively regulate ABA signaling by increasing ABI3 turnover (Zhang et al., 2005). Interestingly, AIP2 transcription was downregulated upon *Bgt* infection at 48 hai as indicated by a single microarray experiment (Table 8.7, p.204, row 39).

Like in the case of *PRL1*, interpretation of transcriptional upregulation of *AIP2* and *PP2C* (possible *ABI1* or *ABI2*) in response to sylA treatment is difficult. Since for example ABI1, ABI2 and AIP2 all act as negative regulators in ABA signaling it could either be that their expression suppresses transcription of genes regulated by the plant hormone ABA. Alternatively, the regulators might accumulate in the context of negative feedback tuning of

ABA signaling and their transcriptional upregulation might therefore also reflect elevated ABA signaling. In addition, the situation is complicated by their potential to integrate signaling of multiple plant hormones (in this case ABA and auxin). With respect to this, a concerted activity of auxin and ABA might explain the complete cessation of root growth observed in sylA-containing medium (Figure 5.5). Unfortunately, the present knowledge of plant responses to ABA is still fragmented. Nevertheless, sylA-induced anoxia-like plant metabolism, anoxia-related accumulation of ABA, possible regulation of Snf1 kinase by PP2C and inhibition of root growth by ABA indicate that the transcriptional upregulation of ABA signaling factors is closely related to the metabolic change induced by syringolin in wheat. Whether the suspected hormonal signaling is an integral part of syringolin action in the plant or whether the regulatory factors are transcriptionally upregulated to counteract sylA-induced changes remains an open question.

5.3.6. Lipid metabolism

The cDNA fragment *OA_b1D11,* which exhibited transcriptional induction at 12 hat (Table 4.4, row 57), showed 98 % sequence identity (of 275 bp) to the temperature stress-induced lipocalin TaTIL, a novel wheat member of ligand-binding lipocalins (accession #AY077702) (Charron et al., 2002). Lipocalins are a large family of small extracellular ligand binding proteins involved in diverse processes such as protein transport, regulation of cell growth and metabolism, binding of cell surface receptors and membrane biogenesis in animals (Flower, 1996; Flower et al., 2000). Transcripts corresponding to TaTIL were found to specifically accumulate upon cold and heat stress in wheat leaves (Charron et al., 2002). Based on its high similarity to the steroid hormone-binding mammalian lipocalin ApoD and the ability of brassinosteroids to increase heat and cold stress tolerance in plants, it was hypothesized that TaTIL might be involved in brassinosteroid signaling upon temperature stress adaptation in plants (Charron et al., 2002).

The mammalian ApoD is represented in some high-density-lipoprotein particles where it is closely associated with the lecithin-cholesterol acyltransferase (Flower, 1996). In this respect it is interesting that transcripts corresponding to a lecithin-cholesterol acyltransferase (*OA_b2D12*) were also found to accumulate upon sylA treatment at 12 hat (Table 4.4, row 45). Lecithin-cholesterol acyltransferase (LCAT) is an enzyme that reversibly transfers an acyl residue from the membrane phospholipid lecithin to cholesterol, forming 1-acylglycerophosphocholine (lysolecithin) and a cholesterol ester (Lima et al., 2004). In the absence of a sterol acceptor, the enzyme also exhibits phospholipase A_2 or esterase activity (Lima et al., 2004). In plants, hydrolysis of membrane phospholipids occurs in response to

stress and appears to be related to the activation of phospholipase D, but the cellular function of this phenomenon is not clear yet (Zhang et al., 2003). Still, it should be mentioned that the activity of phospholipase D results in accumulation of phosphatidic acid which similarly reduces H_2O_2-induced cell death and regulates ABA signaling by inhibiting the function of ABI1 in *Arabidopsis* (Zhang et al., 2003; Zhang et al., 2004a).

5.3.7. Additional genes of interest

5.3.7.1. Cdc48

Transcripts corresponding to the AAA-type ATPase Cdc48 (cell division control 48; *OA_a3F09*) accumulated in response to sylA-treatment of wheat at 12 hat (Table 4.4, rows 65 & 66). Cdc48 (mammalian homologue p97) forms homo-complexes consisting of 6 subunits arranged in a barrel-like ring structure resembling the 26S proteasome (reviewed by Woodman, 2003). It is involved in a remarkable range of different functions such as membrane fusion, proteolysis and cell cycle control (Fu et al., 2003; Bazirgan and Hampton, 2005; Elsasser and Finley, 2005). The proteolytic activity of Cdc48 requires interaction with additional proteins such as Ufd1 and Npl4, and the ability of Cdc48 to directly bind polyubiquitin lead to the hypothesis that it may target ubiquitylated proteins to the proteasome (Woodman, 2003). Cdc48 is involved in proteolytic release of NFκB from IκB and plays an important role in quality-control by proteasomal degradation of misfolded membrane proteins in the cytosol (Elsasser and Finley, 2005). The activity of Cdc48 related to membrane fusion is thought to be similar like NSF (N-ethylmaleimide-sensitive fusion protein), which breaks cis complexes of v-SNARE and t-SNARE after membrane fusion (Woodman, 2003). In yeast, Cdc48 is required for the cells to pass through G1 and mitosis, and recent investigations indicate that its regulatory function is achieved by Cdc48-mediated proteasomal proteolysis of the cell cycle arrest promoting factor Far1 (Fu et al., 2003). Degradation of Far1 is mediated by ubiquitination via SCF^{Cdc4} E3 ubiquitin ligase containing SKP1 and Cdc53, the yeast homologue of plant cullin1 (Fu et al., 2003). The authors hypothesized that Far1 might inhibit cyclin expression and Cdc28 kinase activity and by this means promotes cell cycle arrest at G1 to S transition.

The cell cycle promoting activity of Cdc48 was somewhat surprising with regard to the strong inhibition of root growth observed upon sylA-treatment (Figure 5.5). Thus, the transcriptional induction of *Cdc48* was interpreted in the context of induction of the whole proteasome machinery and the hypothesized elevated demand for proteolytic activity (chapter 5.3.1). Due to its versatile nature, no concrete conjunction of *Cdc48* transcript

accumulation and other syringolin-related effects such as metabolic change or root growth suppression was identified.

5.3.7.2. DMI1

Transcripts corresponding to *OA_b2E04* accumulated in response to syringolin treatment at 12 hat (Table 4.4, row 58). The deduced sequence of *OA_b2E04* exhibited 83 % identity (of 210 aa) to DMI1 (does not make infections) from *Medicago truncatula. DMI1* was cloned recently by Ané et al. (2004) and genomic investigations revealed that only one conserved ortholog is present in the genome of rice and *Arabidopsis*. Based on sequence similarities, the deduced protein is hypothesized to function like a receptor-complex forming transmembrane protein with possible ion channeling capacity (Ané et al., 2004). Together with the receptor-like protein kinase DMI2 and the calcium-dependent protein kinase DMI3, DMI1 is involved in the perception of Nod factors by the plant which is required for the initiation of symbiotic rhizobial interactions in leguminous plants (reviewed in Endre et al., 2002; Marx, 2004; Mitra et al., 2004). In addition, the three genes are also mediating symbiotic interactions of plants and micorrhizal fungi (Mitra et al., 2004). As described by J. Marx (2004), perception of Nod factors by leguminous plants causes rapid calcium influx in root hair cells which is followed by a second phase of oscillating calcium concentrations, the so-called 'calcium spiking'. According to the present model, DMI1 might allow calcium influx or movement whereas DMI3 perceives and transduces the Ca^{2+} signal (Marx, 2004). Interestingly, calcium oscillation is also observed before stomatal closure in response to the plant hormone ABA (Staxén et al., 1999).

5.3.7.3. Putative glutamate receptor-like protein

OA_a2B04 (accession #AJ888614) exhibited high similarity (> 90% nt identity) to two barley ESTs (accession #BQ659530 and #BQ460935) upon blastn analysis. The two ESTs gave rise to a contig of 805 bp and the 376 bp wheat DNA fragment was overlapping at the central region (a sequence alignment is shown on p.218). Blastx analysis of the consensus sequence revealed 56 % sequence similarity (of 189 aa) to a rice putative Avr9/Cf-9 rapidly elicited (ACRE) protein 141 (accession #Q69NA4) and 41 % similarity (of 183 aa) to the corresponding original protein from tomato (ACRE141; accession #Q84QE2). Transcript profiling of flagellin-induced nonhost resistance and Avr9-induced race specific resistance recently demonstrated considerable overlaps between the two types of resistance (Navarro

et al., 2004). Yet, the *Arabidopsis* ACRE141 homolog (accession #AY220478) was not found to be regulated in response to flagellin (Navarro et al., 2004).

Blastx analysis of the consensus sequence revealed that *OA_a2B04* belongs to ligand-gated ion channels and similarly exhibits similarity to 7-transmembrane glutamate receptor-like proteins (41 % similarity of 186 aa to AtGLR2.8, one of 20 glutamate receptor-like proteins from *Arabidopsis*). Evolutionary, plant glutamate receptors were suggested to provide a link between animal ionotropic and G-protein-coupled (metabotropic) glutamate receptors (proposed by Turano et al., 2001). Metabotropic glutamate receptors are involved in protection from cell death in neuronal and vascular tissues which includes protein kinase A, B and C-related deactivation of pro-apoptotic BAD (BCL2-antagonist of cell death), caspase inhibition, poly(ADP-ribose) polymerase (PARP) stabilization and prevented cytochrome c release from mitochondria (reviewed by Lin et al., 2002). At present, the capacity of glutamate guiding and ligand interaction of plant homologues is being investigated, yet they are often found to behave like constitutive non-selective cation channels possibly involved in Ca^{2+} signaling and inter-/intracellular trafficking of NH_4^+ (reviewed by Davenport, 2002). Interestingly, heterologous expression of AtGLR2.8 in oocytes is not found to induce currents indicative for alternative activities in this case (communicated by Davenport, 2002).

It might be noteworthy that a recently identified plant regulator of G protein signaling (AtRGS1) also has similarity to metabotropic glutamate receptors (Chen et al., 2003). RGS proteins are important components of heterotrimeric G protein signaling and mediate rapid $G\alpha$ deactivation by accelerating $G\alpha$ GTP hydrolysis (De Vries et al., 2000).

5.3.7.4. Receptor kinases

Reminiscent of the animal innate immune system, plants are able to sense PAMPs by LRR domain-containing plasma membrane-bound receptor kinases (RLKs) like for example the flagellin sensing FLS2 (reviewed by Nürnberger et al., 2004). Treatment of *Arabidopsis* with the flg22 recognition element of flagellin causes transcriptional induction of a large number of proteins and more than half of them is involved in signal perception and transduction including more than 100 receptor-like kinases (Zipfel et al., 2004). In contrast, only one cDNA fragment which exhibited moderate similarity to receptor-like kinases was isolated in the present study. *OA_b1B08* exhibited clear transcriptional induction in response to sylA treatment at 12 hat and 24 hat (Table 4.4, row 63). Blast analysis revealed high similarity (89% of 205 nt) with a wheat EST (accession #BE517637) which is part of a UniGene EST contig (accession #Ta.36614). Blast analysis of the corresponding consensus

sequence similarly revealed moderate similarity to light repressible receptor kinases and mechano-sensitive ion channel domain-containing proteins, but no further specification was achieved.

RLKs not only are involved in recognition of non-self in plant immunity but also mediate perception of plant hormones (Boller, 2005). Recently, Osakabe et al. (2005) identified an *Arabidopsis* LRR-type RLK (RLK1) which appears to be required for early ABA perception. One of the best characterized LRR-RLKs is the brassinosteroid (BR) receptor, BR-insensitive1 (BRI1, reviewed by Boller, 2005). SSH resulted in the isolation of a cDNA fragment (*OA_a1E09*) which was found to be part of an EST UniGene cluster (accession #Ta.8488). Interestingly, blastx analysis of the corresponding consensus sequence revealed the presence of a 50 aa-spanning domain found in the rice BRI1-interacting protein 130 (BIP130). BIP130 is phosphorylated by BRI1 and strongly binds to the BRI1-kinase domain (BRI1-KD) but at present, nothing is known about its molecular function (Hirabayashi et al., 2004). Still, the correlation of *OA_a1E09* and BIP130 might indicate that the encoded protein could be involved in RLK signaling. *OA_a1E09* exhibited clear transcriptional induction upon analysis by reverse northern dot blot hybridization (Table 4.2, p.36). However, the t/c ratio upon microarray analysis was 1.49 at 12 hat in the absence of *Bgt* and although differential expression was statistically significant as judged by one sample T-test, the fragment was not included in Table 4.4 because of weak differential expression (not shown).

5.3.7.5. R-genes

As mentioned earlier, SSH yielded three cDNA fragments with homology to R-genes or associated elements. By microarray analysis, only one of them was confirmed to be transcriptionally upregulated by sylA treatment of wheat. Thus, with regard to the transcriptional induction of a large number of nearly 50 different R-genes in the nonhost resistance induced by flg22 in *Arabidopsis*, the situation was found to resemble the one observed for RLKs described above.

OA_a1E08 transcripts accumulated at 12 and 24 hat (Table 4.4, row 59). It might be of interest that *OA_a1E08* was found to be one of only five fragments which exhibited t/c ratios which were more than 1.3-fold higher in the infected case after sylA treatment as compared to the uninfected situation (Table 4.7, row: 55). *OA_a1E08* showed 87 % (of 153 bp) and 86 % (of 134 bp) DNA sequence identity at the 5'-end to two wheat ESTs (accessions #CA654986 and #CA698654) and 85 % (of 64 bp) sequence identity at the 3'-end to another wheat EST (accession #BE405507) upon blastn comparison. An alignment of the corresponding sequences is shown in the Appendix (p.215). Blastx comparisons

revealed 65 % sequence identity (in 127 aa) with the deduced protein sequence of a 3.3 kb barley cDNA sequence (accession #AJ507096) corresponding to the NBS-LRR disease resistance protein homologue of the barley rga *S-9204* gene, an R-protein lacking a coiled coil (CC) domain (Madsen et al., 2003). S-9204 was found to exhibit closest homology to the disease resistance protein RPP8 (resistance to *Peronospora parasitica*) from *Arabidopsis*. Intriguingly, the latter was found to act independently from RAR1 and SGT1 (Figure 3.8 & Tör et al., 2003).

5.4. Conclusion

Powdery mildew is able to suppress host defense which results in increased susceptibility of infected cells to subsequent infection with compatible but also incompatible pathogens (Kunoh et al., 1985; Lyngkjaer and Carver, 1999). Wäspi et al. (2001) discussed two probable modes of HR induction by sylA. In one scenario, syringolin acts as an elicitor re-inducing plant defense by contributing to the elicitor activity already present by fungal elicitors. This reflects an additive effect resulting in a breakdown of pathogen-related defense and cell death suppression. Alternatively, syringolin may target the pathogen and impair the fungal host defense suppression mechanism (Wäspi et al., 2001). The present data indicate that syringolin predominantly acts on the host plant. Syringolin appears to strongly affect plant metabolism as indicated by the induction of numerous genes. Together with the absence of powdery mildew and epidermis specific transcriptional upregulation of individual genes, this supports earlier theories of additive effects of syringolin and fungal elicitor activity.

The bacterial pathogen *Pseudomonas syringae* pv. *syringae* causes canker in many economically important stone and pome fruit trees (Agrios, 1997). *P. syringae* pathovars *syringae* and *atrofaciens,* which only can be distinguished on the basis of disease symptoms, are also causal agents of leaf blight and glume rot, which is favored under long periods of wet weather, and can severely reduce grain quality of wheat and barley (Duveiller et al., 1997). Besides, certain species of *Pseudomonas* were found to seasonally exhibit growth inhibitory effects in roots of winter wheat (Elliott and Lynch, 1985). As described by Thaler et al. (2004), *P. syringae* is a hemibiotrophic pathogen which can switch from biotrophic to necrogenic lifestyle. The bacteria are widespread on leaf surfaces during sustained epiphytic growth, which, under appropriate weather conditions is rapidly changed to a pathogenic life style upon which it can multiply to high numbers in the apoplast of host plants (Duveiller et al., 1997). Pathogenicity of *Pseudomonas* is dependent on functional *hrp* gene products (hypersensitive response and pathogenicity) which encode a type III

secretion system but eventually are recognized by nonhost plants resulting in the induction of defense-associated HR (Alfano and Collmer, 1996). The Hrp system secrets proteins which are thought to be required for pathogenicity including HR-inducing harpins and numerous avirulence proteins (Avr), the latter eliciting race-specific resistance in the presence of cognate plant R-proteins (Alfano and Collmer, 1996).

In addition, *Pseudomonas* secrete a number of broad-range phytotoxins which are generally required for virulence and like syringolin are nonribosomally synthesized polypeptides (reviewed by Bender et al., 1999). The finding that like the synthesis of the phytotoxin syringomycin or syringopeptin, syringolin production is under the control of the *lemA*/*gacA* global signal transduction system lead to the speculation that syringolin may contribute to virulence of *P. syringae* pv. *syringae* (Wäspi et al., 1998a). Lately, Lu et al. (2005) have found that *sylD,* which encodes two peptide synthetase modules required for syringolin synthesis (Amrein et al., 2004), is under the control of SalA, which controls the expression of genes essential for bacterial pathogenesis and is a member of the *lemA*/*gacA* regulon. Interestingly, transcription of *sylE* encoding a putative syringolin exporter, and also of *syrE* encoding syringomycin synthetase, was found to be induced during epiphytic growth of *P. syringae* pv. *syringae* on bean (Marco et al., 2005). Since environmental conditions rapidly change in the phyllosphere, the authors hypothesized that the production of certain 'early' virulence factors might also be essential during epiphytic growth allowing the bacteria to eventually get in closer contact with the plant cells.

Intriguingly, syringomycin and syringopeptin exhibit striking similarity in their phytotoxic activity (Bender et al., 1999). They both induce stomatal closure with an efficiency resembling the effect of exogenous ABA application, probably mediated by their capability of forming ion conductive pores in lipid bilayers (Di Giorgio et al., 1996).

It is in this context that the results obtained in the present work may tempt to speculate that instead of acting as avirulence factor, syringolin may act like a virulence factor in wheat repressing host defense by inducing an anoxia-like metabolism. Repression of defense may likely be a consequence of far reaching inhibition of biosynthetic processes, which occurs during low oxygen metabolism (Geigenberger, 2003). Unfortunately, no information is presently available on the capacity of plant cells to launch expression of PR proteins under anoxic conditions and the only argument comes from the observation of increased susceptibility against bacterial soft rot under low oxygen conditions (Butler et al., 1990). The mechanism by which syringolin may induce the anoxia-like metabolism is purely speculative. It is presently not known whether syringolin like syringomycin induces stomatal closure or whether it also forms conductive pores in lipid membranes. Membrane integration might at least explain the strong unspecific binding of radioactively-labeled

syringolin to cellular extracts of rice protoplasts which yet prevented identification of putative receptors in the nonhost plant (U. Wäspi, personal communication). Alternatively, the numerous mitochondrial enzymes induced by syringolin indicate that it might predominantly act on mitochondria where intriguingly also the O_2-sensing system is thought to be located (Geigenberger, 2003).

The fact that syringolin does not induce cell death at high concentrations demonstrates that its activity clearly differs from the one of syringomycin or syringopeptin. The present data even indicate pro-survival activity since many proteins like for example AOX, Hsps or prohibitin which show transcriptional upregulation are reported to protect from cellular damage. This would then make syringolin particularly meaningful during early virulence which appears to be relevant also during epiphytic growth of the bacteria.

This raises the question of why application of sylA on powdery mildew-infected wheat blocks fungal spread and finally induces infection specific HR? A plausible explanation would be that fungal growth is primarily paused due to nutrient limitation. The dramatic changes in plant metabolism observed after sylA treatment might have disastrous effects for a biotrophic pathogen like *Blumeria* and nutrient transfer which is thought to occur by uptake of glucose (Sutton et al., 1999) could be effectively disturbed. However, the lack of HR observed when the fungus is simply killed by application of a fungicide such as cyprodinil (Wäspi et al., 2001) indicates that fungal death caused by nutrient starvation is probably unlikely to induce HR of infected cells. With respect to this, it might be of importance that re-aeration is a critical phase which causes severe oxidative stress and markedly decreases viability of plants which had been adapted to anoxic or hypoxic conditions (Biemelt et al., 1998). In accordance with this, a re-induction of PR gene expression is observed at 48 hat in *Bgt*-infected wheat treated with syringolin (Wäspi et al., 2001). Likewise, microscopical examinations of sylA-treated infected wheat leaves revealed that infection-specific autofluorescence can be observed at 72 hat at the earliest and is fully pronounced after 96 hat (not shown). These findings prompted us to carry out an additional microarray experiment, thereby investigating transcriptional changes in infected and uninfected wheat leaves occurring at 48 h after sylA treatment. The results of a single experiment are presented in (Figure 8.3, p.211 & Table 8.9, p.212).

Re-induction of PR-gene transcription by syringolin treatment as described by Wäspi et al*,* (2001) was confirmed in the case of *WIR2* (row 12) encoding a thaumatin-like protein (accession #X58394), which was also represented by *RB_c085* (row 6)*.* Re-induction was also indicated in the case of other PR-genes not previously tested such as *RB_c079* encoding β-1,3-glucanase or *WCI2* and *RB_c072* encoding a wheat PR-1 protein (Table 8.9). Furthermore, the experiment revealed that a number of sylA-responsive genes (20)

encoding for example VDAC, Hsp23.6 or wheat Pir7b still exhibits transcriptional upregulation even at 2 days after sylA treatment (rows 19 - 39). However, only two syringolin-responsive genes also exhibited re-induction reflected by higher t/c ratios in the presence of *Bgt* (rows 1 & 2). Intriguingly, this was most pronounced for *OA_a2F04*, the fragment which had previously been identified as a putative HR marker gene during race specific interactions in wheat cv. MA (chapt. 4.3.3, p.110). The second fragment (*OA_a1B01*) encoded mitochondrial sHsp23.5.

Thus, the observation of re-induction of a putative HR marker gene (*OA_a2F04*) at 48 hat supports findings obtained by microscopical examination and affirms the hypothesis that syringolin-induced HR only occurs at a later time point. The fact that a second gene which encodes a mitochondrial chaperonin was also re-induced indicates that cells are indeed stressed at the mitochondria at around 48 hat.

As mentioned above, transcriptional induction of numerous genes encoding protective enzymes may lead to the speculation that syringolin mediates cell death protection in a first phase after treatment. Indeed, at the earliest time point investigated, transcripts of *OA_a2F04* were found to accumulate but only in the presence of *Bgt* after sylA treatment at 2 hat (Figure 4.27 & Table 4.9, p.97). The same was true for the PR gene *WIR3* encoding a peroxidase, which was shown to efficiently protect from powdery mildew infection upon overexpression in the epidermis (Schweizer et al., 1999b; Altpeter et al., 2005). No accumulation of *WIR3* transcripts was observed at the later time points investigated in ceA and ceB. Furthermore, transcription of *OA_a2F04* exhibited the normal pattern of syringolin-responsive genes in ceA and ceB since t/c ratios were lower in the infected samples and no epidermis specificity was indicated (Table 4.4, row 107 & Table 4.7, row 93). Thus, the early *Bgt* specific induction of an important PR gene (*WIR3*) and a putative HR marker gene (*OA_a2F04*) may be indicative for early initiation of plant defense which subsequently was suppressed as obvious from investigations in the later time points (ceA and ceB). Interestingly, the two sHsps (*OA_a1B01* and *OA_a1H02*) which also were shown to rapidly accumulate during harpin-induced HR were also found to accumulate early after syringolin treatment (Table 4.9, rows 1 & 4).

Ironically, despite the fact that HR may not occur during the time points of SSH screening, the present study still resulted in the identification of a putative HR marker gene (*OA_a2F04*, accession #AJ888625). In the interaction study of wheat and different strains of powdery mildew (chapt 4.3.3), the expression pattern of *OA_a2F04* coincided with the one of *OA_a1H06* (Figure 4.36, p.113) Indeed, DNA sequence comparison revealed 58 % identity (of 149 bp) in the central part of *OA_a2F04* between position 216 and 354 (Figure 5.8).

Figure 5.8: Alignment of *OA_a2F04* and *OA_a1H06.* Identical nucleotides conserved are in black boxes and similar nucleotides (purin or pyrimidin) are in gray boxes. Gaps introduced to improve the alignment are indicated by dots. Multiple sequence alignment was done using PILEUP program (GCG).

Blast analysis of the *OA_a2F04* DNA sequence turned out to be difficult. Upon blastn comparisons, the DNA fragment *OA_a2F04* was found to exhibit between 80 and 90 % DNA sequence identity (of 80 to 100 bp) to a heterologous group consisting of more than 20 wheat and barley ESTs. Pileup revealed the presence of several subgroups and one representative EST each was aligned together with *OA_a2F04* (Appendix, p.217). Highest homology with 99 % sequence identity (of 471 bp) was found to a wheat mRNA (accession #CK215536) cloned in the context of functional genomics of abiotic stress. A barley homologue (accession #CD055978) was found to be transiently induced at 12 hai with *Bgh* in a Mlo/mlo independent manner (Zierold et al., 2005, suppl. data).

The longest open reading frame (orf) only encompassed 222 bp (73 aa) indicating that *OA_a2F04* corresponded to untranslated DNA sequence. The small orf encoded two common motifs (KEGKeKKRS and PFHSRPGL), the former also being found in a human

arginine/serine-rich splicing factor or an *Arabidopsis* BSD domain containing protein (accession #NP_569021). BSD domains were recently discovered to occur in basal transcription factors, synapse-associated proteins and proteins carrying Ubox domains involved in ubiquitination (Doerks et al., 2002). It was also considered that *OA_a2F04* might represent uncoding sequence as found in the long terminal repeat of LTR-retrotransposons. Retrotransposons were found to be activated and transcribed upon various stress situations such as wounding or pathogen attack (Wessler, 1996; Grandbastien, 1998; Sugimoto et al., 2000; Melayah et al., 2001) and the phenomenon was hypothesized to contribute to genetic polymorphism under selective pressure (Vicient et al., 1999). Yet, blast analysis only indicated low homology to retrotransposons (T. Wicker, personal communication).

Due to the fact that plant material investigated by microarray analysis contained infected as well as uninfected cells, it may as well be speculated that a putative function of *OA_a2F04* in HR may be either pro- as well as anti-apoptotic, since local HR may also trigger a cell death protective response in nearby surrounding cells. Likewise, transcript accumulation of the anti-apoptotic BI-1 in barley at 24 - 48 hai is pronounced in *Bgh*-infected lines undergoing HR (Hückelhoven et al., 2001). BI-1 is a suppressor of cell death which can functionally substitute cell death suppressor Mlo (reviewed by Watanabe and Lam, 2004).

To sum up, the present work indicates that syringolin which elicits nonhost resistance in rice (Wäspi et al., 1998a) is not recognized by the plant defense machinery of wheat where it exhibits virulence activity. It is speculated that syringolin suppresses host defense by an elaborate mechanism which involves a switch to a metabolism normally observed under anoxic conditions. This also implies that the syringolin-induced HR occurring in powdery mildew-infected wheat rather is a side-effect which may be related to metabolic changes induced by syringolin. The hypothesis that fungal growth inhibition primarily occurs due to nutrient starvation also would explain the fact that syringolin exhibits strong curative activity whereas protection by prior application is less effective (Wäspi et al., 2001). Thus, it is interesting that also nonribosomally synthesized peptides like syringolin, which per definition are neither true PAMPs nor typical virulence factors, may induce nonhost resistance in inappropriate host species but similarly exhibit virulence activity which may involve suppression of host defense and HR. Likewise, Cui et al. (2005) have recently shown that infection of *Arabidopsis* by virulent *P. syringae* causes systemic induced susceptibility (SIS) towards secondary infection. They found that the phenomenon is caused by coronatine which structurally mimics the plant phytohormone jasmonate (JA) and together with syringomycin and syringopeptin was classified as bacterial phytotoxin (Bender

et al., 1999). Cell death suppression activity (CDS) including supression of Bax-induced PCD is also found to mediate suppression of nonhost resistance and investigations in the case of numerous bacterial avirulence factors like AvrPtoB indicate that their perception by plant resistance proteins and additional factors can result in both virulence or defense-related HR, respectively (Abramovitch et al., 2003; Jamir et al., 2004; Kang et al., 2004; Li et al., 2005b; reviewed by Nomura et al., 2005). In a first approach, a model explaining the different reactions has been proposed by Abramovitch and Martin (2005).

5.5. Future prospects

The present work provided novel and unexpected insights into the molecular events accompanying the plant response to syringolin, a small peptide synthesized by *P. syringae* pv. *syringae*. The results lead to the formulation of an alternative hypothesis describing the complex reaction of powdery mildew-infected wheat upon treatment with syringolin. Thus, it will be of major importance to test whether syringolin indeed suppresses innate resistance in wheat. Although powdery mildew due to its biotrophy might be generally unsuitable for this purpose, it would still be interesting to see if transcriptional induction of PR proteins is reduced when syringolin is applied before powdery mildew infection. Of course it has to be tested if syringolin is required for pathogenicity of *P. syringae*. Unfortunately, the three strains which are known to synthesize syringolin are not pathogenic on wheat and no suitable test system has been found thus far (R. Dudler, personal communication). Nevertheless, microarray comparison of transcription in wheat infiltrated with a bacterial suspension of wild type *P. syringae* pv. *syringae* strain B301D-R and a knock-out mutant deficient for syringolin synthesis indicated that some of the PR genes including *WIR2* and *WIR3* indeed exhibit stronger transcriptional induction in the knock out mutant (preliminary results). The syringolin-producing *P. syringae* pv. *syringae* strain B301D-R isolated from pear and strain B728a isolated from bean were both reported to be moderately pathogenic when injected into 10-week-old peach seedlings (Little et al., 1998). However, with respect to the suspicion that syringolin might particularly be required during early virulence, it is highly recommended to carry out spray inoculation as described in Duveiller et al, (1997). Therefore it will first be necessary to test known wheat or barley pathogenic strains for their ability to produce syringolin.

Suppression subtractive hybridization and subsequent microarray analysis resulted in the identification of 124 genes responsive to syringolin treatment, 30 of which were tested for their participation in HR via inhibition of transcript accumulation by transiently induced RNAi. Yet, microarray analysis finally indicated that this approach likely would not be successful since none of the syringolin-responsive genes showed HR-specific elevated transcript accumulation. Yet, two genes which both exhibited elevated transcript accumulation in the interaction of wheat cv. Michigan Amber with *BgtAvr2* were identified to be putative marker genes for the hypersensitive response in the race specific interaction. At first it will be desirable to clone full length cDNAs in order to get additional information about putative biological functions of the proteins encoded by *OA_a2F04* and *OA_a1H06.* Next it will be necessary to test the effect of transient overexpression and RNAi by expression in an appropriate system such as wheat cv. Michigan Amber, which was established in the time course of the present work. In the case of transiently induced RNAi it has to be considered that many homologous transcripts appear to be present in wheat and tests may alternatively have to be carried out in the diploid barley *Hordeum vulgare*.

Transcript profiling using the Affymetrix ATH1 genome array in syringolin-treated *Arabidopsis* which had been infected with the powdery mildew fungus *Erysiphe cichoracearum* largely confirmed results obtained in the present work (K. Michel, personal communication) which opens up the possibility to carry out experiments in the model plant *Arabidopsis thaliana*. A reverse genetical approach with mutagenized plants expressing a herbicide resistance gene under the control of a syringolin-inducible promoter has already been initiated in order to identify regulators of the plant response to syringolin (S. Rau, personal communication).

6. Materials and Methods

If not indicated otherwise, chemicals were obtained from Fluka (Buchs, Switzerland) and DNA manipulations were conducted as descirbed in Maniatis et al. (1982). Enzymes were obtained from Roche Applied Science (Penzberg, Germany).

6.1. Plant and fungal growth conditions and treatments

6.1.1. Plant material

Most experiments were carried out in the susceptible *Triticum aestivum* cv. Fidel. Investigations of nonhost and race-specific resistance interactions (chapt. 4.3) were carried out in *Triticum aestivum* cv. Michigan Amber (MA), the donor line of the *Pm3f* allele (N. Yahiaoui, personal communication) and the susceptible *Triticum aestivum* cv. Kanzler.

6.1.2. Fungal strains

Swiss field isolates of powdery mildew were obtained from P. Streckeisen, (FAL Reckenholz, Zürich, Switzerland). If not indicated otherwise, experiments were carried out with the virulent *Blumeria graminis* f.sp. *tritici* isolate 92315, referred to as *Bgt* or *BgtVir*. Isolates 96244 (*BgtAvr1*), 98229 (*BgtAvr2*) and 96236 (*BgtAvr3*) which all cause a resistance response in wheat carrying the *Pm3f* allele (N. Yahiaoui, personal communication) were used for investigations of race-specific resistance (chapt. 4.3). Investigations of nonhost resistance were carried out with a Swiss field isolate of barley powdery mildew *Blumeria graminis* f.sp. *hordei* isolate 4.8 (referred to as *Bgh*).

6.1.3. Inoculation and syringolin treatment

One hundred plants were grown in pots (∅ 12 cm) on standard soil (Einheitserde, Buchenberg, Germany) in a growth chamber (16 h light period at 22°C, 8 h dark period at 18°C; 60 % relative humidity).

Powdery mildew was cultivated by weekly inoculating 7-day-old wheat or barley seedlings. Inoculated plants were kept in a growth chamber Type 3755 (Brouwer, Luzern, Switzerland) with 16 h light period at 22°C and 60 % relative humidity.

Inoculation of wheat plants with powdery mildew was performed with 7-day-old-seedlings at a spore density of 100-150 conidia / mm^2. Plants were inoculated in inoculation chambers by brushing plants infected one week earlier over the test plants.

Syringolin treatment of infected plants was carried out 48 hours after inoculation. Pots were placed on a rotating platform and sprayed with 10 ml of distilled water containing 100 µM syringolin A and 0.05 % (v/v) Tween 20 or a control solution. Cyprodinil (Novartis AG, Basel, Switzerland) was kindly provided by Dr. M. Oostendorp (Novartis Crop Protection AG, Basel, Switzerland). The substance was dissolved in an 8:2 (v/v) water/acetone mixture at a concentration of 888 µM and sprayed as described above. Control plants were sprayed with the solvent only.

Plant material was collected from different tissues at various time points after treatment. For differential screening, whole seedlings were harvested. For microarray experiments, only primary leaves were harvested. In the case of ceB (chapt. 4.2.4.1), the abaxial epidermis was stripped off the leaf using a scalpel and a pair of tweezers. The separated plant tissue was immediately frozen in liquid nitrogen.

Root growth inhibition experiments were carried out in sterilized 50 ml glass tubes half filled with half strength Muarashige and Skoog (MS) medium containing 2 % (w/v) sucrose and 0.25 % (w/v) phytagar (Gibco BGL, Paisley, UK) with or without 2 µM syringolin A. Seeds of wheat cv. Fidel were surface sterilized by immersion for 5 min in water containing 70 % ethanol followed by 15 min in water containing 1 % (v/v) sodium hypochlorite. Seeds were rinsed 3-times with autoclaved water, stratified 4 days at +4°C in autoclaved water and placed onto the medium under sterile conditions. The glass tubes were capped and plant growth was monitored in a growth chamber (16 h light period at 22°C, 8 h dark period at 18°C; 60 % relative humidity).

Microscopical investigations were carried out with wheat leaf segments. The central 4 cm of primary leaves was placed on petri dishes containing 0.5 % (w/v) water-phytagar (Gibco BGL, Paisley, UK) and 20 mg L^{-1} benzimidazole senescence inhibitor. Inoculation with fungal conidia was done by blowing spores from heavily infected wheat leaves into the inoculation chambers until spore density was at 10 spores / mm^2. Incubation was done in a growth chamber (16 h light period at 22°C, 8 h dark period at 18°C; 85-90 % relative humidity).

6.2. Syringolin A isolation

Syringolin A was isolated from still cultures of *Pseudomonas syringae* pv. *syringae* strain B301D-R as described (Wäspi et al., 1999). Three-step purification included partition chromatography on an Amberlite XAD 16 column (2.6 x 40 cm; Rohm and Haas, Philadelphia (PA), USA), reversed phase HPLC on a Nucleosil 100 7 C_{18} 250/20 column (Macherey-Nagel, Duren, Germany) and FPLC on a Superdex 30 16/60 gel filtration column (Pharmacia, Uppsala, Sweden, for details, see Wäspi et al., 2001).

6.3. Microscopy

To monitor autofluorescence of plant cells, wheat leaves were destained by overnight immersion at 37°C in either chloral hydrate (2.5 g/ml) or a 1:2 (v/v) dilution of a lactophenol stock solution (phenol : lactic acid : glycerol : water = 1:1:2:1) with ethanol. For the next two days, leaves were cleared 3-times with sterile water and kept at +10°C. If desired, fungal structures were stained with Coomassie blue (0.3 % (w/v) in a 1:1 mixture of water and methanol). Leaf segments were mounted onto microscopic slides in 40 % (v/v) glycerol. Microscopic investigation with the Axioplan microscope (Carl Zeiss AG, Oberkochen, Germany) was done by bright-field or blue light incident fluorescence microscopy (excitation filter 450-490 nm; bypass filter 515-565 nm). Images were captured with the Magna Fire 2.0 digital camera (Optronics, Goleta (CA), USA) using auto exposure settings.

6.4. RNA extraction and mRNA isolation

RNA was isolated from collected plant material that was ground to a fine powder in liquid nitrogen using pestle and mortar. The material was suspended in Trizol extraction buffer containing phenol (Invitrogen BV, Groningen, The Netherlands) at a ratio of 1:10 (w/v), shaken for 3 min and pooled on ice. 0.25 ml of chloroform per 1 ml of Trizol was added and after vigorous shaking, samples were centrifuged at 3000 x g for 15 min and the supernatant was transferred to a fresh RNase-free tube. Chloroform extraction was repeated and the RNA was subsequently precipitated by addition of 1 Vol of isopropyl alcohol. After incubation for 15 min at room temperature, the RNA was collected by centrifugation at 12'000 x g for 30 min at +4°C. The pellet was washed with 80 % (v/v) ethanol by centrifugation at 12'000 x g for 15 min at +4°C. The supernatant was discarded

and the RNA was dissolved in proteinase K-treated autoclaved TE buffer (Maniatis et al., 1982).

Poly(A)$^+$ RNA was isolated from 200 to 2000 µg of total RNA. In the case of SSH screening, oligo(dT) OLIGOTEX (Qiagen AG, Hombrechtikon, Switzerland) was used. In the case of microarray experiments, poly(A)$^+$ RNA was isolated with the mTRAP kit (Active Motif, Rixensart, Belgium). Purifications were performed according to the protocols of the manufacturer.

Total RNA used for linear amplification (Van Gelder et al., 1990) was first purified on RNeasy spin-columns (Qiagen AG, Hombrechtikon, Switzerland) according to the protocols of the manufacturer.

RNA integrity was checked on a bioanalyzer (Agilent Technologies, Inc., Palo Alto (CA), USA) and on agarose gels containing formaldehyde (Maniatis et al., 1982).

6.5. cDNA subtraction and differential screening

6.5.1. cDNA subtraction

cDNA subtraction and differential screening was carried out according to Diatchenko et al. (1999) by using the PCR-Select™ cDNA Subtraction kit (Clontech Laboratories Inc., Mountain View (CA), USA). Total RNA of the 2 hat and 6 hat time points (α-subtraction) and total RNA of the 12 hat and 24 hat time points (β-subtraction) was combined at a ratio of 1:1 (w/w) prior to poly(A)$^+$ RNA isolation. To minimize variation, experiments were repeated twice and total RNA was combined at a ratio of 1:1 (w/w). Forward and reverse subtractions were carried out with 2 µg of poly(A)$^+$ RNA. For cDNA digestion, *Rsa*I restriction endonuclease was obtained from Roche Applied Science (Penzberg, Germany). First and second hybridizations lasting 10 h and 18 h, respectively, were carried out at 68°C. The BD Advantage™ 2 Polymerase Mix (Clontech Laboratories Inc., Mountain View (CA), USA) containing *Taq* DNA polymerase was used for hot start PCR amplification of recombinant cDNA hybrids. The first PCR included 27 rounds of amplification and the second PCR included 10 rounds of amplification. All cDNA inserts obtained by SSH contain the five prime NstPrm1 5'-TCGAGCGGCCGCCCGGGCAGGT and three prime NstPrm2R 5'-AGCGTGGTCGCGGCCGAGGT adaptor sequences which has been used to prime PCR amplification at up to 68°C annealing temperature.

To monitor cDNA digestion, ligation and subtraction efficiency, 3 gene specific primers each for wheat glyceraldehyde-3-phosphate dehydrogenase (accession #AF25127)

and wheat α-tubulin (accession #U76558) suitable for PCR amplifications with annealing temperatures of up to 65° C were designed: w_G3PDH_s 5'-GCTCCCATGTTTGTCTGTGG; w_G3PDH_a 5'-ATGCTGGACCTGTTGTCACC; w_G3PDH_a_RsaI 5'-CTCATTT ACTTGGTGCTGTGC and w_aTubu_s 5'-TGAGGGAGTGCATCTCGATC; w_aTubu_a 5'-CAAGGAATCCCTGGAGACCA; w_aTubu_RsaI **5'-** CCATCAAACCTCAGGGAAGC. *WIR2* transcript abundance (accession #X58394) was monitored with the help of w_WIR2_s2 5'-ACGACATCTCGGTGATCGAC and w_WIR2_a2 5'-GGTGCGACGTATAGAGGCTT. cDNA obtained from wheat cv. Fidel RNA by RT-PCR with M-MuLV RTase (Pharmacia, Uppsala, Sweden) and Taq DNA polymerase (Amersham Biosciences, Uppsala, Sweden) using the two primer combinations (w_G3PDH_s / w_G3PDH_a_RsaI) and (w_aTubu_s / w_aTubu_RsaI) was blunt end-ligated with T4 DNA ligase (Roche Applied Science, Penzberg, Germany) into *EcoR*V-digested pBSK$^+$ (Stratagene, La Jolla; USA) carrying an ampicillin resistance gene and transformed into *E. coli* DH5α according to standard protocols (Maniatis et al., 1982). The two fragments were sequenced using phage M13 standard primers (Maniatis et al., 1982) and sequences were registered at the European Bioinformatics Institute (www.ebi.ac.uk/cgi-bin/expasyfetch; accession #AJ890249 and #AJ890248).

6.5.2. Differential screening

The cDNA pool obtained in the forward subtraction was screened for differentially expressed genes as described by Diatchenko et al. (1999) with the help of the PCR-Select Differential Screening kit (Clontech Laboratories Inc., Mountain View (CA), USA). Secondary PCR products were purified with GFX spin columns (Pharmacia, Uppsala, Sweden), subcloned into pCRII-TOPO (Invitrogen BV, Groningen, The Netherlands) and transformed into *E. coli* TOP10F' following protocols of the TOPO TA cloning kit (Invitrogen BV, Groningen, The Netherlands). Transformed bacteria were plated onto selective LB agar containing ampicillin (100 µg/ml) and clones containing recombinant plasmid DNA were identified by IPTG/X-Gal-dependent blue-white color selection as described (chapt. 4.1.4). PCR amplification of cDNA inserts from liquid cultures in a 96-well format and subsequent transfer to membranes was carried out as described in the Differential Screening protocol. 5 µl of PCR was diluted in 440 µl of 0.2 M NaOH and quadruplicate cDNA dot blots were prepared by blotting 100 µl DNA dilution onto nylon membranes (Hybond-XL, Amersham Biosciences, Uppsala, Sweden) using a MilliBlot-D vacuum blotting manifold (Micropore Corp., Bedford (MA), USA). DNA was cross linked by baking at 80°C. Amplification quality and insert size was estimated by analyzing 5 µl of the PCR reactions on a 2 % (w/v) agarose

gel. ^{32}P-radioactively labeled probes were prepared from 60 ng of DNA corresponding to the forward and reverse-subtracted cDNA pool and from 100 ng of dscDNA corresponding to syringolin-treated and untreated samples according to standard procedures (Maniatis et al., 1982). Probes were equalized for radiation using a TRI-CARB 2900TR liquid scintillation analyzer (Packard Bio Science, Meriden (CT), USA) and hybridized to the dot-blotted membranes for 1 h at 72°C using Express Hyb buffer (Clontech Laboratories Inc., Mountain View (CA), USA). After washing, hybridized membranes were exposed to a Kodak Biomax MS film (Kodak, New Haven, USA) and qualitatively judged for signal intensities as described on page 191.

6.6. DNA handling

6.6.1. Oligonucleotides and primers

All oligonucleotides were obtained from Microsynth AG (Balgach, Switzerland).

6.6.2. DNA isolation, sequencing and sequence analysis

Plasmid DNA was automatically purified (BioRobot 9600, Qiagen AG, Hombrechtikon, Switzerland) with the Wizard SV96 plasmid DNA purification system (Promega Corp., Madison (WI), USA).

The dideoxy termination method (Sanger et al., 1977) was used for sequencing and sequences were determined using an automated sequencer (ABI377, Applied Biosystems, Foster City, U.S.A.). cDNA inserts obtained by SSH were all sequenced with vector-specific primers TOPOforward1 5'-TGCATCAAGCTTGGTACCGAGC and TOPOreverse1 5'-ATTGGGCCCTCTAGATGCATGC using an annealing temperature of 55°C. The sequencing strategy for hairpin loop expression vectors is explained in chapt. 6.8.

SSH-derived sequences were first investigated with the Staden Package Software (Staden, 1996). Sequence quality was assessed by Phred base calling using default parameters (Ewing and Green, 1998; Ewing et al., 1998) and vector / primer sequence detection was done with PREGAP4. Sequences were assembled by Phrap assembly (developed by Phil Green). The second assembly and sequence analysis was done with the Sequencher software (Gene Codes Corp. Ann Arbor, USA) using the parameters described in chapt. 4.1.5 on page 34.

Sequences were compared to DNA databases 'nr', 'dbest' and 'UniGene' and protein databases 'Swiss-Prot' and 'non redundant' using the blast programs blastn, blastx

and tblastx (Altschul et al., 1990) implemented in the Wisconsin Package Version 10.3 (Accelrys Inc., San Diego (CA), USA). Subsequent detailed blast searches were done with the Advanced Blast internet service provided by EMBnet (http://www.ch.embnet.org/).

6.7. Microarray analysis

6.7.1. Probe preparation

SSH microarray probes were amplified by PCR with Taq DNA polymerase (Amersham Biosciences, Uppsala, Sweden) using NstPrm1 and NstPrm2R carrying an amino group at the 5'-hydroxy end (94°C, 2 min, [94°C, 1 min; 60°C, 45 sec; 72°C, 2 min] 35 cycles, 72°C, 2 min). The other probes were either PCR-amplified with amino-modified M13 standard primers (94°C, 2 min, [94°C, 1 min; 55°C, 1 min 30 sec; 72°C, 1 min 30 sec] 35 cycles, 72°C, 2 min) or amino-modified ITEC1_amino 5'-CGCGCCATTGTGTTGGTACC and ITEC2_amino 5'-CATGCATAAGCTTGCTCGAGTC (94°C, 2 min, [94°C, 1 min; 60°C, 45 sec; 72°C, 2 min] 35 cycles, 72°C, 2 min).

For microarray series 5, two 150 µl reactions per probe were carried out and combined whereas one 100 µl reaction was sufficient for series 6 and 7. Five µl of each reaction were analyzed on a 1.5 % agarose gel. The PCR products were purified on Millipore 96 columns (Cat. # MANU03010, Millipore, Volketswil, Switzerland) and 0.5 µl of the clean product was again analyzed on a 1.5 % agarose gel.

6.7.2. Microarray fabrication

Microarray fabrication was performed according to published methods (Schena et al., 1995; Shalon et al., 1996).

Microarray series 5 was printed onto epoxy-coated glass slides (#UAS0005E NoAb BioDiscoveries, Mississauga Ontario, Canada) using a modified GMS 417 arrayer equipped with a robotic printhead carrying 4 pin ring assemblies (Affymetrix, Santa Clara (CA), USA). Purified PCR products were rearranged in 384-well microtiter plates and dissolved in a final volume of 50 µl with average printing concentration of 0.3 µg / µl in 150 mM sodium phosphate printing buffer at pH 8.5. The array was organized in a test design and the whole array was printed twice per slide (dot spacing 325 µm). The arrayer was calibrated according to the protocol of the manufacturer and the probe DNA was deposited by 3 hits per dot. Printing was operated at full capacity using 42 slides at a time. Average printing

duration was 8 min 34 sec per array (12 hours in total). Printed slides were air-dried over night. Shortly before hybridization, DNA was denatured by boiling in distilled water for 2 minutes followed by 2 h of blocking in blocking buffer (pH 8.4) containing 1 mg/ml ethanolamine, 1 mg/ml glycine and 1 mg/ml lysine in a 1:4 (v/v) mixture of Pierce SuperBlock-TRIS (Pierce Biotechnology Inc., Rockford (IL), USA) and 50 mM TBS (Sigma-Aldrich, Buchs (SG), Switzerland).

Fabrication of Microarray series 6 & 7 was carried out as described (Bruggmann et al., 2005) under guidance of P. Reymond following published protocols (Reymond et al., 2000). Microarray series 7 was printed onto QMT Aldehyde slides (#S112025, Quantifoil Micro Tools GmbH, Jena, Germany). using an OmniGrid 100 spotting robot (Genomic Solutions, Ann Arbor, USA) equipped with a printhead harboring 8 printing pins (TeleChem International, Sunnyvale (CA), USA). Purified PCR products were dissolved in final volume of 10 µl 3 x SSC printing buffer containing 1.5 M betaine with average DNA printing concentration of > 0.5 µg / µl. Dot spacing was 270 µm and the array design is illustrated in the Appendix (p. 194). Arrays were printed only once per slide. Printing was operated at full capacity using 100 slides at a time. Average printing duration was 4 min 20 sec per array (7 hours in total). Average temperature was 25°C and relative humidity was adjusted to 55 % rel. hum. Printed slides were kept at room temperature for 3 days to increase binding efficiency. DNA was covalently linked to the surface by baking for 1 h at 60°C. After denaturing by boiling in distilled water for 2 min, slides were all blocked for 5 min in blocking solution containing 66 mM sodium tetrahydridoborate in a 3:1 mixture of PBS and ethanol.

All slides were examined for missing (unprinted) spots after printing and the information was used to flag individual spots in downstream data analysis.

6.7.3. Microarray target preparation and hybridization

Target labeling and hybridization was carried out as described (Bruggmann et al., 2005) except that 2 µg of total RNA was used as starting material for the amplification with the MessageAmp aRNA-Kit (Ambion, Cambridgeshire, UK). In vitro transcription was carried out for 15 h and the primer mix containing 21-mer oligo-dT was used for all indirect labeling. Slides were scanned twice at two characteristic wavelength with the G2505B microarray scanner (Agilent Technologies Inc., Palo Alto (CA), USA) at 100 % laser power and 100 % photo multiplier gain setting at a resolution of 10 µm/pixel. Fluorescence signal strength was acquired with the ImaGene 4.2 software (BioDiscovery Inc, El Segundo (CA), USA) using fixed cycle segmentation with the following cut off settings: Signal low 0.1; signal high 0.95; background buffer low 0; background buffer high 0.8 and acquisition settings: Background

buffer 4 pxls; background width 20 pxls. Individual Net spot intensities were calculated by subtracting the medium fluorescence signal obtained from the background area off the average fluorescence signal obtained in the spot area. t/c ratios were calculated by dividing net spot intensities derived from the test hybridization by net spot intensities derived from the control hybridization.

6.7.4. Data normalization

Calculations with the Microsoft Excel 2002 software (Microsoft Corp., Redmond (WA), USA) for data normalization were done on a logarithmic scale. Data normalization was permanently surveilled on MA-plots (Dudoit et al., 2002) using the ORIGIN 7.0 software (OriginLab Corp., Northhampton (MA), USA). Standard data normalization which included three steps is explained below. Differentially expressed genes were identified by one-sample t-test statistics (Dudoit et al., 2002) using the TIGR MIDAS V2.20 software (Saeed et al., 2003). Cluster analysis was carried out with the TIGR MeV V3.1 software (Saeed et al., 2003).

1. Signal intensities of in-slide replicated probes were integrated by calculating the average logged signal intensity of unflagged replicates (illustrated in Figure 4.11, p. 49).
2. Centering of log(ratios) around zero was achieved by iterative log(ratio) mean centering (ILMC) as implemented in TIGR MIDAS V2.20 software (Saeed et al., 2003) using a mean centering data range setting of ± 1.0 standard deviation (Figure 4.11, p. 49).
3. High and low signal intensity cut off values were applied (Figure 4.12, p. 50). The upper limit (HiCut) was set to 55'000 units whereas the lower limit (LoCut) was set to twice the median of net signal intensities obtained for empty water control spots. If required, cut off limits were adjusted when indicated by MA-plot investigation. Signal intensities of spots lower that LoCut or higher than HiCut were set to the respective value.

Option 1:

If required, data were leveled by between-slide standard deviation regularization (TIGR MIDAS V2.20 software; Saeed et al., 2003) in order to balance for technical and biological variations (Yang et al., 2002b).

Option 2:

Exceptionally, log(ratios) were centered around zero by global locally weighted regression (Lowess) normalization (Quackenbush, 2002) using default smooth parameter settings of 33% (TIGR MIDAS V2.20 software Saeed et al., 2003). Option 2 was used instead of step 2 of standard normalization. The strategy was only applied in the case of investigations of *Bgt*-background induction (chapt. 4.2.6, p.90) and investigations at 2 hat (chapt. 4.2.7, p.95).

6.7.5. Epidermis specificity

The epidermis specificity was calculated as described in the Appendix (p.200). Reliability of the data was again evaluated by t-test statistics assuming one-sided distribution. ϵ_s-factors derived from three independent biological repetitions were assessed for reproducibility in logarithmic scale. ϵ_s-factors were considered to be relevant when p-values were < 0.05 and ϵ_s-factors were larger than 2 or smaller than 0.5.

6.8. Transient silencing constructs

pOA_FB hairpin loop expression constructs suitable for transient induction of RNAi were obtained by cloning PCR fragments derived from individual cDNAs in sense and anti-sense orientation into the pJP26 backbone using conventional DNA cloning procedures (Maniatis et al., 1982). pJP26 is based on pGY1 and carries an ampicillin resistance gene and the CaMV 35S promoter and terminator sequence separated by the second intron of a wheat resistance gene analog (accession #AY270159) as well as two multiple cloning sites located at both ends of the intron (Christensen et al., 2004). Cloning was done in two major steps including separate insertion of the anti-sense fragment followed by insertion of the sense fragment. Sense and anti-sense DNA inserts were PCR-amplified with *Taq* DNA polymerase (Amersham Biosciences, Uppsala, Sweden) using gene specific primers which carry appropriate restriction sites at the 5'-ends (95°C, 30 sec, [95°C, 10 sec; 65°C, 30 sec; 72°C, 2 min] 30 cycles, 72°C, 5 min). A list of primers is given in Table 12 (next page). After amplification, PCR fragments were directly digested in the PCR reaction buffer with the appropriate restriction enzymes to create compatible ends for ligation into the precut DNA vector at 16°C with T4 DNA ligase. For directed insertion of the anti-sense insert, pJP26 was digested with *Spe*I and *Pst*I. Digested PCR fragments and DNA vector were run on 1.5 % (w/v) agarose gels and extracted with the QIAquick Gel Extraction Kit (Qiagen AG, Hombrechtikon, Switzerland). After ligation, the intermediate construct was transformed into

E. coli DH5α and harvested from overnight liquid cultures using the NucleoSpin Plus plasmid DNA purification kit (Macherey-Nagel, Duren, Germany).

The same procedure was repeated for the directed insertion of the sense insert at the 5-prime end of the intron, except that the intermediate constructs were digested with *Sma*I and *Xba*I restriction enzymes.

Table 12: Primers for cloning of foldback constructs. Forward and reverse inserts were amplified with different forward primers but identical reverse primers (only 3 primers per construct needed). Primers contain appropriate restriction sites (indicated) used for directed cloning.

construct	insert length	5'-forward insert forward primer	 reverse primer	3'-reverse insert forward primer
OAa1E06_FB	170 bp	**OAa1E06_c** (*Sma* I) 5'AATTAACCCGGGTCGGATACCACTGAGGCTGG	**OAa1E06_b** (*Spe* I) 5'AATTAAACTAGTCCAAAGGAGCAACAATTGCAAC	**OAa1E06_a** *(PstI)* 5'AATTAACTGCAGTCGGATACCACTGAGGCTGG
pOAa1H02_FB	368 bp	**OAa1H02_c** (*Sma* I) 5'AATTAACCCGGGTCAAGGCCGAGATGAAGAATG	**OAa1H02_b** (*Spe* I) 5'AATTAAACTAGTGCCAAACTTGAGGAAACCAAC	**OAa1H02_a** (*Pst* I) 5'AATTAACTGCAGTCAAGGCCGAGATGAAGAATG
pOAa2C11_FB	279 bp	**OAa2C11_c** (*Sma* I) 5'AATTAACCCGGGAGCAGTCACCAAGATTCATCAG	**OAa2C11_b** (*Spe* I) 5'AATTAAACTAGTTTCAAGAACCTCATCGATACGG	**OAa2C11_a** (*Pst* I) 5'AATTAACTGCAGAGCAGTCACCAAGATTCATCAG
pOAa3B03_FB	376 bp	**OAa3B03_c** (*Sma* I) 5'AATTAACCCGGGAACCTTGCCATCATTCTACCTC	**OAa3B03_b** (*Spe* I) 5'AATTAAACTAGTGTAACAAAGCAAGCAATAGCCC	**OAa3B03_a** (*Pst* I) 5'AATTAACTGCAGAACCTTGCCATCATTCTACCTC
pOAa3C11_FB	233 bp	**OAa3C11_c** (*Sma* I) 5'AATTAACCCGGGCAAAACCCTTAGTAACCTCCC	**OAa3C11_b** (*Spe* I) 5'AATTAAACTAGTGAATATGTCTTGCTTTGGATGC	**OAa3C11_a** (*Pst* I) 5'AATTAACTGCAGCAAAACCCTTAGTAACCTCCC
pOAa3F09_FB	385 bp	**OAa3F09_c** (*Sma* I) 5'AATTAACCCGGGTATTGCATTGTGGCACCAGAC	**OAa3F09_b** (*Spe* I) 5'AATTAAACTAGTCTGCTTCTTCAAATGCCTTCC	**OAa3F09_a** (*Pst* I) 5'AATTAACTGCAGTATTGCATTGTGGCACCAGAC
pOAa3G10_FB	145 bp	**OAa3G10_c** (*Sma* I) 5'AATTAACCCGGGACTCCAACGTGTGCTCCTTTC	**OAa3G10_b** (*Spe* I) 5'AATTAAACTAGTGCACAACACGCAGAAGAAGAG	**OAa3G10_a** (*Pst* I) 5'AATTAACTGCAGACTCCAACGTGTGCTCCTTTC
pOAa3H01_FB	306 bp	**OAa3H01_c** (*Sma* I) 5'AATTAACCCGGGGTAAAGCGAGCGACTACTACC	**OAa3H01_b** (*Spe* I) 5'AATTAAACTAGTGATCCTCCAGCCGTTCTTCC	**OAa3H01_a** (*Pst* I) 5'AATTAACTGCAGGTAAAGCGAGCGACTACTACC
pOAb2A02_FB	178 bp	**OAb2A02_c** (*Dra* I) 5'AATTAATTTAAAAGGTGCTATTTACAAAGACCAAG	**OAb2A02_b** (*Spe* I) 5'AATTAAACTAGTGTTGAGAAGGCTGATAAGTCTG	**OAb2A02_a** (*Pst* I) 5'AATTAACTGCAGAGGTGCTATTTACAAAGACCAAG
pOAb2A06_FB	272 bp	**OAb2A06_c** (*Sma* I) 5'AATTAACCCGGGCAAGGCACTCTCAAGCTCCG	**OAb2A06_b** (*Spe* I) 5'AATTAAACTAGTTGCCAACCAACAGAGAACCAG	**OAb2A06_a** (*Pst* I) 5'AATTAACTGCAGCAAGGCACTCTCAAGCTCCG
pOAb3F11_FB	245 bp	**OAb3F11_c** (*Sma* I) 5'AATTAACCCGGGCTATCTTCTCTTTTGCACCGTC	**OAb3F11_b** (*Spe* I) 5'AATTAAACTAGTGTTCGGAGGATCATCCAAAAAC	**OAb3F11_a** (*Pst* I) 5'AATTAACTGCAGCTATCTTCTCTTTTGCACCGTC

Nineteen pOA_IPK constructs were kindly provided by P. Schweizer, (IPK Gatersleben, Germany). They represent hairpin loop expression constructs obtained by inserting PCR fragments in sense and anti-sense orientation into pIPKTA30N (Douchkov et al., 2005), a pJP26-based vector suitable for Gateway cloning (Invitrogen BV, Groningen, The Netherlands). pOA_IPK constructs were obtained by blunt-end ligating PCR fragments which were amplified from SSH-derived OA-cDNA fragments with the universal primers NstPrm1 and NstPrm2R into the pENTR1-MCS entry vector followed by recombination into pIPKTA30N in a single-step reaction (P. Schweizer, personal communication).

The presence of all inserts and correct orientation was checked by sequencing for all hairpin loop expression constructs used in this study (a list is given in the Table 4.10, p.107). Therefore, the sense insert was PCR-amplified with primers FB_s1 5'-AATCCCACTATCCTTCGCAAGAC and FB_a2 5'-CAGGACTCGGAAGCTGGAAAAT and the anti-sense insert was amplified with FB_s2 5'-AACACATGTGCAGGTGACATGG and FB_a1 5'-TGAGCGAAACCCTATAAGAACCC using BD Advantage™ 2 Polymerase Mix (Clontech Laboratories Inc., Mountain View (CA), USA) (95°C, 1 min, [94°C, 15 sec; 65°C, 30 sec; 68°C, 2 min] 30 cycles, 68°C, 5 min). The primers were annealing inside the 5'- and 3'-multiple cloning site as well as inside the intron which gave rise to overlapping PCR products. The products were excised from an agarose gel, purified as described above and subjected to sequencing using the amplification primers.

6.9. Loss of gene function study

The study of loss of gene function by transient biolistic transformation was conducted according to published protocols (Schweizer et al., 1999b; Schweizer et al., 2000). The following DNA vectors were used for bombardment: The overexpression vector pGY1 (Shinshi et al., 1990), the hairpin loop expression vector pJP26 (Christensen et al., 2004), the alternative hairpin loop expression vector pIPKTA30N kindly provided by P. Schweizer, (IPK Gatersleben, Germany Douchkov et al., 2005), the resistance gene overexpression vectors based on pGY1 containing the Pm3b gene (referred to as pPm3b), the Pm3f gene (referred to as pPm3f) and the inactive M23 mutant allele of the Pm3b gene (referred to as pM23) were kindly provided by N. Yahiaoui (Inst. of Plant Biol., University of Zuerich, Switzerland ,Yahiaoui et al., 2004; Srichumpa et al., 2005), and the reporter gene construct pUbiGUS containing the *uidA* β-glucuronidase gene of *E. coli* under the control of a maize polyubiquitin promoter (Schweizer et al., 1999b).

All transformations were carried out with a delivery pressure of 10 bar and a transformation chamber pressure of 100 mbar. Microcarrier loading quantity (MLQ) was 375 µg / shot (15 µl Tungsten particles ∅ 1.1 µm, 25 mg / ml) and DNA loading ratio (DLR) was 3.2 µg DNA / mg Tungsten (375 µg DNA / shot). For each DNA combination tested, 5 shots were carried out on 6 leaves each, with a target distance of 15 cm. Powdery mildew infection was done 3 h after transformation (250 - 300 conidia / mm^2) and leaves were harvested 48 h post transformation. Crucially, bombarded and infected leaves had to be incubated in a growth chamber (16 h light period at 20°, 8 h dark period at 20°C; 85-90 % relative humidity).

Pool transformations contained pUbiGUS, pPm3b, and three candidate foldback constructs at ratios of 2:1:1:1:1 (w/w). To maintain DLR and MLQ, candidate foldback constructs were substituted by pGY1 (or pJP26 or pIPKTA30N) [pUbiGUS : pPm3b : pGY1 = 2:1:3 (w/w)] for reference transformations. For negative control transformations, also the resistance gene construct was substituted by pGY1 [pUbiGUS : pGY1 = 2 : 4 (w/w)]

Single construct transformations contained pUbiGUS, pGY1 and the candidate foldback constructs at ratios of 2:2:2 (w/w). For reference transformation, the foldback construct was substituted by pGY1.

7. References

Abramovitch, R.B., and Martin, G.B. (2005). AvrPtoB: A bacterial type III effector that both elicits and suppresses programmed cell death associated with plant immunity. FEMS Microbiol. Lett. **245,** 1-8.

Abramovitch, R.B., Kim, Y.J., Chen, S.R., Dickman, M.B., and Martin, G.B. (2003). *Pseudomonas* type III effector AvrPtoB induces plant disease susceptibility by inhibition of host programmed cell death. Embo J. **22,** 60-69.

Adams, J.M., and Cory, S. (2001). Life-or-death decisions by the Bcl-2 protein family. Trends Biochem.Sci. **26,** 61-66.

Agilent Technologies Inc. (2003). Agilent G2565AA and Agilent G2565BA microarray scanner system - user manual (Palo Alto, CA, USA).

Agrios, G.N. (1997). Plant pathology. (San Diego, CA, USA: Academic Press).

Alfano, J.R., and Collmer, A. (1996). Bacterial pathogens in plants: Life up against the wall. Plant Cell **8,** 1683-1698.

Alméras, E., Stolz, S., Vollenweider, S., Reymond, P., Mène-Saffrané, L., and Farmer, E.E. (2003). Reactive electrophile species activate defense gene expression in *Arabidopsis*. Plant J. **34,** 202-216.

Altpeter, F., Varshney, A., Abderhalden, O., Douchkov, D., Sautter, C., Kumlehn, J., Dudler, R., and Schweizer, P. (2005). Stable expression of a defense-related gene in wheat epidermis under transcriptional control of a novel promoter confers pathogen resistance. Plant Molecular Biology **57,** 271-283.

Altschul, S.F., Gish, W., Miller, W., Myers, E.W., and Lipman, D.J. (1990). Basic local alignment search tool. J. Mol. Biol. **215,** 403-410.

Amrein, H., Makart, S., Granado, J., Shakya, R., Schneider-Pokorny, J., and Dudler, R. (2004). Functional analysis of genes involved in the synthesis of syringolin A by *Pseudomonas syringae* pv. *syringae* B301D-R. Mol. Plant-Microbe Interact. **17,** 90-97.

Ané, J.M., Kiss, G.B., Riely, B.K., Penmetsa, R.V., Oldroyd, G.E.D., Ayax, C., Levy, J., Debelle, F., Baek, J.M., Kalo, P., Rosenberg, C., Roe, B.A., Long, S.R., Denarie, J., and Cook, D.R. (2004). *Medicago truncatula* DMI1 required for bacterial and fungal symbioses in legumes. Science **303,** 1364-1367.

Asai, T., Tena, G., Plotnikova, J., Willmann, M.R., Chiu, W.L., Gomez-Gomez, L., Boller, T., Ausubel, F.M., and Sheen, J. (2002). MAP kinase signalling cascade in *Arabidopsis* innate immunity. Nature **415,** 977-983.

Ashburner, M., Ball, C.A., Blake, J.A., Botstein, D., Butler, H., Cherry, J.M., Davis, A.P., Dolinski, K., Dwight, S.S., Eppig, J.T., Harris, M.A., Hill, D.P., Issel-Tarver, L., Kasarskis, A., Lewis, S., Matese, J.C., Richardson, J.E., Ringwald, M., Rubin, G.M., and Sherlock, G. (2000). Gene Ontology: Tool for the unification of biology. Nature Genet. **25,** 25-29.

Assaad, F.F., Qiu, J.L., Youngs, H., Ehrhardt, D., Zimmerli, L., Kalde, M., Wanner, G., Peck, S.C., Edwards, H., Ramonell, K., Somerville, C.R., and Thordal-Christensen, H. (2004). The PEN1 syntaxin defines a novel cellular compartment upon fungal attack and is required for the timely assembly of papillae. Mol. Biol. Cell **15,** 5118-5129.

Azevedo, C., Sadanandom, A., Kitagawa, K., Freialdenhoven, A., Shirasu, K., and Schulze-Lefert, P. (2002). The RAR1 interactor SGT1, an essential component of *R* gene-triggered disease resistance. Science **295,** 2073-2076.

Baerson, S.R., Sanchez-Moreiras, A., Pedrol-Bonjoch, N., Schulz, M., Kagan, I.A., Agarwal, A.K., Reigosa, M.J., and Duke, S.O. (2005). Detoxification and transcriptome response in *Arabidopsis* seedlings exposed to the allelochemical benzoxazolin-2(3H)-one. J. Biol. Chem. **280,** 21867-21881.

Banerjee, J., and Ghosh, S. (2004). Bax increases the pore size of rat brain mitochondrial voltage-dependent anion channel in the presence of tBid. Biochem. Biophys. Res. Commun. **323,** 310-314.

Baugh, L.R., Hill, A.A., Brown, E.L., and Jimter, C.P. (2001). Quantitative analysis of mRNA amplification by *in vitro* transcription. Nucleic Acids Res. **29,** 1-9.

Bazirgan, O.A., and Hampton, R.Y. (2005). Cdc48-Ufd2-Rad23: the road less ubiquitinated? Nat. Cell Biol. **7,** 207-209.

Beere, H.M. (2004). The stress of dying: The role of heat shock proteins in the regulation of apoptosis. J. Cell Sci. **117,** 2641-2651.

Bélanger, R.R., Bushnell, W.R., Dik, A.J., and Carver, T.L.W. (2002). The powdery mildews: A comprehensive treatise. (St. Paul, Minnesota, USA: APS Press).

Bender, C.L., Alarcon-Chaidez, F., and Gross, D.C. (1999). *Pseudomonas syringae* phytotoxins: Mode of action, regulation, and biosynthesis by peptide and polyketide synthetases. Microbiol. Mol. Biol. Rev. **63,** 266-292.

Bengtsson, H., Jonsson, G., and Vallon-Christersson, J. (2004). Calibration and assessment of channel-specific biases in microarray data with extended dynamical range. BMC Bioinformatics **5,** 1-17.

Benz, R. (1994). Permeation of hydrophilic solutes through mitochondrial outer membranes - review on mitochondrial porins. Biochimica et Biophysica Acta - Reviews on Biomembranes **1197,** 167-196.

Bhalerao, R.P., Salchert, K., Bako, L., Okresz, L., Szabados, L., Muranaka, T., Machida, Y., Schell, J., and Koncz, C. (1999). Regulatory interaction of PRL1 WD protein with *Arabidopsis* SNF1-like protein kinases. Proc. Natl. Acad. Sci. U. S. A. **96,** 5322-5327.

Biemelt, S., Keetman, U., and Albrecht, G. (1998). Re-aeration following hypoxia or anoxia leads to activation of the antioxidative defense system in roots of wheat seedlings. Plant Physiol. **116,** 651-658.

Biemelt, S., Keetman, U., Mock, H.P., and Grimm, B. (2000). Expression and activity of isoenzymes of superoxide dismutase in wheat roots in response to hypoxia and anoxia. Plant Cell Environ. **23,** 135-144.

Bieri, S., Mauch, S., Shen, Q.H., Peart, J., Devoto, A., Casais, C., Ceron, F., Schulze, S., Steinbiss, H.H., Shirasu, K., and Schulze-Lefert, P. (2004). RAR1 positively controls steady state levels of barley MLA resistance proteins and enables sufficient MLA6 accumulation for effective resistance. Plant Cell **16,** 3480-3495.

Bolduc, N., and Brisson, L.F. (2002). Antisense down regulation of NtBI-1 in tobacco BY-2 cells induces accelerated cell death upon carbon starvation. FEBS Lett. **532,** 111-114.

Boller, T. (2005). Peptide signalling in plant development and self/non-self perception. Curr. Opin. Cell Biol. **17,** 116-122.

Bonas, U., and Lahaye, T. (2002). Plant disease resistance triggered by pathogen-derived molecules: refined models of specific recognition. Curr. Opin. Microbiol. **5,** 44-50.

Boyes, D.C., Nam, J., and Dangl, J.L. (1998). The *Arabidopsis thaliana* RPM1 disease resistance gene product is a peripheral plasma membrane protein that is degraded coincident with the hypersensitive response. Proc. Natl. Acad. Sci. U. S. A. **95,** 15849-15854.

Brady, S.M., Sarkar, S.F., Bonetta, D., and McCourt, P. (2003). The *ABSCISIC ACID INSENSITIVE 3* (*ABI3*) gene is modulated by farnesylation and is involved in auxin signaling and lateral root development in *Arabidopsis*. Plant J. **34,** 67-75.

Bras, M., Queenan, B., and Susin, S.A. (2005). Programmed cell death via mitochondria: Different modes of dying. Biochem.-Moscow **70,** 231-239.

Bruggmann, R., Abderhalden, O., Reymond, P., and Dudler, R. (2005). Analysis of epidermis- and mesophyll-specific transcript accumulationin powdery mildew-inoculated wheat leaves. Plant Molecular Biology **58,** 247-267.

Buchanan, B.B., Gruissem, W., and Jones, R.L. (2001). Biochemistry & Molecular Biology of Plants. (Rockville, Maryland, USA: American Society of Plant Physiologists).

Bull, J., Mauch, F., Hertig, C., Rebmann, G., and Dudler, R. (1992). Sequence and expression of a wheat gene that encodes a novel protein associated with pathogen defense. Mol. Plant-Microbe Interact. **5,** 516-519.

Butler, W., Cook, L., and Vayda, M.E. (1990). Hypoxic stress inhibits multiple aspects of the potato-tuber wound response. Plant Physiol. **93,** 264-270.

Cao, H., Bowling, S.A., Gordon, A.S., and Dong, X.N. (1994). Characterization of an *Arabidopsis* mutant that is nonresponsive to inducers of systemic acquired-resistance. Plant Cell **6,** 1583-1592.

Carver, T.L.W., Wright, A., and Thomas, B. (2001). The ups and downs of a plant pathogen's early life. IGER Innovations**,** 17-21.

Carver, T.L.W., Ingersonmorris, S.M., Thomas, B.J., and Zeyen, R.J. (1995). Early interactions during powdery mildew infection. Canadian Journal of Botany-Revue Canadienne De Botanique **73,** S632-S639.

Carver, T.L.W., Kunoh, H., Thomas, B.J., and Nicholson, R.L. (1999). Release and visualization of the extracellular matrix of conidia of *Blumeria graminis*. Mycol. Res. **103,** 547-560.

Carver, T.L.W., Zeyen, R.J., Robbins, M.P., Vance, C.P., and Boyles, D.A. (1994). Suppression of host cinnamyl alcohol-dehydrogenase and phenylalanine ammonia-lyase increases oat epidermal-cell susceptibility to powdery mildew penetration. Physiological and Molecular Plant Pathology **44,** 243-259.

Charron, J.B.F., Breton, G., Badawi, M., and Sarhan, F. (2002). Molecular and structural analyses of a novel temperature stress-induced lipocalin from wheat and *Arabidopsis*. FEBS Lett. **517,** 129-132.

Chen, J.G., Willard, F.S., Huang, J., Liang, J.S., Chasse, S.A., Jones, A.M., and Siderovski, D.P. (2003). A seven-transmembrane RGS protein that modulates plant cell proliferation. Science **301,** 1728-1731.

Chen, Y., and Chelkowski, J. (1999). Genes for resistance to wheat powdery mildew. Journal of Applied Genetics **40,** 317-334.

Christensen, A.B., Thordal-Christensen, H., Zimmermann, G., Gjetting, T., Lyngkjaer, M.F., Dudler, R., and Schweizer, P. (2004). The germinlike protein GLP4 exhibits superoxide dismutase activity and is an important component of quantitative resistance in wheat and barley. Mol. Plant-Microbe Interact. **17,** 109-117.

Ciccarelli, F.D., and Bork, P. (2005). The WHy domain mediates the response to desiccation in plants and bacteria. Bioinformatics **21,** 1304-1307.

Clarke, P.G.H. (1990). Developmental cell-death: Morphological diversity and multiple mechanisms. Anat. Embryol. **181,** 195-213.

Coffeen, W.C., and Wolpert, T.J. (2004). Purification and characterization of serine proteases that exhibit caspase-like activity and are associated with programmed cell death in *Avena sativa*. Plant Cell **16,** 857-873.

Collins, N.C., Thordal-Christensen, H., Lipka, V., Bau, S., Kombrink, E., Qiu, J.L., Huckelhoven, R., Stein, M., Freialdenhoven, A., Somerville, S.C., and Schulze-Lefert, P. (2003). SNARE-protein-mediated disease resistance at the plant cell wall. Nature **425,** 973-977.

Colombini, M. (1980). Pore-size and properties of channels from mitochondria isolated from *Neurospora crassa*. J. Membr. Biol. **53,** 79-84.

Crompton, M., Barksby, E., Johnson, N., and Capano, M. (2002). Mitochondrial intermembrane junctional complexes and their involvement in cell death. Biochimie **84,** 143-152.

Cruciat, C.M., Hell, K., Folsch, H., Neupert, W., and Stuart, R.A. (1999). Bcs1p, an AAA-family member, is a chaperone for the assembly of the cytochrome bc_1 complex. Embo J. **18,** 5226-5233.

Cui, J., Bahrami, A.K., Pringle, E.G., Hernandez-Guzman, G., Bender, C.L., Pierce, N.E., and Ausubel, F.M. (2005). *Pseudomonas syringae* manipulates systemic plant defenses against pathogens and herbivores. Proc. Natl. Acad. Sci. U. S. A. **102,** 1791-1796.

Dangl, J.L., and Jones, J.D.G. (2001). Plant pathogens and integrated defence responses to infection. Nature **411,** 826-833.

Davenport, R. (2002). Glutamate receptors in plants. Ann. Bot. **90,** 549-557.

Day, B., Dahlbeck, D., Huang, J., Chisholm, S.T., Li, D.H., and Staskawicz, B.J. (2005). Molecular basis for the RIN4 negative regulation of RPS2 disease resistance. Plant Cell **17,** 1292-1305.

De Vries, L., Zheng, B., Fischer, T., Elenko, E., and Farquhar, M.G. (2000). The regulator of G protein signaling family. Annu. Rev. Pharmacol. Toxicol. **40,** 235-271.

Delaney, T.P., Friedrich, L., and Ryals, J.A. (1995). *Arabidopsis* signal-transduction mutant defective in chemically and biologically induced disease resistance. Proc. Natl. Acad. Sci. U. S. A. **92,** 6602-6606.

Delledonne, M., Zeier, J., Marocco, A., and Lamb, C. (2001). Signal interactions between nitric oxide and reactive oxygen intermediates in the plant hypersensitive disease resistance response. Proc. Natl. Acad. Sci. U. S. A. **98,** 13454-13459.

Di Giorgio, D., Camoni, L., Mott, K.A., Takemoto, J.Y., and Ballio, A. (1996). Syringopeptins, *Pseudomonas syringae* pv. *syringae* phytotoxins, resemble syringomycin in closing stomata. Plant Pathol. **45,** 564-571.

Diatchenko, L., Lukyanov, S., Lau, Y.F.C., and Siebert, P.D. (1999). Suppression subtractive hybridization: A versatile method for identifying differentially expressed genes. In cDNA Preparation and Characterization (San Diego: Academic Press Inc.), pp. 349-380.

Diatchenko, L., Lau, Y.F.C., Campbell, A.P., Chenchik, A., Moqadam, F., Huang, B., Lukyanov, S., Lukyanov, K., Gurskaya, N., Sverdlov, E.D., and Siebert, P.D. (1996). Suppression subtractive hybridization: A method for generating differentially regulated or tissue-specific cDNA probes and libraries. Proc. Natl. Acad. Sci. U. S. A. **93,** 6025-6030.

Dickman, M.B., Park, Y.K., Oltersdorf, T., Li, W., Clemente, T., and French, R. (2001). Abrogation of disease development in plants expressing animal antiapoptotic genes. Proc. Natl. Acad. Sci. U. S. A. **98,** 6957-6962.

Diehl, F., Grahlmann, S., Beier, M., and Hoheisel, J.D. (2001). Manufacturing DNA microarrays of high spot homogeneity and reduced background signal. Nucleic Acids Research **29,** E38.

Dixon, R.A. (2001). Natural products and plant disease resistance. Nature **411,** 843-847.

Doerks, T., Huber, S., Buchner, E., and Bork, P. (2002). BSD: a novel domain in transcription factors and synapse-associated proteins. Trends Biochem.Sci. **27,** 168-170.

Douchkov, D., Nowara, D., U. Zierold, U., and Schweizer, P. (2005). A high-throughput gene silencing system for the functional assessment of defense-related genes in barley epidermal cells. Molecular Plant Microbe Interactions **18,** 755-761.

Drew, M.C. (1997). Oxygen deficiency and root metabolism: Injury and acclimation under hypoxia and anoxia. Annu. Rev. Plant Physiol. Plant Molec. Biol. **48,** 223-250.

Dudoit, S., Yang, Y.H., Callow, M.J., and Speed, T.P. (2002). Statistical methods for identifying differentially expressed genes in replicated cDNA microarray experiments. Stat. Sin. **12,** 111-139.

Duveiller, E., Fucikovsky, L., and Rudolph, K. (1997). The bacterial diseases of wheat: Concepts and methods of disease management. (Mexico: D.F.:CIMMYT).

Eden Bioscience. (2004). Discovery of harpin binding protein 1 (HrBP1) (Eden Bioscience).

Edwards, R., Dixon, D.P., and Walbot, V. (2000). Plant glutathione S-transferases: Enzymes with multiple functions in sickness and in health. Trends in Plant Science **5,** 193-198.

Eisen, M.B., and Brown, P.O. (1999). DNA arrays for analysis of gene expression. In cDNA Preparation and Characterization (San Diego: Academic Press Inc.), pp. 179-205.

Elliott, L.F., and Lynch, J.M. (1985). Plant growth-inhibitory *Pseudomonads* colonizing winter wheat (*Triticum aestivum* L.) roots. Plant Soil **84,** 57-65.

Elsasser, S., and Finley, D. (2005). Delivery of ubiquitinated substrates to protein-unfolding machines. Nat. Cell Biol. **7,** 742-749.

Emel'yanov, V.V., Kirchikhina, N.A., Lastochkin, V.V., and Chirkova, T.V. (2003). Hormonal status in wheat and rice seedlings under anoxia. Russ. J. Plant Physiol. **50,** 827-834.

Enari, M., Sakahira, H., Yokoyama, H., Okawa, K., Iwamatsu, A., and Nagata, S. (1998). A caspase-activated DNase that degrades DNA during apoptosis, and its inhibitor ICAD. Nature **391,** 43-50.

Endre, G., Kereszt, A., Kevei, Z., Mihacea, S., Kalo, P., and Kiss, G.B. (2002). A receptor kinase gene regulating symbiotic nodule development. Nature **417,** 962-966.

Ewing, B., and Green, P. (1998). Base-calling of automated sequencer traces using phred. II. Error probabilities. Genome Res. **8,** 186-194.

Ewing, B., Hillier, L., Wendl, M.C., and Green, P. (1998). Base-calling of automated sequencer traces using phred. I. Accuracy assessment. Genome Res. **8,** 175-185.

Falk, A., Feys, B.J., Frost, L.N., Jones, J.D.G., Daniels, M.J., and Parker, J.E. (1999). EDS1, an essential component of R gene-mediated disease resistance in *Arabidopsis* has homology to eukaryotic lipases. Proc. Natl. Acad. Sci. U. S. A. **96,** 3292-3297.

Farras, R., Ferrando, A., Jasik, J., Kleinow, T., Okresz, L., Tiburcio, A., Salchert, K., del Pozo, C., Schell, J., and Koncz, C. (2001). SKP1-SnRK protein kinase interactions mediate proteasomal binding of a plant SCF ubiquitin ligase. Embo J. **20,** 2742-2756.

Fath, A., Bethke, P., Beligni, V., and Jones, R. (2002). Active oxygen and cell death in cereal aleurone cells. J. Exp. Bot. **53,** 1273-1282.

Feldman, A.L., Costouros, N.G., Wang, E., Qian, M., Marincola, F.M., Alexander, H.R., and Libutti, S.K. (2002). Advantages of mRNA amplification for microarray analysis. Biotechniques **33,** 906-914.

Ferri, K.F., and Kroemer, G. (2001). Organelle-specific initiation of cell death pathways. Nat. Cell Biol. **3,** E255-E263.

Fleischmann, J., and Liu, H. (2001). Polyadenylation of ribosomal RNA by *Candida albicans*. Gene **265,** 71-76.

Fleischmann, J., Liu, H., and Wu, C.P. (2004). Polyadenylation of ribosomal RNA by *Candida albicans* also involves the small subunit. BMC Mol. Biol. **5,** 1-6.

Flower, D.R. (1996). The lipocalin protein family: Structure and function. Biochem. J. **318,** 1-14.

Flower, D.R., North, A.C.T., and Sansom, C.E. (2000). The lipocalin protein family: structural and sequence overview. Biochim. Biophys. Acta-Protein Struct. Molec. Enzym. **1482,** 9-24.

Francis, D., and Sorrell, D.A. (2001). The interface between the cell cycle and plant growth regulators: a mini review. Plant Growth Regul. **33,** 1-12.

Francois, P., Bento, M., Vaudaux, P., and Schrenzel, J. (2003). Comparison of fluorescence and resonance light scattering for highly sensitive microarray detection of bacterial pathogens. J. Microbiol. Methods **55,** 755-762.

Fraser, M., Leung, B., Jahani-Asl, A., Yan, X., Thompson, W.E., and Tsang, B.K. (2003). Chemoresistance in human ovarian cancer: The role of apoptotic regulators. Reprod Biol Endocrinol. **1,** 66.

Freialdenhoven, A., Orme, J., Lahaye, T., and Schulze-Lefert, P. (2005). Barley *Rom1* reveals a potential link between race-specific and nonhost resistance responses to powdery mildew fungi. Mol. Plant-Microbe Interact. **18,** 291-299.

Freialdenhoven, A., Peterhansel, C., Kurth, J., Kreuzaler, F., and SchulzeLefert, P. (1996). Identification of genes required for the function of non-race-specific *mlo* resistance to powdery mildew in barley. Plant Cell **8,** 5-14.

Fretland, A.J., and Omiecinski, C.J. (2000). Epoxide hydrolases: Biochemistry and molecular biology. Chem.-Biol. Interact. **129,** 41-59.

Frickey, T., and Lupas, A.N. (2004). Phylogenetic analysis of AAA proteins. J. Struct. Biol. **146,** 2-10.

Fu, X.R., Ng, C., Feng, D.R., and Liang, C. (2003). Cdc48p is required for the cell cycle commitment point at start via degradation of the G1-CDK inhibitor Far1p. J. Cell Biol. **163,** 21-26.

Fusaro, G., Wang, S., and Chellappan, S. (2002). Differential regulation of Rb family proteins and prohibitin during camptothecin-induced apoptosis. Oncogene **21,** 4539-4548.

Fusaro, G., Dasgupta, P., Rastogi, S., Joshi, B., and Chellappan, S. (2003). Prohibitin induces the transcriptional activity of p53 and is exported from the nucleus upon apoptotic signaling. J. Biol. Chem. **278,** 47853-47861.

Gaffney, T., Friedrich, L., Vernooij, B., Negrotto, D., Nye, G., Uknes, S., Ward, E., Kessmann, H., and Ryals, J. (1993). Requirement of salicylic-acid for the induction of systemic acquired-resistance. Science **261,** 754-756.

Garcia-Higuera, I., Fenoglio, J., Li, Y., Lewis, C., Panchenko, M.P., Reiner, O., Smith, T.F., and Neer, E.J. (1996). Folding of proteins with WD-repeats: Comparison of six members of the WD-repeat superfamily to the G protein beta subunit. Biochemistry **35,** 13985-13994.

Geigenberger, P. (2003). Response of plant metabolism to too little oxygen. Curr. Opin. Plant Biol. **6,** 247-256.

Goerlach, J., Volrath, S., KnaufBeiter, G., Hengy, G., Beckhove, U., Kogel, K.H., Oostendorp, M., Staub, T., Ward, E., Kessmann, H., and Ryals, J. (1996). Benzothiadiazole, a novel class of inducers of systemic acquired resistance, activates gene expression and disease resistance in wheat. Plant Cell **8,** 629-643.

Gomez-Gomez, L., Felix, G., and Boller, T. (1999). A single locus determines sensitivity to bacterial flagellin in *Arabidopsis thaliana*. Plant J. **18,** 277-284.

Gopalan, S., Wei, W., and He, S.Y. (1996). *hrp* gene-dependent induction of *hin1*: A plant gene activated rapidly by both harpins and the *avrPto* gene-mediated signal. Plant J. **10,** 591-600.

Grandbastien, M.A. (1998). Activation of plant retrotransposons under stress conditions. Trends in Plant Science **3,** 181-187.

Grant, J.J., and Loake, G.J. (2000). Role of reactive oxygen intermediates and cognate redox signaling in disease resistance. Plant Physiol. **124,** 21-29.

Granville, D.J., and Gottlieb, R.A. (2003). The mitochondrial voltage-dependent anion channel (VDAC) as a therapeutic target for initiating cell death. Curr. Med. Chem. **10,** 1527-1533.

Gray, W.M., del Pozo, J.C., Walker, L., Hobbie, L., Risseeuw, E., Banks, T., Crosby, W.L., Yang, M., Ma, H., and Estelle, M. (1999). Identification of an SCF ubiquitin-ligase complex required for auxin response in *Arabidopsis thaliana*. Genes Dev. **13,** 1678-1691.

Greenberg, J.T., and Yao, N. (2004). The role and regulation of programmed cell death in plant-pathogen interactions. Cell Microbiol. **6,** 201-211.

Guo, A., Durner, J., and Klessig, D.F. (1998). Characterization of a tobacco epoxide hydrolase gene induced during the resistance response to TMV. Plant J. **15,** 647-656.

Gupta, S., and Knowlton, A.A. (2005). HSP60, Bax, apoptosis and the heart. J. Cell. Mol. Med. **9,** 51-58.

Gurskaya, N.G., Diatchenko, L., Chenchik, A., Siebert, P.D., Khaspekov, G.L., Lukyanov, K.A., Vagner, L.L., Ermolaeva, O.D., Lukyanov, S.A., and Sverdlov, E.D. (1996). Equalizing cDNA subtraction based on selective suppression of polymerase chain reaction: Cloning of Jurkat cell transcripts induced by phytohemaglutinin and phorbol 12-myristate 13-acetate. Anal. Biochem. **240,** 90-97.

Hamilton, E.W., and Heckathorn, S.A. (2001). Mitochondrial adaptations to NaCl. Complex I is protected by anti-oxidants and small heat shock proteins, whereas complex II is protected by proline and betaine. Plant Physiol. **126,** 1266-1274.

Hassa, P., Granado, J., Freydl, E., Wäspi, U., and Dudler, R. (2000). Syringolin-mediated activation of the Pir7b esterase gene in rice cells is suppressed by phosphatase inhibitors. Mol. Plant-Microbe Interact. **13,** 342-346.

Heath, M.C. (1998). Apoptosis, programmed cell death and the hypersensitive response. Eur. J. Plant Pathol. **104,** 117-124.

Heckathorn, S.A., Downs, C.A., Sharkey, T.D., and Coleman, J.S. (1998). The small, methionine-rich chloroplast heat-shock protein protects photosystem II electron transport during heat stress. Plant Physiol. **116,** 439-444.

Hengartner, M.O. (2000). The biochemistry of apoptosis. Nature **407,** 770-776.

Heredia, A. (2003). Biophysical and biochemical characteristics of cutin, a plant barrier biopolymer. Biochim. Biophys. Acta-Gen. Subj. **1620,** 1-7.

Hirabayashi, S., Matsushital, Y., Sato, M., Oh-I, R., Kasaharai, M., Abe, H., and Nyunoyai, H. (2004). Two proton pump interactors identified from a direct phosphorylation screening of a rice cDNA library by using a recombinant BR11 receptor kinase. Plant Biotechnology, **21,** 35-45.

Hoeren, F.U., Dolferus, R., Wu, Y.R., Peacock, W.J., and Dennis, E.S. (1998). Evidence for a role for AtMYB2 in the induction of the Arabidopsis alcohol dehydrogenase gene (ADH1) by low oxygen. Genetics **149,** 479-490.

Holloway, A.J., van Laar, R.K., Tothill, R.W., and Bowtell, D.D.L. (2002). Options available - from start to finish - for obtaining data from DNA microarrays. Nature Genet. **32,** 481-489.

Holmquist, M. (2000). Alpha/beta-hydrolase fold enzymes: Structures, functions and mechanisms. Current Protein and Peptide Science **1,** 209-235.

Holt, B.F., Belkhadir, Y., and Dangl, J.L. (2005). Antagonistic control of disease resistance protein stability in the plant immune system. Science **309,** 929-932.

Hrabak, E.M., and Willis, D.K. (1992). The *lem*A gene required for pathogenicity of *Pseudomonas syringae* pv. *syringae* on bean is a member of a family of 2-component regulators. J. Bacteriol. **174,** 3011-3020.

Hrabak, E.M., and Willis, D.K. (1993). Involvement of the *Iem*A gene in production of syringomycin and protease by *Pseudomonas syringae* pv. *syringae*. Mol. Plant-Microbe Interact. **6,** 368-375.

Huang, X.Q., Hsam, S.L.K., Mohler, V., Roder, M.S., and Zeller, F.J. (2004). Genetic mapping of three alleles at the Pm3 locus conferring powdery mildew resistance in common wheat (Triticum aestivum L.). Genome **47,** 1130-1136.

Hückelhoven, R., and Kogel, K.H. (2003). Reactive oxygen intermediates in plant-microbe interactions: Who is who in powdery mildew resistance? Planta **216,** 891-902.

Hückelhoven, R., Dechert, C., and Kogel, K.H. (2003). Overexpression of barley BAX inhibitor 1 induces breakdown of mlo-mediated penetration resistance to *Blumeria graminis*. Proc. Natl. Acad. Sci. U. S. A. **100,** 5555-5560.

Hückelhoven, R., Fodor, J., Preis, C., and Kogel, K.H. (1999). Hypersensitive cell death and papilla formation in barley attacked by the powdery mildew fungus are associated with hydrogen peroxide but not with salicylic acid accumulation. Plant Physiol. **119,** 1251-1260.

Hückelhoven, R., Dechert, C., Trujillo, M., and Kogel, K.H. (2001). Differential expression of putative cell death regulator genes in near-isogenic, resistant and susceptible barley lines during interaction with the powdery mildew fungus. Plant Molecular Biology **47,** 739-748.

Hughes, T.R., Mao, M., Jones, A.R., Burchard, J., Marton, M.J., Shannon, K.W., Lefkowitz, S.M., Ziman, M., Schelter, J.M., Meyer, M.R., Kobayashi, S., Davis, C., Dai, H.Y., He, Y.D.D., Stephaniants, S.B., Cavet, G., Walker, W.L., West, A., Coffey, E., Shoemaker, D.D., Stoughton, R., Blanchard, A.P., Friend, S.H., and Linsley, P.S. (2001). Expression profiling using microarrays fabricated by an ink-jet oligonucleotide synthesizer. Nat. Biotechnol. **19,** 342-347.

Imai, J., Maruya, M., Yashiroda, H., Yahara, I., and Tanaka, K. (2003). The molecular chaperone Hsp90 plays a role in the assembly and maintenance of the 26S proteasome. Embo J. **22,** 3557-3567.

Jabs, T. (1999). Reactive oxygen intermediates as mediators of programmed cell death in plants and animals. Biochem. Pharmacol. **57,** 231-245.

Jamir, Y., Guo, M., Oh, H.S., Petnicki-Ocwieja, T., Chen, S.R., Tang, X.Y., Dickman, M.B., Collmer, A., and Alfano, J.R. (2004). Identification of *Pseudomonas syringae* type III effectors that can suppress programmed cell death in plants and yeast. Plant J. **37,** 554-565.

Jirage, D., Tootle, T.L., Reuber, T.L., Frost, L.N., Feys, B.J., Parker, J.E., Ausubel, F.M., and Glazebrook, J. (1999). *Arabidopsis thaliana* PAD4 encodes a lipase-like gene that is important for salicylic acid signaling. Proc. Natl. Acad. Sci. U. S. A. **96,** 13583-13588.

Johnson, L.E.B., Bushnell, W.R., and Zeyen, R.J. (1982). Defense patterns in non-host higher-plant species against 2 powdery mildew fungi. I. Monocotyledonous species. Canadian Journal of Botany **60,** 1068-1083.

Joo, J.H., Wang, S.Y., Chen, J.G., Jones, A.M., and Fedoroff, N.V. (2005). Different signaling and cell death roles of heterotrimeric G protein alpha and beta subunits in the *Arabidopsis* oxidative stress response to ozone. Plant Cell **17,** 957-970.

Jorgensen, J.H. (1992). Discovery, characterization and exploitation of *Mlo* powdery mildew resistance in barley. Euphytica **63,** 141-152.

Jorgensen, J.H. (1994). Genetics of Powdery Mildew Resistance in Barley. Crit. Rev. Plant Sci. **13,** 97-119.

Kane, D.J., Sarafian, T.A., Anton, R., Hahn, H., Gralla, E.B., Valentine, J.S., Ord, T., and Bredesen, D.E. (1993). Bcl-2 inhibition of neural death - decreased generation of reactive oxygen species. Science **262,** 1274-1277.

Kang, L., Tang, X.Y., and Mysore, K.S. (2004). *Pseudomonas* type III effector AvrPto suppresses the programmed cell death induced by two nonhost pathogens in *Nicotiana benthamiana* and tomato. Mol. Plant-Microbe Interact. **17,** 1328-1336.

Karlin, S., and Altschul, S.F. (1990). Methods for assessing the statistical significance of molecular sequence features by using general scoring schemes. Proc. Natl. Acad. Sci. U. S. A. **87,** 2264-2268.

Karlin, S., and Altschul, S.F. (1993). Applications and statistics for multiple high-scoring segments in molecular sequences. Proc. Natl. Acad. Sci. U. S. A. **90,** 5873-5877.

Kawai-Yamada, M., Jin, L.H., Yoshinaga, K., Hirata, A., and Uchimiya, H. (2001). Mammalian Bax-induced plant cell death can be down-regulated by overexpression of *Arabidopsis* Bax Inhibitor-1 (AtBl-1). Proc. Natl. Acad. Sci. U. S. A. **98,** 12295-12300.

Kepler, T.B., Crosby, L., and Morgan, K.T. (2002). Normalization and analysis of DNA microarray data by self-consistency and local regression. Genome Biology **3,** 1-12.

Kerr, J.F.R., Wyllie, A.H., and Currie, A.R. (1972). Apoptosis: A basic biological phenomenon with wide-ranging implications in tissue kinetics. Br. J. Cancer **26,** 239-257.

Khurana, S.M.P., Pandey, S.K., Sarkar, D., and Chanemougasoundharam, A. (2005). Apoptosis in plant disease response: A close encounter of the pathogen kind. Curr. Sci. **88,** 740-752.

Kiyosue, T., Beetham, J.K., Pinot, F., Hammock, B.D., Yamaguchishinozaki, K., and Shinozaki, K. (1994). Characterization of an *Arabidopsis* cDNA for a soluble epoxide hydrolase gene that is inducible by auxin and water-stress. Plant J. **6,** 259-269.

Klein, M., Perfus-Barbeoch, L., Frelet, A., Gaedeke, N., Reinhardt, D., Mueller-Roeber, B., Martinoia, E., and Forestier, C. (2003). The plant multidrug resistance ABC transporter AtMRP5 is involved in guard cell hormonal signalling and water use. Plant J. **33,** 119-129.

Klok, E.J., Wilson, I.W., Wilson, D., Chapman, S.C., Ewing, R.M., Somerville, S.C., Peacock, W.J., Dolferus, R., and Dennis, E.S. (2002). Expression profile analysis of the low-oxygen response in *Arabidopsis* root cultures. Plant Cell **14,** 2481-2494.

Kmecl, A., Mauch, F., Winzeler, M., Winzeler, H., and Dudler, R. (1995). Quantitative field-resistance of wheat to powdery mildew and defense reactions at the seedling stage - identification of a potential marker. Physiological and Molecular Plant Pathology **47,** 185-199.

Kmita, H., Antos, N., Wojtkowska, M., and Hryniewiecka, L. (2004). Processes underlying the upregulation of Tom proteins in *S. cerevisiae* mitochondria depleted of the VDAC channel. J. Bioenerg. Biomembr. **36,** 187-193.

Knauf-Beiter, G., Dahmen, H., Heye, U., and Staub, T. (1995). Activity of cyprodinil - optimal treatment timing and site of action. Plant Dis. **79,** 1098-1103.

Knippers, R. (1997). Molekulare Genetik. (Stuttgart, Germany: Georg Thieme Verlag).

Kobayashi, Y., Kobayashi, I., Funaki, Y., Fujimoto, S., Takemoto, T., and Kunoh, H. (1997). Dynamic reorganization of microfilaments and microtubules is necessary for the expression of non-host resistance in barley coleoptile cells. Plant J. **11,** 525-537.

Koga, H., Mayama, S., and Shishiyama, J. (1980). Correlation between the deposition of fluorescent compounds in papillae and resistance in barley against *Erysiphe graminis* f.sp. *hordei*. Canadian Journal of Botany-Revue Canadienne De Botanique **58,** 536-541.

Koga, H., Bushnell, W.R., and Zeyen, R.J. (1990). Specificity of cell type and timing of events associated with papilla formation and the hypersensitive reaction in leaves of *Hordeum vulgare* attacked by *Erysiphe graminis* f.sp. *hordei*. Canadian Journal of Botany-Revue Canadienne De Botanique **68,** 2344-2352.

Koga, H., Zeyen, R.J., Bushnell, W.R., and Ahlstrand, G.G. (1988). Hypersensitive cell-death, autofluorescence, and insoluble silicon accumulation in barley seaf epidermal-cells under attack by *Erysiphe graminis* f.sp. *hordei.* Physiological and Molecular Plant Pathology **32,** 395-409.

Kolesnick, R., and Fuks, Z. (2003). Radiation and ceramide-induced apoptosis. Oncogene **22,** 5897-5906.

Krause, M., and Durner, J. (2004). Harpin inactivates mitochondria in *Arabidopsis* suspension cells. Mol. Plant-Microbe Interact. **17,** 131-139.

Kuai, L., Fang, F., Butler, J.S., and Sherman, F. (2004). Polyadenylation of rRNA in *Saccharomyces cerevisiae*. Proc. Natl. Acad. Sci. U. S. A. **101,** 8581-8586.

Kunoh, H., Hayashimoto, A., Harui, M., and Ishizaki, H. (1985). Induced susceptibility and enhanced resistance at the cellular level in barley coleoptiles I. The significance of timing of fungal invasion. Physiological Plant Pathology **27,** 43-54.

Kunoh, H., Kuroda, K., Hayashimoto, A., and Ishizaki, H. (1986). Induced susceptibility and enhanced resistance at the cellular level in barley coleoptiles II. Timing and localization of induced susceptibility in a single coleoptile cell and its transfer to an adjacent cell. Canadian Journal of Botany-Revue Canadienne De Botanique **64,** 889-895.

Kürsteiner, O., Dupuis, I., and Kuhlemeier, C. (2003). The pyruvate decarboxylase 1 gene of *Arabidopsis* is required during anoxia but not other environmental stresses. Plant Physiol. **132,** 968-978.

Lacomme, C., and Cruz, S.S. (1999). Bax-induced cell death in tobacco is similar to the hypersensitive response. Proc. Natl. Acad. Sci. U. S. A. **96,** 7956-7961.

Lallemant, C.A. (2002). Introduction to microarray analysis (Amersham Pharmacia).

Lam, E. (2004). Controlled cell death, plant survival and development. Nat. Rev. Mol. Cell Biol. **5,** 305-315.

Lam, E., Kato, N., and Lawton, M. (2001). Programmed cell death, mitochondria and the plant hypersensitive response. Nature **411,** 848-853.

Lamb, C., and Dixon, R.A. (1997). The oxidative burst in plant disease resistance. Annu. Rev. Plant Physiol. Plant Molec. Biol. **48,** 251-275.

Lane, B.G., Dunwell, J.M., Ray, J.A., Schmitt, M.R., and Cuming, A.C. (1993). Germin, a protein marker of early plant development, is an oxalate oxidase. J. Biol. Chem. **268,** 12239-12242.

Lane, B.G., Bernier, F., Dratewkakos, E., Shafai, R., Kennedy, T.D., Pyne, C., Munro, J.R., Vaughan, T., Walters, D., and Altomare, F. (1991). Homologies between members of the germin gene family in hexaploid wheat and similarities between these wheat germins and certain *physarum spherulins*. J. Biol. Chem. **266,** 10461-10469.

Lawton, K.A., Friedrich, L., Hunt, M., Weymann, K., Delaney, T., Kessmann, H., Staub, T., and Ryals, J. (1996). Benzothiadiazole induces disease resistance in *Arabidopsis* by activation of the systemic acquired resistance signal transduction pathway. Plant J. **10,** 71-82.

Lee, J., Klessig, D.F., and Nurnberger, T. (2001). A harpin binding site in tobacco plasma membranes mediates activation of the pathogenesis-related gene *HIN1* independent of extracellular calcium but dependent on mitogen-activated protein kinase activity. Plant Cell **13,** 1079-1093.

Lee, P.D., Sladek, R., Greenwood, C.M.T., and Hudson, T.J. (2002). Control genes and variability: Absence of ubiquitous reference transcripts in diverse mammalian expression studies. Genome Res. **12,** 292-297.

Leist, M., and Nicotera, P. (1997). The shape of cell death. Biochem. Biophys. Res. Commun. **236,** 1-9.

Lemeshko, V.V. (2002). Model of the outer membrane potential generation by the inner membrane of mitochondria. Biophys. J. **82,** 684-692.

Lemeshko, V.V., and Lemeshko, S.V. (2004). The voltage-dependent anion channel as a biological transistor: Theoretical considerations. Eur. Biophys. J. Biophys. Lett. **33,** 352-359.

León, J., Lawton, M.A., and Raskin, I. (1995). Hydrogen-peroxide stimulates salicylic acid biosynthesis in tobacco. Plant Physiol. **108,** 1673-1678.

Leung, J., Merlot, S., and Giraudat, J. (1997). The *Arabidopsis* abscisic acid-insensitive2 (ABI2) and ABI1 genes encode homologous protein phosphatases 2C involved in abscisic acid signal transduction. Plant Cell **9,** 759-771.

Leung, Y.F., and Cavalieri, D. (2003). Fundamentals of cDNA microarray data analysis. Trends Genet. **19,** 649-659.

Li, C.M., Haapalainen, M., Lee, J., Nurnberger, T., Romantschuk, M., and Taira, S. (2005a). Harpin of *Pseudomonas syringae* pv. *phaseolicola* harbors a protein binding site. Mol. Plant-Microbe Interact. **18,** 60-66.

Li, X., Lin, H., Zhang, W., Zou, Y., Zhang, J., Tang, X., and Zhou, J. (2005b). Flagellin induces innate immunity in nonhost interactions that is suppressed by *Pseudomonas syringae* effectors. Proc. Natl. Acad. Sci. U. S. A. **102,** 12990–12995.

Li, Y., Li, T., Liu, S.Z., Qiu, M.Y., Han, Z.Y., Jiang, Z.L., Li, R.Y., Ying, K., Xie, Y., and Mao, Y.M. (2004). Systematic comparison of the fidelity of aRNA, mRNA and T-RNA on gene expression profiling using cDNA microarray. J. Biotechnol. **107,** 19-28.

Liang, H., Yao, N., Song, L.T., Luo, S., Lu, H., and Greenberg, L.T. (2003). Ceramides modulate programmed cell death in plants. Genes Dev. **17,** 2636-2641.

Lima, V.L.M., Coelho, L., Kennedy, J.F., Owen, J.S., and Dolphin, P.J. (2004). Lecithin-cholesterol acyltransferase (LCAT) as a plasma glycoprotein: An overview. Carbohydr. Polym. **55,** 179-191.

Lin, S.-H., Chong, Z.Z., and Maiese, K. (2002). The metabotropic glutamate receptor system: G-protein mediated pathways that modulate neuronal and vascular cellular injury. In Curr. Med. Chem. - Central Nervous System Agents, pp. 17-28.

Little, E.L., Bostock, R.M., and Kirkpatrick, B.C. (1998). Genetic characterization of *Pseudomonas syringae* pv. *syringae* strains from stone fruits in California. Appl. Environ. Microbiol. **64,** 3818-3823.

Liu, F.L., VanToai, T., Moy, L.P., Bock, G., Linford, L.D., and Quackenbush, J. (2005). Global transcription profiling reveals comprehensive insights into hypoxic response in *Arabidopsis*. Plant Physiol. **137,** 1115-1129.

Liu, X.S., Zou, H., Slaughter, C., and Wang, X.D. (1997). DFF, a heterodimeric protein that functions downstream of caspase-3 to trigger DNA fragmentation during apoptosis. Cell **89,** 175-184.

Liu, Y., Schiff, M., Serino, G., Deng, X.W., and Dinesh-Kumar, S.P. (2002). Role of SCF ubiquitin-ligase and the COP9 signalosome in the N gene-mediated resistance response to Tobacco mosaic virus. Plant Cell **14,** 1483-1496.

Lu, C.G., Koroleva, O.A., Farrar, J.F., Gallagher, J., Pollock, C.J., and Tomos, A.D. (2002). Rubisco small subunit, chlorophyll a/b-binding protein and sucrose: Fructan-6-fructosyl transferase gene expression and sugar status in single barley leaf cells in situ. Cell type specificity and induction by light. Plant Physiol. **130,** 1335-1348.

Lu, S.E., Wang, N., Wang, J.L., Chen, Z.J., and Gross, D.C. (2005). Oligonucleotide microarray analysis of the salA regulon controlling phytotoxin production by *Pseudomonas syringae* pv. *syringae*. Mol. Plant-Microbe Interact. **18,** 324-333.

Lyngkjaer, M.F., and Carver, T.L.W. (1999). Induced accessibility and inaccessibility to *Blumeria graminis* f.sp *hordei* in barley epidermal cells attacked by a compatible isolate. Physiological and Molecular Plant Pathology **55,** 151-162.

Mackey, D., Holt, B.F., Wiig, A., and Dangl, J.L. (2002). RIN4 interacts with *Pseudomonas syringae* type III effector molecules and is required for RPM1-mediated resistance in *Arabidopsis*. Cell **108,** 743-754.

MacKintosh, C. (1998). Regulation of cytosolic enzymes in primary metabolism by reversible protein phosphorylation. Curr. Opin. Plant Biol. **1,** 224-229.

Madsen, L.H., Collins, N.C., Rakwalska, M., Backes, G., Sandal, N., Krusell, L., Jensen, J., Waterman, E.H., Jahoor, A., Ayliffe, M., Pryor, A.J., Langridge, P., Schulze-Lefert, P., and Stougaard, J. (2003). Barley disease resistance gene analogs of the NBS-LRR class: Identification and mapping. Mol. Genet. Genomics **269,** 150-161.

Maniatis, T., Fritsch, E.F., and Sambrook, J. (1982). Molecular Cloning. A Laboratory Manual. (Cold Spring Harbor: Cold Spring Harbor Laboratory Press).

Marco, M.L., Legac, J., and Lindow, S.E. (2005). *Pseudomonas syringae* genes induced during colonization of leaf surfaces. Environ. Microbiol. **7,** 1379-1391.

Martinoia, E., Klein, M., Geisler, M., Bovet, L., Forestier, C., Kolukisaoglu, U., Muller-Rober, B., and Schulz, B. (2002). Multifunctionality of plant ABC transporters - more than just detoxifiers. Planta **214,** 345-355.

Martinova, E.A. (2003). Apoptotic regulation of caspase activity. Russ. J. Bioorg. Chem. **29,** 471-495.

Marx, J. (2004). The roots of plant-microbe collaborations. Science **304,** 234-236.

Maxwell, D.P., Wang, Y., and McIntosh, L. (1999). The alternative oxidase lowers mitochondrial reactive oxygen production in plant cells. Proc. Natl. Acad. Sci. U. S. A. **96,** 8271-8276.

Meijer, H.J.G., and Munnik, T. (2003). Phospholipid-based signaling in plants. Annu. Rev. Plant Biol. **54,** 265-306.

Meiners, S., Heyken, D., Weller, A., Ludwig, A., Stangl, K., Kloetzel, P.M., and Kruger, E. (2003). Inhibition of proteasome activity induces concerted expression of proteasome genes and *de Novo* formation of mammalian proteasomes. J. Biol. Chem. **278,** 21517-21525.

Melayah, D., Bonnivard, E., Chalhoub, B., Audeon, C., and Grandbastien, M.A. (2001). The mobility of the tobacco Tnt1 retrotransposon correlates with its transcriptional activation by fungal factors. Plant J. **28,** 159-168.

Merlot, S., Gosti, F., Guerrier, D., Vavasseur, A., and Giraudat, J. (2001). The ABI1 and ABI2 protein phosphatases 2C act in a negative feedback regulatory loop of the abscisic acid signalling pathway. Plant J. **25,** 295-303.

Millenaar, F.F., and Lambers, H. (2003). The alternative oxidase: In vivo regulation and function. Plant Biol. **5,** 2-15.

Mitra, R.M., Gleason, C.A., Edwards, A., Hadfield, J., Downie, J.A., Oldroyd, G.E.D., and Long, S.R. (2004). A Ca2+/calmodulin-dependent protein kinase required for symbiotic nodule development: Gene identification by transcript-based cloning. Proc. Natl. Acad. Sci. U. S. A. **101,** 4701-4705.

Mittler, R., Vanderauwera, S., Gollery, M., and Van Breusegem, F. (2004). Reactive oxygen gene network of plants. Trends in Plant Science **9,** 490-498.

Molecular Probes. (2004). The Handbook - A guide to fluorescent probes and labeling technologies (Molecular Probes).

Moon, J., Parry, G., and Estelle, M. (2004). The ubiquitin-proteasome pathway and plant development. Plant Cell **16,** 3181-3195.

Muthukrishnan, S., Liang, G.H., Trick, H.N., and Gill, B.S. (2001). Pathogenesis-related proteins and their genes in cereals. Plant Cell Tissue Organ Cult. **64,** 93-114.

Nardini, M., and Dijkstra, B.W. (1999). Alpha/beta hydrolase fold enzymes: The family keeps growing. Curr. Opin. Struct. Biol. **9,** 732-737.

Navarro, L., Zipfel, C., Rowland, O., Keller, I., Robatzek, S., Boller, T., and Jones, J.D.G. (2004). The transcriptional innate immune response to flg22. interplay and overlap with Avr gene-dependent defense responses and bacterial pathogenesis. Plant Physiol. **135,** 1113-1128.

Nemeth, K., Salchert, K., Putnoky, P., Bhalerao, R., Koncz-Kalman, Z., Stankovic-Stangeland, B., Bako, L., Mathur, J., Okresz, L., Stabel, S., Geigenberger, P., Stitt, M., Redei, G.P., Schell, J., and Koncz, C. (1998). Pleiotropic control of glucose and hormone responses by PRL1, a nuclear WD protein, in *Arabidopsis*. Genes Dev. **12,** 3059-3073.

Nicotera, P., and Leist, M. (1997). Energy supply and the shape of death in neurons and lymphoid cells. Cell Death Differ. **4,** 435-442.

Nijtmans, L.G.J., de Jong, L., Sanz, M.A., Coates, P.J., Berden, J.A., Back, J.W., Muijsers, A.O., van der Spek, H., and Grivell, L.A. (2000). Prohibitins act as a membrane-bound chaperone for the stabilization of mitochondrial proteins. Embo J. **19,** 2444-2451.

Nishimura, M., and Somerville, S. (2002). Plant biology - Resisting attack. Science **295,** 2032-2033.

Nomura, K., Melotto, M., and He, S.Y. (2005). Suppression of host defense in compatible plant-*Pseudomonas syringae* interactions. Curr. Opin. Plant Biol. **8,** 361-368.

Nugroho, L.H., Verberne, M.C., and Verpoorte, R. (2002). Activities of enzymes involved in the phenylpropanoid pathway in constitutively salicylic acid-producing tobacco plants. Plant Physiol. Biochem. **40,** 755-760.

Nürnberger, T., Brunner, F., Kemmerling, B., and Piater, L. (2004). Innate immunity in plants and animals: Striking similarities and obvious differences. Immunol. Rev. **198,** 249-266.

Oka, M., Yaginuma, K., Numata, K., Konishi, M., Oki, T., and Kawaguchi, H. (1988a). Glidobactins A, B and C - New antitumor antibiotics II Structure elucidation. J. Antibiot. **41,** 1338-1350.

Oka, M., Numata, K., Nishiyama, Y., Kamei, H., Konishi, M., Oki, T., and Kawaguchi, H. (1988b). Chemical modification of the antitumor antibiotic glidobactin. J. Antibiot. **41,** 1812-1822.

Opalski, K.S., Schultheiss, H., Kogel, K.H., and Hückelhoven, R. (2005). The receptor-like MLO protein and the RAC/ROP family G-protein RACB modulate actin reorganization in barley attacked by the biotrophic powdery mildew fungus *Blumeria graminis* f.sp *hordei*. Plant J. **41,** 291-303.

Ordog, S.H., Higgins, V.J., and Vanlerberghe, G.C. (2002). Mitochondrial alternative oxidase is not a critical component of plant viral resistance but may play a role in the hypersensitive response. Plant Physiol. **129,** 1858-1865.

Ortega, J., Heymann, J.B., Kajava, A.V., Ustrell, V., Rechsteiner, M., and Steven, A.C. (2005). The axial channel of the 20 S proteasome opens upon binding of the PA200 activator. J. Mol. Biol. **346,** 1221-1227.

Osakabe, Y., Maruyama, K., Seki, M., Satou, M., Shinozaki, K., and Yamaguchi-Shinozaki, K. (2005). Leucine-rich repeat receptor-like kinase1 is a key membrane-bound regulator of abscisic acid early signaling in *Arabidopsis*. Plant Cell **17,** 1105-1119.

Ouchi, S., Oku, H., and Hibino, C. (1976). Localization of induced resistance and susceptibility in barley leaves inoculated with powdery mildew fungus. Phytopathology **66,** 901-905.

Pabon, C., Modrusan, Z., Ruvolo, M.V., Coleman, I.M., Daniel, S., Yue, H., Arnold, L.J., and Reynolds, M.A. (2001). Optimized T7 amplification system for microarray analysis. Biotechniques **31,** 874-879.

Paillard, S., Schnurbusch, T., Winzeler, M., Messmer, M., Sourdille, P., Abderhalden, O., Keller, B., and Schachermayr, G. (2003). An integrative genetic linkage map of winter wheat (*Triticum aestivum* L.). Theor. Appl. Genet. **107,** 1235-1242.

Panstruga, R. (2003). Establishing compatibility between plants and obligate biotrophic pathogens. Curr. Opin. Plant Biol. **6,** 320-326.

PerkinElmer. (2002). ScanArray Express microarray scanner (PerkinElmer Life Sciences, Inc.).

Petersen, D., Chandramouli, G.V.R., Geoghegan, J., Hilburn, J., Paarlberg, J., Kim, C.H., Munroe, D., Gangi, L., Han, J., Puri, R., Staudt, L., Weinstein, J., Barrett, J.C., Green, J., and Kawasaki, E.S. (2005). Three microarray platforms: An analysis of their concordance in profiling gene expression. BMC Genomics **6,** 1-14.

Piffanelli, P., Zhou, F.S., Casais, C., Orme, J., Jarosch, B., Schaffrath, U., Collins, N.C., Panstruga, R., and Schulze-Lefert, P. (2002). The barley MLO modulator of defense and cell death is responsive to biotic and abiotic stress stimuli. Plant Physiol. **129,** 1076-1085.

Pirkkala, L., Nykanen, P., and Sistonen, L. (2001). Roles of the heat shock transcription factors in regulation of the heat shock response and beyond. Faseb J. **15,** 1118-1131.

Polacek, D.C., Passerini, A.G., Shi, C.Z., Francesco, N.M., Manduchi, E., Grant, G.R., Powell, S., Bischof, H., Winkler, H., Stoeckert, C.J., and Davies, P.F. (2003). Fidelity and enhanced sensitivity of differential transcription profiles following linear amplification of nanogram amounts of endothelial mRNA. Physiol. Genomics **13,** 147-156.

Pryce-Jones, E., Carver, T., and Gurr, S.J. (1999). The roles of cellulase enzymes and mechanical force in host penetration by *Erysiphe graminis* f.sp *hordei*. Physiological and Molecular Plant Pathology **55,** 175-182.

Quackenbush, J. (2002). Microarray data normalization and transformation. Nature Genet. **32,** 496-501.

Randolph, J.B., and Waggoner, A.S. (1997). Stability, specificity and fluorescence brightness of multiply-labeled fluorescent DNA probes. Nucleic Acids Research **25,** 2923-2929.

Rapizzi, E., Pinton, P., Szabadkai, G., Wieckowski, M.R., Vandecasteele, G., Baird, G., Tuft, R.A., Fogarty, K.E., and Rizzuto, R. (2002). Recombinant expression of the voltage-dependent anion channel enhances the transfer of Ca^{2+} microdomains to mitochondria. J. Cell Biol. **159,** 613-624.

Rasmusson, A.G., Soole, K.L., and Elthon, T.E. (2004). Alternative NAD(P)H dehydrogenases of plant mitochondria. Annu. Rev. Plant Biol. **55,** 23-39.

Reade, J.P.H., Milner, L.J., and Cobb, A.H. (2004). A role for glutathione S-transferases in resistance to herbicides in grasses. Weed Sci. **52,** 468-474.

Rebmann, G., Mauch, F., and Dudler, R. (1991). Sequence of a wheat cDNA encoding a pathogen-induced thaumatin-like protein. Plant Molecular Biology **17,** 283-285.

Reimmann, C., Hofmann, C., Mauch, F., and Dudler, R. (1995). Characterization of a rice gene induced by *Pseudomonas syringae* pv. *syringae* - requirement for the bacterial *lemA* gene-function. Physiological and Molecular Plant Pathology **46,** 71-81.

Reymond, P., Weber, H., Damond, M., and Farmer, E.E. (2000). Differential gene expression in response to mechanical wounding and insect feeding in *Arabidopsis*. Plant Cell **12,** 707-719.

Ricoult, C., Cliquet, J.B., and Limami, A.M. (2005). Stimulation of alanine amino transferase (AlaAT) gene expression and alanine accumulation in embryo axis of the model legume *Medicago truncatula* contribute to anoxia stress tolerance. Physiol. Plant. **123,** 30-39.

Rifkin, I.R., Leadbetter, E.A., Busconi, L., Viglianti, G., and Marshak-Rothstein, A. (2005). Toll-like receptors, endogenous ligands, and systemic autoimmune disease. Immunol. Rev. **204,** 27-42.

Robson, C.A., and Vanlerberghe, G.C. (2002). Transgenic plant cells lacking mitochondrial alternative oxidase have increased susceptibility to mitochondria-dependent and -independent pathways of programmed cell death. Plant Physiol. **129,** 1908-1920.

Roeder, A., Kirschning, C.J., Rupec, R.A., Schaller, M., Weindl, G., and Korting, H.C. (2004). Toll-like receptors as key mediators in innate antifungal immunity. Med. Mycol. **42,** 485-498.

Rojo, E., Martin, R., Carter, C., Zouhar, J., Pan, S.Q., Plotnikova, J., Jin, H.L., Paneque, M., Sanchez-Serrano, J.J., Baker, B., Ausubel, F.M., and Raikhel, N.V. (2004). VPE gamma exhibits a caspase-like activity that contributes to defense against pathogens. Current Biology **14,** 1897-1906.

Roskams, A.J.I., Friedman, V., Wood, C.M., Walker, L., Owens, G.A., Stewart, D.A., Altus, M.S., Danner, D.B., Liu, X.T., and McClung, J.K. (1993). Cell cycle activity and expression of prohibitin mRNA. J. Cell. Physiol. **157,** 289-295.

Ross, A.F. (1961a). Localized acquired resistance to plant virus infection in hypersensitive hosts. Virology **14,** 329-339.

Ross, A.F. (1961b). Systemic acquired resistance induced by localized virus infections in plants. Virology **14,** 340-358.

Rostovtseva, T., and Colombini, M. (1997). VDAC channels mediate and gate the flow of ATP: Implications for the regulation of mitochondrial function. Biophys. J. **72,** 1954-1962.

Rostovtseva, T.K., Antonsson, B., Suzuki, M., Youle, R.J., Colombini, M., and Bezrukov, S.M. (2004). Bid, but not Bax, regulates VDAC channels. J. Biol. Chem. **279,** 13575-13583.

Rotari, V.I., He, R., and Gallois, P. (2005). Death by proteases in plants: whodunit. Physiol. Plant. **123,** 376-385.

Sachs, M.M., Freeling, M., and Okimoto, R. (1980). The anaerobic proteins of maize. Cell **20,** 761-767.

Saeed, A.I., Sharov, V., White, J., Li, J., Liang, W., Bhagabati, N., Braisted, J., Klapa, M., Currier, T., Thiagarajan, M., Sturn, A., Snuffin, M., Rezantsev, A., Popov, D., Ryltsov, A., Kostukovich, E., Borisovsky, I., Liu, Z., Vinsavich, A., Trush, V., and Quackenbush, J. (2003). TM4: A free, open-source system for microarray data management and analysis. Biotechniques **34,** 374-378.

Salchert, K., Bhalerao, R., Koncz-Kalman, Z., and Koncz, C. (1998). Control of cell elongation and stress responses by steroid hormones and carbon catabolic repression in plants. Philos. Trans. R. Soc. Lond. Ser. B-Biol. Sci. **353,** 1517-1520.

Sanger, F., Nicklen, S., and Coulson, A.R. (1977). DNA sequencing with chain-terminating inhibitors. Proc. Natl. Acad. Sci. U. S. A. **74,** 5463-5467.

Sanmartin, M., Jaroszewski, L., Raikhel, N.V., and Rojo, E. (2005). Caspases. Regulating death since the origin of life. Plant Physiol. **137,** 841-847.

Schaffrath, U., Freydl, E., and Dudler, R. (1997). Evidence for different signaling pathways activated by inducers of acquired resistance in wheat. Mol. Plant-Microbe Interact. **10,** 779-783.

Scharf, K.D., Siddique, M., and Vierling, E. (2001). The expanding family of Arabidopsis thaliana small heat stress proteins and a new family of proteins containing alpha-crystallin domains (Acd proteins). Cell Stress Chaperones **6,** 225-237.

Scheideler, M., Schlaich, N.L., Fellenberg, K., Beissbarth, T., Hauser, N.C., Vingron, M., Slusarenko, A.J., and Hoheisel, J.D. (2002). Monitoring the switch from housekeeping to pathogen defense metabolism in *Arabidopsis thaliana* using cDNA arrays. J. Biol. Chem. **277,** 10555-10561.

Schena, M., Shalon, D., Davis, R.W., and Brown, P.O. (1995). Quantitative monitoring of gene-expression patterns with a complementary-DNA microarray. Science **270,** 467-470.

Schlegel, T.K., Schönherr, J., and Schreiber, L. (2005). Size selectivity of aqueous pores in stomatous cuticles of *Vicia faba* leaves. Planta **221,** 648-655.

Schulze-Lefert, P., and Vogel, J. (2000). Closing the ranks to attack by powdery mildew. Trends in Plant Science **5,** 343-348.

Schulze-Lefert, P., and Bieri, S. (2005). Recognition at a distance. Science **308,** 506-508.

Schwantes, H.O., and Weberling, F. (1981). Pflanzensystematik. Einführung in die systematische Botanik. Grundzüge des Pflanzensystems. (Stuttgart, Germany: Eugen Ulmer Gmbh & Co.).

Schwechheimer, C., Serino, G., Callis, J., Crosby, W.L., Lyapina, S., Deshaies, R.J., Gray, W.M., Estelle, M., and Deng, X.W. (2001). Interactions of the COP9 signalosome with the E3 ubiquitin ligase SCF^{TIR1} in mediating auxin response. Science **292,** 1379-1382.

Schweizer, P., Hunziker, W., and Moesinger, E. (1989). cDNA cloning, invitro transcription and partial sequence-analysis of messenger-RNAs from winter-wheat (*Triticum aestivum* L.) with induced resistance to *Erysiphe graminis* f.sp *tritici*. Plant Molecular Biology **12,** 643-654.

Schweizer, P., Christoffel, A., and Dudler, R. (1999a). Transient expression of members of the germin-like gene family in epidermal cells of wheat confers disease resistance. Plant J. **20,** 540-552.

Schweizer, P., Pokorny, J., Abderhalden, O., and Dudler, R. (1999b). A transient assay system for the functional assessment of defense-related genes in wheat. Mol. Plant-Microbe Interact. **12,** 647-654.

Schweizer, P., Schlagenhauf, E., Schaffrath, U., and Dudler, R. (1999c). Different patterns of host genes are induced in rice by *Pseudomonas syringae*, a biological inducer of resistance, and the chemical inducer benzothiadiazole (BTH). Eur. J. Plant Pathol. **105,** 659-665.

Schweizer, P., Pokorny, J., Schulze-Lefert, P., and Dudler, R. (2000). Double-stranded RNA interferes with gene function at the single-cell level in cereals. Plant J. **24,** 895-903.

Seidegard, J., and Ekstrom, G. (1997). The role of human glutathione transferases and epoxide hydrolases in the metabolism of xenobiotics. Environ. Health Perspect. **105,** 791-799.

Sela-Buurlage, M.B., Ponstein, A.S., Bresvloemans, S.A., Melchers, L.S., Vandenelzen, P.J.M., and Cornelissen, B.J.C. (1993). Only specific tobacco (*Nicotiana tabacum*) chitinases and beta-1,3-glucanases exhibit antifungal activity. Plant Physiol. **101,** 857-863.

Shalon, D., Smith, S.J., and Brown, P.O. (1996). A DNA microarray system for analyzing complex DNA samples using two-color fluorescent probe hybridization. Genome Res. **6,** 639-645.

Sheng, L. (2003). Protein phosphatases in plants. Annu. Rev. Plant Biol. **54,** 63-92.

Shimada, T., Yamada, K., Kataoka, M., Nakaune, S., Koumoto, Y., Kuroyanagi, M., Tabata, S., Kato, T., Shinozaki, K., Seki, M., Kobayashi, M., Kondo, M., Nishimura, M., and Hara-Nishimura, I. (2003). Vacuolar processing enzymes are essential for proper processing of seed storage proteins in *Arabidopsis thaliana*. J. Biol. Chem. **278,** 32292-32299.

Shimizu, S., Narita, M., and Tsujimoto, Y. (1999). Bcl-2 family proteins regulate the release of apoptogenic cytochrome c by the mitochondrial channel VDAC. Nature **399,** 483-487.

Shimizu, S., Ide, T., Yanagida, T., and Tsujimoto, Y. (2000). Electrophysiological study of a novel large pore formed by Bax and the voltage-dependent anion channel that is permeable to cytochrome c. J. Biol. Chem. **275,** 12321-12325.

Shinshi, H., Neuhaus, J.M., Ryals, J., and Meins, F. (1990). Structure of a tobacco endochitinase gene: Evidence that different chitinase genes can arise by transposition of sequences encoding a cysteine-rich domain. Plant Molecular Biology **14,** 357-368.

Shirasu, K., and Schulze-Lefert, P. (2003). Complex formation, promiscuity and multi-functionality: protein interactions in disease-resistance pathways. Trends in Plant Science **8,** 252-258.

Shirasu, K., Nielsen, K., Piffanelli, P., Oliver, R., and Schulze-Lefert, P. (1999). Cell-autonomous complementation of mlo resistance using a biolistic transient expression system. Plant J. **17,** 293-299.

Shoji, J., Hinoo, H., Kato, T., Hattori, T., Hirooka, K., Tawara, K., Shiratori, O., and Terui, Y. (1990). Isolation of cepafungins I, II and III from *Pseudomonas* species. J. Antibiot. **43,** 783-787.

Shomura, Y., Dragovic, Z., Chang, H.C., Tzvetkov, N., Young, J.C., Brodsky, J.L., Guerriero, V., Hartl, F.U., and Bracher, A. (2005). Regulation of Hsp70 function by HspBP1: Structural analysis reveals an alternate mechanism for Hsp70 nucleotide exchange. Mol. Cell **17,** 367-379.

Sidler, M., Hassa, P., Hasan, S., Ringli, C., and Dudler, R. (1998). Involvement of an ABC transporter in a developmental pathway regulating hypocotyl cell elongation in the light. Plant Cell **10,** 1623-1636.

Smith, J.A., and Métraux, J.P. (1991). *Pseudomonas syringae* pv. *syringae* induces systemic resistance to *pyricularia oryzae* in Rice. Physiological and Molecular Plant Pathology **39,** 451-461.

Snedden, W.A., and Fromm, H. (1997). Characterization of the plant homologue of prohibitin, a gene associated with antiproliferative activity in mammalian cells. Plant Molecular Biology **33,** 753-756.

Sommer, T., Jarosch, E., and Lenk, U. (2001). Compartment-specific functions of the ubiquitin-proteasome pathway. In Reviews of Physiology Biochemistry and Pharmacology (Berlin: Springer Verlag, Berlin, Germany), pp. 97-160.

Soukas, A., Cohen, P., Socci, N.D., and Friedman, J.M. (2000). Leptin-specific patterns of gene expression in white adipose tissue. Genes Dev. **14,** 963-980.

Srichumpa, P., Brunner, S., Keller, B., and Yahiaoui, N. (2005). Allelic series of four powdery mildew resistance genes at the *Pm3* locus in hexaploid bread wheat. Plant Physiol. **(in press)**.

Staden, R. (1996). The Staden sequence analysis package. Mol. Biotechnol. **5,** 233-241.

Staxén, I., Pical, C., Montgomery, L.T., Gray, J.E., Hetherington, A.M., and McAinsh, M.R. (1999). Abscisic acid induces oscillations in guard-cell cytosolic free calcium that involve phosphoinositide-specific phospholipase C. Proc. Natl. Acad. Sci. U. S. A. **96,** 1779-1784.

Stein, M., and Somerville, S.C. (2002). MLO, a novel modulator of plant defenses and cell death, binds calmodulin. Trends in Plant Science **7,** 379-380.

Stryer, L. (1988). Biochemistry. (New York: Freeman & Co.).

Subbaiah, C.C., and Sachs, M.M. (2003). Molecular and cellular adaptations of maize to flooding stress. Ann. Bot. **91,** 119-127.

Subramanian, V., Rothenberg, A., Gomez, C., Cohen, A.W., Garcia, A., Bhattacharyya, S., Shapiro, L., Dolios, G., Wang, R., Lisanti, M.P., and Brasaemle, D.L. (2004). Perilipin A mediates the reversible binding of CGI-58 to lipid droplets in 3T3-L1 adipocytes. J. Biol. Chem. **279,** 42062-42071.

Sugimoto, K., Takeda, S., and Hirochika, H. (2000). MYB-related transcription factor NtMYB2 induced by wounding and elicitors is a regulator of the tobacco retrotransposon Tto1 and defense-related genes. Plant Cell **12,** 2511-2527.

Sullivan, J.A., Shirasu, K., and Deng, X.W. (2003). The diverse roles of ubiquitin and the 26S proteasome in the life of plants. Nat. Rev. Genet. **4,** 948-958.

Sutton, P.N., Henry, M.J., and Hall, J.L. (1999). Glucose, and not sucrose, is transported from wheat to wheat powdery mildew. Planta **208,** 426-430.

Suzuki, M., Kao, C.Y., Cocciolone, S., and McCarty, D.R. (2001). Maize VP1 complements *Arabidopsis abi3* and confers a novel ABA/auxin interaction in roots. Plant J. **28,** 409-418.

Takahashi, A., Casais, C., Ichimura, K., and Shirasu, K. (2003). HSP90 interacts with RAR1 and SGT1 and is essential for RPS2-mediated disease resistance in *Arabidopsis*. Proc. Natl. Acad. Sci. U. S. A. **100,** 11777-11782.

Takeda, K., and Akira, S. (2005). Toll-like receptors in innate immunity. Int. Immunol. **17,** 1-14.

Takeuchi, J., Fujimuro, M., Yokosawa, H., Tanaka, K., and Toh-e, A. (1999). Rpn9 is required for efficient assembly of the yeast 26S proteasome. Mol. Cell. Biol. **19,** 6575-6584.

Thaler, J.S., Owen, B., and Higgins, V.J. (2004). The role of the jasmonate response in plant susceptibility to diverse pathogens with a range of lifestyles. Plant Physiol. **135,** 530-538.

Thompson, W.E., Ramalho-Santos, J., and Sutovsky, P. (2003). Ubiquitination of prohibitin in mammalian sperm mitochondria: Possible roles in the regulation of mitochondrial inheritance and sperm quality control. Biol. Reprod. **69,** 254-260.

Thordal-Christensen, H. (2003). Fresh insights into processes of nonhost resistance. Curr. Opin. Plant Biol. **6,** 351-357.

Thordal-Christensen, H., Zhang, Z.G., Wei, Y.D., and Collinge, D.B. (1997). Subcellular localization of H_2O_2 in plants. H_2O_2 accumulation in papillae and hypersensitive response during the barley-powdery mildew interaction. Plant J. **11,** 1187-1194.

Tör, M., Yemm, A., and Holub, E. (2003). The role of proteolysis in *R* gene mediated defence in plants. Mol. Plant Pathol. **4,** 287-296.

Tsujimoto, Y. (1997). Apoptosis and necrosis: Intracellular ATP level as a determinant for cell death modes. Cell Death Differ. **4,** 429-434.

Turano, F.J., Panta, G.R., Allard, M.W., and van Berkum, P. (2001). The putative glutamate receptors from plants are related to two superfamilies of animal neurotransmitter receptors via distinct evolutionary mechanisms. Mol. Biol. Evol. **18,** 1417-1420.

Ustrell, V., Hoffman, L., Pratt, G., and Rechsteiner, M. (2002). PA200, a nuclear proteasome activator involved in DNA repair. Embo J. **21,** 3516-3525.

Van Gelder, R.N., Vonzastrow, M.E., Yool, A., Dement, W.C., Barchas, J.D., and Eberwine, J.H. (1990). Amplified RNA Synthesized from limited quantities of heterogeneous cDNA. Proc. Natl. Acad. Sci. U. S. A. **87,** 1663-1667.

Vicient, C.M., Suoniemi, A., Anamthamat-Jonsson, K., Tanskanen, J., Beharav, A., Nevo, E., and Schulman, A.H. (1999). Retrotransposon BARE-1 and its role in genome evolution in the genus *Hordeum*. Plant Cell **11,** 1769-1784.

Vierstra, R.D. (2003). The ubiquitin/26S proteasome pathway, the complex last chapter in the life of many plant proteins. Trends in Plant Science **8,** 135-142.

von Röpenack, E., Parr, A., and Schulze-Lefert, P. (1998). Structural analyses and dynamics of soluble and cell wall-bound phenolics in a broad spectrum resistance to the powdery mildew fungus in barley. J. Biol. Chem. **273,** 9013-9022.

von Stein, O.D., Thies, W.G., and Hofmann, M. (1997). A high throughput screening for rarely transcribed differentially expressed genes. Nucleic Acids Research **25,** 2598-2602.

Wang, H.X., He, X.M., Band, M., Wilson, C., and Liu, L. (2005). A study of inter-lab and inter-platform agreement of DNA microarray data. BMC Genomics **6**.

Wang, M., Hoekstra, S., van Bergen, S., Lamers, G.E.M., Oppedijk, B.J., van der Heijden, M.W., de Priester, W., and Schilperoort, R.A. (1999). Apoptosis in developing anthers and the role of ABA in this process during androgenesis in *Hordeum vulgare* L. Plant Molecular Biology **39,** 489-501.

Wang, W.X., Vinocur, B., Shoseyov, O., and Altman, A. (2004). Role of plant heat-shock proteins and molecular chaperones in the abiotic stress response. Trends in Plant Science **9,** 244-252.

Ward, E.R., Uknes, S.J., Williams, S.C., Dincher, S.S., Wiederhold, D.L., Alexander, D.C., Ahlgoy, P., Metraux, J.P., and Ryals, J.A. (1991). Coordinate gene activity in response to agents that induce systemic acquired-resistance. Plant Cell **3,** 1085-1094.

Wäspi, U., Schweizer, P., and Dudler, R. (2001). Syringolin reprograms wheat to undergo hypersensitive cell death in a compatible interaction with powdery mildew. Plant Cell **13,** 153-161.

Wäspi, U., Blanc, D., Winkler, T., Ruedi, P., and Dudler, R. (1998a). Syringolin, a novel peptide elicitor from *Pseudomonas syringae* pv. *syringae* that induces resistance to *Pyricularia oryzae* in rice. Mol. Plant-Microbe Interact. **11,** 727-733.

Wäspi, U., Hassa, P., Staempfli, A.A., Molleyres, L.P., Winkler, T., and Dudler, R. (1999). Identification and structure of a family of syringolin variants: Unusual cyclic peptides from *Pseudomonas syringae* pv. *syringae* that elicit defense responses in rice. Microbiol. Res. **154,** 89-93.

Wäspi, U., Misteli, B., Hasslacher, M., Jandrositz, A., Kohlwein, S.D., Schwab, H., and Dudler, R. (1998b). The defense-related rice gene *Pir7b* encodes an alpha/beta hydrolase fold protein exhibiting esterase activity towards naphthol AS-esters. Eur. J. Biochem. **254,** 32-37.

Watanabe, N., and Lam, E. (2004). Recent advance in the study of caspase-like proteases and Bax inhibitor-1 in plants: their possible roles as regulator of programmed cell death. Mol. Plant Pathol. **5,** 65-70.

Wei, F.S., Wong, R.A., and Wise, R.P. (2002). Genome dynamics and evolution of the *Mla* (powdery mildew) resistance locus in barley. Plant Cell **14,** 1903-1917.

Wessler, S.R. (1996). Plant retrotransposons: Turned on by stress. Current Biology **6,** 959-961.

Whiteford, J.R., and Spanu, P.D. (2002). Hydrophobins and the interactions between fungi and plants. Mol. Plant Pathol. **3,** 391-400.

Windsor, B., Roux, S.J., and Lloyd, A. (2003). Multiherbicide tolerance conferred by AtPgp1 and apyrase overexpression in *Arabidopsis thaliana*. Nat. Biotechnol. **21,** 428-433.

Woltering, E.J. (2004). Death proteases come alive. Trends in Plant Science **9,** 469-472.

Woltering, E.J., van der Bent, A., and Hoeberichts, F.A. (2002). Do plant Caspases exist? Plant Physiol. **130,** 1764-1769.

Woodman, P.G. (2003). p97, a protein coping with multiple identities. J. Cell Sci. **116,** 4283-4290.

Wyand, R.A., and Brown, J.K.M. (2003). Genetic and forma specialis diversity in *Blumeria graminis* of cereals and its implications for host-pathogen co-evolution. Mol. Plant Pathol. **4,** 187-198.

Xanthoudakis, S., and Nicholson, D.W. (2000). Heat-shock proteins as death determinants. Nat. Cell Biol. **2,** E163-E165.

Xiao, S.Y., Calis, O., Patrick, E., Zhang, G.G., Charoenwattana, P., Muskett, P., Parker, J.E., and Turner, J.G. (2005). The atypical resistance gene, *RPW8*, recruits components of basal defence for powdery mildew resistance in *Arabidopsis*. Plant J. **42,** 95-110.

Yahiaoui, N., Srichumpa, P., Dudler, R., and Keller, B. (2004). Genome analysis at different ploidy levels allows cloning of the powdery mildew resistance gene *Pm3b* from hexaploid wheat. Plant J. **37,** 528-538.

Yang, I.V., Chen, E., Hasseman, J.P., Liang, W., Frank, B.C., Wang, S., Sharov, V., Saeed, A.I., White, J., Li, J., Lee, N.H., Yeatman, T.J., and Quackenbush, J. (2002a). Within the fold: assessing differential expression measures and reproducibility in microarray assays. Genome Biology **3,** 1-13.

Yang, P.Z., Fu, H.Y., Walker, J., Papa, C.M., Smalle, J., Ju, Y.M., and Vierstra, R.D. (2004). Purification of the *Arabidopsis* 26 S proteasome - Biochemical and molecular analyses revealed the presence of multiple isoforms. J. Biol. Chem. **279,** 6401-6413.

Yang, Y.H., Dudoit, S., Luu, P., Lin, D.M., Peng, V., Ngai, J., and Speed, T.P. (2002b). Normalization for cDNA microarray data: a robust composite method addressing single and multiple slide systematic variation. Nucleic Acids Research **30**.

Yao, N., Eisfelder, B.J., Marvin, J., and Greenberg, J.T. (2004). The mitochondrion - an organelle commonly involved in programmed cell death in *Arabidopsis thaliana*. Plant J. **40,** 596-610.

Yu, L.H., Gaitatzes, C., Neer, E., and Smith, T.E. (2000). Thirty-plus functional families from a single motif. Protein Sci. **9,** 2470-2476.

Zalman, L.S., Nikaido, H., and Kagawa, Y. (1980). Mitochondrial outer-membrane contains a protein producing nonspecific diffusion channels. J. Biol. Chem. **255,** 1771-1774.

Zeller, F.J., Lutz, J., and Stephan, U. (1993). Chromosome Location of Genes for Resistance to Powdery Mildew in Common Wheat (*Triticum-Aestivum* L) .1. *Mlk* and Other Alleles at the *Pm3* Locus. Euphytica **68,** 223-229.

Zeyen, R.J., Carver, T.L.W., and Lingkjaer, M.F. (2002). Epidermal cell papillae. In The powdery mildews, R.R. Bélanger, W.R. Bushnell, A.J. Dik, and T.L.W. Carver, eds (St. Paul, MN: APS Press), pp. 107-125.

Zhang, W.H., Qin, C.B., Zhao, J., and Wang, X.M. (2004a). Phospholipase D alpha 1-derived phosphatidic acid interacts with ABI1 phosphatase 2C and regulates abscisic acid signaling. Proc. Natl. Acad. Sci. U. S. A. **101,** 9508-9513.

Zhang, W.H., Wang, C.X., Qin, C.B., Wood, T., Olafsdottir, G., Welti, R., and Wang, X.M. (2003). The oleate-stimulated phospholipase D, PLD delta, and phosphatidic acid decrease H_2O_2-induced cell death in *Arabidopsis*. Plant Cell **15,** 2285-2295.

Zhang, X.R., Garreton, V., and Chua, N.H. (2005). The AIP2 E3 ligase acts as a novel negative regulator of ABA signaling by promoting ABI3 degradation. Genes Dev. **19,** 1532-1543.

Zhang, Y., Dorey, S., Swiderski, M., and Jones, J.D.G. (2004b). Expression of RPS4 in tobacco induces an AvrRps4-independent HR that requires EDS1, SGT1 and HSP90. Plant J. **40,** 213-224.

Zhou, F.S., Kurth, J.C., Wei, F.S., Elliott, C., Vale, G., Yahiaoui, N., Keller, B., Somerville, S., Wise, R., and Schulze-Lefert, P. (2001). Cell-autonomous expression of barley *Mla1* confers race-specific resistance to the powdery mildew fungus via a *Rar1*-independent signaling pathway. Plant Cell **13,** 337-350.

Zierold, U., Scholz, U., and Schweizer, P. (2005). Transcriptome analysis of *mlo*-mediated resistance in the epidermis of barley. Mol. Plant Pathol. **6,** 139-151.

Zipfel, C., Robatzek, S., Navarro, L., Oakeley, E.J., Jones, J.D.G., Felix, G., and Boller, T. (2004). Bacterial disease resistance in *Arabidopsis* through flagellin perception. Nature **428,** 764-767.

8. Appendix

8.1. Hybridization signal classes

Table 8.1: Signal class overview for dot blot data acquisition. Since overall signal intensities derived from cDNA hybridization was comparably lower than the one corresponding to subtracted pool hybridization, classes on the cDNA hybridizations were shifted towards lower signals.

signal classes	+++	++	+	(+)	-
subtraction hybridizations					
cDNA hybridizations					

8.2. Similarity groups overview

Table 8.2: Similarity groups (SGs) identified by phrap assembly. cDNA fragments used for microarray downstream analysis are outlined in bold letters. Horizontal lines inside SGs delimit contigs indicative for isoenzymes. SGs were obtained by low-pass assembly with min. percentage overlap = 20 bp and min. match percentage = 75 %. Contigs were obtained by high-pass assembly with min. percentage overlap = 100 bp and min. match percentage = 98 %. Hybridization classes obtained by reverse northern dot blot hybridization (chapt. 4.1.5) are given in the following order: forward subtracted probe, reverse subtracted probe, probe corresponding to syringolin treatment-derived cDNA and probe corresponding to control cDNA. Accession numbers of sequences submitted to the European Bioinformatics Institute (EBI) are listed. #N/A denotes no submission.

SG 01	***α1B01***	AJ874072	+++	-	+	-
hsp 23.5	*α2B12*	#N/A	+++	-	+	-
	α2C10	AJ890230	+++	(+)	+	-

SG 02	***α1C12***	AJ888600	+++	-	+	-
fructose-bisphosphate aldolase	*α1F02*	#N/A	+++	+	+	-
	α1F09	#N/A	+++	-	+	-
	α2D02	#N/A	+++	-	+	-
	β1F10	#N/A	+	(+)	+	-
	β3B02	#N/A	++	(+)	+	-
	β2C02	AJ890240	(+)	-	(+)	(+)

SG 03	***α1D09***	AJ888604	+++	-	+	-
cytochrome P450	*α2B01*	#N/A	++	-	(+)	-
	α1F06	#N/A	+++	-	(+)	-
	β1G02	AJ890236	++	-	(+)	-

SG 04	***α2G01***	AJ888626	+++	-	+	-
enolase 1	*α3B07*	#N/A	+++	-	+	-
	α3C07	#N/A	+++	-	+	-
	α3E02	#N/A	+++	(+)	+	-
	α3E03	#N/A	+++	(+)	+	-
	β1D04	#N/A	+++	-	++	-
	β2G02	#N/A	+++	(+)	++	-
	α3G04	#N/A	+++	-	+	-
	β2H04	#N/A	+++	-	++	-

SG 05	***α3A01***	AJ888631	+	(+)	-	-
glutathione-S-transferase	*α3B10*	#N/A	+	(+)	-	-
	α3D03	#N/A	+	(+)	-	-

SG 06						
enolase 2	*α2A04*	#N/A	+++	-	+	-
	α3D01	#N/A	+++	(+)	+	-
	α3H09	#N/A	+++	(+)	+	-
	β1B02	#N/A	+++	-	+	-
	β1E06	#N/A	+++	-	+	-
	β2F02	AJ890241	+++	(+)	++	(+)
	β2A09	AJ888670	+++	+	++	+
	β2F11	#N/A	+++	-	++	-
	β1H01	#N/A	(+)	-	(+)	-

SG 07						
unknown	*β2E02*	#N/A	(+)	(+)	-	-
	β3B01	AJ888698	+	-	(+)	-

SG 08						
glyceraldehyde 3-	*α1H03*	#N/A	+++	+	+	(+)
phosphate	*α2H10*	#N/A	+++	(+)	+	-
dehydrogenase	*α2H11*	#N/A	+++	+	+	(+)
(cytosolic)	*β1G06*	#N/A	+++	-	++	(+)
	β3C10	AJ874100	+++	+	++	+
	β3F07	#N/A	+++	+	++	+
	β2A12	AJ890238	+++	++	++	+

SG 09						
unknown	***α1F05***	AJ888609	+++	+	(+)	-
	β3A06	#N/A	++	(+)	+	(+)
	β3H01	AJ890245	+	-	(+)	-
	α3B12	#N/A	++	+	-	-
	β1C05	AJ890246	+	(+)	(+)	-

SG 10						
epoxide hydrolase	***β3B10***	AJ888700	+	-	(+)	-
	β3F10	#N/A	+	-	(+)	-
	α1H10	AJ890243	++	++	(+)	(+)
	α1B12	#N/A	+++	-	(+)	-
	α3H11	#N/A	+++	+	+	
	β2H01	AJ888690	+++	-	+	-
	β2A10	#N/A	+++	-	+	-
	α1C10	#N/A	+++	(+)	(+)	-
	β1B11	#N/A	+++	-	(+)	-
	β3H05	AJ890244	+	-	+	+

SG 11						
pir7b	*α2D06*	#N/A	+++	(+)	+	-
SA-binding protein	***β1B01***	AJ874087	+++	-	++	-
Ethylene-induced /	*β2G03*	#N/A	+++	-	+	-
Polyneuridine-	*β3C07*	#N/A	+++	-	++	-
aldehyde esterase	*β1A02*	#N/A	+	-	(+)	-
	β2D04	#N/A	+++	-	+	-
	β3A02	#N/A	+++	-	+++	-
	β1B06	AJ890242	+++	-	++	-
	β1H09	#N/A	+++	-	++	-
	β2H06	#N/A	+++	-	++	-
	β1G01	#N/A	+++	-	++	-
	β2A07	AJ874094	+++	-	++	-
	β2F03	#N/A	+++	-	++	-
	β3D03	#N/A	+++	-	++	-

SG 12						
20S proteasome α4	***β1A08***	AJ888652	+	(+)	(+)	-
	β2D01	#N/A	+	+	(+)	

SG 13						
voltage-dependent	*α1D05*	#N/A	+++	-	+	-
anion channel 1	***β1F04***	AJ888662	+++	-	+	-
	β2A01	#N/A	+++	-	+	-
	β3D02	#N/A	+	-	(+)	-
	β3G06	#N/A	++	(+)	(+)	-

SG 14						
alcohol dehydrogenase	***α1D06***	AJ888602	+++	-	+	-
ADH1	*α1G05*	#N/A	+++	(+)	+	-
	α3F11	#N/A	+++	(+)	(+)	-
	α2A09	#N/A	++	-	(+)	-
	β1A04	AJ890239	+++	-	+	-

SG 15						
sucrose synthase 1	***α3A03***	AJ888632	+++	(+)	(+)	(+)
	α3F06	#N/A	++	-	(+)	(+)

SG 16						
succinyl-CoA-ligase β	***β1E11***	AJ874090	+	-	+	(+)
	α3B05	#N/A	++	(+)	(+)	(+)

SG 17						
ABI3-interacting	***β2A06***	AJ888668	+++	-	+	-
protein 2	*β2C08*	#N/A	+++	-	+	-
	β3H06	#N/A	+++	-	+	-
	β2G08	AJ890233	+++	-	+	-

SG 18						
proteasome regulatory	***β1C03***	AJ888656	+	-	(+)	-
	β2H02	#N/A	+	-	(+)	-

SG 19						
enoyl-CoA hydratase	*α1E01*	#N/A	+	(+)	-	-
	α2E05	AJ888621	++	+	-	-

SG 20						
pyruvate kinase	***β1B10***	AJ888655	++	-	++	(+)
	β1F09	#N/A	+++	-	++	(+)

SG 21						
hsp 70	***α3C06***	AJ888638	++	+	+	(+)
	α3F02	#N/A	+++	+	++	(+)

SG 22						
cytochrome P450	***α1C04***	AJ888598	+++	+	+	-
	α2D12	AJ890237	+++	-	(+)	
	β1D06	AJ888659	++	-	(+)	-
	β1D10	#N/A	+	-	(+)	-

SG 23						
ubiquitin conjugating	***β1D12***	AJ888661	(+)	-	(+)	(+)
	β2G06	#N/A	+	-	(+)	(+)

SG 24]						
20S proteasome β2	*β2D09*	#N/A	+++	-	+	(+)
	β3H03	AJ888717	+++	-	+	-

SG 25						
succinyl-CoA-ligase β	***β1D01***	AJ874089	++	-	+	(+)
	β1E08	#N/A	++	-	+	(+)

SG 26						
no significant hit	***α1D08***	AJ888603	+++	-	+	(+)
	β1A06	AJ874086	+++	-	(+)	-
	β2B07	AJ888674	+++	-	+	-
	β1E03	#N/A	++	-	(+)	-

SG 27	***β1A07***	AJ888651	(+)	-	(+)	-
nuclear coiled-coil	*β1D09*	#N/A	(+)	-	(+)	(+)

SG 28	*α3G03*	#N/A	(+)	-	-	-
glutath. S-transferase	***α3G10***	AJ888647	+	(+)	(+)	-

SG 29	*β1H06*	#N/A	++	-	+	-
glutath. S-transferase	***β3D05***	AJ874102	+++	-	++	-

SG 30	***β1G05***	AJ874091	++	-	+	-
20S proteasome α5	*β3C04*	#N/A	+++	-	+	(+)

SG 31	***α1E09***	AJ888607	++	-	+	-
BRI1-KD interacting	*α2G06*	#N/A	++	(+)	+	(+)
protein 130	*α3B06*	#N/A	++	-	(+)	(+)

SG 32	***α1H02***	AJ874076	+++	(+)	++	-
hsp 23.6	*α3F05*	AJ890231	++	(+)	(+)	(+)
	α3C08	#N/A	+++	+	++	-
	α3H06	AJ890232	+++	+	++	-
	α3H08	#N/A	+++	+	++	-

SG 33	***α1C01***	AJ888597	++	++	+	(+)
unknown	*α1F01*	#N/A	++	++	+	(+)

SG 34	*β1H07*	#N/A	+	-	+	(+)
20S proteasome β6	***β2C07***	AJ888678	++	(+)	+	+

SG 35	***α1A10***	AJ888594	+++	++	++	+
polyubiquitin	*α2G10*	AJ890235	+++	+	++	+

SG 36	***α1E06***	AJ874074	+++	-	(+)	-
alternative oxidase	*α2G07*	#N/A	+++	(+)	(+)	-

SG 37	*α1D02*	AJ890234	++	(+)	-	-
proteasome regulatory	***α2C11***	AJ888616	+++	(+)	(+)	-

SG 38	*α2A10*	AJ890247	++	-	+	-
ABC transporter	***α3H01***	AJ888649	+++	(+)	+	-

SG 39	***α2A05***	AJ888612	++	-	(+)	-
alcohol dehydrogen.	*β2D06*	#N/A	+++	-	+	-

SG 40	*α1C05*	#N/A	++	+	-	-
no significant hit	***α1D03***	AJ888601	++	+	+	-

SG 41	***β2B04***	AJ888672	+++	(+)	++	-
pyruvate kinase	*β3H11*	#N/A	+++	-	+	+

8.3. Array design

Table 8.3: Control probes (subset 3). Control probe categories are 'ITEC' for ESTs of the International *Triticeae* EST Cooperative, 'PR' for PR genes, 'HOUSE' for putative housekeeping genes, 'HYB' for surveillance of hybridizations and experiments and 'RNA' for surveillance of target quality.

probe ID	access. #no	origin	category	function
BE437387	BE437387	barley	ITEC	histone H2A
BE437255	BE437255	barley	ITEC	ascorbate peroxidase
BE437261	BE437261	barley	ITEC	actin
BE437288	BE437288	barley	ITEC	hsp90
BE437291	BE437291	barley	ITEC	nucleolar protein
BE437451	BE437451	barley	ITEC	ribulose-bisphosphate carboxylase small subunit
BE437465	BE437465	barley	ITEC	unknown
BE437518	BE437518	barley	ITEC	unknown
BE437539	BE437539	barley	ITEC	60S ribosomal protein L11
BE437593	BE437593	barley	ITEC	phospho-2-dehydro-3-deoxyheptonate aldolase 1
BE437599	BE437599	barley	ITEC	elongation factor 1-α
BE437621	BE437621	barley	ITEC	cytochrome c oxidase subunit 6B
BE437646	BE437646	barley	ITEC	protein kinase
BE437656	BE437656	barley	ITEC	protein kinase
BE437752	BE437752	barley	ITEC	ubiquitin-conjugating enzyme
BE437891	BE437891	barley	ITEC	glyceraldehyde-3-phosphate dehydrogenase
BE437892	BE437892	barley	ITEC	ribulose-bisphosphate carboxylase small subunit
BE437899	BE437899	barley	ITEC	glyceraldehyde-3-phosphate dehydrogenase
BE437979	BE437979	barley	ITEC	carbamoyl-phosphate synthetase small subunit
BE437985	BE437985	barley	ITEC	protein phosphatase 2A regulatory subunit
BE437994	BE437994	barley	ITEC	ubiquitin
BE437996	BE437996	barley	ITEC	chlorophyll a/b-binding protein light harvesting
BE438183	BE438183	barley	ITEC	phosphoribosyl pyrophosphate synthase
M94959	M94959	wheat	PR	Wir1
X58394	X58394	wheat	PR	Wir2 thaumatin-like protein
X56011	X56011	wheat	PR	Wir3 peroxidase
Wir5E123	(X56012)	wheat	PR	glutathione-S-transferase (exons of)
U32427	U32427	wheat	PR	WCI-1
U32428	U32428	wheat	PR	WCI-2 lipoxygenase
U32430	U32430	wheat	PR	WCI-4 thiol protease
U32431	U32431	wheat	PR	WCI-5
Y18212	Y18212	wheat	PR	TaGLUC2 beta-1,3-endoglucanase
OA5	AJ890250	wheat	PR	TaGLUC5 beta-1,3-endoglucanase
AJ237942	AJ237942	wheat	PR	TaGLP4 germin-like protein
BE419039	BE419039	wheat	PR	harpin induced gene homolog
GapC	#N/A	arabidopsis	HOUSE	glyceraldehyde-3-phosphate dehydrogenase
X16280	X16280	rice	HOUSE	actin
OA_aTubuRsa	AJ890248	wheat	HOUSE	α-tubulin
OA_G3PDHRsa	AJ890249	wheat	HOUSE	glyceraldehyde-3-phosphate dehydrogenase
AF216581	AF216581	arabidopsis	HYB	AP2/EREBP-like transcription factor leafy petiole

Table 8.3 (continued)

probe ID	access. #no	origin	category	function
AA115962	AA115962	human	HYB	haemoglobin beta-chain
H24390	H24390	human	HYB	dihydrofolate reductase
OA_R1	#N/A	human	HYB	testis-specific protein
OA_R2	#N/A	human	HYB	semenogelin II mRNA
R13084	R13084	human	HYB	low affinity nerve growth factor receptor
RUB_3'	#N/A	wheat	RNA	ribulose-bisphosphate carboxylase 3' end
RUB_5'_2	#N/A	wheat	RNA	ribulose-bisphosphate carboxylase 5' end
RUB_5'_3'	#N/A	wheat	RNA	ribulose-bisphosphate carboxylase middle part
TEF_3'	#N/A	wheat	RNA	translation initiation factor 3' end
TEF_5'_2	#N/A	wheat	RNA	translation initiation factor 5' end
TEF_5'_3'	#N/A	wheat	RNA	translation initiation factor middle part
UBI_3'	#N/A	wheat	RNA	ubiquitin 3' end
UBI_5'	#N/A	wheat	RNA	ubiquitin 5' end

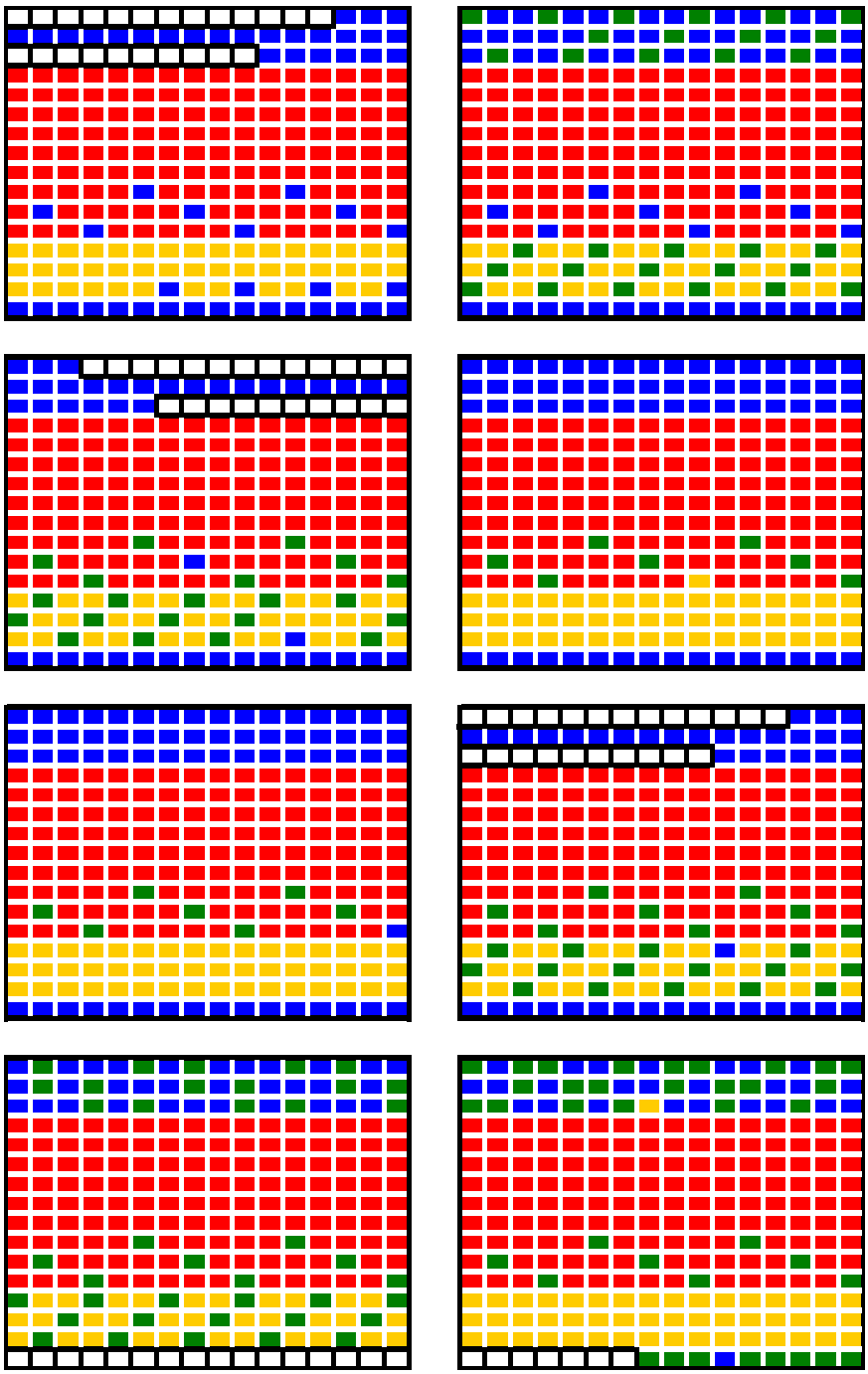

Figure 8.1: Layout of microarray series 6 and 7. The arrays were printed onto aldehyde slides using an OmniGrid 100 spotting robot equipped with 8 printing pins (in collaboration with the Department of Plant Molecular Biology at the University of Lausanne). Yellow probes: subset one (SSH fragments), red probes: subset two (AFLP fragments), green probes: subset three (Controls), white probes: subset four (ScoreCard) and blue probes: water controls.

8.4. Probe quality control

cDNA yield

$$\text{cDNA [ng]} = \frac{\left(A_{260} - CF_{260\,dye} \times A_{\lambda_{\max} dye}\right) \times 37 ng/\mu L}{l} \times Vol_{probe}$$

Amount of incorporated dye

$$\text{Dye [µmol]} = Vol_{probe} \times c_{dye} \quad (*)$$

$$= \frac{Vol_{probe} \times A_{\lambda_{\max} dye}}{\varepsilon_{\lambda_{\max} dye}} \times l$$

$$\text{Dye [pmol]} = \frac{Vol_{probe} \times A_{\lambda_{\max} dye}}{\varepsilon_{\lambda_{\max} dye}} \times l \times 10^6$$

Frequency of incorporation (foi): *No of labeled nucleotides per 1000 nucleotides*

$$\text{foi}_{\text{dye}} = \frac{Dye[pmol]}{cDNA[ng]} \times MW_{Nucleotide}$$

Base/dye ratio (bdr): *No. of bases per incorporated dye*

$$\text{bdr} = \frac{\left(A_{260} - CF_{260_{dye}} A_{\lambda_{\max} dye}\right)}{\times \varepsilon_{ssDNA}} \times \frac{\varepsilon_{\lambda_{\max} dye}}{A_{\lambda_{\max} dye}}$$

(*)Lambert-Beer law

$$A = \varepsilon \times c \times l \qquad \rightarrow \qquad c = \frac{A}{\varepsilon \times l}$$

A	=	absorbance			
c	=	molar concentration [mol L^{-1}]			
ε	=	molar absorption coefficient [L mol^{-1} cm^{-1}]			
l	=	path length [cm]			
Vol_{probe}	=	probe volume [µl]			
$CF_{260\ AF555}$	=	0,08 (correcction factor for dye-specific absorption at 260 nm)			
$CF_{260\ AF647}$	=	0,00			
$\varepsilon_{\text{AF555}}$	=	150'000 [L mol^{-1} cm^{-1}]	$MW_{Nucleotide}$	=	324.5 [g mol^{-1}]
$\varepsilon_{\text{AF647}}$	=	239'000 [L mol^{-1} cm^{-1}]	MW_{AF555}	=	~1250 [g mol^{-1}]
ε_{ssDNA}	=	8919 [L mol^{-1} cm^{-1}]	MW_{AF647}	=	~1300 [g mol^{-1}]

8.5. Evaluations / Estimations

8.5.1. Estimation of proportion of epidermal cells in wheat leaves

Microscopic investigations on leaf cross-sections revealed average numbers of 5.5 mesophyll cells per 2 epidermal cells along the transversal axes. With respect to the proportions along the longitudal extension of the leaf, numbers of cells corresponding to epidermis and mesophyll were determined by light microscopy by bringing corresponding layers into focus. It was found that due to smaller cell size, numbers of mesophyll cells in the palisade parenchyma were 6.4-fold higher as compared to the epidermis lying beyond. Based on this, it was calculated that the leaves consist of 95 % mesophyll cells (5.5 x 6.4 / (5.5 x 6.4 + 2)) and only 5 % epidermal cells (2 / (5.5 x 6.4 + 2)).

8.5.2. Estimation of proportion of *Bgt*-infected cells in wheat leaves

Wheat seedlings were infected at high spore density following protocols described for typical microarray experiments (Materials and Methods). Eighteen hours after infection, 10 primary leaves were randomly chosen for investigation by light microscopy along the longitudal axes. Determinations of spore numbers on 110 fields of view on the adaxial leaf surface revealed high variability and resulted in 6.59 spores on average per field of view. Counting of average epidermal cell numbers present in one field of view resulted in 42.3 cells. By assigning similar proportions of infected cells also to the abaxial side of the leaf, it was concluded that in a typical microarray experiment, 15.6 % of all cells of the leaf surface were primarily infected with wheat powdery mildew. Infection on the abaxial side was considered to be generally lower than on the adaxial side and thus, 15.6 % represents a rather overestimated proportion. Finally, it was further calculated that on average, the proportion of infected cells in relation to all cells of the leaf was 0.78 % (0.156 x 0.05).

8.5.3. Estimation of proportion of stomata cells in the epidermis

Microscopic investigations of wheat leaves on the adaxial surface revealed that 30.3 % of epidermal cells were stomatal cells.

8.6. Global SD regularization on data derived from infected and uninfected syringolin-treated wheat leaves

Table 8.4 Genes exhibiting differing induction ratios (larger than 1.5-fold) after SD-regularization. All experiments of ceA were repeated three times (the average t/c ratio is shown in columns 5 to 8). Bold t/c ratios: $p < 0.05$ (one-sample t-test). Fragments forming contigs identified after data normalization are separated by horizontal lines. #N/A denotes that corresponding data were not available. Column 9: Direct comparison of epidermal tissue harvested between 2 and 8 hat from infected and uninfected leaves sprayed with control solution (one single repetition; ceB). t/c ratios greater than 2 are listed. Additional data is given in chapt. 8.8.

	Putative function & [Blast hit]	EST ID	access. no#	E-val	sylA on total leaf material (p < 0.05) *Bgt*-infected 12 hat	*Bgt*-infected 24 hat	uninfected 12 hat	uninfected 24 hat	*Bgt* infected -08 hat
	1	2	3	4	5	6	7	8	9
	***stronger induction in the PRESENCE of* Bgt**								
1	glutathione S-transferase [CN013161]	***OA_b3D05***	AJ874102	1.00E-152	**18.3**	**11.1**	**8.9**	**9.5**	-
2	28S ribosomal RNA gene [AY064705]	***RB_c116***	AJ888238	4.00E-71	**2.2**	**2.3**	1.4	1.0	11.9
3	pir7b / salicylic acid-binding protein / Ethylene-induced esterase / Polyneuridine aldehyde esterase [Q43360]	***OA_b1B01***	AJ874087	2.00E-67	**21.8**	**11.5**	**12.3**	**13.8**	-
4	pir7b / salicylic acid-binding protein / Ethylene-induced esterase / Polyneuridine aldehyde esterase [CB864680]	***OA_b2A07***	AJ874094	3.00E-79	**16.9**	**12.8**	**8.8**	**16.1**	-
5	no significant hit	***OA_b1A06***	AJ874086	#N/A	**16.0**	**9.8**	**16.7**	**9.8**	-
6	no significant hit	***OA_b2B07***	AJ888674	#N/A	**21.7**	**9.3**	**13.1**	**9.7**	-
	***stronger induction in the ABSENCE of* Bgt**								
7	20S proteasome alpha 5 subunit [Q9LSU1]	***OA_b3D01***	AJ888705	1.00E-20	**2.4**	1.5	**3.4**	**1.7**	-
8	hsp 23.6 [Ta.214]	***OA_a1H02***	AJ874076	1.00E-143	**4.1**	**2.0**	**6.3**	**2.8**	-
9	sucrase (ferredoxin-like) [BQ458888]	***OA_b3C03***	AJ888702	6.00E-99	**1.9**	1.2	**2.9**	1.2	-
10	sucrase (ferredoxin-like) [Hv.12867]	***RB_c020***	AJ888720	6.00E-12	1.3	0.9	**2.1**	1.0	-
11	MDR-like ABC transporter [Ta.9295]	***OA_a2E02***	AJ888620	0.00E+00	**2.5**	1.2	**4.0**	**1.6**	-
12	glutathione S-transferase [CK217249]	***OA_a3G10***	AJ888647	9.00E-77	**1.8**	0.9	**2.7**	1.0	-
13	glutathione S-transferase [CK205115]	***RB_c017***	AJ873967 AJ873968	4.00E-25	**2.9**	1.6	**6.4**	1.8	2.7
14	cytochrome P450 [AF321867]	***OA_a1D09***	AJ888604	3.00E-67	2.6	1.0	**4.2**	1.5	-
15	cytochrome P450 [AP002839]	***OA_a1C04***	AJ888598	1.00E-78	1.8	0.8	**2.7**	1.0	-
16	ABI3-interacting protein 2 (abscisic acid insensitive interacting protein) [Ta.6216]	***OA_b2A06***	AJ888668	0.00E+00	1.7	0.7	**3.3**	1.2	0.4
17	prohibitin [AF236371]	***OA_a3C03***	AJ874085	1.00E-114	**3.1**	1.3	**4.9**	**2.2**	-
18	BCS1-like protein / AAA-type ATPase-like protein [Ta.11182]	***OA_a1B08***	AJ874073	1.00E-130	**2.8**	**1.5**	**6.1**	1.4	6.3
19	TipC / VPS13 - like protein [Ta.8446]	***OA_b1G10***	AJ888664	1.00E-148	1.8	1.1	**3.0**	1.6	-
20	gigantea mRNA [BG909229]	***RB_c001***	AJ873936 AJ873963 AJ873964	1.00E-117	0.7	1.0	0.5	**0.4**	6.6
21	B12D protein [BQ170981]	***RB_96.2***	AJ888727	1.00E-31	**2.5**	**1.7**	**4.1**	**2.1**	2.8
22	epoxide hydrolase [Ta.26236]	***OA_b3B10***	AJ888700	2.00E-78	**7.2**	**2.0**	**11.5**	**3.2**	-

Table 8.4 (continued)

	Putative function & [Blast hit]	EST ID	access. no#	E-val	sylA on total leaf material (p < 0.05) *Bgt*-infected 12 hat	*Bgt*-infected 24 hat	uninfected 12 hat	uninfected 24 hat	*Bgt* infected -08 hat
	1	2	3	4	5	6	7	8	9
23	monooxygenase [CD452994]	***RB_53.1***	AJ888726	8.00E-85	**2.2**	1.0	**4.6**	1.3	-
24		***RB_53.3***	#N/A	#N/A	1.5	0.9	**3.0**	1.2	-
25		***RB_53.6***	#N/A	#N/A	**2.4**	1.2	**4.5**	1.4	-
26		***RB_53.7***	#N/A	#N/A	2.0	1.1	**3.9**	1.3	-
27	unknown [CN011234]	***OA_a1H06***	AJ888610	3.00E-84	1.8	1.0	**3.1**	1.3	-
28	unknown [BQ768185]	***OA_a3E09***	AJ888643	1.00E-104	2.9	1.2	**4.4**	1.3	-
29	unknown [BJ291998]	***OA_b2G10***	AJ888688	3.00E-66	**1.9**	1.2	**3.7**	1.3	-
30	unknown [AW448695]	***RB_240.4***	AJ888722	2.00E-55	1.5	1.1	**2.2**	1.5	-
31		***RB_240.5***	#N/A	#N/A	1.4	1.1	**2.1**	1.5	-
32	no significant hit [Str.21194]	***OA_a3C05***	AJ888637	5.40E-01	1.2	0.9	**2.1**	1.3	-

8.7. Epidermal specificity

To determine the expression levels of arbitrary genes in epidermis and mesophyll, their spot intensities were correlated to spot intensities of ribulose 1,5-bisphosphate carboxylase/oxygenase (rubisco) probes present on the microarray.

The parenchyma of leaves of the C_3-plant wheat consists of an upper palisade parenchyma and a lower spongy parenchyma. Yet, unlike C_4-plants like maize, no division of physiological tasks exist and fixation of CO_2 in all chloroplasts occurs directly by the action of ribulose 1,5-bisphosphate carboxylase in the calvin cycle. Thereby, carboxylation of ribulose 1,5-bisphosphate yields two molecules of 3-phosphoglycerate, the first stable intermediate in photosynthesis. The plant ribulose 1,5-bisphosphate carboxylase/oxygenase (rubisco) is an oligomeric complex of eight copies of a large subunit and eight copies of a small subunit. Whereas the large subunit is encoded by the chloroplast DNA, the small subunit is encoded in the nuclear genome (Buchanan et al., 2001). Thus, apart from guard cells, no transcripts of the large subunit of rubisco are found in epidermal cells due to their lack of chloroplasts. Additionally, no expression also of the small subunit was observed by RT-PCR experiments in barley epidermal cells under different light conditions (Lu et al., 2002). Furthermore, probes corresponding to small subunits of rubisco present in the microarray manufactured in our lab exhibited similar expression patterns like probes corresponding to large subunits in wheat (data not shown). Thus, signal intensities derived from targets corresponding to large but also small subunits of rubisco were all included for the calculation of epidermis specificity.

To calculate a measure for gene expression in the epidermis, the relations between intensities of arbitrary genes and rubisco in the epidermal samples were compared to the ones in the mesophyll samples. The resulting value referred to as epidermis specificity factor (ϵ_s) was calculated according to the equation given below.

$$\varepsilon_s = \frac{I_{x_{epi}}}{\rho_{epi}} \Big/ \frac{I_{x_{mes}}}{\rho_{mes}}$$

$I_{x_{epi}}$ = Spot intensity in the epidermal sample of an arbitary gene.

$I_{x_{mes}}$ = Spot intensity in the mesophyll sample of an arbitary gene.

ρ_{epi} = Average rubisco intensity in the epidermal sample

ρ_{mes} = Average rubisco intensity in the mesophyll sample

The equation above was transformed to separate spot intensities of arbitrary genes and rubisco as shown below.

$$\varepsilon_s = \frac{I_{x_{epi}}}{I_{x_{mes}}} \times \rho \qquad \rho = \frac{\rho_{mes}}{\rho_{epi}} = \text{Rubisco proportion}$$

To minimize deviations, rubisco intensities were related to intensities of six different rubisco probes each of them present in three copies on the microarray. Signals of two additional probes were not included because of very high signal intensities which occasionally required correction by application of cutoff values due to saturated scanning (chapt. 4.2.1.4). The probes used to calculate rubisco proportions are listed in Table 8.5.

Table 8.5: Probes used for the calculation of ρ. As an example, average log-intensities of three experiments of ceB derived from sylA-treated epidermal and mesophyll samples are given (rows 3 & 4).

	Gene ID	function	epidermis avr Log2(c_val)	mesophyll avr Log2(c_val)	average ρ c_val_{mes} / c_val_{epi}
	1	2	3	4	5
1	**BE437451**	rubisco small subunit (barley)	12.0305	12.6975	
2	**BE437892**	rubisco small subunit (barley)	13.0773	13.6647	
3	**RUB_3'**	rubisco 3prime end (wheat)	13.2083	14.2989	
4	**RUB_5'**	rubisco 5prime end (wheat)	11.4716	12.0806	
5	**RUB_5'_3'**	rubisco middle part (wheat)	12.7202	13.2698	
6	**OA_b3E01**	rubisco small subunit (wheat)	13.2088	14.2319	
7	**average**		**12.6195**	**13.3739**	**1.6870**

The rubisco proportion used to calculate epidermis specificity factors (ϵ_s) corresponded to the relation between the average log intensity derived from mesophyll samples (Table 8.5, column 4) and average log intensity derived from epidermal samples (Table 8.5, column 3). Over all three repetitions listed in Table 8.5, the average ρ was found to be equal to 1.6870. Average rubisco proportions of all repetitions in ceB are listed in Table 8.6.

Table 8.6: Average rubisco proportions as calculated from three independent repetitions of ceB.

Experiments	Average ρ
- 08 hat control	1.826
- 08 hat syringolin	1.687
- 32 hat control	1.688
- 32 hat syringolin	1.808

ϵ_s of genes exhibiting equal signal intensities in epidermal and mesophyll samples would be equal to ρ (1.7512 on average). Conversely, ϵ_s-factors of genes exhibiting similar expression patterns like rubisco would be equal to 1.0. By using an average ρ of 1.7512, estimations revealed that epidermal tissue in epidermis samples accounted for at least 50 % reflecting an enrichment of 10-fold as compared to total leaf samples (data not shown). Furthermore, simulations of epidermis specificities revealed that genes expressed exclusively in the mesophyll would exhibit ϵ_s around 0.9 whereas ϵ_s higher than 2.0 strongly indicated expression of corresponding genes in the abaxial epidermis (mentioned in chapt. 4.2.4, p.74; data not shown).

8.8 *Bgt* pre-induction

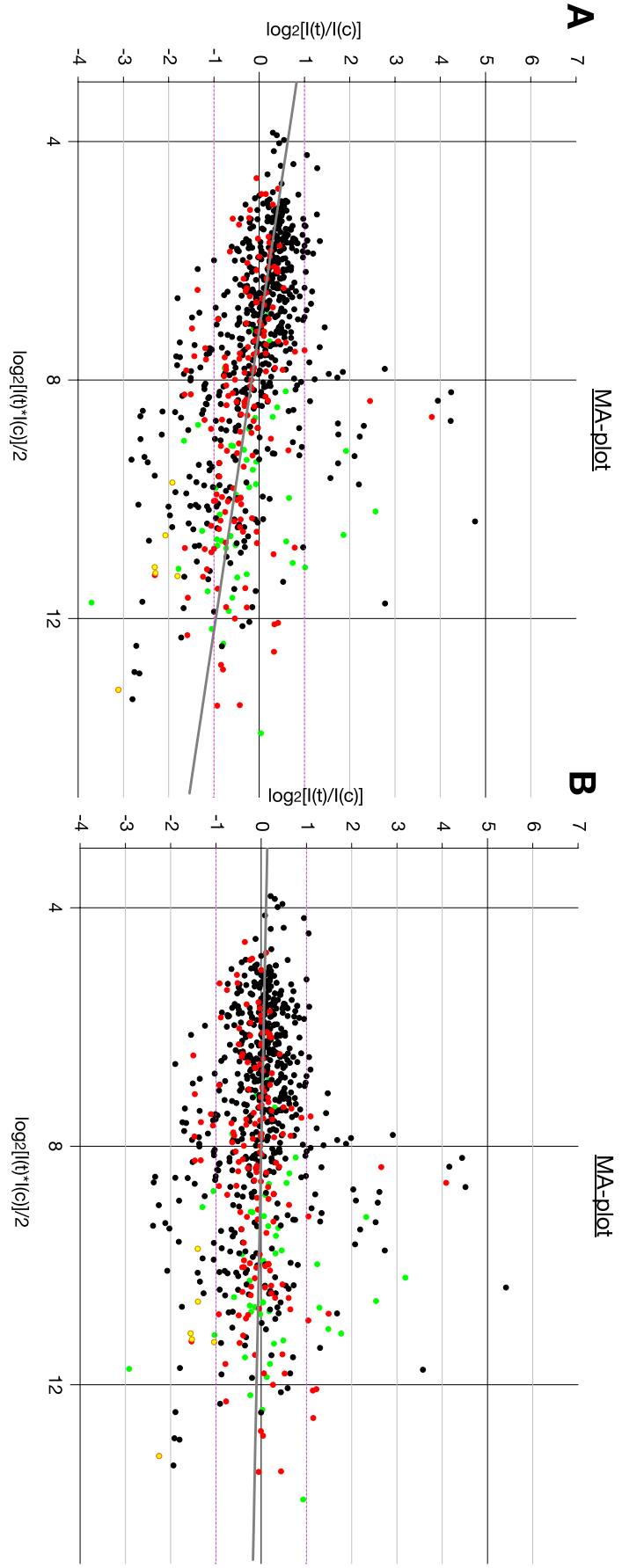

Figure 8.2: MA-plot visualizing data of one single experiment exhibiting channel intensity-dependent variability before (Panel A) and after (Panel B) Lowess normalization. Red dots: Targets corresponding to subset one (SSH-derived OA-fragments). Black dots correspond to subset two (cDNA AFLP-derived RB-clones). Green dots: Control targets corresponding to subset three (including WIR and WCI genes). Yellow dots: Ribulose bisphosphate carboxylase. Trend line (grey): Trends were visualized by linear regression using ORIGIN 7.0 (OriginLab Corporation, Northampton (MA), USA). Pink line: Threshold limits applied for the selection presented in Table 8.7

Data was derived from direct comparison of RNA corresponding to epidermis of *Bgt*-infected (t) and uninfected (c) wheat leaves sprayed with mock solution only (48 hai). Epidermis was separated from the remainder of the leaf and collected at 1 to 8 hat. Causes of tilted trend lines were discussed in chapt. 5.1.2

Table 8.7: Genes regulated by *Bgt*-infection at -08 and -32 hat following mock treatment (H_2O and 0.05 % (v/v) Tween20. Data were derived from one single repetition of ceB (Figure 4.26). Only genes exhibiting more than 2-fold induction / repression in at least one of the time points and treatments were listed. Black regular t/c ratios: Ratios exceeding threshold limit of 2. Genes found to be regulated by syringolin treatment (Table 4.7) were highlighted by arrows (⇦). Genes described elsewhere to be epidermally induced by barley powdery mildew attack are marked with 'Bgh', genes found to be ubiquitously induced by *Bgh* are marked with 'bgh' (Bruggmann et al., 2005).

	Putative function & [Blast hit]	EST ID	access. no#	E-val	*Bgt* infection - 56 hai epi	- 56 hai meso	- 80 hai epi	- 80 hai meso	
	1	2	3	4	5	6	7	8	
1	AP2/EREBP-like transcription factor LEAFY PETIOLE gene AF216581 (*Arabidopsis*)	***AF216581***	AF216581	#N/A	**2.4**	1.0	**3.1**	1.0	
2	TaGLP4 (germin-like protein)	***AJ237942^{Bgh}***	AJ237942	#N/A	**5.8**	**5.0**	**14.9**	**11.3**	
3	TaGLUC5 (beta-1,3-endoglucanase) [AF055328]	***OA5***	AJ890250	1.0E-154	**0.5**	1.2	0.6	1.6	
4	TaGLUC2 (beta-1,3-endoglucanase)	***Y18212***	Y18212	#N/A	1.0	**4.9**	**2.3**	**6.8**	
5	actin (barley)	***BE437261***	BE437261	5.0E-24	**2.8**	1.1	**2.3**	1.3	
6	protein kinase (barley)	***BE437646***	BE437646	3.0E-25	**0.1**	0.6	**0.2**	**0.5**	
7	WCI-1 (wheat)	***U32427***	U32427	#N/A	**0.5**	0.9	**0.3**	**0.1**	
8	WCI-2 (lipoxygenase) (wheat)	***U32428***	U32428	#N/A	**0.4**	**0.4**	**0.3**	**0.1**	
9	WCI-4 (thiol protease) (wheat)	***U32430***	U32430	#N/A	1.5	0.9	1.3	**0.3**	
10	WCI-5 (wheat)	***U32431***	U32431	#N/A	**2.4**	**2.2**	**2.3**	**2.2**	
11	Wir1 (wheat)	***M94959***	M94959	#N/A	**3.4**	1.9	**3.6**	1.7	
12	Wir3 (peroxidase) (wheat)	***X56011***	X56011	#N/A	**9.1**	**14.1**	**11.1**	**13.6**	
13	Wir2 (thaumatin-like protein) (wheat)	***X58394***	X58394	#N/A	**5.0**	**7.1**	**4.2**	**6.2**	
14	exon of glutathione-S-transferase (wheat X56012)	***Wir5E123***	(X56012)	#N/A	1.9	**2.4**	1.3	**2.4**	
15	ribulose-bisphosphate carboxylase small subunit (barley)	***BE437451***	BE437451	2.0E-22	**0.4**	**0.4**	0.5	**0.4**	
16	ribulose-bisphosphate carboxylase small subunit (barley)	***BE437892***	BE437892	6.0E-13	**0.5**	**0.5**	0.6	**0.5**	
17	Rubisco 3' end (wheat)	***RUB$_{3prime}$***	#N/A	#N/A	**0.4**	**0.3**	**0.5**	**0.4**	
18	Rubisco 5' end (wheat)	***RUB$_{5prime_2}$***	#N/A	#N/A	**0.4**	**0.4**	0.7	**0.4**	
19	Rubisco middle part (wheat)	***RUB$_{5prime_3prime}$***	#N/A	#N/A	**0.3**	**0.4**	**0.5**	**0.4**	
20	unknown [BJ457050]	***OA_a1A05***	AJ888592	4.0E-55	**0.5**	**0.5**	**0.4**	**0.5**	
21	BCS1-like protein / AAA-type ATPase-like protein [Ta.11182]	***OA_a1B08^{Bgh}***	AJ874073	1.0E-130	**6.3**	**3.0**	**4.0**	**2.8**	⇦
22	unknown [CK160607]	***OA_a1C01***	AJ888597	2.0E-20	**2.2**	1.0	2.0	1.2	
23	no significant hit [BG415498]	***OA_a1D03***	AJ888601	1.0E-03	**2.3**	1.1	**2.7**	1.3	⇦
24	cytochrome P450 [AF321867]	***OA_a1D09***	AJ888604	3.0E-67	0.6	0.7	**0.4**	0.7	⇦
25	alternative oxidase [AF174004]	***OA_a1E06^{Bgh}***	AJ874074	4.0E-87	**2.1**	1.3	1.7	1.8	⇦
26	unknown [BE445384]	***OA_a1F05***	AJ888609	6.0E-97	**2.1**	1.0	**2.0**	1.3	⇦
27	MRP-like ABC transporter [CA733405]	***OA_a2A06***	AJ888613	1.0E-161	0.5	0.8	**0.5**	0.7	⇦
28	unknown [AK103640]	***OA_a2H01***	AJ888627	2.0E-98	**0.4**	0.6	0.5	**0.5**	⇦

Table 8.7 (continued)

	Putative function & [Blast hit]	EST ID	access. no#	E-val	*Bgt* infection - 56 hai epi	- 56 hai meso	- 80 hai epi	- 80 hai meso	
	1	2	3	4	5	6	7	8	
29	d-TDP-glucose dehydratase [AJ295156]	***OA_a2H02^{bgh}***	AJ874080	1.0E-109	1.2	1.7	1.2	**2.7**	
30	PDR-like ABC transporter [CD881196]	***OA_a3A04^{Bgh}***	AJ874081	1.0E-88	**17.0**	**3.5**	**10.7**	**3.5**	⇦
31	hsp70-interacting protein [CA719392]	***OA_a3A05***	AJ888633	8.0E-35	**0.4**	**0.5**	**0.5**	**0.4**	
32	rubisco L [AY328025]	***OA_a3B08***	AJ888636	2.0E-38	**0.2**	1.0	**0.5**	0.7	
33	no significant hit [Str.21194]	***OA_a3C05***	AJ888637	5.4E-01	0.7	0.6	**0.5**	**0.5**	⇦
34	Pto kinase interactor 1 (Pti1) [Ta.7365]	***OA_a3C11***	AJ888639	1.0E-160	**0.5**	0.8	**0.5**	0.6	
35	unknown [AV836689]	***OA_a3F01***	AJ888644	2.0E-54	**2.2**	0.9	**2.7**	1.2	
36	no significant hit	***OA_a3H02***	AJ888650	#N/A	**2.8**	1.0	**3.5**	1.0	
37	temperature stress-induced lipocalin / Apolipoprotein D (APOD) [AY077702]	***OA_b1D11***	AJ888660	1.0E-142	1.6	1.9	1.6	**2.5**	⇦
38	20S proteasome alpha 5 subunit [CD936318]	***OA_b1G05^{bgh}***	AJ874091	0.0E+00	1.4	1.5	1.2	**2.3**	⇦
39	ABI3-interacting protein 2 (abscisic acid insensitive interacting protein) [Ta.6216]	***OA_b2A06***	AJ888668	0.0E+00	**0.4**	0.9	**0.5**	0.7	⇦
40	pir7b / salicylic acid-binding protein / Ethylene-induced esterase / Polyneuridine aldehyde esterase [CB864680]	***OA_b2A07^{bgh}***	AJ874094	3.0E-79	1.2	**2.4**	1.1	**2.3**	⇦
41	enolase 2 [P42895]	***OA_b2A09***	AJ888670	2.0E-44	**0.4**	0.8	0.5	0.7	⇦
42	thioredoxin (F-type) [BG908661]	***OA_b2E11***	AJ888685	2.0E-24	0.6	0.6	**0.4**	0.7	
43	glucose transport protein fused to Caffeoyl-CoA O-methyltransferase [CA685905]	***OA_b2H03***	AJ874099	3.0E-47	**2.1**	**3.0**	**2.3**	**2.7**	
44	glutathione S-transferase [CN013161]	***OA_b3D05^{Bgh}***	AJ874102	1.0E-152	1.9	1.4	**2.1**	1.4	⇦
45	rubisco (small subunit) [AB042066]	***OA_b3E01***	AJ888707	4.0E-55	**0.3**	0.5	**0.5**	**0.5**	
46	unknown [CK212249]	***OA_b3E06***	AJ888709	2.0E-67	**0.4**	**0.4**	**0.3**	**0.3**	
47	unknown [CV771156]	***OA_b3E08***	AJ888710	4.0E-32	0.6	0.7	**0.5**	0.8	
48	NAM-like (No apical meristem) [Ta.3949]	***OA_b3F11***	AJ888713	0.0E+00	0.5	0.6	**0.5**	0.5	
49	AAA-metalloprotease FtsH (*P. sativum*) [AP003240]	***OA_b3G10***	AJ888715	1.0E-49	**0.4**	0.9	0.6	1.1	
50	gigantea mRNA [BG909229]	***RB_c001^{Bgh}***	AJ873936 AJ873963 AJ873964	1.0E-117	**6.6**	**3.4**	1.9	**2.3**	⇦
51	mitochondrial phosphate transporter, *O. sativa*	***RB_c003***	#N/A	5.0E-04	**2.0**	1.0	**2.4**	1.0	
52	beta-1,3-endoglucanase, *T. aestivum*	***RB_c006^{bgh}***	AJ873940	3.0E-28	**2.1**	**3.2**	**2.5**	**2.9**	
53	cDNA clone C00255, mRNA sequence, *Blumeria graminis* f. sp. *hordei*	***RB_c010^{Bgh}***	AJ888234	3.0E-68	**5.8**	1.2	**6.4**	1.2	
54	Phenylalanine ammonia-lyase, *H. vulgare*	***RB_c011^{bgh}***	AJ873947	1.0E-43	1.4	**2.4**	2.0	**2.3**	
55	cDNA clone WHE2831_H03_P05, *T. monococcum*	***RB_c013^{Bgh}***	AJ873953 AJ873954 AJ873955	1.0E-30	**4.0**	**2.3**	**5.1**	**4.0**	
56	beta-1,3-endoglucanase (Y18212), *T. aestivum*	***RB_c015^{bgh}***	AJ874005	1.0E-140	1.6	**5.2**	**3.1**	**7.5**	
57	glutathione S-transferase [CK205115]	***RB_c017^{bgh}***	AJ873967 AJ873968	4.0E-25	**2.7**	**2.4**	**2.3**	**3.2**	⇦
58	Thaumatin-like protein TLP8	***RB_c018bgh***	AJ873969 AJ873970 AJ873971 AJ873981	2.0E-06	2.0	1.8	**2.1**	1.8	
59	Appressorium stage EST library of *Blumeria graminis* f.sp. *hordei* cDNA clone A00191-R	***RB_c022^{Bgh}***	AJ888235 AJ888236	2.0E-92	**4.1**	1.3	**5.9**	1.4	

Table 8.7 (continued)

	Putative function & [Blast hit]	EST ID	access. no#	E-val	*Bgt* infection - 56 hai epi	- 56 hai meso	- 80 hai epi	- 80 hai meso
	1	2	3	4	5	6	7	8
60	Glutamate carboxypeptidase-like protein, *Saccharomyces cerevisiae*	***RB_c024***	#N/A	5.5E-01	**7.5**	0.8	**9.7**	0.9
61	histidine-rich protein, *O. sativa*	***RB_c025^{bgh}***	AJ873984	1.0E-01	**3.2**	**3.5**	**2.0**	**2.7**
62	cis-zeatin O-glucosyltransferase [Q8S465]	***RB_c027^{bgh}***	AJ873990 AJ873991	3.0E-10	1.2	1.8	1.5	**2.2**
63	subtilisin-chymotrypsin inhibitor 2 [Y08625]	***RB_c029^{bgh}***	AJ874007	3.0E-24	**2.5**	**5.9**	**5.1**	**9.0**
64	Putative histidine kinase, *O. sativa*	***RB_c033^{bgh}***	AJ873992 AJ874021	7.0E-21	1.0	**2.1**	0.8	1.5
65	partial mRNA clone cMWG0676.uni, *H. vulgare*	***RB_c034***	#N/A	5.0E-12	0.6	0.6	**0.3**	**0.4**
66	no significant hit	***RB_c037^{Bgh}***	AJ874025 AJ874026	#N/A	**2.1**	1.9	2.0	**2.2**
67	glutamine synthetase 2, *H. vulgare*	***RB_c038***	#N/A	6.0E-56	**0.5**	0.5	**0.5**	**0.5**
68	cDNA clone C01137, *Blumeria graminis* f. sp. *hordei*	***RB_c040^{Bgh}***	AJ888229	9.0E-31	**2.1**	1.0	1.5	0.8
69	NAD- dependent formate dehydrogenase, mitochondrial precursor, *H. vulgare*	***RB_c045^{Bgh}***	AJ874031 AJ874060 AJ874064	4.0E-53	**4.6**	**3.5**	**5.5**	**4.1**
70	Putative immediate-early salicylate-induced glucosyltransferase [Ta.23340]	***RB_c048^{bgh}***	AJ874027	2.0E-29	**6.1**	**10.9**	**6.0**	**7.0**
71	clone wlm24.pk0027.a6:fis, full insert mRNA sequence (GDSL-motif lipase/hydrolase-like), *T. aestivu*m	***RB_c049^{bgh}***	AJ873944	1.0E-19	1.6	**2.7**	1.1	**2.6**
72	Similar to wak4 (wall-associated kinase), *A. thaliana* [Q9LWG6]	***RB_c052^{bgh}***	AJ874036 AJ874037	1.0E-08	**2.3**	**2.1**	1.5	2.0
73	Berberine bridge enzym-like protein, *A. thaliana*	***RB_c055^{Bgh}***	AJ874071	1.0E-12	**2.3**	**2.0**	**2.3**	1.3
74	Germin 9f-2.8 gene, *T. aestivum*	***RB_c057^{bgh}***	AJ873945 AJ873948	4.0E-75	**4.2**	**8.7**	**9.9**	**13.0**
75	Elongation factor 1 alpha-subunit (TEF1), *T. aestivum*	***RB_c066^{bgh}***	AJ874057	2.0E-67	1.2	1.6	1.7	**2.6**
76	beta-1,3-endoglucanase, *T. aestivum*	***RB_c069^{bgh}***	AJ873974	1.0E-83	1.5	**5.9**	**2.9**	**8.4**
77	Putative cytochrome P450, *O. sativa*	***RB_c070^{bgh}***	AJ874023	4.0E-44	2.0	1.2	**2.3**	1.1
78	Pathogenesis related protein 1.1 (PR-1.1), *T. aestivum*	***RB_c072^{bgh}***	AJ874038 AJ874039	1.0E-73	1.9	**2.3**	1.7	1.9
79	Beta-1,3-glucanase (Glb3), *T. aestivum*	***RB_c079^{bgh}***	AJ885878	1.0E-109	0.7	**2.3**	1.1	1.7
80	T4 cDNA library under conditions of nitrogen deprivation, *Botrytis cinerea* strain	***RB_c082^{Bgh}***	AJ888237	1.0E-11	**42.5**	**2.6**	**38.6**	**4.2**
81	Thaumatin-like protein TLP4, *H. vulgare*	***RB_c083^{bgh}***	AJ874018 AJ874050	8.0E-44	**2.0**	**3.5**	**2.6**	**3.4**
82	Thaumatin-like protein, *T. aestivum*	***RB_c085^{bgh}***	AJ874044	2.0E-66	**2.2**	**2.8**	1.9	**2.4**
83	beta-1,3-endoglucanase (Y18212), *T. aestivum* [Y18212]	***RB_c091^{bgh}***	AJ874012	1.0E-100	**2.1**	**3.1**	**2.4**	**3.0**
84	APS reductase (PRH), *A. thaliana*	***RB_c093***	#N/A	7.0E-66	0.8	0.8	1.6	**2.1**
85	cDNA clone:J013161I06, *O. sativa*	***RB_c094^{bgh}***	AJ874006	5.0E-21	1.5	1.9	1.2	**2.2**
86	Phenylalanine ammonia-lyase, *H. vulgare*	***RB_c101^{Bgh}***	AJ873941 AJ873961	1.0E-108	1.1	2.0	1.4	**2.1**
87	Putative protein kinase, *O. sativa*	***RB_c105^{Bgh}***	AJ874066	2.0E-07	1.7	1.7	**2.0**	1.9
88	stress-related peroxidase, *H. vulgare*	***RB_c114^{Bgh}***	AJ874040 AJ874041	7.0E-06	**2.5**	1.3	1.9	1.5
89	PAL mRNA for phenylalanine ammonia-lyase (1831 bp), *H.vulgare*	***RB_c115^{bgh}***	AJ874042	9.2E-02	1.4	1.9	1.8	**2.3**
90	fungal 28S ribosomal RNA gene [AY064705]	***RB_c116^{Bgh}***	AJ888238	4.0E-71	**11.9**	1.3	**11.0**	1.1
91	Glyceraldehyde 3-phosphate dehydrogenase, *Blumeria graminis* f.sp. *hordei*	***RB_c122^{Bgh}***	AJ888233	1.0E-71	**22.8**	**2.2**	**26.8**	**3.7**

Table 8.7 (continued)

	Putative function & [Blast hit]	EST ID	access. no#	E-val	*Bgt* infection - 56 hai epi	- 56 hai meso	- 80 hai epi	- 80 hai meso	
	1	2	3	4	5	6	7	8	
92	#N/A	***RB_22.3***	#N/A	#N/A	**0.2**	0.5	**0.2**	**0.4**	
93	#N/A	***RB_22.4***	#N/A	#N/A	**0.2**	**0.5**	**0.2**	**0.3**	
94	#N/A	***RB_22.5***	#N/A	#N/A	**0.2**	**0.5**	**0.2**	**0.3**	
95	#N/A	***RB_22.6***	#N/A	#N/A	**0.3**	**0.4**	**0.2**	**0.3**	
96	#N/A	***RB_22.7***	#N/A	#N/A	**0.2**	**0.5**	**0.2**	**0.3**	
97	#N/A	***RB_22.8***	#N/A	#N/A	**0.2**	**0.5**	**0.2**	**0.3**	
98	Hypothetical protein, *O. sativa*	***RB_25.5***	#N/A	9.0E-51	**0.4**	0.6	**0.2**	**0.2**	
99	#N/A	***RB_25.7***	#N/A	#N/A	**0.4**	0.6	**0.2**	**0.2**	
100	Hypothetical protein, *O. sativa*	***RB_25.8***	#N/A	1.0E-38	**0.5**	0.7	**0.4**	#N/A	
101	#N/A	***RB_31.3***	#N/A	#N/A	**0.4**	**0.4**	**0.2**	**0.2**	
102	#N/A	***RB_33.1***	#N/A	#N/A	**0.4**	0.7	**0.2**	**0.2**	
103	WIR5; Glutathione S-transferase 1 (EC 2.5.1.18) (GST class-phi), *T. aestivum*	***RB_37.4***	#N/A	8.0E-09	1.4	**2.2**	1.2	2.0	
104	Ripening-related protein-like [CD872650]	***RB_39.2***	AJ888725	5.0E-67	**0.3**	**0.5**	**0.2**	**0.2**	⇦
105	#N/A	***RB_39A.1***	#N/A	#N/A	**0.3**	**0.4**	**0.2**	**0.2**	⇦
106	#N/A	***RB_39B.1***	#N/A	#N/A	**0.4**	**0.4**	**0.2**	**0.2**	
107	#N/A	***RB_39B.2***	#N/A	#N/A	**0.3**	0.6	0.5	0.7	
108	#N/A	***RB_39B.4***	#N/A	#N/A	**0.3**	**0.4**	**0.2**	**0.2**	
109	#N/A	***RB_39B.6***	#N/A	#N/A	**0.4**	**0.4**	**0.2**	**0.2**	
110	cDNA clone D01275 similar to retinal short-chain, *Blumeria graminis* f. sp. *hordei*	***RB_43A.5^{Bgh}***	AJ888230	1.0E-107	**21.7**	**2.6**	**30.0**	**3.3**	
111	chromosome 1 YAC yUP8H12 complete sequence, *A. thaliana*	***RB_74.2^{Bgh}***	#N/A	4.0E-01	**2.5**	**2.2**	1.3	**2.5**	
112	#N/A	***RB_86.3***	#N/A	#N/A	0.9	**0.4**	0.7	**0.5**	
113	*B. graminis* f. sp. *hordei* cDNA clone D01017 similar to s-adenosylmethionine synthetase	***RB_96.1^{Bgh}***	AJ888231	8.0E-86	**17.8**	**2.4**	**28.1**	**2.0**	
114	B12D protein [BQ170981]	***RB_96.2^{Bgh}***	AJ888727	1.0E-31	**2.8**	1.2	**3.2**	1.2	⇦
115	fructose-1,6-bisphosphatase [CD894371]	***RB_97.3***	AJ888728	4.0E-40	**0.4**	**0.4**	**0.4**	**0.5**	⇦
116	putative monosaccharide transporter [25415126]	***RB_104.3^{bgh}***	AJ874105	9.0E-65	0.6	1.0	**0.5**	0.8	
117	#N/A	***RB_124.7***	#N/A	#N/A	0.5	0.5	**0.5**	0.6	
118	#N/A	***RB_139.2***	#N/A	#N/A	0.5	#N/A	**0.3**	**0.4**	
119	putative glutamine synthase, *Lycopersicon esculentum*	***RB_144.1^{bgh}***	#N/A	7.0E-04	1.5	**3.7**	**2.2**	**4.3**	
120	genomic DNA, chromosome 7, BAC clone:OSJNBb0018L13, *O. sativa*	***RB_144.3^{bgh}***	#N/A	3.7E+00	1.4	**2.2**	1.3	**2.4**	
121	#N/A	***RB_165.1***	#N/A	#N/A	**0.4**	0.6	**0.4**	0.5	
122	Beta-1,3-glucanase (Glb3), *T. aestivum*	***RB_182.3***	#N/A	1.0E-111	**0.5**	0.6	0.5	0.5	
123	Ubiquitin-protein ligase 2, *A. thaliana*	***RB_182.4***	#N/A	9.0E-05	**0.5**	**0.4**	**0.5**	0.5	
124	#N/A	***RB_182.7***	#N/A	#N/A	**0.5**	0.6	0.6	0.6	

Table 8.7 (continued)

	Putative function & [Blast hit]	EST ID	access. no#	E-val	*Bgt* infection - 56 hai epi	- 56 hai meso	- 80 hai epi	- 80 hai meso
	1	2	3	4	5	6	7	8
125	#N/A	***RB_182.9***	#N/A	#N/A	**0.5**	0.5	**0.5**	0.6
126	#N/A	***RB_183.4***	#N/A	#N/A	0.8	**0.5**	0.7	**0.2**
127	#N/A	***RB_183.6***	#N/A	#N/A	1.8	0.9	1.4	**0.3**
128	#N/A	***RB_190.1***	#N/A	#N/A	0.6	0.5	0.6	**0.5**
129	unknown [CD373989]	***RB_190.3^{bgh}***	AJ873980	2.0E-04	1.7	#N/A	1.6	**2.4**
130	#N/A	***RB_190.5***	#N/A	#N/A	**0.3**	0.5	**0.3**	0.5
131	#N/A	***RB_206.1***	#N/A	#N/A	0.5	0.6	**0.5**	0.7
132	#N/A	***RB_206.5***	#N/A	#N/A	**3.7**	0.6	**5.0**	0.7
133	#N/A	***RB_206.6***	#N/A	#N/A	0.5	0.6	**0.5**	0.7
134	Carbonic anhydrase, chloroplast precursor, *H. vulgare*	***RB_212.2***	#N/A	3.0E-09	0.5	**0.5**	0.6	**0.5**
135	#N/A	***RB_212.3***	#N/A	#N/A	**0.2**	**0.5**	**0.4**	**0.5**
136	#N/A	***RB_212.4***	#N/A	#N/A	1.4	1.0	**2.3**	0.9
137	#N/A	***RB_214.4***	#N/A	#N/A	**0.4**	0.6	0.6	0.5
138	Hypothetical protein (Myosin-like protein), *A. thaliana*	***RB_226.3^{bgh}***	AJ873994	7.0E-14	1.6	**3.8**	1.0	**2.8**
139	#N/A	***RB_240.3***	#N/A	#N/A	0.8	0.8	**0.5**	0.6
140	cyclophilin, *T. aestivum*	***RB_244.2^{bgh}***	AJ874000	6.0E-49	1.8	1.8	1.7	**2.8**
141	genomic DNA, chromosome 7, BAC clone:OJ1714_H10, *O. sativa*	***RB_255.8^{Bgh}***	AJ874004	2.4E-01	1.4	0.9	**2.1**	0.8
142	#N/A	***RB_257.8***	#N/A	#N/A	**0.3**	**0.3**	**0.3**	**0.3**
143	#N/A	***RB_264.1***	#N/A	#N/A	**2.5**	1.0	**2.3**	1.1
144	#N/A	***RB_264.7***	#N/A	#N/A	**6.0**	1.1	**6.9**	1.2
145	apospory-associated protein C [CA655323]	***RB_265.2***	AJ888723	3.0E-29	**0.4**	0.8	**0.3**	0.7
146	#N/A	***RB_265.5***	#N/A	#N/A	**0.5**	0.8	**0.4**	0.8
147	Osr40g3 protein, *O. sativa*	***RB_282.5^{bgh}***	AJ874013	3.0E-04	**3.2**	**8.3**	**5.9**	**11.3**
148	#N/A	***RB_285.12***	#N/A	#N/A	**0.3**	**0.5**	**0.3**	**0.4**
149	F24O1.18 protein, *A. thaliana*	***RB_286.1***	#N/A	1.0E-03	1.5	1.2	**2.0**	1.2
150	#N/A	***RB_292B.11***	#N/A	#N/A	0.6	0.8	**0.5**	0.8
151	#N/A	***RB_297.3***	#N/A	#N/A	**2.1**	1.2	1.4	1.4
152	#N/A	***RB_301.1***	#N/A	#N/A	**0.3**	0.7	0.7	0.6
153	#N/A	***RB_301.3***	#N/A	#N/A	**0.4**	0.7	0.7	0.5
154	#N/A	***RB_301.6***	#N/A	#N/A	**0.3**	0.6	**0.4**	**0.5**
155	#N/A	***RB_304.1***	#N/A	#N/A	**0.4**	0.7	**0.4**	0.7
156	#N/A	***RB_304.3***	#N/A	#N/A	**0.5**	0.7	**0.5**	0.8
157	#N/A	***RB_304.5***	#N/A	#N/A	**0.4**	0.7	0.6	0.7

Table 8.7 (continued)

	Putative function & [Blast hit]	EST ID	access. no#	E-val	*Bgt* infection - 56 hai epi	- 56 hai meso	- 80 hai epi	- 80 hai meso
	1	2	3	4	5	6	7	8
158	#N/A	***RB_304.8***	#N/A	#N/A	**0.3**	0.8	**0.4**	0.6
159	#N/A	***RB_305.1***	#N/A	#N/A	**0.3**	0.9	**0.3**	0.8
160	#N/A	***RB_305.2***	#N/A	#N/A	**0.4**	**0.5**	0.6	**0.5**
161	#N/A	***RB_305.3***	#N/A	#N/A	0.5	0.8	**0.4**	0.9
162	#N/A	***RB_305.4***	#N/A	#N/A	**0.3**	1.0	**0.4**	0.8
163	#N/A	***RB_305.5***	#N/A	#N/A	**0.3**	1.0	**0.4**	0.9
164	#N/A	***RB_305.6***	#N/A	#N/A	**0.3**	0.9	**0.4**	0.9
165	#N/A	***RB_305.7***	#N/A	#N/A	**0.3**	1.1	**0.3**	0.8
166	#N/A	***RB_318.1***	#N/A	#N/A	0.5	0.5	**0.4**	**0.4**
167	#N/A	***RB_318.2***	#N/A	#N/A	**0.4**	0.6	**0.3**	**0.5**
168	Pheromone receptor V3R2, *M. musculus*	***RB_318.3***	#N/A	1.9E+01	**0.3**	0.6	**0.4**	**0.5**
169	#N/A	***RB_318.8***	#N/A	#N/A	0.7	1.0	**0.5**	0.8
170	#N/A	***RB_323.3***	#N/A	#N/A	0.7	0.8	**0.5**	0.6
171	#N/A	***RB_323.5***	#N/A	#N/A	0.7	0.8	**0.5**	0.6
172	Putative GDP-mannose pyrophosphorylase, *O. sativa*	***RB_327.3^{bgh}***	AJ874028	2.0E-19	**4.3**	1.2	**4.3**	1.3
173	#N/A	***RB_337.5***	#N/A	#N/A	**2.6**	1.3	**2.2**	1.0
174	#N/A	***RB_337.6***	#N/A	#N/A	0.8	0.7	0.6	**0.4**
175	#N/A	***RB_337.7***	#N/A	#N/A	0.5	0.9	**0.3**	**0.5**
176	#N/A	***RB_337.8***	#N/A	#N/A	0.5	0.9	**0.5**	1.1
177	#N/A	***RB_339.1***	#N/A	#N/A	0.7	0.8	**0.4**	**0.5**
178	#N/A	***RB_339.3***	#N/A	#N/A	0.8	0.8	**0.5**	0.5
179	#N/A	***RB_339.4***	#N/A	#N/A	0.6	0.7	**0.5**	**0.5**
180	#N/A	***RB_339.5***	#N/A	#N/A	**0.5**	0.7	**0.4**	**0.4**
181	Ethylene-responsive small GTP-binding protein, Lycopersicon esculentum (Ras-related protein RAB1BV)	***RB_339.8^{Bgh}***	AJ874032	3.0E-18	0.6	1.0	**0.5**	0.6
182	#N/A	***RB_354.1***	#N/A	#N/A	1.8	1.8	2.0	**2.3**
183	#N/A	***RB_358.7***	#N/A	#N/A	**0.5**	0.6	0.6	**0.5**
184	no significant hit	***RB_360.7***	#N/A	#N/A	**0.4**	**2.1**	0.9	**2.2**

8.9. Extendedly induced transcription

Table 8.8 Transcripts extendedly induced by syringolin treatment. Data was derived from ceA (columns 5-8) and ceB (columns 9-14). Genes were considered to be extendedly induced if the t/c ratio at 24 hat was not more than 2.5-fold smaller that the one at the early time point. Experiments were repeated three times (the average t/c ratio is shown). Bold t/c ratios: P-value smaller than 5 % as assigned by one-sample t-test. Fragments forming contigs identified after data normalization are separated by horizontal lines. #N/A denotes that corresponding data were not available. Average ϵ_s calculated by comparison of data corresponding to syringolin-treated epidermis and mesophyll are printed in red (columns 11 & 14). ϵ_s values found to be reliable ($p < 0.05$) according to t-test statistics were printed in bold letters when exceeding threshold limit of 2.0.

	Putative function & [Blast hit]	EST ID	access. no#	E-val	ceA (p < 0.05) sylA on total leaves *Bgt* 12 hat	*Bgt* 24 hat	- 12 hat	- 24 hat	ceB (p < 0.05) sylA on stripped & *Bgt*-infected leaves - 08 hat epi	- 08 hat mes	- 08 hat ϵ_s	- 32 hat epi	- 32 hat mes	- 32 hat ϵ_s
	1	2	3	4	5	6	7	8	9	10	11	12	13	14
2	NBS-LRR disease resistance protein [AJ507096]	***OA_a1E08***	AJ874075	3.00E-49	**4.2**	**2.2**	**9.5**	**4.0**	**6.1**	**4.5**	1.6	**5.4**	**2.7**	**3.9**
3	hsp 23.6 [Ta.214]	***OA_a1H02***	AJ874076	1.00E-143	**3.5**	**1.9**	**7.9**	**3.0**	**5.6**	**7.6**	1.2	**3.5**	**2.7**	**2.5**
4	ligand-gated ion channel 2.8 [BQ659530]	***OA_a2B04***	AJ888614	5.00E-99	**15.8**	**5.0**	**25.0**	**11.0**	**10.4**	**12.6**	0.8	**4.4**	**3.1**	2.5
5	enolase 1 [CD454849]	***OA_a2G01***	AJ888626	8.00E-90	**4.6**	**3.0**	**7.3**	**4.9**	**4.9**	**5.7**	1.2	**4.8**	**2.9**	3.6
6	no significant hit	***OA_b1A06***	AJ874086	#N/A	**11.9**	**8.4**	**24.1**	**11.8**	**15.4**	**16.7**	1.3	**11.4**	**11.4**	3.8
7	no significant hit	***OA_b2B07***	AJ888674	#N/A	**15.5**	**7.8**	**18.2**	**11.7**	**15.3**	**21.2**	1.0	**14.2**	**14.2**	2.1
8	pir7b [Q43360]	***OA_b1B01***	AJ874087	2.00E-67	**15.5**	**9.5**	**16.9**	**17.1**	**17.0**	**17.9**	1.4	**14.7**	**17.2**	1.7
9	hsp 60 [AC027038]	***OA_b1C09***	AJ874088	5.00E-35	**7.8**	**2.3**	**13.6**	**5.7**	**11.0**	**14.2**	1.6	**5.4**	**5.1**	**4.7**
10	cytochrome P450 [AP002839]	***OA_b1D06***	AJ888659	3.00E-47	**13.7**	**5.1**	**21.6**	**9.6**	**12.9**	**16.0**	0.9	**6.0**	**3.3**	3.1
11	voltage-dependent anion channel 1 [X77733]	***OA_b1F04***	AJ888662	2.00E-57	**6.7**	**3.0**	**15.4**	**6.1**	**13.3**	**11.2**	1.5	**6.2**	**3.8**	**4.5**
12	pir7b [CB864680]	***OA_b2A07***	AJ874094	3.00E-79	**12.0**	**10.5**	**11.6**	**20.2**	**13.5**	**11.7**	1.5	**10.7**	**15.2**	1.9
13	epoxide hydrolase [Ta.26236]	***OA_b3B10***	AJ888700	2.00E-78	**5.8**	**2.0**	**15.7**	**3.5**	**10.9**	**11.2**	1.4	4.6	**1.9**	4.2
14	glutathione S-transferase [CN013161]	***OA_b3D05***	AJ874102	1.00E-152	**12.9**	**9.4**	**11.8**	**11.4**	**9.2**	**9.3**	1.5	**9.1**	**13.7**	3.0

8.10 Differential transcription at 48 hat

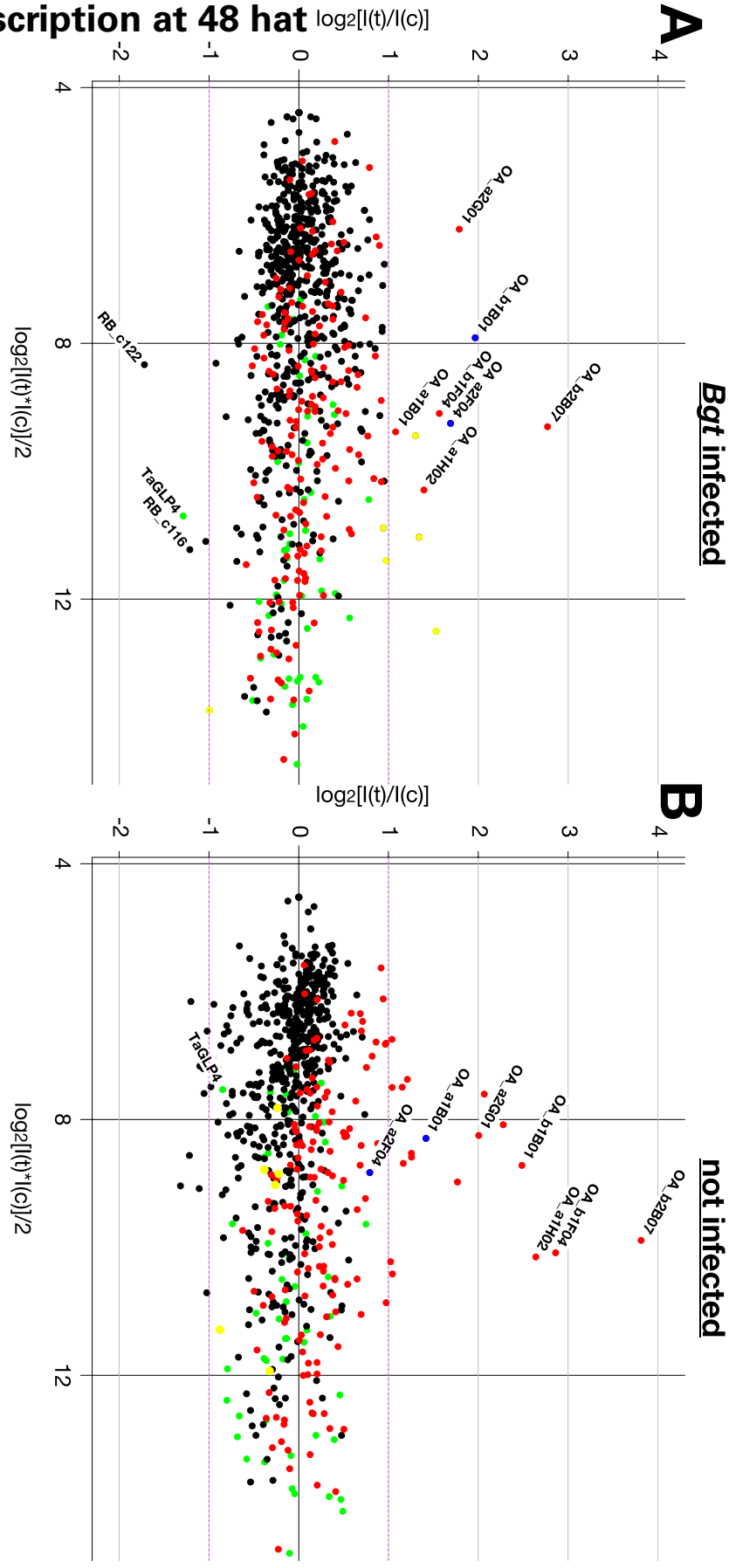

Figure 8.3: MA-plots visualizing microarray experiments corresponding to total leaf material collected 48 hat. Plants were infected (A) or uninfected (B) with *Bgt* 48 h before treatment. Data was derived from pilot experiments and labeling was done according to the poly(A)$^+$ RNA method (chapt. 4.2.1.5). Experiments were carried out only once. Red dots: Probes corresponding to subset one (SSH-derived OA-fragments). Black dots correspond to subset two (cDNA AFLP-derived RB-clones). Green dots: Control targets corresponding to subset three (including WIR and WCI genes). Yellow dots: PR-genes *WIR2*, *WIR5*, *WCI2*, *RB_c072*, *RB_c079* and *RB_c085*. Pink line: Threshold level of 2-fold induction / repression.

Table 8.9: Genes regulated by syringolin at 48 hat of infected and uninfected wheat leaves. Data were derived from one single pilot experiment. Only genes exhibiting more than 1.9-fold variability of expression in at least one of the treatments were listed. Black regular t/c ratios: Ratios exceeding threshold limit of 2. Syringolin-responsive genes identified in ceA and ceB were highlighted by arrows (⇦). Genes described elsewhere to be epidermally induced by barley powdery mildew attack are marked with $^{'Bgh'}$, genes found to be ubiquitously induced by *Bgh* are marked with $^{'bgh'}$ (Bruggmann et al., 2005).

	Putative function & [Blast hit]	EST ID	access. no#	E-val	pilot exp. sylA on total leaves *Bgt* 48 hat	- 48 hat	
	1	2	3	4	5	6	7
	Bgt-dependent induction						
1	hsp 23.5 [Ta.203]	***OA_a1B01^{bgh}***	AJ874072	1.00E-133	**2.1**	**2.7**	⇦
2	unknown [CK215536]	***OA_a2F04***	AJ888625	0.00E+00	**3.2**	1.7	⇦
3	unknown [CA669769]	***RB_c037^{Bgh}***	AJ874025 AJ874026	1.00E-105	1.9	1.1	
4	Pathogenesis related protein 1.1 *(T. aestivum)*	***RB_c072^{bgh}***	AJ874038 AJ874039	1.00E-73	1.9	0.8	
5	Beta-1,3-glucanase (Glb3), *(T. aestivum)*	***RB_c079^{bgh}***	AJ885878	1.00E-109	**2.5**	0.8	
6	Thaumatin-like protein, *(T. aestivum)*	***RB_c085^{bgh}***	AJ874044	2.00E-66	**2.5**	0.9	
7	#N/A	***RB_157.5***	#N/A	#N/A	1.9	0.9	
8	#N/A	***RB_183.4***	#N/A	#N/A	1.9	1.0	
9	#N/A	***RB_285.12***	#N/A	#N/A	1.9	0.9	
10	#N/A	***RB_358.8***	#N/A	#N/A	1.9	0.7	
11	WCI-2 (lipoxygenase) (wheat)	***U32428***	U32428	#N/A	2.0	0.5	
12	Wir2 (thaumatin-like protein) (wheat)	***X58394***	X58394	#N/A	**2.9**	0.8	
	Bgt-dependent repression						
13	TaGLP4 (germin-like protein)	***AJ237942^{Bgh}***	AJ237942	#N/A	**0.4**	0.6	
14	#N/A	***RB_264.6***	#N/A	#N/A	**0.4**	0.7	
15	APS reductase *A. thaliana*	***RB_c093***	#N/A	7.00E-66	**0.5**	0.6	
16	exon of glutathione-S-transferase (wheat; X56012)	***Wir5E123***	(X56012)	#N/A	0.5	0.8	
17	28S ribosomal RNA gene (fungal) [AY064705]	***RB_c116^{Bgh}***	AJ888238	4.00E-71	**0.4**	1.1	
18	G3PDH (Blumeria graminis f.sp. hordei) [X99732]	***RB_c122^{Bgh}***	AJ888233	1.00E-71	**0.3**	1.0	
	extendedly induced						
19	unknown [Hv.10128]	***OA_a1A03***	AJ888591	1.00E-158	1.4	**3.4**	⇦
20	cytochrome P450 [AP002839]	***OA_a1C04***	AJ888598	1.00E-78	1.5	**2.2**	⇦

Table 8.9 (continued)

	Putative function & [Blast hit]	EST ID	access. no#	E-val	pilot exp. sylA on total leaves *Bgt* 48 hat	- 48 hat	
	1	2	3	4	5	6	7
21	fructose-bisphosphate aldolase [CD907979]	***OA_a1C12***	AJ888600	1.00E-141	1.5	**2.1**	⇦
22	unknown [D22421]	***OA_a1D08***	AJ888603	8.00E-06	1.7	**2.3**	⇦
23	cytochrome P450 [AF321867]	***OA_a1D09***	AJ888604	3.00E-67	1.8	**4.2**	⇦
24	ferredoxin-dependent glutamate synthase [BJ323017]	***OA_a1D10***	AJ888605	4.00E-60	1.5	2.0	⇦
25	hsp 23.6 [Ta.214]	***OA_a1H02^{bgh}***	AJ874076	1.00E-143	**2.6**	**6.2**	⇦
26	alcohol dehydrogenase ADH1 [CD868456]	***OA_a2A05***	AJ888612	1.00E-163	1.1	1.9	⇦
27	NADPH-dependent oxidoreductase [CA682777]	***OA_a2C02^{bgh}***	AJ874078	3.00E-99	1.7	**2.4**	⇦
28	enolase 1 [CD454849]	***OA_a2G01***	AJ888626	8.00E-90	**3.5**	**4.0**	⇦
29	no significant hit	***OA_b1A06^{Bgh}***	AJ874086	#N/A	1.2	2.0	⇦
30	no significant hit	***OA_b2B07***	AJ888674	#N/A	**6.8**	**14.1**	⇦
31	pir7b [Q43360]	***OA_b1B01^{bgh}***	AJ874087	2.00E-67	**3.9**	**5.6**	⇦
32	26s proteosome regulatory subunit [CA602939]	***OA_b1C03***	AJ888656	1.00E-47	1.4	**2.1**	⇦
33	cytochrome P450 [AP002839]	***OA_b1D06***	AJ888659	3.00E-47	1.4	**4.8**	⇦
34	voltage-dependent anion channel 1 [X77733]	***OA_b1F04***	AJ888662	2.00E-57	**3.0**	**7.3**	⇦
35	DMI1 [CA027230]	***OA_b2E04***	AJ888682	0.00E+00	1.5	**2.4**	⇦
36	valyl tRNA synthetase [AC084023]	***OA_b2E06***	AJ888683	3.00E-63	1.1	**2.2**	⇦
37	epoxide hydrolase [Ta.26236]	***OA_b3B10***	AJ888700	2.00E-78	1.3	2.0	⇦
38	glutathione S-transferase [CN013161]	***OA_b3D05^{Bgh}***	AJ874102	1.00E-152	1.3	**2.1**	⇦
39	unknown [BU100203]	***OA_b3E09^{bgh}***	AJ874103	0.00E+00	1.9	**2.0**	⇦
	48 hat specific downregulation						
40	Nitrite reductase apoprotein (Nir1), *(H. vulgare)*	***RB_c061***	#N/A	6.00E-18	1.0	**0.5**	
41	lipid transfer protein 3 (LTP3), *(T. aestivum)*	***RB_c092***	#N/A	3.00E-21	1.1	**0.5**	
42	BAC OJ1055_H05,chromosome 12, *(O. sativa)*	***RB_38B.2***	#N/A	1.10E+00	1.2	**0.4**	
43	Hypothetical protein, *(A. thaliana)*	***RB_38B.3^{bgh}***	AJ874051	1.50E-02	#N/A	0.5	
44	#N/A	***RB_42B.2***	#N/A	#N/A	0.8	**0.5**	
45	#N/A	***RB_43A.1***	#N/A	#N/A	0.9	0.5	
46	#N/A	***RB_43A.2***	#N/A	#N/A	0.9	0.5	
47	#N/A	***RB_43A.3***	#N/A	#N/A	#N/A	**0.4**	
48	Phosphoethanolamine methyltransferase, *(T. aestivum)*	***RB_45.3***	#N/A	5.00E-07	0.6	**0.4**	
49	#N/A	***RB_52.2***	#N/A	#N/A	0.9	**0.5**	

Table 8.9 (continued)

	Putative function & [Blast hit]	EST ID	access. no#	E-val	pilot exp. sylA on total leaves *Bgt* 48 hat	pilot exp. sylA on total leaves - 48 hat	
	1	2	3	4	5	6	7
50	#N/A	***RB_87.3***	#N/A	#N/A	1.1	**0.5**	
51	DNA chromosome 4, contig fragment No. 19, *(A. thaliana)*	***RB_153.1***	#N/A	9.60E+00	1.2	**0.5**	
52	#N/A	***RB_155.7***	#N/A	#N/A	1.1	**0.5**	

8.11. Blast analysis & alignments

8.11.1. Wheat pir7b homolog *OA_b1B01, OA_b2A07*

```
b1B01    1                                                        GTGTT
b2A07    1
pir7b  181                                  ...GCCTCAGCGTCGCGCTCGCCATGGAGAGGTT

b1B01    6 CCCCGGCAAGCCGTGTTCGCAGCCGCCGGGATGCCGTGCGTTGGCAAGCACATGGGCGTC
b2A07    1
pir7b  241 CCCGGACAAGCCGTGTTCGTCGCCGCCGCGATGCCGTGCGTCGGCAAGCACATGGGCGTC

b1B01   66 AGTTCATGCGAAGGACATCATCGGAAGG...ACTCATGGACTGCAAGATGATAACAACCA
b2A07    1 AGTTCATGCGAAGAACATCATCGAAGGGACTACTCATGGACTGCGAGATGATAACAACCA
pir7b  301 AGTTCATGAGAAGAACTGCACCTGAAGGATTACTTATGGATTGCGAAATGACAATAGCCA

b1B01  123 CGGTGCAGGGGTTGCAATGATAATGGGCCCAAACTTCTTAACTACCAGCAAAGTTCACCT
b2A07   61 GGGTGCAGGGGTTGCAATCATAATGGGCCCAGACTTCTTAATTACCAGCAAAGTCCACCT
pir7b  361 GGGCTCAGGAGTTGCAATCAATTTGGGACCAACCTTCTTGACTACCAGCAAAGTCCAGCA

b1B01  183 GAGGATTTGGCCCTGGCAAAAATGTTGGTGACCTGTTCATGGAGGATCCGGTGATGAAGG
b2A07  121 GAGGATTTGGCCCTAGCAAAAATGTTGGTGACCAGTTCATGAAGGATCCAGTGATGAAGG
pir7b  421 GAGGATCTGGCACTGGCGAAGATGCTGGTGATCAGTTCATGGATGATCCGGTGATGAAAG

b1B01  243 ATGCAAGCCTGCTCACCGATGGTCGGTGAAGAAGGTATATGTGGTAGCAAAGGCTGATGG
b2A07  181 ATGCAAGCCTGCTCACCGATGGTCGGTGAAGAAGGTATACGTGGTAGCCAAGCCTGATGG
pir7b  481 ATGAGAGCTTGCTCACCAATGATCGGTGAAGAAGGTGTACGTGATCGCCAAGGCTGACAG

b1B01  303 CTCCAGCACCAGCGTTGGATGGTGTTGTTGAGCCCCGGCACGGAGGCCGAGGAGATCGCG
b2A07  241 CTCCAGCACCAGCGTTGGATGGTGATGTTTAGCCCCGACACGGAGGTCGAGGAGATCGCC
pir7b  541 CTCCAGCACCAGCGGTGGATGGTGGCGATGAGCCCTGGCACGGACGTCGAGGAGATCGCC

b1B01  363 ACGCCATCATGAGCTCGGGGCCTAGGGAGCTCTGTGATGCTCTGGTCAAGGCTTAAATAC
b2A07  301 ATGCCATCATGAGCTCTAGGCCTACGGAGCTCTGTGATGCTCTGGTCAAGACTTAAATAC
pir7b  601 ACGCCGTCATGAACTCCAAGCCCAGGGAACTCTGCGACATTCTGATCAAGAATACGAGTA

b1B01  423 TTGCTAAATTGTAC
b2A07  361 TTGCTAAAGTGTAC
pir7b  661 GAAAAATGCCAGTTTGGAAATAATCAGTGCTTC...
```

Figure 8.4: Alignment of nucleic acid sequences of two homologs of the rice pir7b esterase (accession # Z34270). Only the region of *OA_b1B01 and OA_b2A07* is shown and continuing sequences are indicated by '...'. Identical nucleotides conserved are displayed in white letters and similar nucleotides (purin or pyrimidin) are in gray boxes. Gaps introduced to improve the alignment are indicated by dots. Multiple sequence alignment was done using PILEUP program (Wisconsin Package Version 10.3, Accelrys Inc., San Diego, CA). The boxes were drawn using a BOXSHADE 3.21 web site (http://www.ch.embnet.org/software/BOX_form.html).

8.11.2. Wheat NBS-LRR resistance gene homolog *OA_a1E08*

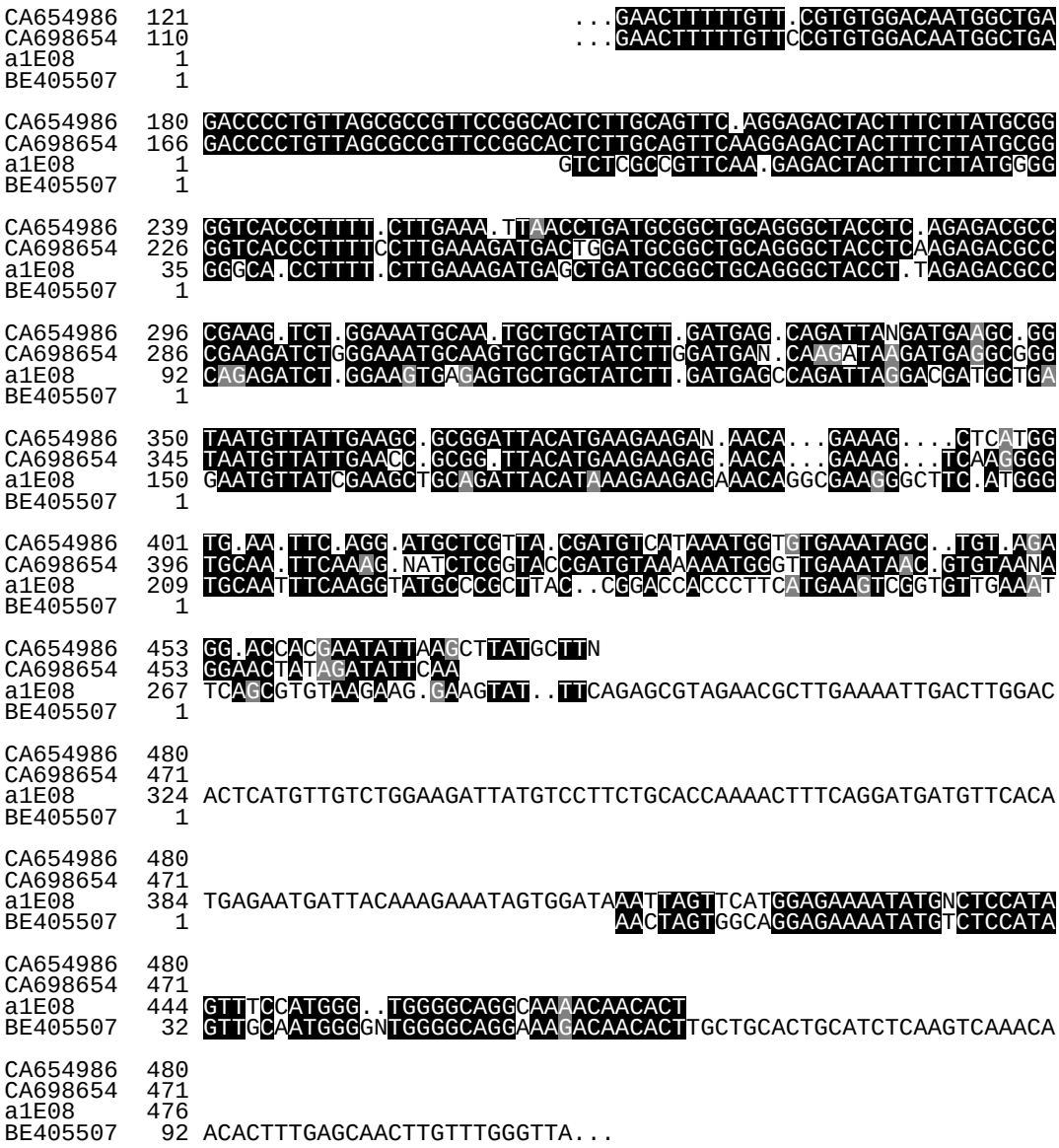

Figure 8.5: Alignment of *OA_a1E08* to wheat ESTs. Only the region of *OA_a1E08* is shown and continuing sequences are indicated by '...'. The total length of the alignment is 1128 bp. Identical nucleotides conserved are displayed in white letters and similar nucleotides (purin or pyrimidin) among at least four members are in gray boxes. Gaps introduced to improve the alignment are indicated by dots. Multiple sequence alignment was done using PILEUP program (Wisconsin Package Version 10.3, Accelrys Inc., San Diego, CA). The boxes were drawn using a BOXSHADE 3.21 web site. (http://www.ch.embnet.org/software/BOX_form.html).

8.11.3. Wheat putative epoxide hydrolase *OA_b2H01* and *OA_b3B10*

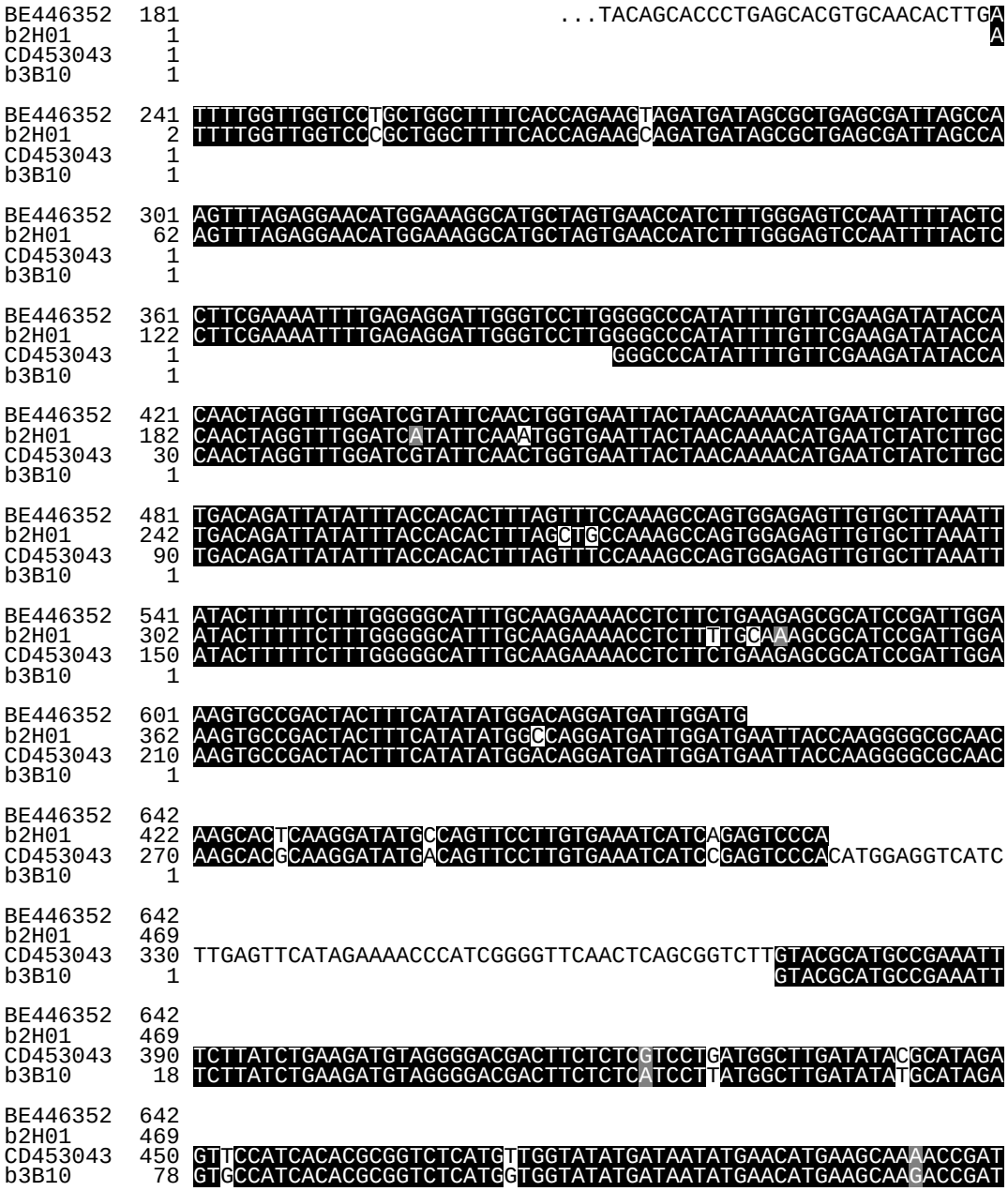

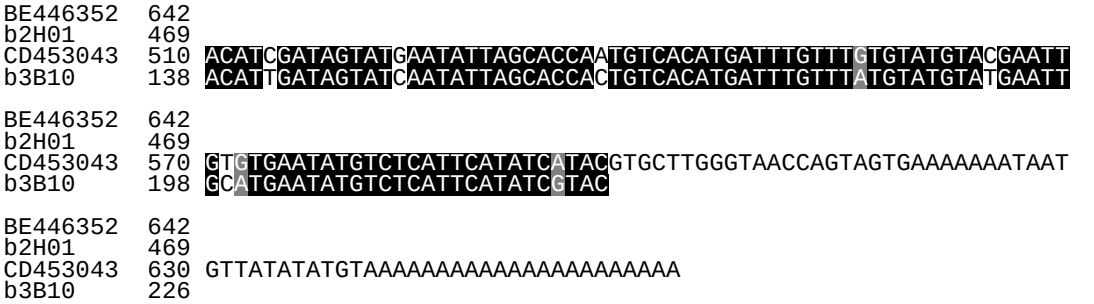

Figure 8.6: Alignment of *OA_b2H01* and *OA_b3B10* to wheat ESTs. Only the 3' region of BE446352 is shown and continuing sequences are indicated by '...'. The total length of the alignment is 1053 bp. Identical nucleotides conserved are displayed in white letters and similar nucleotides (purin or pyrimidin) are in gray boxes. Gaps introduced to improve the alignment are indicated by dots. Multiple sequence alignment was done using PILEUP program (Wisconsin Package Version 10.3, Accelrys Inc., San Diego, CA). The boxes were drawn using a BOXSHADE 3.21 web site. (http://www.ch.embnet.org/software/BOX_form.html).

8.11.4. Wheat cDNA fragment *OA_a2F04*

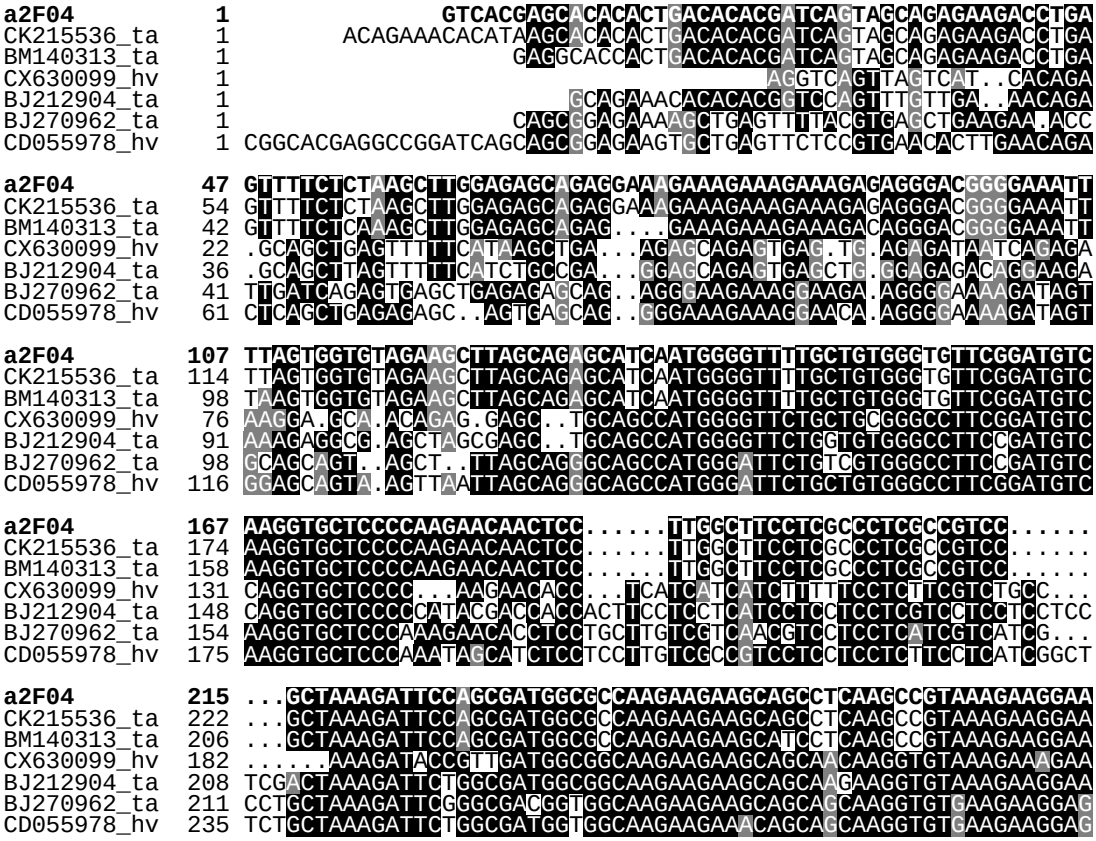

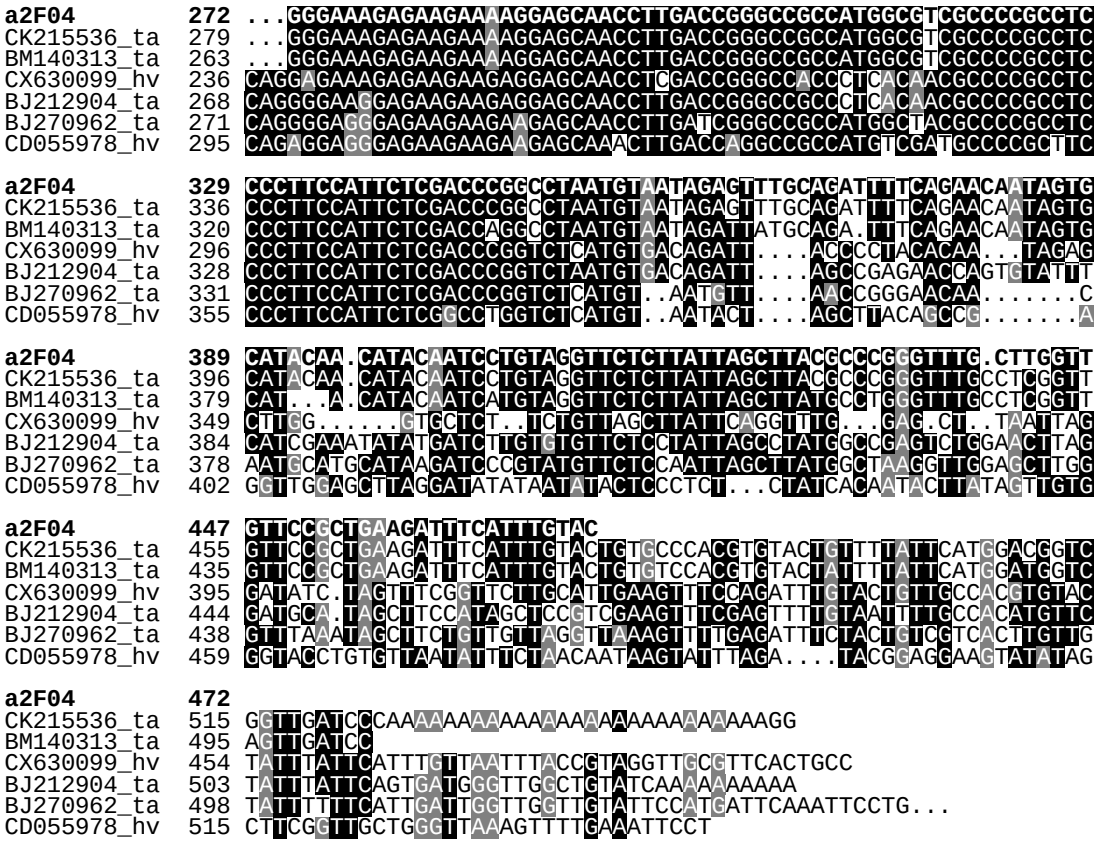

Figure 8.7: Alignment of *OA_a2F04* to wheat (_ta) and barley (_hv) ESTs. Continuing sequences are indicated by '...'. Identical nucleotides conserved are displayed in white letters and similar nucleotides (purin or pyrimidin) are in gray boxes. Gaps introduced to improve the alignment are indicated by dots. Multiple sequence alignment was done using PILEUP program (Wisconsin Package Version 10.3, Accelrys Inc., San Diego, CA). The boxes were drawn using a BOXSHADE 3.21 web site. (http://www.ch.embnet.org/software/BOX_form.html).

8.11.5. Wheat cDNA fragment *OA_a2B04*

Figure 8.8: Alignment of *OA_a2B04* to barley ESTs. Only parts of the barley ESTs are shown and continuing sequences are indicated by '...'. The total length of the alignment is 805 bp. Identical nucleotides conserved are displayed in white letters and similar nucleotides (purin or pyrimidin) are in gray boxes. Gaps introduced to improve the alignment are indicated by dots. Multiple sequence alignment was done using PILEUP program (Wisconsin Package Version 10.3, Accelrys Inc., San Diego, CA). The boxes were drawn using a BOXSHADE 3.21 web site. (http://www.ch.embnet.org/software/BOX_form.html).

8.12. Renamed hairpin loop transcript expression constructs

Table 8.10: List of constructs renamed after sequencing. High throughput cloning brings about the risk of mixing up samples. Sequencing revealed that some of the p_IPK expression constructs contained different DNA sequences than expected. Some of them were still considered to be interesting candidates to study loss of gene function. To avoid further confusion, corresponding sample names were left unchanged (column 3) but construct IDs were referred to with the actual name of the real DNA inserts (column 2).

Construct ID	cDNA fragment	original sample name	cDNA accession#
1	2	3	4
pOA_b3C08_IPK	***OA_b3C08***	pOA_b3C08u_IPK	AJ888703
pOA_a3A04_IPK	***OA_a3A04***	pOA_a3A04u_IPK	AJ874081
pOA_b1G10_IPK	***OA_b1G10***	pOA_a1E08_IPK	AJ888664
pOA_a1D09_IPK	***OA_a1D09***	pOA_b3D01_IPK	AJ888604
pOA_b3C03_IPK	***OA_b3C03***	pOA_b2E04_IPK	AJ888702
pOA_b2G09_IPK	***OA_b2G09***	pOA_b3C08o_IPK	AJ874098

8.13. Incompatible and compatible nonhost and race-specific interactions of wheat and powdery mildew

Table 8.11: Nonhost Resistance: Proportions of cells exhibiting HR during incompatible interactions with wheat and *Blumeria graminis*. Interactions on 10 leaves were scored at 2 dpi. The number of cells exhibiting whole cell AF is labeled with HR resistance. The number of cells exhibiting no or only local autofluorescence is labeled with pen resistance. Colonized cells containing haustoria or esh were labeled with 'esh no HR'.

wheat cv.	pathogen	pen resistance	HR resistance	esh no HR	tot interactions	PE (%)	HR (%)
Fidel	Bgh	92	185	0	277	**0**	**67**
Fidel	Bgt	165	52	57	217	**26**	**24**
Kanzler	Bgh	54	202	0	256	**0**	**79**

Table 8.12: Race-specific resistance: Proportions of cells exhibiting HR during incompatible interactions with wheat and *Blumeria graminis*. Interactions on 2 leaves were scored at 2 dpi. The number of cells exhibiting whole cell AF lacking pre-haustorial structures is labeled with 'pre-hau HR'. Whole cell AF in the presence of pre-haustorial structures is labeled with 'post-hau HR'. The number of cells exhibiting no or only local autofluorescence is labeled with pen resistance. Colonized cells containing haustoria or esh were labeled with 'esh no HR'.

wheat cv.	pathogen	pen resistance	pre-hau HR	post-hau HR	esh no HR	tot interactions	PE (%)	HR (%)
MA	*BgtAvr2*	11	31	95	1	138	**1**	**91**
MA	*BgtAvr3*	227	20	88	6	341	**2**	**32**
MA	*BgtVir*	59	21	2	103	185	**56**	**12**

8.14. Induction of gene transcription by infection of wheat with *Blumeria graminis*

Table 8.13: Genes regulated by *Blumeria graminis*-infection at 08 and 24 hai. Data were derived from one single-pass experiment and labeling was done starting from poly(A)$^+$RNA (chapt. 4.2.1.5). Only genes exhibiting more than 2-fold variability of expression in at least one of the time points and treatments were listed. Bold t/c ratios: Ratios exceeding threshold limit of 2. Names of *Blumeria* isolates were abbreviated: *Vir* for *BgtVir*, *Avr2* for *BgtAvr2*, *Avr3* for *BgtAvr3*. #N/A denotes that corresponding data were not available. In the case of t/c ratios, #N/A denotes missing ore flagged probes on particular microarray slides. Genes found to be regulated by sylA treatment (Table 4.7) were highlighted by arrows ⇦. Arrows of genes exhibiting sylA responsiveness only at the 2 hat time point (Table 4.9) were set into parenthesis (⇦). SylA-responsiveness of *OA_b3C12* (row 88) was indicated only in microarray experiments labeled according to the poly(A)$^+$ RNA method (chapt. 4.2.1.6). Genes described elsewhere to be epidermally induced by barley powdery mildew attack are marked with $^{'Bgh'}$, genes found to be ubiquitously induced by *Bgh* are marked with $^{'bgh'}$ (Bruggmann et al., 2005).

					08 hai						24 hai						
	Putative function		access.		wheat cv. MA				cv. Kanzler		wheat cv. MA				cv. Kanzler		
		EST ID	no#	E-val	*Vir*	*Avr2*	*Avr3*	*Bgh*	*Vir*	*Bgh*	*Vir*	*Avr2*	*Avr3*	*Bgh*	*Vir*	*Bgh*	
	1	2	3	4	5	6	7	8	9	10	11	12	13	14	15	16	
1	TaGLP4 (germin-like protein)	***AJ237942^{Bgh}***	AJ237942	#N/A	**10.8**	**11.7**	**13.3**	**14.2**	**8.5**	**5.2**	**21.7**	**15.4**	**14.4**	**9.6**	**11.4**	**10.3**	
2	glyceraldehyde-3-phosphate dehydrogenase	***GapC***	#N/A	#N/A	0.8	0.9	1.0	1.2	1.0	1.0	0.6	**0.5**	0.5	**0.4**	**0.4**	**0.4**	⇦
3	Wir1	***M94959***	M94959	#N/A	**2.9**	1.8	**3.7**	**2.3**	**4.6**	**5.4**	**2.7**	**2.9**	**3.3**	**3.0**	**2.8**	**3.4**	
4	a-tubulin	***OA_aTubuRsa***	AJ890248	1.E-158	1.1	0.9	0.7	1.1	1.0	1.0	**2.0**	1.0	0.8	1.0	1.5	1.2	
5	glyceraldehyde-3-phosphate dehydrogenase (cytosolic, wheat)	***OA_G3PDHRsa***	AJ890249	1.E-133	1.1	1.1	0.9	1.0	1.2	1.4	**2.8**	1.7	**2.5**	**2.6**	**3.1**	**3.3**	⇦
6	TaGLUC5 (beta-1,3-endoglucanase)	***OA5***	AJ890250	1.E-154	0.9	0.7	0.8	0.9	1.0	0.9	**4.4**	**2.7**	**3.0**	**3.5**	**3.0**	**3.5**	
7	ribulose-bisphosphate carboxylase small subunit	***BE437451***	BE437451	2.E-22	1.0	1.1	1.3	1.3	1.1	1.2	**0.5**	**0.4**	**0.4**	**0.3**	**0.3**	**0.3**	
8	unknown	***BE437465***	BE437465	3.E-79	1.0	0.9	1.0	1.2	1.0	1.0	0.8	**0.5**	0.7	0.7	0.7	0.7	
9	unknown	***BE437518***	BE437518	8.E-53	0.9	0.8	1.1	1.4	0.9	1.0	0.6	0.5	**0.5**	**0.4**	**0.4**	**0.4**	
10	phospho-2-dehydro-3-deoxyheptonate aldolase 1	***BE437593***	BE437593	2.E-75	0.9	1.0	1.1	1.4	1.0	1.0	0.9	0.7	**0.5**	**0.4**	0.6	0.5	
11	glyceraldehyde-3-phosphate dehydrogenase (cytosolic)	***BE437891***	BE437891	1.E-67	1.0	1.0	0.8	1.0	1.3	1.5	**3.0**	1.6	**2.3**	**2.7**	**2.5**	**3.0**	⇦
12	ribulose-bisphosphate carboxylase small subunit	***BE437892***	BE437892	6.E-13	1.0	1.0	1.1	1.1	1.1	1.1	**0.4**	**0.4**	**0.5**	**0.5**	**0.3**	**0.4**	
13	glyceraldehyde-3-phosphate dehydrogenase (cytosolic)	***BE437899***	BE437899	4.E-81	1.0	0.9	0.9	1.1	1.2	1.4	**2.3**	1.5	**2.1**	**2.2**	**2.4**	**2.7**	⇦
14	chlorophyll a/b-binding protein (light harvesting)	***BE437996***	BE437996	3.E-31	0.9	0.9	0.9	1.4	1.0	1.0	**0.5**	**0.3**	**0.2**	**0.3**	**0.2**	**0.3**	
15	WCI-1	***U32427***	U32427	#N/A	1.2	0.9	0.6	1.3	0.7	0.8	**0.4**	**0.3**	**0.2**	**0.3**	**0.3**	**0.2**	
16	WCI-2 (lipoxygenase)	***U32428***	U32428	#N/A	1.9	**4.0**	0.6	1.8	1.4	1.4	0.5	1.0	0.6	0.9	**0.1**	**0.2**	(⇦)
17	WCI-4 (thiol protease)	***U32430***	U32430	#N/A	1.0	0.9	0.8	1.0	0.7	0.9	**0.5**	**0.5**	**0.3**	**0.4**	**0.4**	**0.4**	
18	WCI-5	***U32431***	U32431	#N/A	**4.8**	**4.4**	**5.7**	**4.7**	**3.4**	**3.5**	**4.8**	**6.6**	**5.6**	**5.6**	**2.9**	**5.4**	
19	exon of glutathione-S-transferase (wheat X56012)	***Wir5E123***	(X56012)	#N/A	1.9	1.4	1.6	1.0	**2.2**	2.0	**3.9**	**3.0**	**4.8**	1.6	**5.0**	**2.2**	
20	Wir3 (peroxidase)	***X56011***	X56011	#N/A	**8.8**	**4.4**	**3.6**	**3.5**	**9.0**	**11.1**	**38.6**	**30.6**	**37.1**	**23.2**	**22.3**	**23.4**	(⇦)

Table 8.13 (continued)

	Putative function	EST ID	access. no#	E-val	08 hai wheat cv. MA Vir	08 hai wheat cv. MA Avr2	08 hai wheat cv. MA Avr3	08 hai wheat cv. MA Bgh	08 hai cv. Kanzler Vir	08 hai cv. Kanzler Bgh	24 hai wheat cv. MA Vir	24 hai wheat cv. MA Avr2	24 hai wheat cv. MA Avr3	24 hai wheat cv. MA Bgh	24 hai cv. Kanzler Vir	24 hai cv. Kanzler Bgh	
	1	2	3	4	5	6	7	8	9	10	11	12	13	14	15	16	
21	Wir2 (thaumatin-like protein)	***X58394***	X58394	#N/A	**17.6**	**14.3**	**16.4**	**21.1**	**20.2**	**31.9**	**29.6**	**42.9**	**32.4**	**22.5**	**20.4**	**31.2**	
22	TaGLUC2 (beta-1,3-endoglucanase)	***Y18212***	Y18212	#N/A	1.4	1.0	1.2	1.2	1.8	**2.1**	**11.2**	**9.2**	**9.7**	**11.2**	**10.4**	**13.7**	
23	RUBISCO 3prime end	***RUB_3'***	#N/A	#N/A	0.6	0.9	1.1	1.2	0.9	0.9	**0.2**	**0.2**	**0.3**	**0.2**	**0.2**	**0.2**	
24	RUBISCO 5prime end	***RUB_5'_2***	#N/A	#N/A	0.6	0.7	0.9	1.1	0.7	0.7	**0.2**	**0.2**	**0.2**	**0.1**	**0.1**	**0.1**	
25	RUBISCO middle part	***RUB_5'_3'***	#N/A	#N/A	1.0	1.0	1.1	1.1	1.1	1.1	**0.3**	**0.3**	**0.4**	**0.4**	**0.3**	**0.3**	
26	translation initiation factor middle part	***TEF_5'_3'***	#N/A	#N/A	1.0	0.9	0.9	1.2	1.0	1.2	**2.1**	1.4	1.2	1.3	1.5	1.8	
27	unknown	***OA_a1A03***	AJ888591	1.E-158	1.1	1.0	1.1	0.9	1.1	1.1	**3.0**	**2.4**	1.5	**2.3**	**2.1**	1.4	⇦
28	unknown	***OA_a1A05***	AJ888592	4.E-55	0.8	0.7	0.7	0.8	0.8	0.8	**0.3**	**0.2**	**0.5**	**0.4**	**0.3**	**0.4**	
29	epoxide hydrolase	***OA_a1A07***	AJ888593	5.E-20	1.0	0.9	1.0	1.0	1.1	1.1	0.5	**0.5**	0.6	**0.5**	0.6	**0.5**	
30	DnaJ-1	***OA_a1A12***	AJ888595	2.E-33	0.8	0.8	1.2	1.3	0.9	1.0	**0.4**	**0.4**	**0.3**	**0.3**	**0.2**	**0.3**	
31	hsp 23.5	***OA_a1B01^{bgh}***	AJ874072	1.E-133	**2.8**	**2.4**	**2.8**	1.6	**3.4**	**4.4**	**9.2**	**9.3**	**5.5**	**4.9**	**7.7**	**4.0**	⇦
32	cytochrome P450	***OA_a1C04***	AJ888598	1.E-78	0.9	0.7	1.1	0.8	0.9	1.1	**2.2**	1.7	**2.0**	**4.0**	**2.8**	**3.1**	⇦
33	fructose-bisphosphate aldolase	***OA_a1C12***	AJ888600	1.E-141	0.8	0.7	0.8	1.1	1.1	1.1	**2.7**	1.4	1.0	1.3	1.6	1.5	⇦
34	NBS-LRR disease resistance protein	***OA_a1E08^{bgh}***	AJ874075	3.E-49	1.4	1.2	1.1	0.9	**2.5**	**2.0**	**2.6**	1.9	**3.2**	**2.2**	**3.0**	**3.7**	⇦
35	lysyl-tRNA synthetase	***OA_a1E11***	AJ888608	0.E+00	0.8	0.8	0.9	1.1	1.0	0.7	0.5	**0.4**	**0.4**	**0.4**	**0.4**	**0.4**	⇦
36	hsp 23.6	***OA_a1H02^{bgh}***	AJ874076	1.E-143	1.8	1.6	1.7	1.6	**2.2**	**2.2**	**7.3**	**5.7**	**2.7**	**4.1**	**5.3**	**4.5**	⇦
37	unknown	***OA_a1H06***	AJ888610	3.E-84	1.7	1.8	**3.3**	1.3	2.0	1.0	1.2	**5.0**	**2.2**	1.8	**0.5**	0.6	⇦
38	unknown	***OA_a2A03***	AJ888611	2.E-20	1.3	1.0	1.4	1.0	1.4	1.1	1.4	1.1	1.5	1.6	1.3	**2.4**	
39	MRP-like ABC transporter	***OA_a2A06***	AJ888613	1.E-161	1.2	1.1	0.8	0.9	1.3	0.9	**2.3**	1.0	1.6	**2.1**	1.2	1.1	⇦
40	NADH dehydrogenase	***OA_a2B11^{bgh}***	AJ874077	1.E-101	1.4	1.3	1.2	0.9	1.5	1.3	**5.2**	**3.4**	**4.2**	**3.3**	**4.8**	**3.9**	⇦
41	NADPH-dependent oxidoreductase	***OA_a2C02^{bgh}***	AJ874078	3.E-99	**2.9**	**2.5**	**2.4**	1.5	**2.5**	1.6	**7.9**	**4.3**	**4.4**	**7.6**	**6.6**	**8.3**	⇦
42	26S proteasome regulatory subunit	***OA_a2C11***	AJ888616	3.E-62	0.9	0.8	0.9	0.7	0.9	1.1	1.7	1.4	1.1	1.4	**2.1**	1.6	⇦
43	alanine aminotransferase 2	***OA_a2D10^{bgh}***	AJ874079	0.E+00	1.0	1.0	0.8	0.7	1.2	1.5	**2.4**	1.3	**2.2**	**2.6**	**2.2**	**2.7**	⇦
44	MDR-like ABC transporter	***OA_a2E02***	AJ888620	0.E+00	1.1	1.1	1.2	1.0	1.1	1.0	**2.7**	1.7	1.6	**2.1**	1.9	1.4	⇦
45	unknown	***OA_a2E09***	AJ888622	1.E-51	0.8	0.8	1.0	0.8	0.9	0.8	0.5	0.5	0.6	0.5	**0.5**	0.5	⇦
46	unknown	***OA_a2F04***	AJ888625	0.E+00	**2.6**	**3.0**	**4.9**	1.0	**2.8**	1.2	1.8	**17.8**	**5.6**	**2.8**	**0.4**	**0.4**	⇦
47	60S ribosomal protein L30	***OA_a2H04***	AJ888629	4.E-41	0.9	1.0	1.2	0.9	1.2	1.2	1.5	**3.3**	1.9	1.7	1.0	1.2	⇦
48	glutathione-S-transferase/glutaredoxin	***OA_a3A01***	AJ888631	1.E-144	0.8	0.9	0.8	0.7	1.0	1.2	1.4	1.0	1.7	**2.1**	**2.6**	**3.2**	⇦
49	hsp70-interacting protein	***OA_a3A05***	AJ888633	8.E-35	1.8	1.3	1.2	0.9	1.6	1.1	**3.2**	1.8	1.1	1.2	1.4	0.8	(⇦)
50	adenylate kinase (ATP-AMP transphosphorylase)	***OA_a3A08^{bgh}***	AJ874082	1.E-50	1.1	1.0	1.0	0.8	1.3	1.5	**3.4**	**3.0**	**3.6**	**3.4**	**4.3**	**4.8**	⇦
51	UDP-glucose:salicylic acid glucosyltransferase	***OA_a3B03***	AJ888635	5.E-49	1.5	1.2	1.9	1.2	1.4	1.1	**3.4**	**2.6**	**2.1**	**2.7**	1.2	0.7	⇦
52	rubisco L	***OA_a3B08***	AJ888636	2.E-38	1.3	1.4	**2.1**	**2.1**	1.4	1.4	1.1	1.4	0.8	0.6	0.6	0.7	
53	prohibitin	***OA_a3C03^{bgh}***	AJ874085	1.E-114	1.0	0.8	0.8	0.9	1.1	1.1	**2.3**	1.5	**2.0**	**2.6**	**2.8**	**4.0**	⇦
54	MRP-like ABC transporter	***OA_a3D05***	AJ888640	1.E-93	1.2	1.0	1.1	0.9	1.1	1.0	**2.4**	1.3	1.5	**2.2**	1.3	1.3	⇦

Table 8.13 (continued)

	Putative function	EST ID	access. no#	E-val	08 hai						24 hai						
					wheat cv. MA				cv. Kanzler		wheat cv. MA				cv. Kanzler		
					Vir	*Avr2*	*Avr3*	*Bgh*	*Vir*	*Bgh*	*Vir*	*Avr2*	*Avr3*	*Bgh*	*Vir*	*Bgh*	
	1	2	3	4	5	6	7	8	9	10	11	12	13	14	15	16	
55	ABC transporter	***OA_a3D11***	AJ888641	1.E-119	**2.5**	**2.6**	1.9	1.9	2.0	1.3	**3.7**	**2.7**	**5.0**	**4.9**	**4.2**	**5.7**	
56	(alanine) acetyltransferase	***OA_a3E08***	AJ888642	2.E-82	**3.0**	**2.4**	**3.6**	1.7	**2.5**	1.5	1.6	**3.6**	**2.8**	1.9	1.2	1.0	⇦
57	unknown	***OA_a3F01***	AJ888644	2.E-54	0.9	0.7	1.0	0.8	0.7	1.0	**0.5**	**0.5**	**0.5**	**0.4**	**0.4**	**0.4**	
58	cell division control protein 48 homolog E (Transitional endoplasmic reticulum ATPase E)	***OA_a3F09***	AJ888645	0.E+00	1.1	0.9	0.8	0.9	0.9	1.0	**2.2**	1.2	1.3	1.5	1.8	1.4	⇦
59	unknown	***OA_a3G11***	AJ888648	2.E-17	0.7	0.6	0.8	0.7	0.6	0.8	0.6	0.6	0.5	0.6	0.5	**0.5**	
60	nuclear coiled-coil protein	***OA_b1A07***	AJ888651	0.E+00	**2.0**	**2.0**	1.9	1.1	1.9	1.1	1.7	1.9	**2.2**	1.7	1.9	**2.3**	⇦
61	light repressible receptor protein kinase	***OA_b1B08***	AJ888654	5.E-73	0.7	0.8	0.6	0.7	0.8	0.7	1.0	**0.5**	0.8	1.0	1.1	1.6	⇦
62	succinyl-CoA-ligase beta subunit	***OA_b1D01***^{bgh}	AJ874089	3.E-63	0.9	0.9	0.7	0.7	1.0	0.9	1.2	0.8	1.5	1.9	2.0	**2.8**	⇦
63	cytochrome P450	***OA_b1D06***	AJ888659	3.E-47	1.3	1.2	1.4	0.7	1.4	1.3	**2.5**	**2.1**	**2.7**	**5.9**	**2.5**	**3.0**	⇦
64	succinyl-CoA-ligase beta subunit	***OA_b1E11***^{bgh}	AJ874090	5.E-38	0.9	0.8	0.7	0.7	0.9	0.9	1.1	0.8	1.4	1.6	1.8	**2.5**	⇦
65	voltage-dependent anion channel 1	***OA_b1F04***	AJ888662	2.E-57	1.1	1.0	1.0	0.7	1.2	1.1	**2.1**	1.5	1.8	**2.3**	**2.6**	**2.6**	⇦
66	26S proteasome RPN9b subunit	***OA_b1F08***	AJ888663	1.E-163	1.2	1.0	0.7	0.8	1.0	1.1	**2.1**	1.2	1.8	1.8	**2.6**	**2.4**	⇦
67	dynamin protein	***OA_b1G11***	AJ888665	0.E+00	1.1	1.1	0.9	0.7	1.1	1.2	**2.4**	1.5	**2.2**	**2.6**	**3.0**	**2.4**	
68	glutathione S-transferase	***OA_b1H08***^{bgh}	AJ874092	7.E-81	1.3	1.2	1.4	1.0	1.0	1.2	**2.0**	1.5	1.6	1.9	1.8	**2.3**	⇦
69	citrate synthase	***OA_b1H11***^{bgh}	AJ874093	3.E-59	0.8	0.9	0.7	0.6	0.9	0.9	**2.1**	1.0	**2.6**	**2.6**	**2.9**	**3.5**	⇦
70	autophagy / symbiosis-related microtubule associated protein	***OA_b2A02***	AJ888667	3.E-37	0.9	0.8	0.7	0.7	0.7	0.7	0.5	**0.4**	0.7	0.6	0.6	0.5	
71	phragmoplastin / dynamin-like protein	***OA_b2A08***	AJ888669	2.E-73	1.0	0.8	0.7	0.7	1.0	0.9	1.9	1.1	1.6	1.7	**2.0**	1.9	
72	enolase 2	***OA_b2A09***	AJ888670	2.E-44	0.8	0.7	0.6	0.8	0.8	0.5	0.6	**0.3**	**0.5**	**0.4**	**0.4**	**0.4**	⇦
73	ATP-dependent Clp protease	***OA_b2B02***	AJ888671	2.E-53	**3.2**	**2.3**	1.6	0.8	1.9	1.0	1.9	**2.4**	**4.4**	1.9	**2.7**	1.7	
74	calreticulin	***OA_b2C03***^{bgh}	AJ874095	1.E-105	1.8	1.5	1.2	1.5	1.7	**2.7**	**3.7**	**3.4**	**4.5**	**5.4**	**4.4**	**4.6**	
75	sorting nexin 1	***OA_b2C10***	AJ888679	9.E-95	0.7	0.8	0.7	0.8	0.8	0.8	0.7	**0.5**	1.0	0.9	0.7	1.0	
76	lecithin-cholesterol acyl transferase	***OA_b2D12***	AJ888681	1.E-156	0.6	0.7	0.8	0.9	0.8	0.7	**0.4**	**0.3**	**0.4**	**0.4**	**0.3**	**0.4**	⇦
77	thioredoxin (F-type)	***OA_b2E11***	AJ888685	2.E-24	0.7	0.8	0.9	0.9	0.9	0.8	0.5	**0.5**	0.6	0.5	**0.5**	0.5	
78	aspartate aminotransferase (cytoplasmic)	***OA_b2F07***	AJ888686	4.E-82	0.7	0.8	0.9	1.0	0.9	0.9	0.6	**0.5**	0.5	**0.5**	**0.5**	0.5	⇦
79	2,3-bisphosphoglycerate-independent phosphoglycerate mutase	***OA_b2G09***^{bgh}	AJ874098	1.E-90	1.1	1.0	0.7	0.8	1.0	1.1	1.7	0.8	1.4	2.0	1.9	**2.5**	⇦
80	20S proteasome beta 3 subunit	***OA_b2G11***	AJ888689	6.E-55	1.0	0.8	0.8	0.7	1.0	1.1	1.9	1.2	1.8	**2.3**	**2.8**	**3.2**	⇦
81	epoxide hydrolase	***OA_b2H01***	AJ888690	4.E-69	0.8	0.9	0.6	0.7	0.7	0.6	**0.3**	**0.1**	**0.4**	**0.3**	**0.4**	**0.4**	⇦
82	glucose transport protein fused to Caffeoyl-CoA O-methyltransferase	***OA_b2H03***	AJ874099	3.E-47	**7.1**	**5.3**	**6.8**	**3.7**	**4.3**	**3.2**	**2.8**	**3.3**	**4.0**	**2.9**	**2.3**	**2.4**	
83	NAC6 domain (NAM protein)	***OA_b3A07***	AJ888694	1.E-67	1.3	1.2	0.8	1.0	1.2	0.7	1.1	1.2	0.8	**0.4**	0.9	0.5	
84	20S proteasome beta 5 subunit	***OA_b3A12***	AJ888697	5.E-64	0.9	0.7	0.8	0.8	1.0	0.8	1.6	1.0	1.5	1.6	1.8	**2.2**	⇦
85	similarity to ATP binding protein associated with cell differentiation	***OA_b3B07***	AJ888699	6.E-51	1.0	0.9	0.8	0.8	0.9	0.9	**2.3**	1.8	1.8	**2.0**	**2.2**	**2.1**	
86	epoxide hydrolase	***OA_b3B10***	AJ888700	2.E-78	0.7	0.8	0.9	1.0	0.9	0.8	0.6	**0.4**	**0.5**	**0.4**	**0.3**	**0.4**	⇦

Table 8.13 (continued)

	Putative function	EST ID	access. no#	E-val	08 hai wheat cv. MA Vir	Avr2	Avr3	Bgh	08 hai cv. Kanzler Vir	Bgh	24 hai wheat cv. MA Vir	Avr2	Avr3	Bgh	24 hai cv. Kanzler Vir	Bgh	
	1	2	3	4	5	6	7	8	9	10	11	12	13	14	15	16	
87	glyceraldehyde 3-phosphate dehydrogenase (cytosolic)	***OA_b3C10^{bgh}***	AJ874100	5.E-68	1.1	1.0	0.8	0.9	1.3	1.4	**2.8**	1.6	**2.5**	2.0	**2.8**	**2.7**	⇦
88	unknown	***OA_b3C12^{bgh}***	AJ874101	0.E+00	1.0	0.8	0.7	0.8	1.1	1.3	2.0	1.3	1.8	**2.0**	**2.3**	**2.8**	(⇦)
89	20S proteasome alpha 5 subunit	***OA_b3D01***	AJ888705	1.E-20	1.0	0.7	0.8	0.7	1.0	1.1	**2.2**	1.4	**2.1**	**2.6**	**3.0**	**3.4**	⇦
90	signal sequence receptor, alpha subunit (SSR-alpha)	***OA_b3D11***	AJ888706	2.E-38	0.9	0.8	0.8	0.9	0.9	0.9	0.6	**0.4**	**0.5**	**0.5**	0.5	0.5	
91	rubisco (small subunit)	***OA_b3E01***	AJ888707	4.E-55	1.0	1.0	1.1	1.0	1.1	1.0	**0.5**	**0.5**	0.8	**0.4**	**0.4**	**0.4**	
92	unknown	***OA_b3E03***	AJ888708	1.E-176	0.8	0.8	0.7	0.8	0.8	0.8	0.7	0.6	**0.4**	**0.5**	0.8	0.9	⇦
93	unknown	***OA_b3E09^{bgh}***	AJ874103	0.E+00	1.0	1.0	0.8	0.7	1.1	0.8	1.4	0.7	2.0	**2.2**	**2.3**	**2.7**	⇦
94	NAM-like (No apical meristem)	***OA_b3F11***	AJ888713	0.E+00	1.0	0.8	0.7	0.9	0.9	0.8	0.5	**0.3**	**0.4**	**0.3**	**0.4**	**0.4**	
95	aconitate hydratase (cytoplasmic)	***OA_b3G05^{bgh}***	AJ874104	4.E-57	0.9	1.0	0.8	0.8	1.0	0.9	**2.6**	1.6	**2.3**	**2.4**	**2.4**	**2.7**	⇦
96	MAP kinase	***OA_b3G11***	AJ888716	2.E-63	0.8	0.7	0.9	0.9	0.9	0.7	0.7	**0.5**	0.6	0.5	0.6	0.6	
97	putative membrane associated protein	***RB_c004^{bgh}***	AJ873937 AJ873982 AJ874003	1.E-07	**4.7**	**3.6**	**3.7**	**3.1**	**4.1**	**4.0**	**8.8**	**8.8**	**8.0**	**5.3**	**6.4**	**5.1**	
98	beta-1,3-endoglucanase	***RB_c006^{bgh}***	AJ873940	3.E-28	1.3	1.2	**2.2**	1.0	1.4	1.6	**4.3**	**4.7**	**5.0**	**4.3**	**3.9**	**4.7**	
99	Phenylalanine ammonia-lyase	***RB_c011^{bgh}***	AJ873947	1.E-43	1.1	1.1	1.0	1.0	1.2	1.1	**3.4**	1.3	1.4	1.4	**2.2**	1.8	
100	cDNA clone WHE2831_H03_P05	***RB_c013^{Bgh}***	AJ873953 AJ873954 AJ873955	1.E-30	1.1	1.0	0.9	0.9	1.0	1.1	**2.4**	**2.2**	**2.1**	**2.4**	1.5	1.8	
101	calreticulin fragment (CHR2)	***RB_c014^{bgh}***	AJ873956 AJ874048	1.E-169	**2.1**	1.8	1.7	**2.1**	**2.5**	**3.1**	**4.7**	**4.4**	**5.9**	**6.4**	**5.6**	**6.6**	
102	beta-1,3-endoglucanase (Y18212)	***RB_c015^{bgh}***	AJ874005	1.E-140	1.1	1.1	1.1	1.0	1.3	1.4	**3.4**	**2.8**	**3.3**	**3.3**	**3.2**	**3.8**	
103	beta-1,3-glucanase (GLU2) gene, exons 1-2	***RB_c026^{bgh}***	AJ873987 AJ873988	1.E-52	1.7	1.5	1.6	1.3	1.5	1.5	**2.2**	1.5	**3.1**	**2.2**	**2.2**	**2.4**	
104	chitinase II (PR-3)	***RB_c028^{bgh}***	AJ873995 AJ873996 AJ874022	6.E-22	**2.9**	**2.0**	**2.5**	**2.2**	**2.9**	**4.3**	**7.9**	**9.0**	**8.9**	**10.0**	**5.1**	**5.8**	
105	subtilisin-chymotrypsin inhibitor 2	***RB_c029^{bgh}***	AJ874007	3.E-24	1.1	1.1	1.2	1.0	1.0	0.9	**2.1**	1.9	1.3	1.7	1.6	1.5	
106	Putative histidine kinase	***RB_c033^{bgh}***	AJ873992 AJ874021	7.E-21	0.9	1.0	1.2	1.0	1.8	1.3	0.8	1.0	1.0	0.9	**3.7**	**4.2**	
107	no significant hit ?	***RB_c037^{Bgh}***	AJ874025 AJ874026	#N/A	**2.5**	**2.1**	**2.2**	**2.1**	1.2	1.1	**5.6**	**4.0**	**8.4**	**4.0**	1.0	1.1	
108	glutamine synthetase	***RB_c038***	#N/A	6.E-56	0.7	0.6	0.6	0.8	0.6	0.8	**0.3**	**0.2**	**0.3**	**0.2**	**0.2**	**0.2**	
109	pathogenic related protein in response to Blumeria	***RB_c039^{bgh}***	AJ874034 AJ874035	6.E-08	**6.8**	**6.3**	**6.7**	**2.6**	**5.8**	**3.1**	**15.8**	**12.6**	**11.1**	**10.1**	**9.1**	**7.6**	
110	cDNA clone:J013165K20	***RB_c041^{bgh}***	AJ874045	7.E-04	1.4	1.4	1.5	1.2	1.5	1.5	**2.2**	**2.5**	**2.5**	**2.7**	**2.2**	**3.2**	
111	genomic DNA, chromosome 4, BAC clone: OSJNBb0091E11	***RB_c042^{bgh}***	AJ874054 AJ874055 AJ874056	1.E-10	**2.8**	**2.4**	**2.8**	**2.1**	1.0	1.0	1.7	1.9	**2.3**	1.3	0.8	0.8	
112	calreticulin (CRH2)	***RB_c044^{bgh}***	AJ874047 AJ874058	1.E-40	1.7	1.4	1.3	1.5	1.7	**2.1**	**3.0**	**2.9**	**3.6**	**3.8**	**3.7**	**4.0**	
113	Kaurene synthase	***RB_c047^{bgh}***	AJ873997	4.E-17	**4.8**	**3.9**	**2.7**	1.9	**4.5**	**3.4**	**11.6**	**7.6**	**16.3**	**9.0**	**13.7**	**11.9**	(⇦)
114	immediate-early salicylate-induced glucosyltransferase	***RB_c048^{bgh}***	AJ874027	2.E-29	**2.5**	**2.4**	**2.8**	**2.3**	**2.8**	**2.4**	**5.6**	**5.8**	**4.4**	**3.4**	**4.1**	**3.1**	⇦
115	UDP-galactose/UDP-glucose transporter	***RB_c053^{bgh}***	AJ874049 AJ874061	5.E-88	**2.8**	**2.8**	**2.3**	**2.3**	**2.7**	**2.6**	**3.1**	**2.0**	**3.3**	**2.8**	**5.0**	**3.3**	
116	O-linked GlcNAc transferase like protein (glcNAc-like gene)	***RB_c054***	#N/A	3.E-29	1.1	1.0	0.8	0.7	1.1	1.0	1.6	1.2	1.7	1.7	**2.0**	**2.0**	
117	Nitrite reductase apoprotein (Nir1)	***RB_c061***	#N/A	6.E-18	0.9	0.8	0.8	0.9	0.7	0.6	0.8	0.5	**0.5**	0.6	**0.5**	0.7	
118	Serine/threonine-protein kinase-like protein	***RB_c063***	#N/A	2.E-02	1.5	1.4	1.8	1.2	1.6	1.3	2.0	**2.1**	1.8	1.8	1.6	1.4	
119	superoxide dismutase-4A (Sod4a gene)	***RB_c064^{bgh}***	AJ874033 AJ874067	3.E-22	1.5	1.3	1.4	1.2	1.6	1.5	**2.3**	**2.1**	**2.3**	**2.0**	**2.2**	**2.3**	

Table 8.13 (continued)

	Putative function	EST ID	access. no#	E-val	08 hai						24 hai					
					wheat cv. MA				cv. Kanzler		wheat cv. MA				cv. Kanzler	
					Vir	*Avr2*	*Avr3*	*Bgh*	*Vir*	*Bgh*	*Vir*	*Avr2*	*Avr3*	*Bgh*	*Vir*	*Bgh*
	1	2	3	4	5	6	7	8	9	10	11	12	13	14	15	16
			AJ874068													
120	beta-1,3-endoglucanase	***RB_c069^{bgh}***	AJ873974	1.E-83	1.3	1.1	1.5	1.2	1.6	1.8	**5.4**	**4.1**	**5.6**	**6.0**	**4.9**	**5.3**
121	Putative cytochrome P450	***RB_c070^{bgh}***	AJ874023	4.E-44	1.6	1.4	1.1	1.2	0.9	0.7	**4.6**	**2.9**	**7.5**	**4.4**	**2.2**	1.4
122	Putative cytochrome P450	***RB_c071***	#N/A	4.E-44	1.6	1.4	1.1	1.2	0.9	0.7	**4.6**	**2.7**	**7.1**	**4.4**	**2.0**	1.5
123	Pathogenesis related protein 1.1 (PR-1.1)	***RB_c072^{bgh}***	AJ874038 AJ874039	1.E-73	**3.3**	**2.0**	**2.5**	**2.5**	**5.3**	**9.2**	**9.8**	**9.7**	**13.2**	**11.6**	**11.3**	**17.1**
124	cosmid 69-7-1 Lr21 gene	***RB_c075***	#N/A	1.E-15	0.9	0.8	0.7	0.8	0.8	0.8	0.6	**0.5**	0.7	0.7	0.6	0.6
125	B1144G04.13 protein	***RB_c077^{bgh}***	AJ874014 AJ874015	3.E-09	1.1	1.1	1.2	1.0	1.3	1.0	**2.0**	1.5	2.0	1.8	1.8	1.7
126	Beta-1,3-glucanase (Glb3)	***RB_c079^{bgh}***	AJ885878	1.E-109	**5.3**	**4.8**	**6.7**	**4.2**	**6.2**	**4.9**	**14.4**	**16.4**	**18.1**	**15.3**	**10.1**	**15.2**
127	Thaumatin-like protein TLP4	***RB_c083^{bgh}***	AJ874018 AJ874050	8.E-44	1.7	1.5	1.9	1.6	1.7	1.9	**2.8**	**3.1**	**2.1**	**2.9**	**2.5**	**2.9**
128	Thaumatin-like protein	***RB_c085^{bgh}***	AJ874044	2.E-66	**7.4**	**5.6**	**8.1**	**7.9**	**9.8**	**12.9**	**16.5**	**23.7**	**21.6**	**19.1**	**12.1**	**17.4**
129	clone wlmk8.pk0018.e8:fis, similar to sulfate adenylyltransferase	***RB_c086***	#N/A	1.E-171	0.8	0.8	0.8	1.2	0.8	0.9	0.6	**0.4**	**0.4**	**0.4**	**0.4**	0.5
130	beta-1,3-endoglucanase (Y18212)	***RB_c091^{bgh}***	AJ874012	1.E-100	1.7	1.3	1.8	1.5	**2.2**	**2.7**	**6.3**	**5.8**	**7.0**	**6.9**	**5.4**	**6.7**
131	cDNA clone:J013161I06	***RB_c094^{bgh}***	AJ874006	5.E-21	1.5	1.4	1.3	1.2	1.6	1.6	**2.6**	**2.2**	**2.7**	**2.6**	**3.1**	**2.9**
132	Putative transposon gamma-delta 80.3 kDa protein, E. coli	***RB_c096***	AJ888232	1.E-108	**2.0**	**2.1**	**2.5**	**2.1**	**2.7**	**3.2**	**4.7**	**6.1**	**5.6**	**5.8**	**3.1**	**5.0**
133	Putative peroxidase	***RB_c097***	#N/A	2.E-08	1.3	1.2	1.4	1.2	1.3	1.5	**2.1**	**2.0**	1.8	1.8	**2.4**	**2.1**
134	P0684C01.8 protein	***RB_c100^{bgh}***	AJ873979	6.E-23	1.1	1.0	0.9	0.9	1.0	1.3	**3.4**	**2.5**	1.9	1.9	**2.6**	**2.2**
135	Phenylalanine ammonia-lyase	***RB_c101^{Bgh}***	AJ873941 AJ873961	1.E-108	1.0	0.9	0.9	1.1	0.9	1.1	**7.1**	**3.7**	**2.5**	**2.6**	**3.7**	**3.2**
136	F24O1.18 protein	***RB_c103^{bgh}***	AJ874016	4.E-01	1.3	1.0	1.1	1.1	1.0	1.2	1.8	1.6	**2.1**	**2.0**	**2.0**	**2.7**
137	Putative wall-associated kinase 2	***RB_c104^{bgh}***	AJ873943	5.E-09	1.6	1.4	1.5	1.3	1.4	1.0	1.4	1.6	2.0	1.8	1.8	**2.3**
138	chilling-inducible protein	***RB_c110***	AJ873939	8.E-07	2.0	1.5	1.7	1.3	1.5	2.0	**3.3**	**3.4**	**4.3**	**3.3**	**2.9**	**2.4**
139	Arabinogalactan protein-like	***RB_c111***	#N/A	7.E-38	1.0	1.0	0.9	0.9	0.8	0.9	0.6	**0.4**	0.7	0.7	0.6	0.8
140	fungal 28S ribosomal RNA gene	***RB_c116^{Bgh}***	AJ888238	4.E-71	**2.4**	**3.3**	**2.6**	**3.8**	1.2	1.8	1.0	**2.9**	1.9	1.4	1.4	1.8
141	60S ribosomal protein L10-2 (Putative tumor suppressor SG12)	***RB_c117^{bgh}***	AJ874001 AJ874002	9.E-14	1.2	1.0	1.0	0.9	1.1	1.2	**2.5**	**2.2**	1.7	1.6	**2.1**	1.8
142	embryo-abundant protein	***RB_c118^{bgh}***	AJ873998 AJ873999	8.E-16	1.5	1.3	1.7	1.4	1.7	1.6	1.8	**2.6**	**2.3**	**2.1**	1.8	1.9
143	3-phosphoshikimate 1-carboxyvinyltransferase	***RB_c119^{bgh}***	AJ874053	7.E-21	1.1	1.1	1.1	1.0	1.0	1.1	**2.1**	1.8	1.9	1.8	1.9	1.9
144	WIR1A protein	***RB_c120^{bgh}***	AJ874059	2.E+00	**3.0**	**2.2**	**3.3**	**2.2**	1.3	1.2	**2.4**	**2.7**	**3.0**	**2.5**	1.6	1.6
145	Glyceraldehyde 3-phosphate dehydrogenase, Blumeria graminis f.sp. hordei	***RB_c122^{Bgh}***	AJ888233	1.E-71	**2.4**	**2.1**	1.9	**14.5**	1.6	**4.9**	1.3	1.4	1.2	1.6	1.4	1.6
146	#N/A	***RB_4.5***	#N/A	#N/A	0.9	1.1	0.9	1.3	**0.4**	1.3	**0.3**	0.7	0.6	0.5	0.8	0.8
147	#N/A	***RB_4.6***	#N/A	#N/A	0.9	0.7	1.0	1.2	0.7	1.1	**2.9**	1.8	1.0	1.3	1.5	1.4
148	#N/A	***RB_22.3***	#N/A	#N/A	0.8	0.8	0.8	0.8	0.8	0.7	**0.5**	**0.4**	**0.5**	**0.4**	**0.5**	**0.4**
149	#N/A	***RB_22.4***	#N/A	#N/A	0.7	0.8	0.8	0.8	0.7	0.8	**0.4**	**0.4**	**0.5**	**0.4**	**0.3**	**0.3**
150	#N/A	***RB_22.5***	#N/A	#N/A	0.7	0.8	0.8	0.9	0.8	1.0	**0.5**	**0.2**	0.5	**0.4**	**0.5**	**0.4**
151	#N/A	***RB_22.6***	#N/A	#N/A	0.6	0.8	0.7	0.8	0.6	0.8	**0.3**	**0.3**	**0.4**	**0.4**	**0.3**	**0.3**

Table 8.13 (continued)

	Putative function	EST ID	access. no#	E-val	08 hai wheat cv. MA Vir	08 hai wheat cv. MA Avr2	08 hai wheat cv. MA Avr3	08 hai wheat cv. MA Bgh	08 hai cv. Kanzler Vir	08 hai cv. Kanzler Bgh	24 hai wheat cv. MA Vir	24 hai wheat cv. MA Avr2	24 hai wheat cv. MA Avr3	24 hai wheat cv. MA Bgh	24 hai cv. Kanzler Vir	24 hai cv. Kanzler Bgh
	1	2	3	4	5	6	7	8	9	10	11	12	13	14	15	16
152	#N/A	***RB_22.7***	#N/A	#N/A	0.7	0.7	0.6	0.8	0.7	0.8	**0.3**	**0.3**	**0.4**	**0.3**	**0.3**	**0.3**
153	#N/A	***RB_22.8***	#N/A	#N/A	0.8	0.8	0.7	0.9	0.7	0.8	**0.4**	**0.4**	**0.4**	**0.4**	**0.4**	**0.3**
154	Beta-1,3-glucanase (GLU2)	***RB_24.4^{bgh}***	AJ885877	8.E-10	1.0	0.9	0.8	1.1	1.2	0.9	1.2	0.6	0.8	0.7	**2.1**	1.7
155	#N/A	***RB_25.16***	#N/A	#N/A	0.8	0.7	0.9	0.7	0.8	0.8	1.1	1.0	0.7	0.8	0.8	**0.3**
156	Low molecular weight heat shock protein precursor (hsp22) mRNA, nuclear gene encoding mitochondrial protein	***RB_33.8***	#N/A	2.E+00	1.3	1.1	1.2	1.0	1.3	1.3	**2.7**	1.9	**2.1**	1.8	1.6	1.5
157	clone OJ1012B02, chromosome 3	***RB_34.5^{bgh}***	#N/A	2.E+01	**2.2**	1.8	1.6	1.5	1.9	1.8	**2.8**	**2.7**	**2.6**	**2.5**	**2.5**	**2.6**
158	WIR5	***RB_37.4***	#N/A	8.E-09	1.9	#N/A	1.4	1.0	1.9	1.9	**3.4**	**2.9**	**4.5**	1.4	**4.8**	**2.0**
159	Putative bZIP (Leucine zipper) protein	***RB_37A.4***	#N/A	9.E-28	1.5	1.3	1.1	1.2	1.4	1.3	**2.1**	**2.1**	**2.7**	**2.9**	**2.9**	**3.0**
160	#N/A	***RB_39B.2***	#N/A	#N/A	0.9	1.2	#N/A	1.0	0.7	0.9	0.6	0.8	0.6	0.7	**0.5**	0.7
161	no significant hit	***RB_40.2^{bgh}***	#N/A	#N/A	1.1	1.1	0.8	0.9	1.1	1.0	**2.7**	1.7	**2.2**	**2.5**	**2.1**	**2.7**
162	#N/A	***RB_42B.1***	#N/A	#N/A	1.2	1.0	0.7	0.7	1.1	0.9	1.5	1.3	1.6	1.7	**2.2**	**2.1**
163	#N/A	***RB_42B.2***	#N/A	#N/A	1.2	1.0	0.9	0.7	1.0	1.1	2.0	1.4	1.8	2.0	**2.4**	**2.4**
164	#N/A	***RB_42B.3***	#N/A	#N/A	1.1	0.9	0.8	0.6	0.9	1.0	1.8	1.5	1.8	1.8	**2.2**	**2.1**
165	#N/A	***RB_42B.8***	#N/A	#N/A	1.0	0.9	0.7	0.8	0.9	1.1	1.7	1.3	1.6	1.7	**2.0**	2.0
166	cDNA clone D01275 similar to retinal short-chain, Blumeria graminis f. sp. hordei	***RB_43A.5^{Bgh}***	AJ888230	1.E-107	**3.0**	**2.3**	**3.4**	**5.6**	**2.2**	**3.9**	**5.2**	**6.9**	**4.8**	**4.4**	**2.9**	**4.3**
167	#N/A	***RB_43A.7***	#N/A	#N/A	1.1	1.3	1.3	1.0	1.5	#N/A	1.5	1.8	**2.1**	1.1	**2.3**	**3.0**
168	Phosphoethanolamine methyltransferase	***RB_45.3***	#N/A	5.E-07	0.6	0.6	**0.4**	0.6	0.6	0.7	**0.4**	#N/A	**0.2**	**0.4**	**0.3**	**0.4**
169	#N/A	***RB_50A.4***	#N/A	#N/A	0.7	0.6	**0.5**	0.5	0.6	0.7	**0.4**	**0.2**	0.5	**0.4**	**0.4**	**0.5**
170	#N/A	***RB_50A.5***	#N/A	#N/A	0.7	0.7	0.7	0.8	0.6	0.9	**0.5**	**0.4**	0.5	**0.5**	0.6	0.6
171	#N/A	***RB_50A.8***	#N/A	#N/A	0.6	0.7	0.5	0.6	0.6	0.8	**0.4**	**0.3**	0.6	**0.4**	**0.4**	**0.5**
172	chromosome 1 YAC yUP8H12 complete sequence	***RB_74.2^{Bgh}***	#N/A	4.E-01	**2.1**	**2.2**	**2.1**	1.6	1.2	1.4	1.5	**2.1**	**2.3**	**2.1**	1.1	1.4
173	Similarity to RNA-binding protein	***RB_78_101.10***	#N/A	1.E-70	1.1	1.1	1.1	0.9	1.2	1.0	1.9	1.5	**2.2**	1.4	**2.0**	1.7
174	Mg-chelatase subunit XANTHA-F	***RB_86.1***	#N/A	2.E-26	0.7	0.9	0.7	1.4	0.8	0.8	**0.4**	**0.3**	**0.3**	**0.3**	**0.2**	**0.3**
175	#N/A	***RB_86.3***	#N/A	#N/A	0.7	0.8	0.7	1.3	0.8	0.7	**0.3**	**0.2**	**0.3**	**0.2**	**0.2**	**0.3**
176	methionine sulfoxide reductase	***RB_92.2***	#N/A	6.E-19	1.3	0.9	1.0	1.1	1.0	1.0	**2.6**	1.3	1.7	1.5	1.8	1.3
177	fructose-1,6-bisphosphatase	***RB_97.3***	AJ888728	4.E-40	0.6	0.7	0.7	0.9	0.8	0.7	**0.5**	**0.3**	**0.5**	**0.4**	**0.4**	**0.5**
178	putative monosaccharide transporter	***RB_104.3^{bgh}***	AJ874105	9.E-65	1.7	1.4	1.4	1.3	2.0	2.0	**2.7**	**3.8**	**3.1**	**3.0**	**2.7**	**2.7**
179	Polysaccharide biosynthesis protein	***RB_107.2^{bgh}***	AJ873938	7.E-01	1.3	1.2	1.2	1.2	1.4	1.4	1.9	**2.0**	1.9	1.5	1.8	1.8
180	#N/A	***RB_124.6***	#N/A	#N/A	1.0	1.2	1.1	0.9	0.5	1.0	**0.4**	0.9	0.7	0.5	0.6	0.8
181	clone WPMS17, microsatellite DNA	***RB_132.1^{bgh}***	#N/A	2.E+01	1.2	1.1	1.2	1.2	1.4	1.4	1.7	**2.0**	2.0	**2.3**	2.0	1.9
182	#N/A	***RB_139.2***	#N/A	#N/A	0.9	0.9	0.9	1.0	0.5	1.0	**0.4**	0.7	0.5	**0.5**	0.7	0.6
183	putative glutamine synthase	***RB_144.1^{bgh}***	#N/A	7.E-04	1.1	1.2	1.2	0.9	1.0	1.3	**3.0**	#N/A	1.8	1.7	**2.3**	1.8
184	genomic DNA, chromosome 7, BAC clone:OSJNBb0018L13	***RB_144.3^{bgh}***	#N/A	4.E+00	1.1	1.2	1.0	1.0	0.9	1.2	**2.8**	1.8	1.4	1.2	**2.2**	1.7

Table 8.13 (continued)

	Putative function	EST ID	access. no#	E-val	08 hai						24 hai					
					wheat cv. MA				cv. Kanzler		wheat cv. MA				cv. Kanzler	
					Vir	*Avr2*	*Avr3*	*Bgh*	*Vir*	*Bgh*	*Vir*	*Avr2*	*Avr3*	*Bgh*	*Vir*	*Bgh*
	1	2	3	4	5	6	7	8	9	10	11	12	13	14	15	16
185	plant 18S ribosomal RNA	***RB_148.2***^{Bgh}	AJ873949	2.E-40	0.8	1.0	0.7	1.3	**0.5**	1.0	**0.3**	0.6	0.6	**0.4**	0.6	0.6
186	#N/A	***RB_148.8***	#N/A	#N/A	0.8	0.9	0.8	0.9	1.0	0.9	**0.5**	0.6	0.6	0.5	0.7	0.6
187	#N/A	***RB_157.5***	#N/A	#N/A	1.0	1.1	1.2	1.1	1.0	1.0	**2.1**	1.8	**2.3**	1.8	1.1	1.6
188	BAC OSJNBa0059E14, chromosome 3	***RB_158.1***	#N/A	2.E+01	1.1	1.1	1.1	1.1	1.2	1.5	**3.1**	**2.4**	**2.1**	#N/A	**3.2**	**2.2**
189	#N/A	***RB_159.1***	#N/A	#N/A	0.9	0.9	0.7	0.7	0.9	0.8	0.5	0.6	0.5	0.5	0.5	**0.5**
190	Botrytis cinerea strain	***RB_164.1***^{bgh}	AJ873960	3.E-01	1.1	1.3	1.1	1.1	1.3	1.5	**4.0**	**3.6**	**2.9**	**3.5**	**4.1**	**4.0**
191	BAC OSJNBa0054A12, chromosome 12	***RB_164.4***^{Bgh}	AJ873962	7.E-01	0.8	1.0	0.9	1.0	1.1	1.0	**2.7**	**2.0**	1.4	1.4	**2.2**	1.7
192	#N/A	***RB_165.1***	#N/A	#N/A	0.7	0.6	0.7	0.8	0.7	0.6	**0.3**	**0.3**	**0.3**	**0.2**	**0.3**	**0.3**
193	#N/A	***RB_165.4***	#N/A	#N/A	1.0	1.1	0.8	1.0	**0.4**	1.1	**0.3**	0.7	0.6	**0.4**	0.8	0.6
194	bacterial transposase	***RB_168.2***	#N/A	2.E-72	1.9	1.8	1.8	1.6	1.9	1.9	**3.1**	**2.9**	**2.7**	**2.2**	**2.4**	1.9
195	#N/A	***RB_169.2***	#N/A	#N/A	**2.4**	1.6	1.4	1.3	1.4	1.3	**4.5**	**3.8**	**4.4**	1.8	**3.5**	1.4
196	#N/A	***RB_169.4***	#N/A	#N/A	**2.5**	1.7	1.5	1.1	1.7	1.4	**4.4**	**4.3**	**3.8**	1.6	**3.7**	1.1
197	#N/A	***RB_169.5***	#N/A	#N/A	0.9	1.0	0.8	1.3	**0.4**	1.2	**0.4**	0.7	0.6	0.5	0.8	0.6
198	#N/A	***RB_169.6***	#N/A	#N/A	1.9	1.5	1.3	1.1	1.1	1.3	**3.0**	**3.3**	**3.0**	1.2	1.9	1.3
199	#N/A	***RB_169.7***	#N/A	#N/A	1.0	1.1	1.0	1.3	**0.4**	1.2	**0.4**	0.8	0.7	0.6	0.9	0.6
200	#N/A	***RB_174.7***	#N/A	#N/A	0.9	1.1	0.9	1.4	**0.4**	1.2	**0.3**	0.8	0.7	0.5	0.7	#N/A
201	ubiquitin-conjugating enzyme (UBC)	***RB_178.8***^{bgh}	AJ873972	6.E-10	1.2	1.2	1.0	1.3	1.4	1.3	1.5	**2.2**	1.5	1.6	1.3	1.7
202	no significant hit	***RB_182.1***^{bgh}	AJ885876	#N/A	1.6	1.3	1.9	1.3	1.8	1.8	**2.7**	**2.8**	**3.3**	**2.1**	**2.4**	**2.7**
203	Beta-1,3-glucanase (Glb3)	***RB_182.3***	#N/A	1.E-111	0.8	0.7	0.8	0.7	0.8	0.9	0.5	**0.4**	0.6	**0.4**	**0.4**	**0.5**
204	Ubiquitin-protein ligase 2	***RB_182.4***	#N/A	9.E-05	0.7	0.8	0.8	0.8	0.9	0.7	0.5	**0.4**	0.6	**0.4**	**0.4**	**0.4**
205	#N/A	***RB_182.7***	#N/A	#N/A	0.6	0.6	0.7	0.7	0.7	0.5	**0.4**	**0.3**	**0.4**	**0.3**	**0.3**	**0.3**
206	#N/A	***RB_182.10***	#N/A	#N/A	0.6	0.8	0.7	0.6	0.8	0.6	**0.5**	**0.3**	**0.5**	**0.3**	**0.3**	**0.3**
207	#N/A	***RB_182.11***	#N/A	#N/A	0.6	0.6	0.7	0.7	0.7	0.6	**0.4**	**0.3**	**0.4**	**0.3**	**0.3**	**0.3**
208	#N/A	***RB_182.12***	#N/A	#N/A	0.6	0.6	0.7	0.7	0.7	0.6	**0.4**	**0.3**	**0.4**	**0.3**	**0.3**	**0.3**
209	#N/A	***RB_183.4***	#N/A	#N/A	1.7	**2.3**	0.8	1.2	1.2	1.2	0.6	1.6	0.9	0.8	0.6	**0.5**
210	#N/A	***RB_183.5***	#N/A	#N/A	**2.2**	1.7	1.5	1.0	1.4	1.4	1.3	**4.3**	**2.4**	1.3	**2.1**	1.2
211	#N/A	***RB_190.1***	#N/A	#N/A	0.7	0.7	0.8	0.6	0.8	0.6	**0.4**	**0.3**	**0.4**	**0.4**	**0.4**	**0.3**
212	#N/A	***RB_190.4***	#N/A	#N/A	0.8	0.7	1.0	1.0	0.9	0.7	**0.4**	**0.5**	0.5	**0.4**	**0.5**	**0.4**
213	#N/A	***RB_206.6***	#N/A	#N/A	0.7	0.8	0.9	0.9	0.8	0.8	**0.5**	0.7	0.6	0.6	0.6	0.6
214	Carbonic anhydrase, chloroplast precursor	***RB_212.2***	#N/A	3.E-09	1.0	1.0	1.1	1.5	0.9	1.0	**0.4**	0.7	0.7	0.7	0.7	0.7
215	#N/A	***RB_212.3***	#N/A	#N/A	0.8	0.7	0.8	1.1	0.8	0.7	**0.3**	**0.2**	**0.3**	**0.2**	**0.2**	**0.2**
216	#N/A	***RB_212.4***	#N/A	#N/A	0.8	0.8	0.8	0.8	1.3	0.7	**0.4**	0.6	0.6	0.7	0.5	0.5
217	#N/A	***RB_214.4***	#N/A	#N/A	1.0	1.1	1.0	1.2	1.1	1.0	**0.4**	**0.3**	**0.3**	**0.3**	**0.2**	**0.3**
218	Putative aspartate aminotransferase	***RB_218.2***^{bgh}	AJ873989	8.E-16	1.0	1.0	1.2	1.0	0.9	1.1	**5.5**	**3.7**	**5.2**	**3.7**	**4.0**	**3.3**

Table 8.13 (continued)

	Putative function	EST ID	access. no#	E-val	08 hai						24 hai					
					wheat cv. MA				cv. Kanzler		wheat cv. MA				cv. Kanzler	
					Vir	*Avr2*	*Avr3*	*Bgh*	*Vir*	*Bgh*	*Vir*	*Avr2*	*Avr3*	*Bgh*	*Vir*	*Bgh*
	1	2	3	4	5	6	7	8	9	10	11	12	13	14	15	16
219	Myb-related protein	***RB_226.2***^{bgh}	AJ873993	7.E-09	1.9	1.7	**2.1**	1.3	1.7	1.3	1.9	1.0	**2.4**	1.5	1.3	1.8
220	no significant hit	***RB_240.1***^{bgh}	#N/A	#N/A	0.8	0.8	0.8	0.7	1.0	1.1	1.6	1.4	1.5	2.0	1.5	**2.0**
221	#N/A	***RB_240.2***	#N/A	#N/A	0.5	0.7	0.6	1.1	0.7	0.6	**0.2**	**0.2**	**0.2**	**0.2**	**0.1**	**0.2**
222	#N/A	***RB_240.3***	#N/A	#N/A	0.7	0.8	**2.1**	0.7	0.6	0.8	0.5	0.6	0.8	0.7	0.5	0.6
223	unknown	***RB_240.4***	AJ888722	2.E-55	1.0	0.9	0.8	0.7	1.1	0.9	1.7	1.1	1.6	1.8	1.9	**2.1**
224	#N/A	***RB_240.5***	#N/A	#N/A	1.0	0.9	0.8	0.6	1.1	0.8	1.7	1.1	1.6	1.8	1.7	**2.2**
225	#N/A	***RB_257.8***	#N/A	#N/A	0.7	0.8	0.7	0.9	0.9	1.0	**0.4**	**0.3**	**0.3**	**0.3**	**0.3**	**0.4**
226	#N/A	***RB_261.7***	#N/A	#N/A	1.5	1.1	1.0	1.0	1.1	1.2	1.0	**2.8**	1.6	1.0	1.4	1.0
227	#N/A	***RB_285.5***	#N/A	#N/A	1.3	1.2	1.1	1.0	1.5	1.1	**2.3**	1.7	**2.6**	**2.2**	**2.5**	**2.3**
228	#N/A	***RB_285.6***	#N/A	#N/A	1.6	1.3	1.7	1.2	1.8	1.2	**2.6**	1.2	**3.1**	**2.0**	**2.1**	**2.3**
229	#N/A	***RB_285.11***	#N/A	#N/A	1.7	**3.3**	1.7	1.4	**2.0**	1.3	**3.0**	**2.1**	**3.6**	**3.0**	**2.6**	**2.5**
230	#N/A	***RB_285.12***	#N/A	#N/A	1.5	1.3	1.3	1.1	1.9	1.3	**3.0**	1.8	**3.3**	**2.7**	**2.5**	**2.7**
231	Leucine-rich-like protein	***RB_286.2***^{bgh}	#N/A	1.E-14	1.3	1.3	1.1	1.1	1.3	1.4	**3.0**	**3.2**	**4.1**	**5.2**	**2.3**	**6.0**
232	glucose-6-phosphate isomerase-like protein	***RB_291.4***^{bgh}	AJ874017	5.E-46	1.1	1.0	0.9	1.0	0.9	1.2	1.5	1.2	1.6	1.4	1.6	**2.5**
233	#N/A	***RB_301.4***	#N/A	#N/A	1.0	0.8	1.1	1.1	0.6	1.0	**0.4**	0.7	0.7	0.6	0.6	0.6
234	#N/A	***RB_304.4***	#N/A	#N/A	0.7	0.9	1.0	1.1	0.8	0.7	**0.4**	**0.4**	0.5	**0.4**	**0.4**	**0.5**
235	#N/A	***RB_305.1***	#N/A	#N/A	1.1	1.1	1.2	1.1	0.8	1.0	**0.4**	0.7	0.8	0.6	0.6	0.6
236	#N/A	***RB_305.2***	#N/A	#N/A	1.0	0.7	0.8	0.9	0.8	0.8	0.8	0.6	**0.5**	**0.4**	0.7	0.5
237	#N/A	***RB_305.4***	#N/A	#N/A	1.2	1.2	1.1	1.1	0.9	1.1	**0.4**	0.7	0.8	0.6	0.6	0.6
238	#N/A	***RB_305.5***	#N/A	#N/A	1.2	0.9	1.2	1.3	0.8	1.1	**0.5**	0.6	0.9	0.6	0.6	0.7
239	#N/A	***RB_305.6***	#N/A	#N/A	1.1	1.0	1.0	1.1	0.8	1.0	**0.4**	0.7	0.8	0.6	0.6	0.5
240	#N/A	***RB_305.7***	#N/A	#N/A	1.2	1.3	1.1	1.1	0.9	1.1	**0.4**	0.7	0.8	0.6	0.6	0.7
241	#N/A	***RB_305.8***	#N/A	#N/A	0.9	0.7	0.9	1.0	0.9	0.7	0.8	0.7	0.6	**0.4**	0.7	0.7
242	#N/A	***RB_307.5***	#N/A	#N/A	1.0	1.1	1.0	1.3	1.1	1.0	**2.8**	**2.0**	**3.2**	**2.7**	**2.7**	**3.1**
243	#N/A	***RB_307.7***	#N/A	#N/A	1.0	1.1	0.9	1.0	1.0	1.1	1.9	1.5	**2.6**	1.9	**2.1**	2.0
244	#N/A	***RB_313.5***	#N/A	#N/A	0.9	0.9	1.1	0.8	1.0	0.9	**0.4**	0.6	0.9	0.6	0.6	0.6
245	14-3-3-like protein	***RB_317.4***	#N/A	7.E-01	1.6	1.9	1.7	**2.0**	1.2	1.8	0.9	**2.0**	1.3	1.2	1.3	1.5
246	#N/A	***RB_318.5***	#N/A	#N/A	1.6	1.5	1.8	**3.0**	1.2	1.3	2.0	**2.8**	1.6	1.7	1.1	1.5
247	#N/A	***RB_323.2***	#N/A	#N/A	1.0	0.9	0.9	1.1	0.9	1.0	0.7	0.6	**0.2**	**0.4**	**0.4**	**0.4**
248	#N/A	***RB_323.5***	#N/A	#N/A	0.9	0.7	1.2	0.8	1.0	1.2	**0.3**	**0.3**	**0.3**	**0.3**	**0.2**	**0.2**
249	GDP-mannose pyrophosphorylase	***RB_327.3***^{bgh}	AJ874028	2.E-19	1.4	1.7	1.5	1.8	1.0	1.3	1.9	#N/A	**2.1**	1.7	1.7	**2.4**
250	transformer serine/arginine-rich ribonucleoprotein	***RB_337.2***	#N/A	0.E+00	1.1	1.1	0.9	0.8	1.3	1.2	0.6	**0.5**	0.9	0.8	0.7	0.6
251	#N/A	***RB_337.5***	#N/A	#N/A	2.0	**2.1**	2.0	**2.2**	1.3	1.8	0.9	**2.1**	1.5	1.1	1.3	1.3
252	#N/A	***RB_337.6***	#N/A	#N/A	0.8	0.6	0.8	1.1	0.9	0.9	0.5	**0.5**	**0.5**	**0.4**	**0.4**	**0.4**
253	#N/A	***RB_337.8***	#N/A	#N/A	0.5	**0.5**	0.5	0.8	0.6	0.6	**0.3**	**0.2**	**0.2**	**0.2**	**0.2**	**0.2**

Table 8.13 (continued)

	Putative function	EST ID	access. no#	E-val	08 hai						24 hai					
					wheat cv. MA				cv. Kanzler		wheat cv. MA				cv. Kanzler	
					Vir	*Avr2*	*Avr3*	*Bgh*	*Vir*	*Bgh*	*Vir*	*Avr2*	*Avr3*	*Bgh*	*Vir*	*Bgh*
	1	2	3	4	5	6	7	8	9	10	11	12	13	14	15	16
254	#N/A	***RB_339.1***	#N/A	#N/A	0.8	0.6	0.8	1.1	0.8	0.8	0.6	**0.5**	**0.5**	**0.4**	**0.4**	**0.5**
255	#N/A	***RB_339.3***	#N/A	#N/A	0.8	0.7	0.8	1.1	0.8	0.9	0.5	**0.4**	**0.4**	**0.4**	**0.4**	**0.5**
256	#N/A	***RB_339.4***	#N/A	#N/A	#N/A	0.6	0.8	1.1	0.8	0.8	0.6	**0.4**	**0.5**	**0.4**	**0.4**	**0.5**
257	#N/A	***RB_339.5***	#N/A	#N/A	0.7	0.6	0.7	1.1	0.8	0.8	0.5	**0.4**	**0.5**	**0.4**	**0.4**	**0.4**
258	Ethylene-responsive small GTP-binding protein	***RB_339.8^{Bgh}***	AJ874032	3.E-18	0.8	0.7	0.8	1.1	0.9	0.9	0.7	0.6	0.5	**0.5**	0.6	0.6
259	#N/A	***RB_342.5***	#N/A	#N/A	0.9	0.7	0.8	0.8	0.8	0.8	0.6	0.5	**0.5**	**0.4**	0.5	0.6
260	#N/A	***RB_342.6***	#N/A	#N/A	0.8	0.7	0.8	0.8	1.0	0.7	0.5	0.5	**0.4**	**0.4**	**0.5**	0.6
261	#N/A	***RB_358.7***	#N/A	#N/A	0.7	0.6	0.8	0.8	0.7	0.6	**0.4**	**0.3**	**0.3**	**0.2**	**0.3**	**0.3**
262	WCI-5, T. aestivum	***RB_360.4^{bgh}***	AJ874046	1.E-109	**5.8**	**6.4**	**7.1**	**5.1**	**3.7**	**3.6**	**6.2**	**8.4**	**7.2**	**7.7**	**4.1**	**7.3**
263	no significant hit	***RB_360.7***	#N/A	#N/A	1.3	1.2	1.4	1.4	1.3	1.5	**3.5**	**2.4**	1.6	1.1	1.8	1.3

9. Acknowledgements

I wish to thank...

Prof. Dr. Robert Dudler for giving me the great opportunity to do my Ph.D. thesis in his group. His expertise and his critical comments were a great help and have made this work a creative experience to me.

Prof. Dr. Beat Keller for taking charge of the co-referate.

PD Dr. Patrick Schweizer for introducing me to the transient expression system, for his continuous technical support and for providing the pOA_IPK hairpin loop expression constructs. My special thanks also go to Dr. Urs Wäspi for introducing me into the world of syringolin. Dr. Schweizer and Dr. Wäspi were excellent supervisors during my years of apprenticeship.

Dr. Rémy Bruggmann for the common microarray project, for all the interesting scientific discussions and for his competent technical and bioinformatical contributions.

Jana Schneider for her endeavors during construction of the foldback expression vectors and subsequent testing by biolistic transformation.

PD Dr. Philippe Reymond for the production of the microarrays and the introduction into microarray data analysis.

Kathrin Michel for the critical comments to our numerous theories of syringolin action in plants and for her contributions and inputs from the *Arabidopsis* system.

Dr. Roshani Shakya for the common syringolin purification sessions and for borrowing me some of her precious syringolin stocks.

Dr. Nabila Yahiaoui for kindly providing the Pm3 expression vectors, the powdery mildew isolates and the seeds of wheat cv. Michigan Amber. I also wish to thank Susanne Brunner for the free exchange of information concerning transient *R*-gene expression in wheat.

Prof. Dr. Felix Keller for his patient support during purification of syringolin - my cordial thanks!

Dr. Edith Schlagenhauf for introducing me into UNIX and for her help with the Staden software during the initial stage of DNA sequence analysis.

Dr. Jens Sobeck for the technical inputs and for directing my attention to the Agilent G2505B microarray scanner.

Simone Rau and all the other members of the group for the pleasant and cooperative atmosphere.

The technical personnel of the institute is acknowledged for their excellent support.

I thank E.E. Farmer, University of Lausanne, for the use of the Gene Expression Laboratory Microarray facility at the Department of Plant Molecular Biology. This work was supported by the Swiss National Science Foundation. The Functional Genomics Center Zurich and the Kanton Zürich is acknowledged.

I am especially grateful to my wife Chris and the children for their patience and understanding during intensive periods of work, to my parents for encouraging me and facilitating my studies and to my parents-in-law for their generous support. They all have made this work possible.

10. Curriculum vitae

Name	Olaf Abderhalden
Date of birth	April 28, 1972
Place of origin	Ebnat-Kappel (SG)
1979 - 1985	Primary school in Rafz (ZH)
1985 - 1987	Secondary school in Rafz (ZH)
1987 - 1991	Grammar school in Bülach: Matura type C
1991 - 1992	Military service
1992 - 1999	Undergraduate studies at the University of Zürich
July 1999	Diploma in plant pathology, University of Zürich
1999 - 2000	Studies of resistance of transgenic wheat at the Institute of Plant Biology, University of Zürch
2000 - 2005	Ph.D. thesis at the Institute of Plant Biology at the University of Zürich

Publications:

Michel, K., Abderhalden, O., Bruggmann, R., and Dudler, R. (2006). Transcriptional changes in powdery mildew-infected wheat and *Arabidopsis* leaves undergoing syringolin-triggered hypersensitive cell death at infection sites. Plant Molecular Biology 62, 561-578.

Bruggmann, R., Abderhalden, O., Reymond, P., and Dudler, R. (2005). Analysis of epidermis- and mesophyll-specific transcript accumulation in powdery mildew-inoculated wheat leaves. Plant Molecular Biology 58, 247-267.

Altpeter, F., Varshney, A., Abderhalden, O., Douchkov, D., Sautter, C., Kumlehn, J., Dudler, R., and Schweizer, P. (2005). Stable expression of a defense-related gene in wheat epidermis under transcriptional control of a novel promoter confers pathogen resistance. Plant Molecular Biology 57, 271-283.

Paillard, S., Schnurbusch, T., Winzeler, M., Messmer, M., Sourdille, P., Abderhalden, O., Keller, B., and Schachermayr, G. (2003). An integrative genetic linkage map of winter wheat (*Triticum aestivum* L.). Theor. Appl. Genet. 107, 1235-1242.

Schweizer, P., Pokorny, J., Abderhalden, O., and Dudler, R. (1999). A transient assay system for the functional assessment of defense-related genes in wheat. Mol. Plant-Microbe Interact. 12, 647-654.